

NEW GENES AND MECHANISMS OF RECURRENT HYDATIDIFORM MOLES

Ngoc Minh Phuong Nguyen

Department of Human Genetics

Faculty of Medicine

McGill University

Montreal, Quebec, Canada

December 2018

A thesis submitted to McGill University in partial fulfilment of the requirements of the degree of

Doctor of Philosophy

© Ngoc Minh Phuong Nguyen, 2018

To my future Phuong

I hope when you read this thesis again in the future, you will remember the passion and energy you put in these years of work, the happiness and joy you felt when you learned something new, understood things, and even when the results you got in the end could be not as you expected, or when they were so lovely that you couldn't stop smiling. You learned, and you loved it.

ABSTRACT

Hydatidiform mole (HM) or molar pregnancy is a rare complication of pregnancy characterized by the excessive proliferation of the trophoblast and abnormal embryonic development. Recurrent hydatidiform moles (RHM) are defined by the occurrence of at least two HMs in the same patient. Though there are two genes, *NLRP7* and *KHDC3L*, whose mutations cause RHM, there exist other patients without mutations in the known genes.

Chapter 2 in this thesis describes my MSc project before I fast-tracked to the PhD program. This project focused on the genetic characterization of the conceptions of patients with bi-allelic *NLRP7* mutations. Our work showed that *NLRP7* acts upstream of $p57^{KIP2}$ and regulates the balance between trophoblastic proliferation and tissue differentiation in the HM tissues. This work also corroborated previous data that all conceptions from patients with bi-allelic *NLRP7* mutations are diploid biparental.

Chapters 3 and 4 describe the work of gene identification in patients with RHM. To identify novel genes responsible for this entity, we performed whole exome sequencing on patients with RHM who are negative for mutations in the two known genes, and then targeted sequencing of candidate genes in larger cohorts of patients with milder phenotypes. The main challenge of this work was the high genetic heterogeneity of patients with RHM since we were not able to find any two patients with mutations in the same gene. To overcome this challenge, we retrieved all accessible HM tissues of the patients included in the exome sequencing and comprehensively characterized their genotypes in order to understand the mechanisms underlying them and classify the patients into specific groups (Chapter 3). Our data showed that RHMs from the same patient mostly have the same genotypic type and identified two main mechanisms that recur in patients without mutations in the known genes: diploid androgenetic

(24% of patients) and triploid dispermic (32% of patients), with stronger genetic susceptibility in the former category of patients.

Next, we identified bi-allelic deleterious mutations in three genes, *MEII*, *TOP6BL/C11orf80*, and *REC114*, with roles in meiotic double-strand breaks formation (Chapter 4). Mutations in *MEII* and *TOP6BL* were found in 2 unrelated patients with recurrent androgenetic HMs and their affected siblings. *REC114* is essential in meiotic double-strand breaks formation and its mutation was identified in one patient with androgenetic HM. Our work has revealed that the same genetic defect caused by these three genes can be responsible for both male and female infertility, and uncovered, for the first time in mammals, a mechanism for the genesis of androgenetic zygotes.

RÉSUMÉ

La môle hydatiforme (MH) ou grossesse molaire est une complication rare de la grossesse humaine. Elle est caractérisée par une prolifération excessive du trophoblaste et un développement embryonnaire anormal. Les môles hydatidiformes récurrentes (MHR) sont définies par la présence d'au moins deux MH chez la même patiente. Bien qu'il existe deux gènes dont les mutations causent des MHR, *NLRP7* et *KHDC3L*, il existe d'autres patientes avec MHR et sans mutations dans ces deux gènes.

Le chapitre 2 de cette thèse décrit mon projet de maîtrise en sciences avant que je passe au programme de doctorat. Ce projet était axé sur la caractérisation génétique des conceptions de patientes présentant des mutations bi-alléliques dans *NLRP7*. Nos travaux ont montré que *NLRP7* agissait en amont de $p57^{KIP2}$ et régulait l'équilibre entre la prolifération trophoblastique et la différenciation tissulaire dans les tissus molaire. Ce travail a également confirmé des données antérieures selon lesquelles toutes les conceptions de patientes porteuses de mutations bi-alléliques dans *NLRP7* sont diploïdes biparentales.

Les chapitres 3 et 4 décrivent les travaux d'identification des gènes chez les patientes atteintes de MHR. Pour identifier de nouveaux gènes responsables de cette entité, nous avons effectué un séquençage d'exome complet sur des patientes atteintes de MHR et sans mutations dans les deux gènes connus, puis un séquençage ciblé de gènes candidats dans des cohortes plus importantes de patientes présentant un phénotype moins sévère. Le principal défi de ce travail était la grande hétérogénéité génétique des patientes atteintes de MHR puisque nous n'avons pas été en mesure de trouver deux patientes présentant des mutations dans le même gène. Pour surmonter ce défi, nous avons récupéré les tissus molaire de ces patientes et nous les avons génotypé afin de comprendre les mécanismes sous-jacents et de classer les patientes dans des groupes spécifiques

(Chapitre 3). Nos données ont montré que les MHR provenant de la même patiente avaient généralement le même type génotypique et avons identifié deux mécanismes récurrents chez les patientes ne présentant pas de mutation dans les gènes connus: diploïde androgénétique (24% des patientes) et triploïde dispermique (32% des patientes), avec une susceptibilité génétique plus forte dans la première catégorie de patientes.

Ensuite, nous avons identifié des mutations délétères bi-alléliques dans trois gènes, *MEI1*, *TOP6BL / C11orf80* et *REC114*. Ces derniers ont des rôles dans la formation de rupture à double brin durant la méiose. Ces mutations ont été trouvées chez cinq patientes non apparentées, atteintes d'HM androgéniques récurrentes, de fausses couches et d'infertilité. Aussi, chez deux sœurs avec plusieurs fausses couches et un frère souffrant d'infertilité (chapitre 4). Nos travaux ont révélé que ce défaut génétique causé par ces trois gènes peut être responsable de l'infertilité masculine et féminine. En outre, nos travaux ont montré pour la première fois chez les mammifères, un mécanisme de la genèse des zygotes androgéniques.

TABLE OF CONTENTS

ABSTRACT	3
RÉSUMÉ	5
LIST OF ABBREVIATIONS	9
LIST OF FIGURES	12
LIST OF TABLES	15
ACKNOWLEDGEMENTS	16
FORMAT OF THE THESIS	18
CONTRIBUTION OF AUTHORS	20
CHAPTER 1- LITERATURE REVIEW	23
1.1 Hydatidiform mole.....	24
1.1.1 Introduction.....	24
1.1.2 Epidemiology	24
1.1.3 Classification based on histopathology	25
1.1.4 Sporadic hydatidiform mole	25
1.1.5 Hypotheses about the mechanisms of androgenetic HM formation	26
1.2 Genetics of RHM.....	31
1.2.1 <i>NLRP7</i>	31
1.2.2 <i>KHDC3L</i>	36
1.3 Genomic imprinting in recurrent diploid biparental moles.....	38
1.3.1 Altered DNA methylation at imprinted genes in the conceptions of patients with <i>KHDC3L</i> or <i>NLRP7</i> mutations	38
1.3.2 Altered DNA methylation beyond non-imprinted genes.....	40
1.3.3 Altered expression of <i>CDKN1C</i> in the conceptions of patients with <i>NLRP7</i> mutations	40
1.4 Ovum donation is recommended for patients with RHM	41
1.5 Rationale and objectives	43
1.6. Figures and Table	45
PREFACE TO CHAPTER 2	53
CHAPTER 2	54

Abstract	55
Materials and methods	59
Results.....	62
Discussion	68
Figures	73
Supplementary figure and table.....	81
PREFACE TO CHAPTER 3	83
CHAPTER 3.....	84
Abstract	86
Introduction.....	87
Materials and methods.....	89
Results.....	93
Discussion	103
Figures	108
Supplementary Figures and Tables	117
PREFACE TO CHAPTER 4	123
CHAPTER 4.....	124
Abstract	126
Introduction.....	127
Material and Methods	129
Results.....	134
Discussion	142
Movie titles and legends	148
Figures	149
Supplementary figures and tables.....	156
CHAPTER 5: GENERAL DISCUSSION	174
CHAPTER 6: CONCLUSION AND FUTURE DIRECTIONS	184
CHAPTER 7: REFERENCES.....	186
APPENDIX (ETHICS AND COPYRIGHT PERMISSIONS)	199

LIST OF ABBREVIATIONS

AnCHM	Androgenetic CHM
ASC	Apoptosis-Associated Speck-Like Protein Containing CARD
BO	Blighted ovum
CC	Cumulus cells
CDKN1C	Cyclin dependent kinase inhibitor 1C
CHM	Complete hydatidiform mole
COCs	Cumulus cell-oocyte complexes
CT	Cytotrophoblast
DIC	Differential interference contrast.
DMR	Differentially methylated regions
dpp	Day postpartum
DPPA5	Developmental Pluripotency Associated 5
END	Early neonatal death
FFPE	Formalin-fixed, paraffin-embedded
FISH	Fluorescent in situ hybridization
GTN	Gestational trophoblastic neoplasia;
GV	Germinal vesicles
H&E	Hematoxylin and eosin
hCG	Human chorionic gonadotropin;
HEK293	Human Embryonic Kidney 293 cells
hESCs	Human embryonic stem cells
HM	Hydatidiform mole
ICSI	Intra-cytoplasmic sperm injection.
Il1r1	Type 1 IL-1 receptor
IL-1 β	Interleukin-1 beta
IM	Invasive mole
IVF	In-vitro fertilization
KHDC1	KH homology domain containing 1
Khdc3	KH domain-containing protein 3
KHDC3L	KH domain containing 3 like, subcortical maternal complex member
LCL	Lymphoblastoid cell lines

LRR	Leucine Rich Repeat
MAF	Minor allele frequency
MC	Miscarriages
MEI1	Meiotic double-stranded break formation protein 1
MII	Metaphase II
MKI67	Marker of proliferation Ki-67
MSUC	Meiotic silencing of unsynapsed chromatin regions
NACHT	Domain present in <u>N</u> AIP, <u>C</u> IITA, <u>H</u> ET-E, <u>T</u> P-1
NB	Newborn
NLRP2	NLR family pyrin domain containing 2
NLRP5	NLR family pyrin domain containing 5
NLRP7	NLR family pyrin domain containing 7
NM MC	Nonmolar miscarriages;
NOD	Nucleotide oligomerization domain
NP	Normal pregnancy
NRBC	Nucleated red blood cell
NSV	Non-synonymous variant
OOEP	Oocyte expressed protein
Padi6	Peptidyl arginine deiminase 6
PB	Polar body
PBMC	Peripheral blood mononuclear cells
PGD	Preimplantation genetic diagnosis;
PHM	Partial hydatidiform mole
POC	Products of conception
PTD	Persistent trophoblastic disease
REC114	REC114 meiotic recombination protein
RHM	Recurrent hydatidiform moles
RM	Recurrent miscarriages.
SA	Spontaneous abortion
SB	Still birth
SNP	Single nucleotide polymorphisms
SCMC	Subcortical maternal complex (SCMC)
THP1	Monocytic cell line

TLE6	TLE family member 6, subcortical maternal complex member
TOP6BL (C11orf80)	Type 2 DNA topoisomerase 6 subunit B-like
WES	Whole exome sequencing
Zbed3	Zinc finger BED-type containing 3
ZP	Zona pellucida

LIST OF FIGURES

Chapter 1

Figure 1.1. Gross morphology and histopathological section of HM	45
Figure 1.2. Frequencies and classification of sporadic and recurrent HMs by aetiology, histopathology, and genotype.....	46
Figure 1.3. Schematic representation of the “empty” oocyte mechanism proposed by Kajii 1977.....	47
Figure 1.4. Proposed mechanism of postzygotic diploidization of triploids at the origin of HM formation.	498
Figure 1.5. Schematic representation of the formation of androgenetic zygote in <i>Corbicula</i> species after fertilization.	50
Figure 1.6. Known functions of the two genes <i>NLRP7</i> and <i>KHDC3L</i>	51

Chapter 2

Figure 2.1. Examples of the variations in the expression of p57 ^{KIP2} in diploid biparental hydatidiform moles from patients with two <i>NLRP7</i> -defective alleles	73
Figure 2.2. Representative example of our comprehensive analysis of products of conceptions (POCs) from patients with two defective alleles in <i>NLRP7</i>	74
Figure 2.3. Mosaic mole from a patient with two <i>NLRP7</i> -defective alleles.....	75
Figure 2.4. Recapitulation of p57 ^{KIP2} expression, histopathological features of the hydatidiform moles and <i>NLRP7</i> mutations in the patients.....	76
Figure 2.5. Ki-67 expression in 22 products of conceptions (POCs) from patients with two <i>NLRP7</i> -defective alleles.	78
Figure 2.6. A suggested model of <i>NLRP7</i> action upstream of p57 ^{KIP2} and Ki-67.....	78
Supplementary figure S2.1. Whole villous showing the presence of the XX cells in the villous stroma. Two cellular populations, diploid XY and diploid XX in the villous stroma.	

Chapter 3

Figure 3.1. Location of the Alu insertion in exon 4 of <i>NLRP7</i>	108
Figure 3.2. Summary of the comprehensive characterization of 57 hydatidiform mole tissues from 25 patients with no recessive pathogenic variants in <i>NLRP7</i> or <i>KHDC3L</i>	111
Figure 3.3. Histopathology and genotyping data of the two non-molar miscarriages from patient.....	113
Figure 3.4. Comparison of the genetic susceptibility for recurrent hydatidiform moles between patients with and without recessive mutations in <i>NLRP7</i> or <i>KHDC3L</i>	114
Figure 3.5. A recapitulation of the mutation screening in 113 patients and comprehensive characterization of their hydatidiform mole tissues.	115
Supplementary Figure 3.1A.....	117
Supplementary Figure 3.1B.....	118
Supplementary Figure 3.2.....	119
Supplementary Figure 3.3.....	120

Chapter 4

Figure 4.1. Pedigree structure, reproductive outcomes, and mutation analysis of two families with bi-allelic <i>MEI1</i> mutations	149
Figure 4.2. Pedigree structure, reproductive outcomes, and mutation analyses of <i>TOP6BL/C11ORF80</i> and <i>REC114</i> in three affected women with bi-allelic mutations	151
Figure 4.3. Meiosis I abnormalities in oocytes from wild-type, heterozygous, and homozygous mice.....	152
Figure 4.4. Various spindle and chromosome congression abnormalities after in vitro maturation	153
Figure 4.5. H3K9me2 staining of maternal chromosomes in oocytes and zygotes from wild-type and <i>Mei1</i> ^{-/-}	154
Figure 4.6. Preimplantation Development of <i>Mei1</i> ^{-/-} Oocytes in Culture.....	155
Figure S4.1. Characterization of four HM tissues from proband 1333 with bi-allelic <i>MEI1</i> mutations.	158
Figure S4.2. Characterization of one HM tissue from proband 880 with bi-allelic <i>MEI1</i> mutations.	159

Figure S4.3 . Microarray and flow cytometry analyses on 4 HM from proband 1333 with bi-allelic mutations in <i>MEII</i>	160
Figure S4.4. Flow cytometry analysis of the HM from proband 880 with bi-allelic mutations in <i>MEII</i>	161
Figure S4.5. Transcription of <i>MEII</i>, <i>TOP6BL</i>, and <i>REC114</i> in different stages of oocytes and reproductive tissues.....	162
Figure S4.6. Oocyte matured in vitro stained with anti α-tubulin (gren) and DAPI (blu170	163
Figure S4.7. An empty oocyte matured in vivo	164
Figure S4.8. H3K9me2 immunofluorescence showing the staining of maternal but not paternal chromosomes in a <i>Mei1</i>+/- zygote.	165
Figure S4.9. An in vivo fertilized oocyte stained with anti-H3K9me2 and DAPI.	166
Figure S4.10. An empty in vivo fertilized oocyte from <i>Mei1</i>-deficient female stained with anti-H3K9me2 (green) and DAPI (blue).	167
Figure S4.11. An in vivo fertilized oocyte from <i>Mei1</i>-deficient female stained with anti-H3K9me2 (green) and DAPI.....	168

Chapter 5

Figure 5.1. A suggested model that recapitulates the various roles of NLRP7 in the pathology of recurrent hydatidiform mole (RHM).....	177
Figure 5.2. Schematic representation of proposed mechanisms of recurrent diploid biparental and androgenetic HMs.....	180

LIST OF TABLES

Chapter 1

Table 1.1. Recapitulation of methylation analysis data in diploid biparental molar tissues from patients with NLRP7 or KHDC3L mutations (From Table 2, Nguyen *et al.* 2014 ¹)...53

Chapter 2

Table 2.1. Recapitulation of p57^{KIP2} and Ki-67 expression by immunohistochemistry, presence of embryonic tissues of inner cell mass origin, histopathology and mutations of 32 POCs from patients with two *NLRP7* defective alleles79

Table 2.2 . Correlations between the severity of the mutations, p57^{KIP2} expression, and the HM features.....80

Supplementary Table 2.1. Recapitulation of the reproductive outcomes, mutation analysis, and characterization of 36 POCs from patients with 2 *NLRP7* defective alleles82

Chapter 3

Table 3.1 Recapitulation of the ten novel protein-truncating variants in *NLRP7* with the ethnicities and reproductive histories of the patients 116

Supplementary Table 3.1: Table showing the sequences of the primers used to amplify the junction fragments and the sizes of the PCR-amplified fragments with each primer pair. 121

Supplementary table 3.2. Comprehensive genotypic analyses of the POC of the 25 patients with various methods as well as their full reproductive histories122

Chapter 4

Table S4.1: Primers used to amplify human genomic and complementary DNA169

Table S4.2: Primers used in RT-PCR to amplify mouse genes.....170

Table S4.3: Subjects screened by targeted sequencing for mutations in the three genes.....171

Table S4.4: Summary of data about the mutations found in the 3 genes.....172

Table S4.5: Summary of oocyte stages at time of collection from proband 1333 (at 36 years) and comments on embryo development after ICSI.....173

ACKNOWLEDGEMENTS

First and foremost, I would like to express my greatest gratitude to my supervisor, mentor, Dr. Rima Slim. I feel like I have been treated as a daughter, and sometimes I think “Sorry Rima, at home you have to deal with troubles from your daughters, and in the lab, you have to deal with me”. Thank you for always being there to guide me, pushing me to fully reach my potentials and most importantly, placing your trust and confidence in my abilities to do this work. I thank you for your great and warm care, professionally and personally.

A student must be lucky to have the greatest teachers at each stage of their academic journey, and I’m lucky like so. I would like to show my appreciation to my late high school teacher, Thầy Châu, who brought me to the world of DNA, who inspired me to switch my career just by his own joyful lessons. To my undergraduate program professor, Dr. Madoka Gray-Mitsumune, who listened to me sharing about my passions and told me about the Department of Human Genetics at McGill. To Dr. Asangla Ao, whom I did not have many chances to work with, yet always enthusiastically helped me whenever she could. I would also like to thank the members of my supervisory committee meetings, Dr. Jacek Majewski, Dr. Anna Naumova, Dr. Teruko Taketo, for their guidance and counsel during my PhD program.

I cannot thank my mentors enough. I owe so much to you.

I would like to say my thanks to all the members of the lab in those past years. To Ramesh, I cannot believe that after all of your silence and shyness, we can become such good friends. Friendship speaks itself. To Manuela and Christine, thanks for giving me the unique feeling I can’t find anymore as I grow older, the feeling of being teased and treated as a “little” 22-year old kid who just started at the lab. To Xiao-Yun Zhang, for keenly contacting me for

oocyte collection, which helped me facilitate my work. And to all other lab members, Nawel, Zhao-Jia, Maryam, Adel, thank you guys for being such good lab mates and providing a nice and peaceful work environment. And my most special and biggest gratitude to Yasmine. With our friendship, I know you are always there to help me with anything. Thanks, Yasmine, for being a great companion in the lab and outside, and for being a good listener. I treasure the time and memories we have shared and I'm glad that we have crossed paths in life.

I greatly appreciate the research scholarships from Faculty of Medicine, RQR, RI-MUHC, CRRD, the American Society of Human Genetics and travel awards from various organizers and the departments of Human Genetics. To Ross Mackay and Angela Roussos for their perfect effort in helping students with all the paper work and questions, without whom my student life would have been much harder. To all the housekeepers in the General Hospital and the Glen, thanks for helping us keep the labs clean so we can do our work. Your silent work is always appreciated.

I was born with a family lottery ticket. I know whatever I do, however things turn out to be, I can be home, and feel safe. To my unique brothers, anh hai and Đức đẹp trai, to whom I feel lucky to be siblings, who cooked for me when I was busy with experiments, who picked me up when I stayed late in the lab, who helped me with my English grammar, whom I shared laughter and bickering with. Life is not easy without you two, my beloved and crazy brothers. To my Dad, a physics teacher who gave me lessons in physics and in life, from whom I genetically inherited the academic gift and followed the work of academic path. To my Mom, who I love the most in life, who does everything for us so that we can have the best things in life. Mom, I love you so so much, and I hope my work in this field can give future moms the happiness of hearing the same thing from their children.

FORMAT OF THE THESIS

The thesis is presented in a manuscript-based format according to the Thesis Preparation Guidelines provided by the McGill Graduate and Postdoctoral studies website. The studies described here were performed under the supervision of Dr. Rima Slim. This thesis contains five chapters. Chapter 1 is a literature review that describes the various aspects of the pathology of hydatidiform mole and relevant background to this thesis. Chapter 2 is a manuscript that was published in the **Journal of Medical Genetics** (PMID: 25097207). Chapter 3 is a manuscript that was published in **Modern Pathology** (PMID: 29463882). Chapter 4 is a manuscript that was published in the **American Journal of Human Genetics** (PMID: 30388401). Chapter 5 includes a global synopsis and comparisons of causative genes found in this study and in previous studies.

Parts of Chapter 1 (Introduction) were reproduced from two review articles on which I am the first author and was responsible for their writing:

Chapter 27 in Hydatidiform Moles in the “Textbook of Autoinflammation” - in press (Ngoc Minh Phuong Nguyen, Pierre-Adrien Bolze, and Rima Slim)

- 1.1.1 Introduction
- 1.1.2 Epidemiology
- 1.1.3 Classification based on histopathology
- 1.1.4 Sporadic hydatidiform mole
- 1.2.1 Expression and localization (NLRP7)
- 1.2.1 NLRP7 and early embryonic development (NLRP7)
- 1.2.2 KHDC3L and the Subcortical Maternal Complex (SCMC)

“Genetics and Epigenetics of Recurrent Hydatidiform Moles: Basic Science and Genetic Counselling” (Ngoc Minh Phuong Nguyen and Rima Slim) ¹

- 1.2.1 NLRP7 (introductory paragraph- with some updates about the numbers and types of mutations)
- 1.2.1 Functional roles of NLRP7
- 1.2.1 Overexpressed NLRP7 downregulates intracellular IL-1 β
- 1.2.1 Physiological level of NLRP7 inhibits IL-1 β secretion in monocytic cells
- 1.2.1 An interesting emerging role for NLRP7 in trophoblast differentiation
- 1.2.1 Immune system (NLRP7)
- 1.2.2 Overview (KHDC3L) (first paragraph)
- 1.3 Genomic imprinting in recurrent diploid biparental moles (with some updates about recently published articles)

References for all chapters can be found at the end of this thesis.

CONTRIBUTION OF AUTHORS

Chapter 2: Comprehensive genotype–phenotype correlations between *NLRP7* mutations and the balance between embryonic tissue differentiation and trophoblastic proliferation

Ngoc Minh Phuong Nguyen, Li Zhang, Ramesh Reddy, Christine Déry, Jocelyne Arseneau, Annie Cheung, Urvashi Surti, Lori Hoffner, Muhieddine Seoud, Ghazi Zaatari, Rashmi Bagga, Radhika Srinivasan, Philippe Coullin, Asangla Ao, Rima Slim.

NMPN performed DNA preparation and genotyping, p57^{KIP2} screening, and contributed to the writing of the manuscript. LZ, CD and RR contributed to genotyping experiments and NLRP7 mutation screening. JA and AC examined and scored all POCs for histopathological diagnosis. LH and US performed the FISH analysis. MS, RB and PC referred some patients. GZ and RS provided some POC tissues. AA supervised ABI 3130 Analyzer work. RS supervised the work, provided financial support and wrote the manuscript.

Chapter 3: The genetics of recurrent hydatidiform moles: new insights and lessons from a comprehensive analysis of 113 patients

Ngoc Minh Phuong Nguyen, Yassemine Khawajkie, Nawel Mechtouf, Maryam Rezaei, Magali Breguet, Elvira Kurvinen, Sujatha Jagadeesh, Asli Ece Solmaz, Monica Aguinaga, Reda Hemida, Mehmet Ibrahim Harma, Cécile Rittore, Kurosh Rahimi, Jocelyne Arseneau, Karine Hovanes, Ronald Clisham, Tiffanee Lenzi, Bonnie Scurry, Marie-Claude Addor, Rashmi Bagga, Genevieve Girardet Nendaz, Vildana Finci, Gemma Poke, Leslie Grimes, Nerine Gregersen, Kayla York, Pierre-Adrien Bolze, Chirag Patel, Hossein Mozdarani, Jacques Puechberty, Jessica Scotchie, Majid Fardaei, Muge Harma, R.J. McKinlay Gardner, Trilochan Sahoo, Tracy Dudding-Byth, Radhika Srinivasan, Philippe Sauthier, Rima Slim

NMPN screened for *NLRP7* and *KHDC3L* mutations in some patients, analyzed Cytoscan HD microarray, performed qPCR, genotyped some of the HM tissues and contributed to the writing of the manuscript. YK performed genotyping and flow cytometry of some HM tissues. NM recruited patients and performed genotyping of some HM tissues. MR contributed to the identification of the mutation in patient 1566. MB and PS recruited patients from the Réseau des Maladies Trophoblastiques du Québec. EK, SJ, AAS, MA, RH, MH, CR, RC, TL, BS, MA, RB, GN, VF, GP, LG, NG, KY, PB, CP, HM, JP, JS, MF, MH, RG, TB, RS referred patients and HM tissues. KR and JA provided histopathological analyses. KH and TS performed SNP microarray. RS supervised the work, provided financial support and wrote the manuscript.

Chapter 4: Causative Mutations and Mechanism of Androgenetic Hydatidiform Moles

Ngoc Minh Phuong Nguyen, Zhao-Jia Ge, Ramesh Reddy, Somayyeh Fahiminiya, Philippe Sauthier, Rashmi Bagga, Feride Iffet Sahin, Sangeetha Mahadevan, Matthew Osmond, Magali Breguet, Kurosh Rahimi, Louise Lapensee, Karine Hovanes, Radhika Srinivasan, Ignatia B. Van den Veyver, Trilochan Sahoo Asangla Ao, Jacek Majewski, Teruko Taketo, and Rima Slim

NMPN and ZG equally contributed to this manuscript. NMPN performed a substantial part of the human genetics work (*NLRP7* and *KHDC3L* mutation analysis; sample preparation, analysis and validation of the results of whole exome sequencing and targeted sequencing; the genotyping of 2 conception tissues; RNA extraction and RT-PCR on lymphoblastoid cell lines and human oocytes; and she contributed to the writing of the manuscript). ZG performed all the mouse work and contributed to the writing of the manuscript. RR performed part of the human genetics work. SF and MO carried out bioinformatics analyses of WES raw data, JM supervised bioinformatics analyses of WES raw data. PS, RB, FIS, SM, MB, KR, LL, RS, and IBV referred patients and provided clinical data and patient samples. TS and KH performed SNP

microarray on 5 HM. AA provided human oocytes. TT supervised the mouse work and contributed to the writing of the manuscript. RS supervised the study, provided financial support and wrote the manuscript.

CHAPTER 1- LITERATURE REVIEW

In this thesis, I recapitulate my work on the investigation of molecular mechanisms and gene identification for recurrent hydatidiform mole through the use of different molecular techniques and next generation sequencing. This chapter introduces the genetic background of this condition and its key factors, which served as the foundation for the findings described in Chapters 2, 3 and 4.

Key concepts in the introduction:

- Hydatidiform mole is an abnormal human pregnancy; recurrent hydatidiform mole is defined by the occurrence of at least 2 HM in a patient (Gross morphology and histopathological example in Figure 1)
- There are 3 different genotypes observed in hydatidiform mole: diploid androgenetic, triploid dispermic, and diploid biparental (Figure 2)
- Two genes were identified: *NLRP7* and *KHDC3L* in patients with recurrent diploid biparental hydatidiform mole (Figure 2)
- The mechanism for androgenetic hydatidiform mole formation is unknown. Some hypotheses were proposed (Schematic representations in Figure 3, 4, 5). Patients with recurrent androgenetic hydatidiform mole do not carry bi-allelic mutations in the two known genes.
- Known functions of *NLRP7* and *KHDC3L* are recapitulated in Figure 6.

1.1 Hydatidiform mole

1.1.1 Introduction

In his description of the first case of hydatidiform mole (HM) in New England in 1638, Governor Winthrop wrote, “If you consider each of them according to the representation of the whole, they were altogether without form; but if they were considered in respect of the parts of each lump of flesh, then there was a representation of innumerable distinct bodies in the form of a globe” ². The “innumerable distinct bodies in the form of a globe” is the appearance of hydropic chorionic villi observed in these pregnancies (Figure 1.1A). This unfortunate event of pregnancy considered in the past as a “monstrous birth” is now called HM, which derives from the “hydatid” (Greek for a drop of water) and “mola” (Latin for millstone/false conception). In this condition, embryonic development arrests very early, most likely during preimplantation development and the HM tissue is characterized by the absence of, or abnormal, embryonic development and excessive proliferation of the trophoblast. HM can be sporadic, when it occurs once in the patient’s reproductive life, or recurrent (RHM), when it occurs at least two times in the same patient. HM can also occur in more than one family member and such cases are referred to as familial cases.

1.1.2 Epidemiology

The incidence of HM is 1 in 600 to 1000 pregnancies in Western countries ^{3;4} but is 2 to 10 times higher in Asian, African, and Latin American countries, with the highest frequency being 12 in 1000 pregnancies in Southeastern Asia ⁴⁻⁶. The incidence of HM is higher in women at the extremes of reproductive age, slightly higher in women aged 15-20 and dramatically higher in women over 40 ³⁻⁷. Recurrence of a second HM affects 1-9% of women with a prior

HM depending on populations and studies [8-13](#). A study from the United Kingdom found that 1 in 76 women with a HM will develop a second HM, and 13 out of 100 women with 2 prior HM will experience a third HM [7](#).

1.1.3 Classification based on histopathology

At the histopathological level, HM are classified into two types, complete HM (CHM) and partial HM (PHM), based on several features and most importantly the degree of trophoblastic proliferation and embryonic tissue differentiation. CHM usually have marked circumferential trophoblastic proliferation (Figure 1.1B) with absence of embryonic tissues and extraembryonic membranes, while PHM have moderate trophoblastic proliferation and may contain embryonic tissues and extraembryonic membranes.

1.1.4 Sporadic hydatidiform mole

Etiology

The fact that sporadic HM occur only once in the reproductive life of the patients and may follow or precede normal pregnancies suggest that sporadic HM do not have a strong genetic etiology at their origin. To better understand what could underlie their occurrence, epidemiological studies have looked at various risk factors that could predispose to sporadic HM such as maternal age, reproductive history, ethnicity, and various environmental factors including diet, oral contraception, herbicides, and ionizing radiation. Of all these factors, maternal age [3](#), a history of miscarriages [14](#), maternal ethnicity [15](#), and the use of oral contraceptive drugs [16](#) are well-established risk factors for HM that were replicated in several studies and populations. Advanced maternal age is the strongest and most consistent risk factor for all types of HM, mainly sporadic CHM [4](#); [17](#); [18](#)..

Also the risk for HM increases with a history of two or more miscarriages, fertility problems or difficulties in conceptions [8: 19-21](#).

Genotype

There are 2 main genotypic types of sporadic HMs: diploid androgenetic and triploid dispermic HM (Figure 1.2). CHMs are usually diploid androgenetic with two copies of the paternal genome and no maternal genome, and may originate from monospermic (two identical copies of a haploid paternal genome-85%) or dispermic (two different haploid paternal genomes-15%) fertilization [22-24](#). PHMs are mostly triploid dispermic (99%, with 2 exceptions of triploid monospermic) [25](#) with two copies of the paternal genome and one copy of the maternal genome.

1.1.5 Hypotheses about the mechanisms of androgenetic HM formation

Proposed hypotheses

Different hypotheses were suggested to explain the mechanisms of androgenetic HM formation. The two main hypotheses differ by the stage at which the maternal genome is lost before or after fertilization.

1- Loss of maternal chromosomes before fertilization: The androgenetic origin of HM was first reported in 1977 by Kajii *et al.* and an “empty” oocyte mechanism at the origin of androgenetic HM was proposed [26](#). It was suggested that the diploid androgenetic moles derive from the fertilization of an oocyte without nucleus (for simplicity, referred hereafter as empty oocyte) by one or two haploid spermatozoa (Figure 1.3). The hypothesis of empty oocytes was proposed to originate from the exclusion or degeneration of the maternal chromosome sets before fertilization [27](#). However, until now, there was no experimental evidence about the existence of empty oocytes.

2- Loss of maternal chromosomes after fertilization: With the lack of evidence for empty oocytes and the high frequency of triploidy observed in human reproduction failure, Golubovsky proposed another model about postzygotic diploidization of triploid zygotes [28](#). This model postulates post-fertilization errors of triploid zygotes to explain various types of abnormal genotypic patterns observed in human conceptions (Figure 1.4). In this model, the oocyte is nucleated, not empty, and is fertilized by 2 different spermatozoa. Depending on different errors that may occur after fertilization, the zygotes may be maintained as triploid dispermic conceptions (~25% of the cases), or the trippronuclear zygote can undergo abnormal cleavage and result in 1n, 2n, and 3n derivatives. Some of these 2n cells might develop into HM; other embryos may be maintained as mosaic conceptions including androgenetic cells. The postzygotic model can explain cases of mosaicism/chimerism that are observed in some conceptions that include HM [29-31](#). Another example for such cases is a recent report about a mosaicism with high frequency of androgenetic cells in blood and saliva of a 11-year-old deaf girl who was otherwise normal. In this case, 93% of the cells in the blood and 74% of the cells in her saliva are diploid androgenetic, while other tissues have normal bi-allelic ratio [32](#).

Because of the challenges in working with human oocytes and embryos, there are no experimental evidence demonstrating the mechanism of androgenetic HM formation in humans and no one has seen how such a HM develops during the preimplantation cleavage stages.

Androgenesis and its mechanisms in lower organisms

In general, androgenesis is very rare. Its scarcity could be attributed to one of the following reasons: either because androgenesis is hardly identified and thus overlooked in natural populations, or it is difficult to evolve and be maintained once it arises [33](#). Although androgenesis has not been described in any other mammalian species, several examples have

been observed in lower organisms and are summarized below. In lower organisms, androgenesis is classified into three types: obligate androgenesis, spontaneous androgenesis, and artificial androgenesis (reviewed in Pigneur 2012 [34](#)).

1) Obligate androgenesis: All offsprings have androgenetic genotypes and can develop to term. Obligate androgenesis is known in only a few organisms such as the freshwater clam genus *Corbicula*, the conifer tree *Cupressus dupreziana*, and the little fire ant *Wasmannia auropunctata*.

Corbicula leana (freshwater clam)- The zygotes lose their maternal chromosomes after fertilization

Among all obligate androgenetic species, *Corbicula leana* is the most characterized model. In this species, after fertilization, all maternal chromosomes are extruded simultaneously into two polar bodies and lost [35:36](#). In this species, after fertilization and polar body formation, only one condensed male pronucleus is observed in the cytoplasm and the zygote continues to develop. In this model, the abnormal extrusion of all maternal chromosomes in two polar bodies is attributed to the abnormal orientation of spindle axis, which was found to be parallel to the egg surface instead of being perpendicular as observed in various animals [37-39](#) (Figure 1.4)

Cupressus dupreziana (conifer tree)- uncharacterized mechanism:

In this species, the pollens (male gametes) are diploid and the embryos lack alleles from the mother [40-42](#), indicating that the embryos have androgenetic genotype. This raised the question about the existence of the female gametes in the endosperm, which is the nutritious tissues of the seed and derives from the megametophyte that produce eggs. To answer this

question, the authors performed flow cytometry analysis but did not find any evidence of a haploid maternal genome in the endosperm; they found a mixture of multiple ploidies (2C/4C/8C) ⁴⁰. While the flow cytometry analysis was complex, they concluded that the absence of a haploid peak (1C) indicates the lack of the haploid maternal nucleus in the endosperm). In conclusion, in this species, the evidence of androgenesis was shown but the evidence of empty oocyte is weak and not conclusive.

Wasmannia auropunctata (Little fire ant)- uncharacterized mechanism:

The genotypes of the male ants were found to be completely identical to those of the sperm found in queen's spermatheca, the female organ that receives and stores sperms Fournier 2005 ⁴³. Although in this study, it was suggested that the mechanism could be due to the elimination of the maternal genome in the egg, there have been no studies characterizing the mechanism of androgenesis in this species.

2) Spontaneous androgenesis- Androgenetic offspring are produced accidentally at a low frequency during fertilization.

For sporadic androgenesis, the frequency of androgenetic occurrence during fertilization can range from less than 1% to 30% depending on the species (table 1 in Hedtke 2011 ⁴⁴). Most of spontaneous androgenesis in plants arise from interpopulation or interspecific hybridization. It was suggested by Schwander and Oldroyd that spontaneous androgenesis tends to occur in hybrids since the genomic divergence between genomic regions highly reduces the rate of recombination ⁴⁵, and therefore impairs meiosis and leads to higher frequency of non-nucleated eggs ⁴⁶. This hypothesis is supported by the study of Koehler *et al.* ⁴⁷, who showed in mice an increase in aneuploidy in embryos resulting from mating different inbred mouse strains, *Mus musculus* with *Mus spretus*, with estimated sequence divergence of about 1%.

3) Artificial androgenesis- Androgenetic offspring are induced artificially in the laboratory. All embryos die or develop abnormalities from day 6 to day 11 post-implantation.

While development of androgenesis rarely occurs in nature, it can be induced in the laboratory to study the contribution of parental genome or to analyze gene regulation during embryogenesis. One common technique is the nuclear transplantation, which is performed by removing the maternal pronucleus from the zygote and replacing it with another male pronucleus. Using this method, McGrath *et al.* found that 17% of the genetically engineered androgenetic mouse embryos implanted, but all died during the early post-implantation period from day 6 to day 11 ⁴⁸. In another study, Barton *et al.* reported that 23% of the genetically engineered androgenotes (28 embryos) implanted. Among these 28 embryos, 8 of them displayed retarded and abnormal development at gestational day 10 (e.g. no somites or 4-6 somites instead of 25-35 somites), while there were no embryonic remains detected for the remaining 20 implanted embryos ⁴⁹. It is noteworthy that embryonic day 6 to 11 in the mouse is equivalent to the first month in human pregnancy (https://embryology.med.unsw.edu.au/embryology/index.php/Mouse_Timeline). The study from Barton *et al.* also noted the better development of extraembryonic membranes and trophoblast in androgenotes compared with the embryo itself, suggesting that the paternal genome is essential for the development of extraembryonic tissues. Similarly, in humans, androgenetic HM is also characterized by the excessive proliferation of trophoblast. To date, only one paper reported the birth of two androgenetic female mice ⁵⁰. However, such successful deliveries of genetically engineered androgenetic embryos were not reproduced in any subsequent studies.

In conclusion, among published studies on mice, most genetically engineered androgenetic embryos fail to develop after implantation, and the ones that survive implantation have severe abnormalities in the first 11 days of gestation [48](#); [49](#); [51-54](#).

1.2 Genetics of RHM

RHM is defined by the occurrence of at least two molar pregnancies in the same patient. Two genes, *NLRP7* and *KHDC3L*, have been reported to be causative of RHM. RHM from patients with bi-allelic mutations in *NLRP7* or *KHDC3L* are all diploid biparental (Figure 1.2). There are still other patients without mutations in the known genes, and there were only 3 cases reported to have recurrent androgenetic when I started working in this field in 2011 [55](#); [56](#). Furthermore, the genetic characterization of the genotype of RHM has not always been reported, making it difficult to determine the frequency of the different genotypes in patients without mutations in the two known genes. The next section describes the known functions of the two causative genes responsible for recurrent diploid biparental HM, which are also recapitulated in Figure 1.6.

1.2.1 NLRP7

NLRP7 (nucleotide oligomerization domain like receptor), pyrin containing 7, maps to 19q13.4 and is the first identified causative gene for RHMs [57](#). Studies from various groups and populations concur that *NLRP7* is a major gene for this condition and is mutated in 48-80%, of patients with at least two HMs, depending on patients' ascertainment criteria and populations [58-61](#). To date, approximately, 74 different mutations in *NLRP7* have been reported in patients with two defective alleles (<https://infervers.umai-montpellier.fr/web/>). These mutations include missense mutations, stop codons, small deletions or insertions (less than 20-bp), splice mutations, large deletions or insertions, and complex rearrangements mostly mediated by Alu repeats.

NLRP7 transcripts have been identified in several human tissues including endometrium, placenta, hematopoietic cells, oocytes at all stages, and preimplantation embryos. *NLRP7* transcripts decrease after fertilization and during preimplantation development to reach their lowest level at day 3 of embryonic development, which corresponds to the blastocyst stage, and then increase sharply from day 3 to day 5, which coincides with the transcriptional activation of the embryonic genome.

Functional roles of NLRP7

NLRP7 codes for a 1037 amino acids protein (including all coding exons of all splice isoforms) and has three main domains, pyrin, NACHT (i.e., found in the NAIP, CIITA, HET-E and TP1 family proteins) and 10 leucine rich repeats (LRR). *NLRP7* is a member of the NLR family of proteins with role in inflammation and apoptosis. Below, I outline known roles of *NLRP7* in various cellular models and discuss their potential involvement in the pathophysiology of recurrent moles.

Overexpressed NLRP7 downregulates intracellular interleukin-1 beta (IL-1 β)

Data from three different groups about the role of *NLRP7* indicate that its overexpression in transient transfections downregulates the production of IL-1 β , an important mediator of the inflammatory response. The first study by Kinoshita *et al.* demonstrated that overexpressed *NLRP7* interacts with overexpressed pro-IL-1 β and pro-caspase-1 and downregulates caspase-1-dependent IL-1 β secretion in Human Embryonic Kidney 293 cells (HEK293) cells by inhibiting pro-IL-1 β processing [62](#). Another study by Messaed *et al.* *et* confirmed the inhibitory effect of overexpressed *NLRP7* on IL-1 β but showed that *NLRP7* acts primarily on pro-IL-1 β and inhibits its intracellular synthesis [63](#). In addition, this study showed that *NLRP7* inhibitory function is mediated concomitantly by its three domains and mostly by the LRR. Although the precise

mechanism by which NLRP7 downregulates intracellular IL-1 β (pro- or mature) is not fully understood, NLRP7 was shown to interact physically with IL-1 β , caspase-1, and the inflammasome adaptor protein Apoptosis-Associated Speck-Like Protein Containing CARD (ASC), with the latter interaction being mediated by the pyrin domain [62](#); [64](#).

Physiological level of NLRP7 is required for normal IL-1 β secretion in monocytic cells

Using an ex vivo cellular model, Messaed *et al.* also looked at the consequences of *NLRP7* mutations on IL-1 β secretion by peripheral blood mononuclear cells (PBMCs) from patients with *NLRP7* mutations [63](#). The authors showed that patients' cells secrete lower levels of IL-1 β than control cells despite the fact that these same cells have normal or slightly higher amounts of intracellular pro-IL-1 β synthesis indicating NLRP7's role in IL-1 β secretion into the extracellular milieu. These findings are in line with those obtained by Kinoshita *et al.*, in stable transfections of THP-1 cells (of human monocytic origin) where expressing an N-terminal 35-kDa *NLRP7* fragment, which mimics some protein-truncating mutations observed in patients with RHM, reduced IL-1 β secretion. This finding was also confirmed in a third cellular model described by Khare *et al.* who demonstrated that *NLRP7* knockdown using small interfering RNA in macrophages significantly impairs IL-1 β release upon stimulation with microbial acylated lipopeptides [64](#). Within monocytic cells, NLRP7 co-localizes with the Golgi and microtubule-organizing center, and associates with microtubules. This suggests that *NLRP7* mutations may decrease cytokine secretion by affecting, directly or indirectly, the structure of cytoskeletal microtubules and impairing the trafficking of IL-1 β -containing vesicles [63](#). This was further supported by the fact that treating hematopoietic cells with a microtubule depolymerizing agent, nocodazole, fragmented NLRP7's signal [63](#).

An interesting emerging role for NLRP7 in trophoblast differentiation

Another novel and interesting role for NLRP7 was demonstrated by Mahadevan *et al.* In this study, the authors showed that *NLRP7* knockdown in human embryonic stem cells leads to an earlier expression of two trophoblast differentiation markers, GCM1 and INSL4, suggesting that NLRP7 loss-of-function accelerates trophoblast differentiation [65](#). Another interesting finding in this study is that *NLRP7* knockdown increased the level of human chorionic gonadotropin (hCG), known to be very high in patients with molar pregnancies. This new role of NLRP7 is very important in view of the fact that hydatidiform mole is characterized by hyperproliferation of the trophoblast and production of high levels of hCG.

Possible roles of NLRP7 in the pathology of moles

Immune system

The known functions of NLRP7 in inflammatory signalling in hematopoietic cells raise questions as to whether NLRP7's role in IL-1 β production may be the cause of the early embryonic development arrest observed in molar pregnancies. Available data do indicate some connections between IL-1 β , ovulation, and oocyte maturation. For instance, in several mammalian species, intra-follicular injection of IL-1 β increases the rate of ovulation, but decreases the quality of the oocytes and consequently the rate of normal embryonic development [66: 67](#). However, this role for IL-1 β in oocytes is in contradiction with data on cells from patients with *NLRP7* mutations, which secrete lower amounts of IL-1 β . In addition, mice lacking IL-1 β [68](#) or type 1 IL-1 receptor (*Il1r1*) [69](#) are fertile, indicating that the lack of IL-1 β signalling does not significantly affect fertility and embryo viability in mice. Besides its role in IL-1 β secretion, NLRP7 has been shown to promote cellular proliferation and invasion in testicular and endometrial cancer [70: 71](#), respectively.

Expression and localization

In humans, *NLRP7* is expressed in many tissues with the highest level of its transcripts found in testis [62](#); [70](#). However, among individual human cells, the highest level of *NLRP7* transcripts is found in oocytes at the germinal vesicle stage [72](#). *NLRP7* transcripts are also present in different stages of oocyte development and in preimplantation embryos [72](#).

NLRP7 protein localizes mainly to the cortical region in all stages of human oocytes [73](#). After the first zygotic division, *NLRP7* localization becomes restricted to the outer cortical region and is absent from the cell-to-cell contact region, which is identical to the localisation of other proteins of the subcortical maternal complex (SCMC) [74](#).

NLRP7 and early embryonic development

Despite the fact that in vitro fertilization was introduced into medical practice 40 years ago, it is not known how a conception that leads to a HM develops during the preimplantation stages. The first description of how HM develops was reported by Edwards in 1990 and 1992 [75](#); [76](#) in a patient with RHM and this was followed by two other case reports [77](#); [78](#). Unfortunately, however, the causative genes responsible for RHM in these three patients are not known and nor are the genotypes of their moles known. Recently, Sills *et al.* reported a patient with 5 RHMs and bi-allelic *NLRP7* mutations, recorded the early development of her embryos after intra-cytoplasmic sperm injection, and provided photographs of two embryos [79](#). In this patient, 15 oocytes were retrieved and 10 were fertilized. All embryos had diploid biparental genome, which is in line with the diploid biparental genomes of HM from patients with bi-allelic *NLRP7* mutations. Of the 10 fertilized oocytes, none were morphologically normal and suitable for transfer to the patient. This case is the first detailed account of how a molar pregnancy develops during preimplantation development and suggests that abnormalities in the conceptions of these patients start very early

during preimplantation development. In addition, this case tells us that what leads to HM is perhaps not a healthy, normal growing early cleavage embryo.

1.2.2 KHDC3L

Overview

KHDC3L (KH domain containing 3 like) is a second recessive gene responsible for RHMs and was identified in 2011 [80](#). *KHDC3L* maps to chromosome 6 and available data indicate that this gene is a minor gene for RHMs accounting for 10 to 14% of patients who do not have mutations in *NLRP7*. To date, six mutations in *KHDC3L* have been reported in patients with two defective alleles [80-82](#). *KHDC3L* transcripts have been identified in several human tissues including all oocytes stages, preimplantation embryos, and hematopoietic cells. *KHDC3L* codes for a small protein of 217 amino acids that belongs to the KHDC1 (KH homology domain containing 1) protein family, members of which contain an atypical KH domain that does not bind RNA as opposed to proteins with canonical KH domain. In humans, this family includes KHDC3L, KHDC1, DPPA5 (Developmental Pluripotency Associated 5), and OOEP (oocyte expressed protein) [83](#). Expression of *KHDC3L* is highest in human oocytes at the germinal vesicle (GV) stage then decreases during preimplantation development and become undetectable at the blastocyst stage [80](#), similar to the expression profile of *NLRP7* [72](#).

Mice knockdown for *Khdc3*, the orthologue of human *KHDC3L*, have reduced fecundity and impaired preimplantation embryo development with a high incidence of aneuploidy due to abnormal spindle assembly, chromosome misalignment, and spindle assembly checkpoint inactivation [84](#). Abnormalities of spindle morphology in the embryos were observed in *Khdc3* null mice such as 1-polar, 3-polar, broad polar and irregularly shaped spindles. Also, a high incidence of chromosome misalignments was observed in the embryos. Some morula- and

blastocyst-like structures contained fewer cells than normal (e.g. some E.4.5 blastocysts contain about 15 cells compared with those control blastocysts with more than 36 cells).

Also, *KHDC3L* knockdown in human GV oocytes increases the rate of abnormal spindles in MII oocytes and decreases the fertilization and embryo cleavage rates [85](#). In addition, this downregulation also leads to a significantly lower number of oocytes that can be fertilized and reach the 2-cell stage.

***KHDC3L* and the Subcortical Maternal Complex (SCMC)**

The SCMC is a multi-protein complex expressed only in oocytes and preimplantation embryos at the subcortical region. Recessive mutations in genes coding for the SCMC proteins lead to defective oocytes and consequently early embryonic arrest during preimplantation stages [74](#); [84](#); [86](#); [87](#). In mice, four members of the SCMC were identified (NLRP5, OOEP, TLE6 and KHDC3) [74](#). NLRP5, OOEP, and TLE6 were shown to interact directly with each other while KHDC3, the mouse orthologue of human KHDC3L, interacts in oocytes only with NLRP5. Genetic ablation of *Ooep* or *Nlrp5* in mice results in the destabilization of the SCMC and the diffuse localization of its proteins in the cytoplasm. Other maternal-effect genes such as *Padi6*, *Nlrp2*, *Zbed3* were also suggested to be part of the mouse SCMC [88-90](#).

In humans, four members of the SCMC (*KHDC3L*, *OOEP*, *NLRP5*, and *TLE6*) were shown to interact in transfected cells. *KHDC3L* and other SCMC components localize in the subcortex of early human embryos. Of these, mutations in *KHDC3L* and *TLE6* play causal roles in recurrent diploid biparental HM and female infertility, respectively [80](#); [91](#). In addition, another maternal-effect gene suggested to participate in the SCMC in mice, *PADI6*, was shown to be responsible for female infertility [92](#); [93](#) and recently for recurrent miscarriages and a HM in one of our patients [94](#).

1.3 Genomic imprinting in recurrent diploid biparental moles

1.3.1 Altered DNA methylation at imprinted genes in the conceptions of patients with *KHDC3L* or *NLRP7* mutations

Genomic imprinting refers to epigenetic modifications such as DNA methylation, histone modification or/and chromatin remodeling that lead to the expression of only one of the two parental copies of a gene. The involvement of genomic imprinting in the pathology of hydatidiform moles emerged soon after the demonstration that sporadic complete moles are androgenetic, which made them an important experimental tool in characterizing the expression and/or methylation of imprinted genes [95-97](#). Later, the identification of recurrent familial moles that have the same histopathological features as the sporadic androgenetic moles [98](#) and the finding that such moles are diploid biparental [99](#) entertained the plausible and interesting idea that the causative gene for recurrent moles would be responsible for setting or maintaining the maternal imprints in the oocytes.

To date, six studies have investigated the DNA methylation in diploid biparental HM from patients with bi-allelic mutations in *NLRP7* or *KHDC3L* and revealed a general trend of lack of DNA maternal methylation marks on imprinted genes [60: 100-104](#). The first study demonstrated in one diploid biparental CHM, from a patient with two *KHDC3L* defective alleles, the loss of methylation marks at six out of seven analyzed differentially methylated regions (DMR) that are normally maternally methylated and the gain of methylation marks on one paternally methylated DMR (*NESP55*) that acquires its methylation at the blastocyst stage (Table 1.1). In contrast, the methylation at the H19 DMR, which is normally established in the male germ line, was normal. Two additional diploid biparental moles from the same patient were later studied, but unfortunately at different DMRs, and their analysis showed the same trend of abnormal methylation with the

exception of one gene, *PEG10*, which preserved its normal methylation on the maternal allele (Table 1.1). Other studies also examined the methylation status of DMRs in moles from patients with two *NLRP7* defective alleles and reported abnormal loss and gain of methylation at some of them [60](#); [101](#); [103](#); [104](#). In one of these studies, single nucleotide polymorphisms were used to distinguish parental alleles at some imprinted genes and showed that the abnormal methylation indeed affected the maternal alleles [101](#) (Table 1.1). Sanchez-Delgado *et al.* examined at the whole genome level the methylation profiles of diploid biparental HMs from patients with bi-allelic mutations in *NLRP7*. They also demonstrated a lack of maternal methylation at several additional imprinted DMRs, including *NAPIL5* and *L3MBTL*, which normally acquire methylation in the female germline. However, paternally methylated DMR, which acquire methylation in the male germ line (*H19*, *IG*, *MEG3*) or during early development (*ZNP597*, *ZBDF2*), were found to have normal methylation pattern. Methylation analysis on *LINE-1* sequences, α -satellites and Alu-Yb8 sequences in these HMs revealed a normal DNA methylation profile. These data suggest that only maternally derived methylation is affected in diploid biparental HM. In addition, the study also showed subtle differences in the methylation profiles between HMs from the same patient or from two sisters carrying the same mutation, suggesting inter-RHM variation. It would have been interesting if the authors correlated the methylation profiles of such HMs with their histopathological features to see if the differences in methylation patterns are associated with their histopathological features (e.g. severe form as complete HM versus milder form as partial HM).

In conclusion, these studies consistently demonstrated the lack of DNA methylation marks on maternally methylated regions of imprinted genes, most likely due to defects in the female germline before the acquisition of the methylation marks. This abnormal DNA methylation pattern can also extend to yet uncharacterized imprinted genes that are responsible for regulating cellular

proliferation and differentiation, two features characterizing the morphology of HM as trophoblastic proliferation and absent/abnormal embryonic development.

1.3.2 Altered DNA methylation beyond non-imprinted genes

To investigate the role of *NLRP7* in establishing methylation marks at imprinted genes, recently, Mahadevan *et al.* examined the consequences of *NLRP7* knockdown on the DNA methylation of imprinted genes during the differentiation of human embryonic stem cells (hESCs) into trophoblast cells [65](#). However, they did not observe any DNA methylation changes at imprinted DMRs including those that were previously shown to be abnormally methylated in diploid biparental molar tissues. They explained their findings by the known high degree of epigenetic stability and resistance of hESC lines to perturbations in DNA methylation at imprinted loci [105](#). Instead, they found that *NLRP7* knockdown altered the DNA methylation of many non-imprinted CpGs. Another recent study showed that the DNA methylation of a total 131 imprinted and non-imprinted loci are altered in blood DNA of an individual with multiple anomalies born to a mother with a single heterozygous *NLRP7* mutation (A719V) [106](#). It would have been important in this study to determine if the mutation in the mother occurred de novo or if it was inherited, and from which of her parents. In addition, it is not clear whether the abnormal child inherited his mother's mutation. Surprisingly, comparing the abnormally methylated genes from the studies by Mahadevan *et al.* and Beygo *et al.* [65](#); [106](#) did not reveal any common gene with altered methylation, which raises questions about the specificity and significance of these findings and their relation to *NLRP7* mutations that remain to be clarified in future studies.

1.3.3 Altered expression of *CDKN1C* in the conceptions of patients with *NLRP7* mutations

In line with the above data, one study demonstrated the underexpression of p57^{KIP2}, the product of the paternally imprinted, maternally expressed gene, *CDKN1C*, in the cytotrophoblast and villous stroma of a series of diploid biparental CHMs [107](#). p57^{KIP2} is the protein coded by a cyclin-dependent kinase inhibitor. *Cdkn1c* deficiency in mice leads to altered cellular proliferation and differentiation resulting in a variety of developmental defects [108](#). Although *CDKN1C* is paternally methylated in the cytotrophoblast and villous stroma of normal first trimester placenta, its expression has been shown to depend on the maternal methylation of *KvDMRI*, a CpG island located at the promoter of *KCNQ1OT1* and believed to control the imprinted expression of *Cdkn1c* during embryonic development [109](#); [110](#). The same is observed in humans, where the loss of maternal methylation marks at *KvDMRI* leads to the silencing of *CDKN1C* in patients with Beckwith-Wiedemann Syndromes [111](#), a pediatric overgrowth disorder in which the placenta share some histopathological features with PHMs.

Despite the complexity of the methylation and imprinting data and the variations between studies and samples, the common findings are the lack of DNA maternal methylation marks at several, maternally imprinted, paternally expressed genes and the unspecific/stochastic extension of methylation abnormalities to non-imprinted genes.

1.4 Ovum donation is recommended for patients with RHM

An unfortunate consequence of the genetic abnormalities in RHM is that most patients cannot have normal pregnancies. To date, there are only 5 patients with RHM reported to have had spontaneous conceptions leading to live births [57](#); [112](#); [113](#). There are no treatments for patients with mutations in these two known genes to achieve normal pregnancies. Ovum donation was

suggested to be an option for such patients. Until now, there are 3 patients with bi-allelic *NLRP7* mutations reported to have live births from donated oocytes [113](#):[114](#), suggesting that ovum donation from healthy women remedies the defects of patients with recessive mutations in *NLRP7* (and the same can be applied to patients with mutations in *KHDC3L*).

1.5 Rationale and objectives

Patients with recurrent hydatidiform moles suffer severe emotional distress when their pregnancies arrest in the first trimester, which inevitably brings down their hopes of ever conceiving a healthy baby. Characterization of the mechanisms leading to RHM formation and identification of new genes responsible for this condition are the two main objectives of this thesis:

Objective 1-Comprehensively characterize RHM of patients with *NLRP7* recessive mutations (Chapter 2)

When I started in the lab in September 2011 (as a MSc student before fast-tracking to the PhD program), some studies documented the genotypes of RHM from patients with recessive *NLRP7* mutations, but only with one method [56](#); [58](#); [60](#); [103](#); [115-120](#). At that time, it was not clear to us whether all RHM from these patients are diploid biparental. In addition, mosaicism in HM was also reported [29-31](#). We intended to characterize the HM of these patients using different methods and determine if they are all diploid biparental and to investigate the presence of aneuploidy in these tissues. Extensively characterizing these tissues allowed us to understand the pathogenesis of RHM and correlate the nature of *NLRP7* mutations with the different features of the moles. This work allowed us to determine if RHM caused by defects in the same gene have the same genotype. The results of this analysis are presented in **Chapter 2**.

Objective 2- Identification of causative genes for RHM (Chapter 3 and 4)

The primary objective of my PhD work was to identify novel genes underlying the etiology of RHM in patients without bi-allelic mutations in *NLRP7* and *KHDC3L*. Patients were screened for *NLRP7* and *KHDC3L* mutations before selecting them for whole exome sequencing (WES),

followed by targeted sequencing of candidate genes on a larger cohort of patients with milder defects. During this process, we realized that this condition is highly heterogeneous since we were not able to identify mutations in the same gene in two patients. Therefore, in parallel with the WES work, we decided to comprehensively characterize all available HM tissues of these patients at the histopathological and genotypic levels. This work allowed us to re-evaluate the diagnosis of their HM tissues, remove patients who were misdiagnosed with RHM, and classify the remaining patients according to the genotypes of their RHM, as well as understand the differences between HMs from patients with and without mutations in the known genes. The results of this objective are presented in **Chapter 3**.

With the data obtained from chapter 3, we enriched for patients with the same genotype of RHM as those with mutations in the candidate genes and performed WES on additional patients. This work led to the identification of three novel genes for androgenetic RHM and the characterization of the genesis of androgenesis in a mouse model. The results of this objective are presented in **Chapter 4**.

1.6. Figures and Table

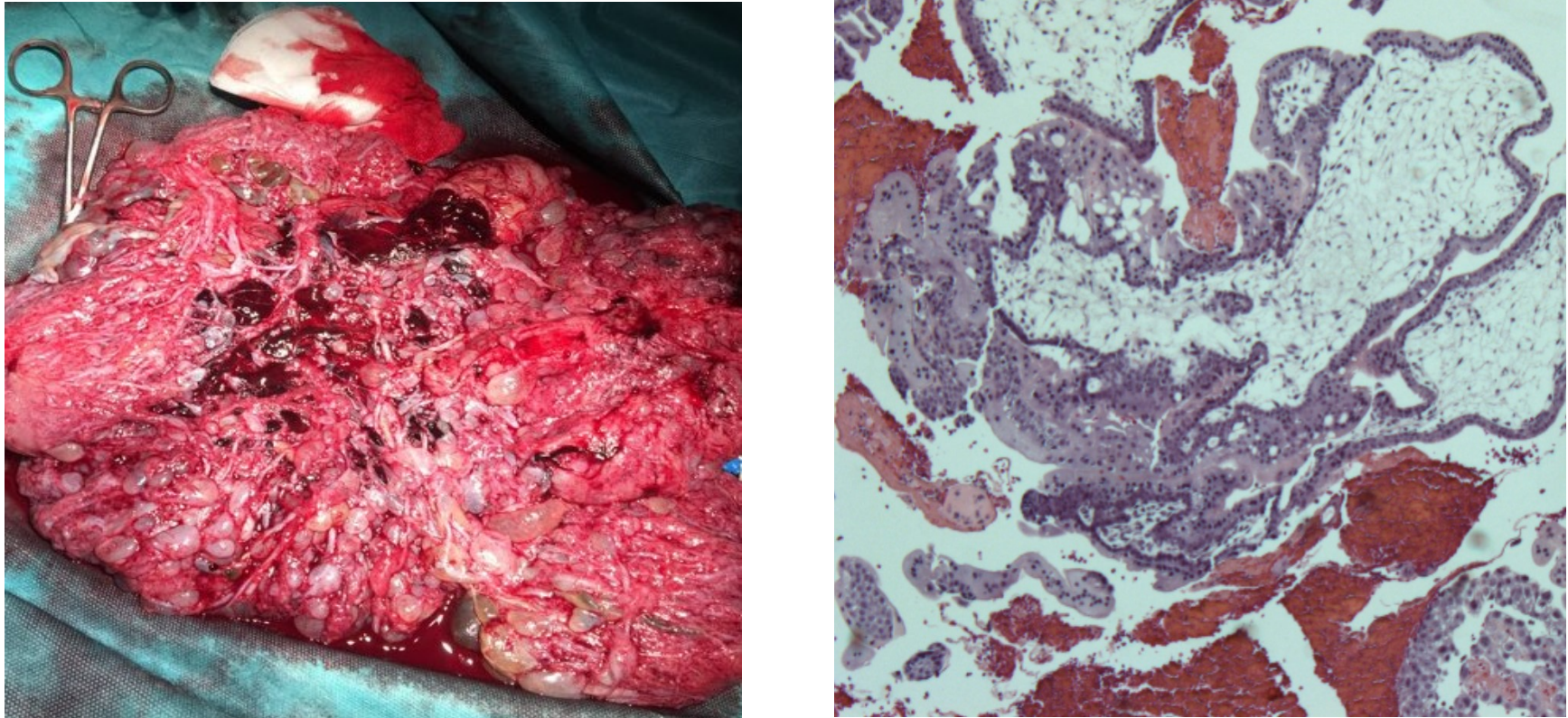


Figure 1.1. Gross morphology and histopathological section of HM. a) Gross morphology of a hydatidiform mole (HM). (b) Histopathological cross-section of an HM showing circumferential trophoblastic proliferation (arrows) around a chorionic villous (CV) (Figure 27.1 from Textbook of Autoinflammation (in press). The gross morphology photo is a courtesy of Drs. Pierre-Adrien Bolze and Jerome Massardier, French Reference Center for Trophoblastic Diseases, Lyon, France)

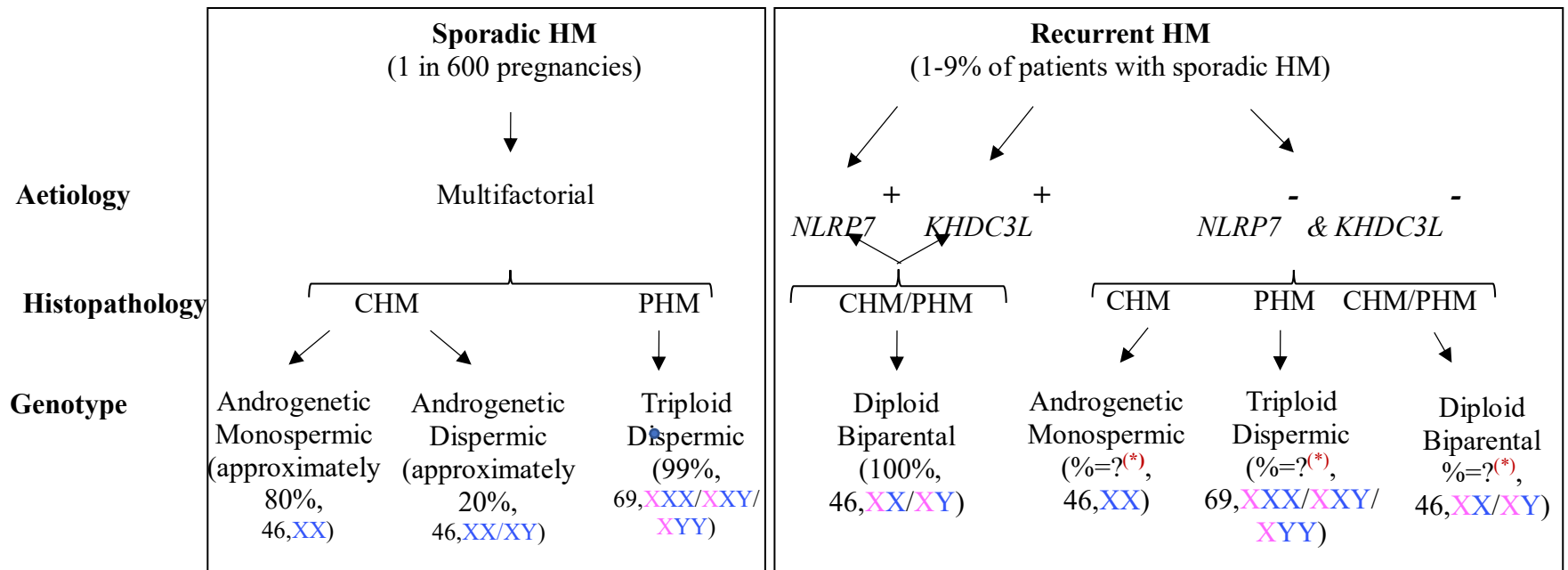


Figure 1.2. Frequencies and classification of sporadic and recurrent HMs by aetiology, histopathology, and genotype. The pink and blue colors refer to the presence of the maternal and paternal genomes, respectively, in the HM.

(*), indicates that the frequencies of these genotypes will be answered in chapter 3; CHM, stands for complete hydatidiform mole; PHM, partial hydatidiform mole; POC, product of conception.

(Adapted from Figure 27.2 from Textbook of Autoinflammation (in press))

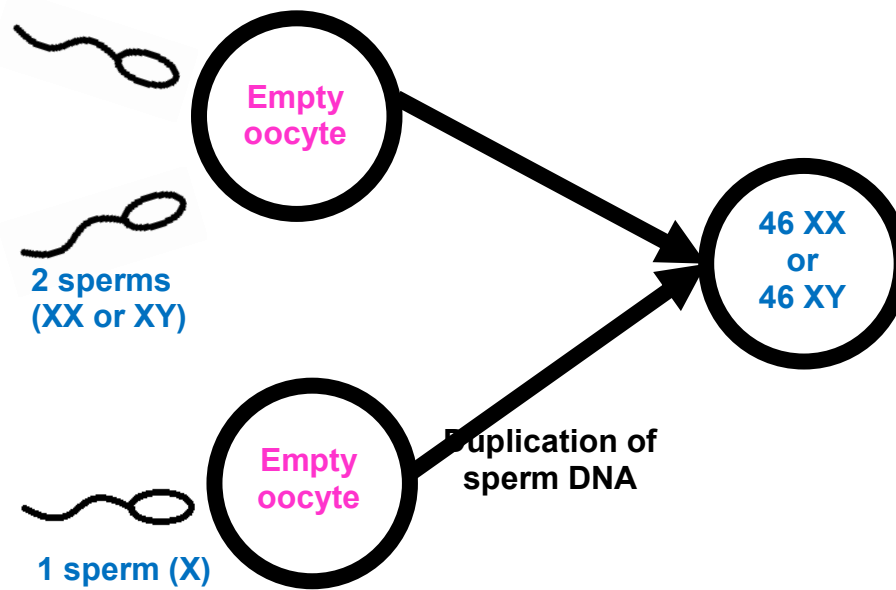


Figure 1.3. Schematic representation of the “empty” oocyte mechanism proposed by Kajii 1977. Maternal chromosomes were suggested to be degenerated or excluded before fertilization. The oocyte is fertilized by either 2 sperms or 1 sperm (which followed by the endoreduplication of the paternal pronucleus), resulting in diploid androgenetic dispermic or monospermic, respectively.

Figure 1.4. Proposed mechanism of postzygotic diploidization of triploids at the origin of HM formation.

Triploid zygote which contains three pronuclei, M (maternal pronucleus), P1 (paternal nucleus1), P2 (paternal nucleus 2) may undergo abnormal cleavage resulting in the 1n, 2n, 3n derivatives. In the first scenario, the zygote can maintain the triploid state and produce a triploid dispermic mole (MP1P2). In the second scenario, abnormal first division of the triploid zygote can result in the mosaic moles with 3n triploid dispermic and 2n biparental derivative or 2n androgenetic derivative. In the third scenario, the maternal pronucleus can be eliminated and a 2n androgenetic derivative can be formed. The division error may also result in the mosaic diploid biparental derivatives. In the fourth scenario, the abnormal first zygotic division results in a 2n diploid biparental derivative and a 1n derivative that undergoes endoreduplication (diploidization), leading to a diploid homozygous androgenetic HM. In the last scenario, a tripolar spindle is formed at the first cleavage division, resulting in abnormalities in chromosome distribution such as trisomy or uniparental disomy (2 copies of the same chromosome coming from the same parent). Androgenetic HM formation is indicated by a red square.

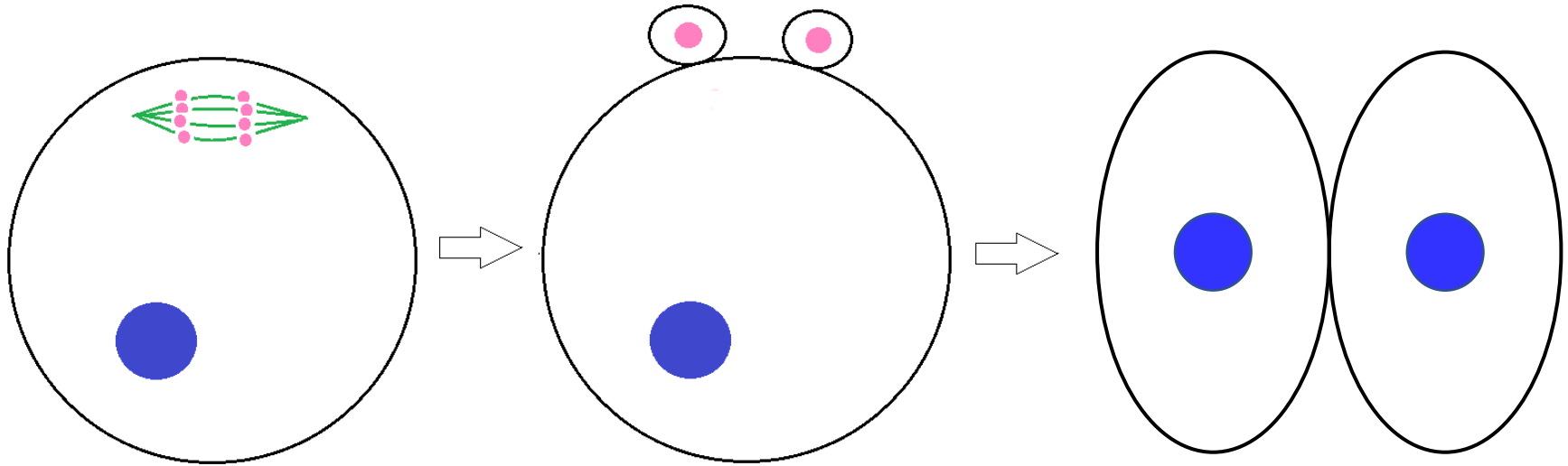


Figure 1.5. Schematic representation of the formation of androgenetic zygote in *Corbicula* species after fertilization. The male pronucleus is indicated in blue. The maternal chromosomes are in pink. The maternal chromosome segregate and are extruded into the two polar bodies. The first cleavage of the zygote continues with only paternal chromosomes.

**Abnormalities in HM from patients with mutations in
NLRP7/*KHDC3L***

***NLRP7* in Immune system**

- *NLRP7* knockdown in macrophages impairs IL-1 β release.
- Patients with *NLRP7* variants secrete low level of IL-1 β secretion.
- *NLRP7* interacts physically with IL-1 β , caspase-1, and ASC in HEK293 cells.

- Abnormal DNA methylation at imprinted genes in HM tissues.
- Silenced expression of p57^{KIP2} in HM tissues.

KHDC3L

- A component of the SCMC.
- *KHDC3L* knockdown in human GV oocytes \uparrow the rate of abnormal spindles in MII oocytes and \downarrow the fertilization and embryo cleavage rates.
- *Khdc3*-null mice have reduced fecundity and impaired preimplantation embryo development.

***NLRP7* knockdown in hES cells**

- Earlier expression of 2 trophoblast differentiation markers GCM1 and ISNL4 \rightarrow accelerate trophoblast differentiation.
- Increases hCG level.



ART outcome and management

- IVF data: all fertilized oocytes develop abnormalities and cannot be transferred.
- Ovum donation is recommended: 3 successful cases reported

Figure 1.6. Known functions of the two genes *NLRP7* and *KHDC3L*. hES cells, stands for human embryonic stem cells. SCMC, for subcortical maternal complex. IVF, for *in vitro fertilization*.

Table 1.1. Recapitulation of methylation analysis data in diploid biparental molar tissues from patients with *NLRP7* or *KHDC3L* mutations (From Table 2, Nguyen *et al.* 2014) ¹

DMR	Chr	<i>KHDC3L</i>		<i>NLRP7</i>			Conclusion
Patient ID		L1	L1	4 & 6	HM70 & HM73	S4	
Number of HMs (n)		n=1	n=2	n=2	n=2	n=1	
Maternal methylated							
<i>KCNQ1OT1a</i>	11	---	---		---	---	---
<i>SNRPNb</i>	15	---		-,---	---		---
<i>PEG1</i>	7	---					---
<i>PEG3</i>	19	---		---	---		---
<i>GNAS-1A a</i>	20	---			---		---
<i>GNAS-AS</i>	20	---			Complex		Inconcl.
<i>GNAS-XLαS b</i>	20	Normal			Normal		Normal
<i>ZACa</i>	6		---			---	---
<i>PEG10 a</i>	7		Normal, --			Normal	Normal
Paternally methylated							
<i>H19 a</i>	11	Normal		+, ++	Normal		Inconcl.
<i>GNAS-NESP55b</i>	20	+++	+++	+++	+++ c	+++	+++

Chr, chromosome; ^a primary imprint; ^b secondary imprint ; ^c gain of methylation at this locus was found in the two diploid biparental moles as well as in one normal term placenta and in one androgenetic mole; Inconcl., inconclusive. Different results on two HM tissues are separated by a comma

PREFACE TO CHAPTER 2

The work in Chapter 2 addresses the question about the genetic mechanism of RHM from patients with bi-allelic mutations in *NLRP7*. While several RHM from such patients were found to be diploid biparental, it was not known if other genotypic types of HM occur in such patients. In addition, data on characterized RHM were generated using only one or two methods and were before the publication of Golubovsky's model proposing that postzygotic abnormalities could be at origin of several genotypic types of HM. Postzygotic abnormalities are very complex and require a combination of several approaches to be detected, especially when working with formalin-fixed paraffin-embedded tissues, in which DNA is degraded and may consequently compromise the quality of DNA genotyping. Therefore, we decided to use four different approaches to investigate the presence of aneuploidies or mosaicisms in these diploid RHM and comprehensively characterized the parental contribution to 36 products of conception (POC) from patients with bi-allelic *NLRP7* mutations.

CHAPTER 2

Comprehensive genotype-phenotype correlations between *NLRP7* mutations and the balance between embryonic tissue differentiation and trophoblastic proliferation

Ngoc Minh Phuong Nguyen^{1,2}, Li Zhang², Ramesh Reddy^{1,2}, Christine Déry^{1,2}, Jocelyne Arseneau³, Annie Cheung⁴, Urvashi Surti⁵, Lori Hoffner⁵, Muhieddine Seoud⁶, Ghazi Zaatari⁷, Rashmi Bagga⁸, Radhika Srinivasan⁹, Philippe Coullin¹⁰, Asangla Ao^{1,2}, Rima Slim^{1,2*}.

¹Departments of Human Genetics and ²Obstetrics and Gynecology, ³Department of Pathology, McGill University Health Centre, Montreal, Quebec, Canada,

⁴Department of Pathology, University of Hong Kong, Queen Mary Hospital, Hong Kong, China

⁵University of Pittsburgh, Department of Pathology, Magee-Women's Hospital, Pittsburgh, Pennsylvania, USA,

⁶ Department of Obstetrics and Gynecology, American University of Beirut, P.O Box 1 1-236, Beirut, Lebanon,

⁷ Department of Pathology, American University of Beirut, P.O Box 1 1-236, Beirut, Lebanon

⁸ Department of Obstetrics & Gynecology, ⁹ Cytology & Gynecological Pathology, Post Graduate Institute of Medical Education and Research, PGIMER, Chandigarh, India

¹⁰ INSERM U 782, Endocrinologie et Génétique de la Reproduction et du Développement, 32 rue des carnets, F 92140 Clamart, France.

Manuscript published in **Journal of Medical Genetics**, September 2014

(PMID: 25097207)

Abstract

Background: Hydatidiform mole (HM) is a human pregnancy with excessive trophoblastic proliferation and abnormal embryonic development that may be sporadic or recurrent. In the sporadic form, the HM phenotype is driven by an abnormal ratio of paternal to maternal genomes while in the recurrent form, the HM phenotype is caused by maternal-recessive mutations, mostly in *NLRP7*, despite the diploid biparental origin of the HM tissues. In this study, we characterized the expression of the imprinted, maternally expressed gene, *CDKN1C* ($p57^{KIP2}$), the genotype, and the histopathology of 36 products of conception (POCs) from patients with two defective alleles in *NLRP7* and looked for potential correlations between the nature of the mutations in the patients and the various HM features.

Methods/results We found that all the 36 POCs are diploid biparental and have the same parental contribution to their genomes. However, some of them expressed variable levels of $p57^{KIP2}$ and this expression was strongly associated with the presence of embryonic tissues of inner cell mass origin and mild trophoblastic proliferation, which are features of triploid PHMs, and were associated with missense mutations. Negative $p57^{KIP2}$ expression was associated with the absence of embryonic tissues and excessive trophoblastic proliferation, which are features of androgenetic complete HMs and were associated with protein-truncating mutations.

Conclusions Our data suggest that *NLRP7*, depending on the severity of its mutations, regulates the imprinted expression of $p57^{KIP2}$ and consequently the balance between tissue differentiation and proliferation during early human development. This role is novel and could not have been revealed by any other approach on somatic cells.

Introduction

Hydatidiform mole (HM) is an abnormal human pregnancy characterized by the absence of, or abnormal, embryonic development, excessive trophoblastic proliferation, and hydropic degeneration of chorionic villi. Common moles are usually sporadic, not recurrent, and affect 1 in 600 pregnancies in western countries [3](#) but have higher frequencies in developing countries [4](#); [5](#). Based on histopathological examination, HMs are divided into two categories, complete HMs (CHMs) and partial HMs (PHMs). CHMs display circumferential trophoblastic proliferation and do not contain extraembryonic membranes (chorion and amnion), fetal nucleated red blood cells (NRBC), or any other embryonic tissue of inner cell mass origin. PHMs have moderate focal trophoblastic proliferation and may contain extraembryonic membranes and/or embryonic tissues of inner cell mass origin.

Common sporadic CHMs are mostly diploid androgenetic with two copies of the paternal genome. Common sporadic PHMs are mostly triploid dispermic with two different copies of the paternal genome and one copy of the maternal genome. $p57^{KIP2}$ is the product of the paternally imprinted, maternally expressed gene, *CDKN1C*, which is expressed in the nuclei of cytotrophoblast and some stromal cells of triploid dispermic PHMs, but not in those of diploid androgenetic CHMs [121](#). Consequently, $p57^{KIP2}$ immunohistochemistry is an ancillary marker that is commonly used by pathologists to indirectly identify the presence of the maternal genome and help them in dividing HMs into PHMs and CHMs, which may share some histopathological features, when evacuated at early gestational stages [122](#). This differential expression of $p57^{KIP2}$ is believed to be due to the absence of the maternal genome in androgenetic CHMs. However, even in androgenetic CHMs, $p57^{KIP2}$ is expressed in the nuclei of extravillous trophoblast cells, which indicates that $p57^{KIP2}$ imprinting is not maintained on paternal alleles in all trophoblastic cells.

Consequently, the exact mechanism underlying the imprinted expression of p57^{KIP2} only in some cellular types of first trimester placenta is not known [123](#); [124](#). Ki-67 is a nuclear protein coded by *MKI67* (antigen identified by monoclonal antibody Ki-67) and a proliferation marker known to be expressed in all active phases of the cell cycle (G1, S, G2, and mitosis), but not in resting G₀ cells [125](#). Ki-67 is expressed in normal first trimester human placenta; however, its expression level is higher in sporadic HMs. Among these, triploid PHMs express lower Ki-67 levels than androgenetic CHMs [126](#); [127](#), which reflects their milder trophoblastic proliferation. Recurrent hydatidiform moles occur in 1-6% of patients with a prior mole [8](#); [10-13](#); [128](#); [129](#) and may occur in patients with no family history of HMs (singleton cases) or in related women from the same family (familial cases). By studying familial cases of recurrent HMs, two maternal effect genes, *NLRP7* and *KHDC3L*, responsible for recurrent HMs have been identified [57](#); [80](#). *NLRP7* is a major gene for recurrent HMs and is mutated in 48-80% of patients, depending on patients' ascertainment criteria and populations [58-60](#); [130](#). *KHDC3L* is a minor gene for recurrent HMs and is mutated in only 10-14% of patients with no *NLRP7* mutations [80](#); [81](#); [130](#). To date, approximately 47 different mutations have been reported in patients with two *NLRP7*-defective alleles (<http://fmf.igh.cnrs.fr/ISSAID/infervers/>). The role of *NLRP7* protein in the pathophysiology of moles is not fully understood, but we do know that *NLRP7* down regulates intracellular inflammation and impairs IL-1 β secretion in various cellular models [62-64](#) including peripheral blood mononuclear cells from patients with two *NLRP7*-defective alleles [63](#). Recently, a study by Mahadevan *et al.* demonstrated that *NLRP7* knockdown in human embryonic stem cells accelerates trophoblast differentiation [131](#).

At the genotypic level, the parental contribution to approximately 80 HMs from patients with two *NLRP7*-defective alleles have been analyzed so far and were found all diploid biparental

[56](#); [58](#); [60](#); [115-120](#); [130](#); [132-135](#) with the exception of two moles that were found to be triploid digynic [130](#) and triploid diandric [134](#). Despite their diploid biparental genome, HMs from patients with *NLRP7* or *KHDC3L* mutations lack maternal methylation marks on several imprinted, paternally expressed genes and display gain of methylation marks on some imprinted, maternally expressed genes [60](#); [100](#); [101](#); [103](#). Recently, altered DNA methylation in cells with *NLRP7* mutations or knockdown has been shown to extend beyond imprinted genes and affect many non-imprinted genes [106](#); [131](#); [136](#). Using immunohistochemistry, four studies have investigated the imprinted expression of p57^{KIP2} in diploid biparental CHMs from patients with two *NLRP7*-defective alleles. These studies demonstrated the absence of p57^{KIP2} expression in the cytotrophoblast and villous stroma of these diploid biparental moles similar to the absence of p57^{KIP2} expression in androgenetic CHMs [107](#); [130](#); [133](#); [135](#). To date, no studies have investigated Ki-67 expression in diploid biparental moles caused by *NLRP7* mutations.

To better understand the role of *NLRP7* mutations in HMs, we first characterized p57^{KIP2} expression in 36 products of conception (POCs), mostly HMs, from patients with two *NLRP7* defective alleles. We found that some of them express variable levels of p57^{KIP2} in the cytotrophoblast and villous stroma, which was in contradiction with previously reported data in the field and suggested either the presence of aneuploidies, genotypic mosaicisms or incomplete inactivation of p57^{KIP2}. We next used three DNA-based approaches to comprehensively characterize these tissues and demonstrated their diploid biparental genome. We looked for potential correlation between p57^{KIP2} expression, the nature of mutations, Ki-67 expression, and morphological features of the HMs. We found that some missense mutations do not completely repress p57^{KIP2} expression and are associated with the presence of embryonic tissues of inner cell mass origin, mild trophoblastic proliferation, and low expression of Ki-67. However, protein-

truncating mutations repress p57^{KIP2} expression, and are associated with the absence of embryonic tissues of inner cell mass origin, and the presence of excessive trophoblastic proliferation.

Materials and methods

Patients and mutation analysis

A total of 36 POCs from 17 patients were included in this study. Patients were referred to our laboratory from various national and international collaborators for DNA testing. All the patients have been screened for *NLRP7* mutations as previously described [57](#) and the results of their mutation analysis were either previously reported [57](#); [59](#); [115](#); [120](#); [137](#) or generated during this study and are described in the “Results” section and Supplementary Table 2.1.

Histopathological characterization of the POCs

Morphological examination

For morphological examination and diagnosis, sections from the POCs were stained with H&E, examined, and scored independently by two pathologists for the degree of trophoblastic proliferation, the degree of hydropic changes, and the presence of extra-embryonic membranes, NRBC, and/or other embryonic tissues according to previously reported guidelines [138](#). The two pathologists were blinded to the data generated by the other methods and we deliberately did not change the histopathological diagnosis based on the results of the other methods because our aim is to look for correlations between the parental contribution to the POC genomes, the histopathological features, and the mutations in the patients. The number of available blocks and/or slides from each POC is provided in Supplementary Table 2.1.

p57^{KIP2} immunohistochemistry

p57^{KIP2} immunohistochemistry were performed on 4- μ m sections from formalin-fixed paraffin-embedded tissues as previously described [122](#). For all cases of p57^{KIP2} immunohistochemistry, the presence or absence of nuclear staining was assessed in cells from the cytotrophoblast, villous stroma, extravillous trophoblast and maternal decidua, independent of histopathological and genotyping data. p57^{KIP2} was considered “conclusive” when maternal decidua or/and extravillous trophoblastic cells, serving as internal positive control, exhibited nuclear expression of p57^{KIP2} in several areas of the analyzed slides. Cases were considered “inconclusive” when maternal decidua and/or extravillous trophoblastic cells did not express p57^{KIP2} or when the staining of p57^{KIP2} was not nuclear due to non-optimal quality of tissue preparation or immunohistochemistry.

Ki-67 immunohistochemistry

Ki-67 expression level was evaluated by scoring the percentage of positive cells in the cytotrophoblast in 10 different fields. Immunohistochemistry analysis was performed under light microscopy at 200x magnification.

Comprehensive characterization of the parental contribution to products of conception

Microsatellite genotyping

Five serial 8- μ m sections were prepared from paraffin blocks containing the largest amount of chorionic villi that are separated from maternal tissues. These sections were stained with Hematoxylin and Eosin and areas containing chorionic villi were defined using a stereomicroscope or an inverted microscope. Pinpoint solution (Zymo Research, Orange, CA, USA) was applied to

the areas that only contain chorionic villi and was left to dry for 30-45 min at room temperature [139](#). The tissues were removed with the Pinpoint gel and were used for DNA extraction using phenol-chloroform. Multiplex fluorescent microsatellite genotyping was performed with PowerPlex® 16 HS System (Promega, Corporation, Fitchburg, WI, USA). The reaction consisted of short tandem repeat multiplex PCR assays that amplify DNA at 15 different short tandem repeat loci and a fragment from the Amelogenin gene that distinguishes the X and Y chromosomes. Amplified PCR products were resolved by capillary electrophoresis using an ABI3130 Genetic Analyzer and the genotypes of the molar tissues were compared to those of the patients and their available partners in order to determine the parental origin of the alleles. The average number of amplified loci was 12.

Flow cytometry

Ten sections of 20 µm containing a substantial amount of chorionic villi from each available POC were used to assess the ploidy of the tissues by flow cytometry using propidium iodide according to standard methods [140](#).

Fluorescent *in situ* hybridization

Fluorescent *in situ* hybridization (FISH) was performed on 4-µm sections. Slides were hybridized with probes from the centromeres of three chromosomes, X, Y, and 18 as previously described [31](#). In addition, probes from other chromosomes were also used on some tissues to solve some genotypic discrepancies and to investigate whether additional peaks detected occasionally with microsatellite markers are due to trisomies. For each POC, more than 100 cells from different microscopic fields were scored with each probe.

Statistics

The significance of the association between the tissues with p57^{KIP2} expression and the presence of embryonic tissues of inner cell mass origin (fetal membranes, nucleated red blood cells, or fetus) was determined by Fisher's exact test. Similar statistical test was used to compare between p57^{KIP2} expression and the severity of the mutations, between the presence of embryonic tissues and the severity of the mutations. The significance of association between Ki-67 and p57^{KIP2} expression was determined by two-tailed unpaired t test. All statistical tests were done using GraphPad Prism software; p values <0.05 were considered statistically significant.

Results

Identification of three novel protein-truncating mutations in *NLRP7*

In this study, we analysed 36 POCs from a total of 17 patients, each with two *NLRP7* defective alleles. *NLRP7* mutations found in 13 out of the 17 patients were previously reported [57](#); [115](#); [120](#); [137](#). Mutation analysis in the remaining four new patients, 1074, 1142, 1200, and 2000, whose POCs are included in this study, was performed during this study as previously described [57](#). This analysis identified three novel protein-truncating mutations, a stop codon, c.2616C>A, p. Tyr872Stop in exon 8; a splice mutation, c.2130-2A>G affecting the invariant acceptor site at the junction of intron 5 and exon 6; and an insertion of 22-bp, c.1517_1518ins22, p.Glu508Aspfs*27 in exon 4 (Supplementary Table 2.1). In some new or previously reported patients, in which more than one mutation was found, the phase was established either by testing the parents for the identified DNA changes or by amplifying a PCR fragment containing both mutations, cloning, and sequencing.

The results of this analysis are summarized in Supplementary Table 2.1 and are annotated according to the Human Genome Variation Society guidelines (<http://www.hgvs.org/>) for haplotype annotations. In conclusion, all the patients, whose POCs are included in this study, had two defective alleles in *NLRP7*.

Some HMs from patients with two *NLRP7*-defective alleles express p57^{KIP2}

Using immunohistochemistry, we first analyzed the expression of p57^{KIP2} in 36 POCs from 17 patients with two *NLRP7*-defective alleles. Of the analyzed tissues, 32 were conclusive. Of these, 19 (59%) did not express p57^{KIP2} in the cytotrophoblast or the villous stroma and were therefore p57^{KIP2} negative and 13 (41%) displayed variable levels of p57^{KIP2} positive cells ranging from 20-100% (Table 2.1 and figure 2.1A-C). Among the 13 POCs with some p57^{KIP2} expression, six expressed p57^{KIP2} strongly in all cytotrophoblast and villous stroma cells (figure 1A); three expressed p57^{KIP2} only in the cytotrophoblast, but not in the villous stroma and this pattern was observed in all chorionic villi (figure 2.1B); and four expressed p57^{KIP2} in 20-50% of cytotrophoblast cells but not in villous stroma cells and this pattern was observed only in 5% of chorionic villi (Table 2.1 and figure 2.1C). These data demonstrate that p57^{KIP2} silencing does not occur in all diploid biparental moles and that some diploid biparental HMs from patients with two *NLRP7*-defective alleles do express p57^{KIP2} in cytotrophoblast and villous stroma cells. The expression of p57^{KIP2} in diploid biparental moles from patients with two *NLRP7* defective alleles is novel and has not been previously reported.

Comprehensive characterization of the parental contribution to HMs from patients with recessive *NLRP7* mutations

The presence of HMs with variable levels of positive p57^{KIP2} expression raised the possibility that these tissues may be aneuploid, for instance triploid, in mosaic or non-mosaic state. We therefore undertook a comprehensive genotypic characterization of the parental contribution to these 36 POCs using three different DNA-based approaches, microsatellite DNA genotyping, flow cytometry, and fluorescent in situ hybridization (FISH). Each of the used methods has its advantages and limitations. Of the three methods used in our genotypic evaluation, microsatellite DNA genotyping is the only one that allows determining the parental origin of DNA present in the POCs. A distortion in the heights of the maternal and paternal alleles is indicative of an imbalance in the ratio between the parental genomes. Flow cytometry is an easy and fast method to determine ploidy (2n or 3n). FISH is another method to determine ploidy and the only method to identify mosaicism, but only in cases of mixed cellular populations with different ploidies, different gender, or high frequency of aneuploidy cells. An example of our comprehensive genotyping approach is provided in figure 2.2.

The detailed results of the three approaches are summarized in Supplementary Table 2.1 and demonstrated that all the POCs are diploid biparental. Among these 36 tissues, 35 had a single cellular population and one was found mosaic with two cellular populations. In this mosaic molar tissue, the main cellular population was diploid XY and was found in all cytotrophoblast cells and in 90% of villous stroma cells. The second minor cellular population was diploid XX and was found only in 10% of cells from the villous stroma (figure 2.3; Supplementary figure S2.1). It is important to note that the mosaicism in this POC was not detected by the multiplex DNA genotyping due to the low amount of cells from the minor cellular population, which prevented us

from determining its parental origin. However, we had noticed an imbalance in the heights of the X and Y allele peaks at the Amelogenin gene marker, which was not due to contamination with maternal DNA as judged by the profiles of other informative microsatellite markers (figure 2.3). It is therefore possible that this POC may have originated from a dispermic fertilization followed by postzygotic diploidization at the first cellular division leading to a diploid biparental XY cell and another diploid XX cell [28](#). Such mosaicism would be in agreement with the mosaic p57^{KIP2} pattern observed with this POC, but does not explain the positive expression of p57^{KIP2} in the major cell line of this POC, which is diploid biparental. Therefore, our genotyping data on the 36 POCs demonstrate that molar tissues from patients with two *NLRP7* defective alleles are mostly diploid biparental with a single cellular population but failed to identify aneuploidies that could underlie their positive p57^{KIP2} expression.

p57^{KIP2} expression correlates with the presence of embryonic tissues of inner cell mass origin

We next used histopathological examination to characterize the 36 POCs from patients with two *NLRP7* defective alleles. Hematoxylin and Eosin slides were reviewed independently by two pathologists who were blinded to the genotyping results and p57^{KIP2} staining. Of the analyzed 36 POCs, there was an agreement between the two pathologists on the diagnosis of 81% of the cases, which is in line with previously reported data in the field [141-143](#). Among the 32 POCs that were conclusive for p57^{KIP2} staining, 13 expressed p57^{KIP2} in the cytotrophoblast and/or the villous stroma and six (46%) of them had embryonic tissues of inner cell mass origin, namely, extraembryonic membranes and nucleated red blood cells inside the chorionic villi (Table 2.1) (figure 2.4, upper panel). These six POCs had mild trophoblastic proliferation and consequently were diagnosed as PHMs or non-molar SAs. However, none of the 19 POCs that did not express

p57^{KIP2} had extra-embryonic membranes or nucleated red blood cells (figure 2.4, lower panel). The association between positive expression of p57^{KIP2} and the presence of embryonic tissues was highly significant (p=0.00189) (Table 2.2). In addition, among the 32 analyzed tissues, 12 were from patients with at least one protein-truncating mutation in the coding region (E99X, Q310Hfs, E340Qfs, Y872X, E508Dfs, C931X) and all these POCs did not have embryonic tissues of inner cell mass origin (p=0.04277) (Table 2.2) and had strong trophoblastic proliferation. Moreover, 10 of these 12 tissues did not express p57^{KIP2} at all (p=0.03191) (Table 2.2).

These data demonstrate a significant association between missense *NRLP7* mutations (presumably with some residual activity), positive p57^{KIP2} expression, the presence of embryonic tissues of inner cell mass origin, and mild trophoblastic proliferation. On the contrary, truncating *NRLP7* mutations (presumed to completely abolish the function) correlated with negative p57^{KIP2} expression and absence of embryonic tissues of inner cell mass origin. We note that some patients with invariant splice mutations had more variability in their reproductive outcomes than patients with protein-truncating mutations in the coding region. The best example of these is the case of family MoLb1, in which three patients are homozygous for an invariant splice mutation, c.352+1G>A, p.Gly118fs, and had the full spectrum of reproductive loss ranging from moles to early neonatal death and including spontaneous abortions and stillbirths [57](#). In addition, two patients from this family had, each, one live birth of a healthy baby and now adults. In this family, MoLb1, four moles were found p57^{KIP2} positive (Table 2.1).

Negative correlation between p57^{KIP2} and Ki-67 expression

In the histopathological analysis, the degree of trophoblastic proliferation was evaluated by the two pathologists based on microscopic examination, which is a descriptive analysis known to be subject to interobserver and intraobserver variabilities [141-143](#). To have a more accurate evaluation of the trophoblastic proliferation of the POCs from patients with two defective *NLRP7* alleles, we analyzed 22 of the 32 POCs that were analyzed with p57^{KIP2} and from which sufficient materials were available, for Ki-67 expression by immunohistochemistry. This analysis showed that the eight POCs that expressed p57^{KIP2} had significantly lower levels of Ki-67 immunoreactivity in the cytotrophoblast than the fourteen POCs that did not express p57^{KIP2} (p=0.0012) (figure 2.5A-C).

Discussion

To date, approximately 80 molar tissues from patients with two *NLRP7* mutations have been genotyped, but only with one method, and found mostly diploid biparental [56](#); [58](#); [60](#); [115-120](#); [130](#); [132-135](#). Of these, 37 were characterized for p57^{KIP2} expression and were all found to be negative [107](#); [130](#); [133](#); [135](#). In this study, we performed p57^{KIP2} immunohistochemistry on 36 POCs, from patients with two *NLRP7* defective alleles and found that six of them are p57^{KIP2} positive in all chorionic villi and seven express variable levels of p57^{KIP2} protein in some chorionic villi. This raised the question about possible genomic aneuploidies, for instance, triploidy or mosaicism that could explain positive or mosaic p57^{KIP2} expression.

We, therefore, undertook a comprehensive characterization of the 36 POCs using three DNA-based approaches to determine their parental contribution. We found that all the analyzed POCs are diploid biparental with a single cellular population with the exception of only one that was found mosaic. Therefore, our data confirm previous reports [56](#); [58](#); [60](#); [115-120](#); [130](#); [132-135](#) and demonstrate that HMs from patients with two mutated copies of *NLRP7* are mostly diploid biparental and exclude the presence of aneuploidies at the origin of positive p57^{KIP2} expression in some of these tissues.

We next evaluated these tissues independently by two pathologists and found that missense mutations in *NLRP7* were associated with positive p57^{KIP2} expression, the presence of embryonic tissues of inner cell mass origin, and mild trophoblastic proliferation. However, protein-truncating mutations in the coding region of *NLRP7* were associated with negative p57^{KIP2} expression, absence of embryonic tissues of inner cell mass origin, and severe trophoblastic proliferation. Interestingly, in all the analyzed tissues, the trophoblastic proliferation was inversely correlated with that of p57^{KIP2} expression, which indicates that these two functions, proliferation and

differentiation, are tightly linked and regulated by the severity of *NLRP7* mutations. Among the four studies that have investigated p57^{KIP2} expression in diploid biparental HMs from patients with two *NLRP7* defective alleles [107](#); [130](#); [133](#); [135](#), one major and important study included 34 HMs and demonstrated that all of them are p57^{KIP2} negative [133](#). We explain the difference between p57^{KIP2} expression in our study and that of Sebire *et al* by mainly three factors. First, in our analysis, we deliberately did not revise the histopathological diagnosis of the different POCs after the analysis of p57^{KIP2} staining while Sebire *et al.* by analogy to the diagnosis of common sporadic androgenetic and triploid HMs, revised the final diagnosis of the conceptions based on p57^{KIP2} expression. Second, in our study, we analyzed all available POCs from the patients while Sebire *et al.* analyzed only the POCs that were diagnosed as HMs. Third, our analysis included more POCs from patients with missense mutations than that of Sebire *et al.* Therefore, our data are not in contradiction with those of Sebire *et al.* but simply, the two studies are not comparable because of their different inclusion criteria and design. Indeed, our study was designed to comprehensively characterize all the conceptions of patients with two *NLRP7*-defective alleles to better understand the effects of the various mutations and the origin of the variability in their reproductive outcomes.

CDKN1C is an imprinted, maternally expressed, gene in several mouse and human tissues. In humans, maternal loss-of-function mutations in *CDKN1C* are responsible for Beckwith-Wiedemann syndrome [111](#), a pediatric overgrowth disorder in which the placenta share some histopathological features with PHMs [144](#); [145](#). In addition, a homozygous frameshift mutation in *NLRP2*, the closest *NLRP* gene to *NLRP7*, in the mother has been shown to be responsible for Beckwith-Wiedemann syndrome in her two offspring [146](#). In mice, maternal p57^{KIP2} null mutations lead to perinatal lethality due to altered cellular proliferation and differentiation in several tissues [108](#); [147](#); [148](#). During mouse embryogenesis, positive p57^{KIP2} expression is associated with terminally

differentiated cells in several tissues [149](#). Our data on molar tissues with the same parental contribution, diploid biparental, and caused by recessive mutations in the same gene, indicate that *NLRP7* plays, directly or indirectly, a role in the decision to switch between cellular differentiation and proliferation at a critical time during early development. Severe *NLRP7* mutations may prevent cytotrophoblast cells from exiting the cell-cycle to terminally differentiate and acquire p57^{KIP2} expression and consequently these cells continue to proliferate. However, mild mutations may allow some cytotrophoblast cells to exit the cell-cycle to terminally differentiate, acquire p57^{KIP2} expression, and consequently these cells stop to proliferate. Similar inverse correlations between p57^{KIP2} and Ki-67 expression, tissue differentiation and proliferation have been observed in other cellular types, such as muscles, neurons, hepatocellular and pancreatic cancers [150-153](#).

The most striking findings of our analyses are the similarities between partial diploid biparental moles, caused by mild *NLRP7* defective alleles, and common partial triploid dispermic moles. The same similarities are observed between complete diploid biparental moles caused by severe *NLRP7* defective alleles and common complete androgenetic moles (figure 2.6). Despite their different genotypes, both sporadic triploid dispermic moles and some diploid biparental moles caused by mild *NLRP7* mutations are p57^{KIP2} positive, express low levels of Ki-67, have mild trophoblastic proliferation, and may have some embryonic tissues. However, sporadic androgenetic moles and most diploid biparental moles caused by *NLRP7* protein-truncating mutations are p57^{KIP2} negative, express high levels of Ki-67, have important trophoblastic proliferation, and do not have embryonic tissues (figure 2.6). These data indicate that all mechanisms leading to HMs, including *NLRP7* mutations, act upstream of p57^{KIP2} and Ki-67, and regulate the balance between tissue differentiation and proliferation.

The time at which *NLRP7* affects p57^{KIP2} expression cannot be determined from our study,

but the two genes are expressed in all oocytes and preimplantation stages [57](#); [72](#); [154](#). Furthermore, previous studies have shown that mouse trophoblast stem cells express p57^{KIP2} upon differentiation into trophoblast giant cells [155](#), which are the equivalent of human extra-villous trophoblast. The fact that p57^{KIP2} expression was normal in the extra-villous trophoblast of all molar tissues from patients with *NLRP7* mutations, but abnormal in the cytotrophoblast and the villous stroma indicates that *NLRP7* defects start to manifest after the terminal differentiation of the extra villous trophoblast and before the terminal differentiation of the cytotrophoblast and villous stroma cells. Our proposed role of *NLRP7* in regulating the balance between tissue differentiation and proliferation is in line with a recent interesting study demonstrating that reduced *NLRP7* expression in human embryonic stem cells alters trophoblast lineage differentiation [131](#).

In conclusion, we report the most comprehensive and thorough analysis of 36 POCs from patients with two *NLRP7* mutations. Our data suggest that *NLRP7* mutations shift the cellular machinery from differentiation to proliferation at a very critical time during early development, a role that could not have been revealed by other approaches on somatic cells.

CONFLICT OF INTEREST

All authors declare no conflict of interest.

ACKNOWLEDGMENT

We thank the patients and their families for their participation in the study. Ngoc Minh Phuong Nguyen was supported by the Réseau Québécois en Reproduction and the Alexander McFee McGill Faculty of Medicine Fellowships. This project was supported by the Canadian Institute for Health Research for RS (MOP-102469). We thank Dr Adel Giaid for providing access to the microtome and acknowledge the use of the Rosalind and Morris Goodman Histopathology

Services. We also thank the Departments of Pathology of the following hospitals and Medical centre, St-Alexius Medical Center, UTS Medical Center, Auckland City Hospital, Victoria General Hospital, Cypress Surgical Center, Fletcher Allen Healthcare, Womack Army Medical Center, Piedmont Henry Hospital, Georgia, Capital Health, Royal Jubilee Hospital, Credit Valley Hospital, for providing archived molar tissues.

Figures

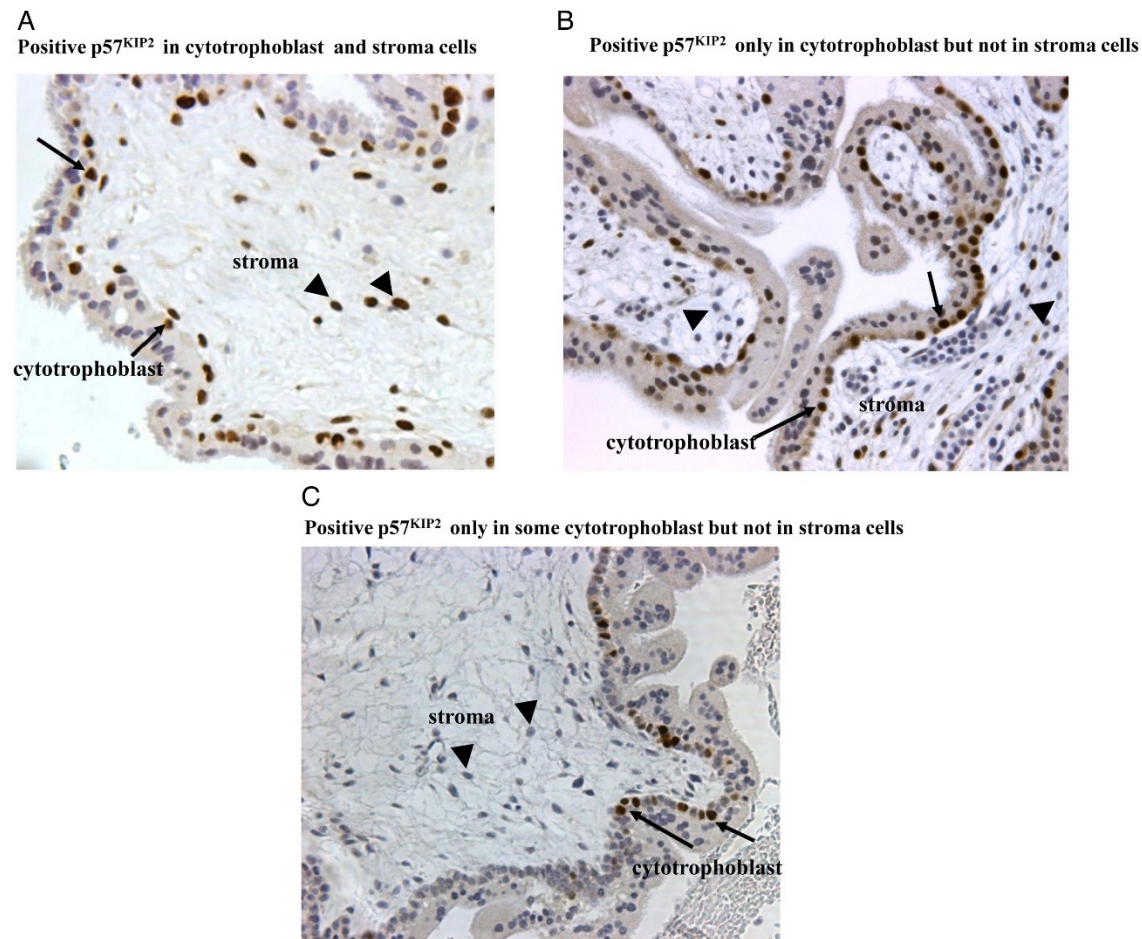


Figure 2.1. Examples of the variations in the expression of p57^{KIP2} in diploid biparental hydatidiform moles from patients with two *NLRP7*-defective alleles. (A) In products of conception (POC) 6526 from patient 655, p57^{KIP2} is expressed strongly (brown) in all nuclei of cytotrophoblast (CT) (arrow) and villous stroma cells (arrowhead) (magnification 200×). (B) In POC 1554 from patient 655, p57^{KIP2} is expressed in all nuclei of CT (arrow) but not in villous stroma cells (arrowhead) (200×). (C) In POC 2777 from patient 655, p57^{KIP2} is expressed in 20%–50% of CT (arrow) but not in villous stroma cells (arrowhead) (200×).

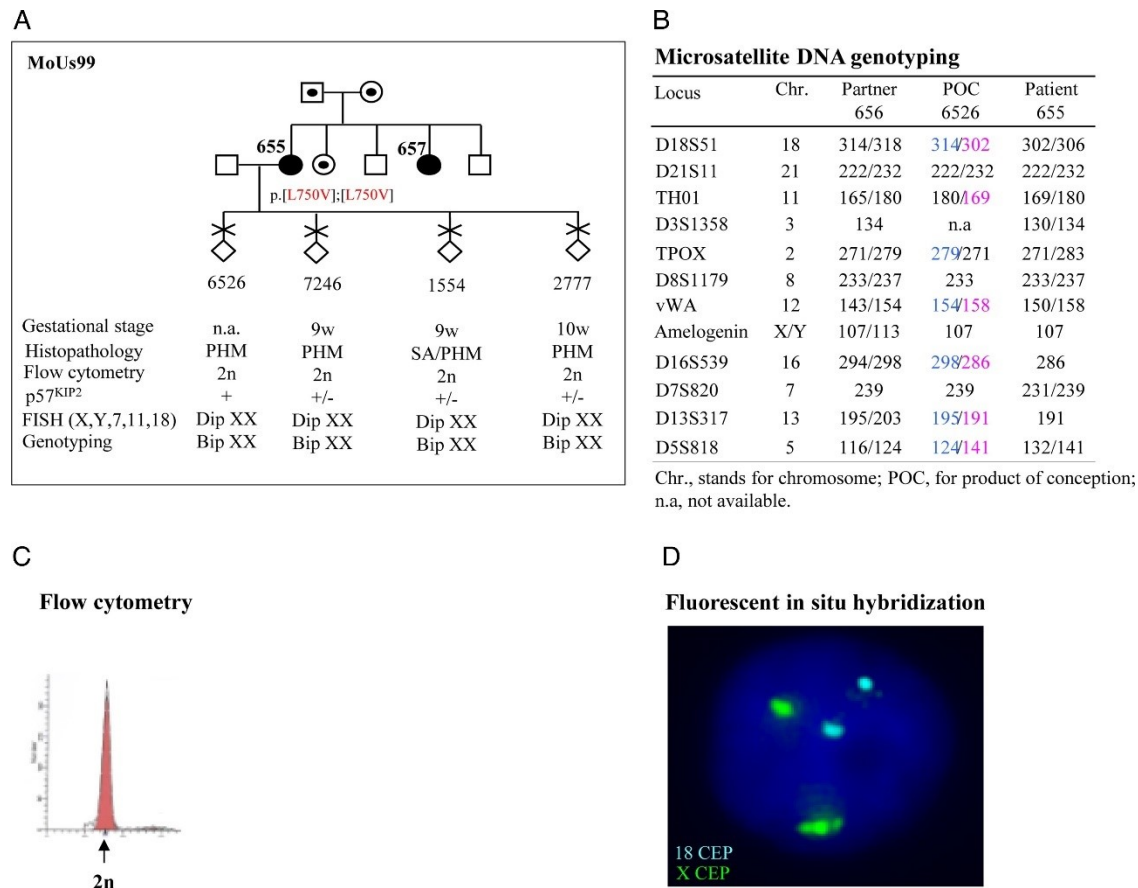


Figure 2.2. Representative example of our comprehensive analysis of products of conceptions (POCs) from patients with two defective alleles in *NLRP7*. (A) Pedigree structure, reproductive outcomes, and recapitulation of the results of the characterization of 4 POCs from patient 655 using three DNA-based approaches. (B) DNA genotyping demonstrating the biparental contribution to POC 6526. Maternal alleles are in pink and paternal alleles in blue. (C) Flow cytometry results demonstrating the presence of a single diploid DNA peak. (D) FISH with centromeric probes from chromosomes X, Y, and 18 confirming diploidy and the presence of two X chromosomes in the POC. . HM, hydatidiform moles; Dip, diploid; Bip, biparental; w, week; n.a., not available; PHM, partial hydatidiform mole; SA, spontaneous abortion.

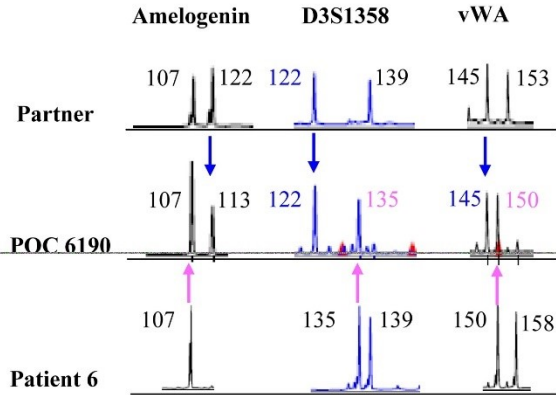
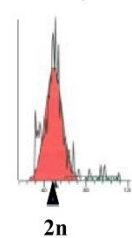
A

Multiplex microsatellite genotyping				
Loci	Chr	Partner	POC 6190	Patient 6
D21S11	21	222/232	222	222
TH01	11	166/178	178 /170	170/181
D3S1358	3	122/139	122 /135	135/139
vWA	12	145/153	145 /150	150/158
Amelogenin	X/Y	107/113	<u>107</u> /113	107
D16S539	16	281	281/294	281/294
D7S820	7	227/231	227 /235	227/235
D13S317	13	191/199	191 /199	199
D5S818	5	133/137	133/137	133/137

Chr., stands for chromosome; POC, product of conception. The X allele with a higher peak at the Amelogenin marker is underlined.

B

Flow cytometry



C

Fluorescent in situ hybridization

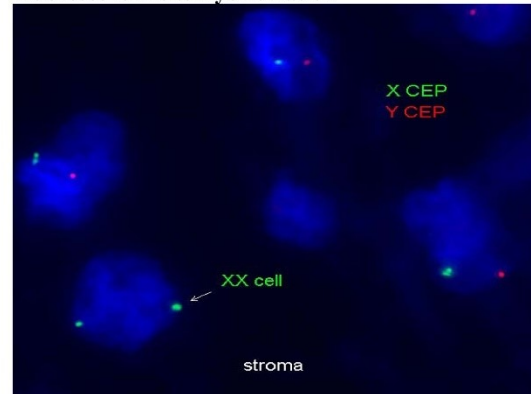


Figure 2.3. Mosaic mole from a patient with two *NLRP7*-defective alleles. (A)

DNA genotyping demonstrating the biparental contribution to this hydatidiform mole. Maternal alleles are in pink and paternal alleles in blue. **(B)** Flow cytometry results demonstrating the presence of a single diploid DNA peak. **(C)** FISH with centromeric probes from chromosomes X and Y showed two cellular populations, diploid XY in the cytotrophoblast and villous stroma and diploid XX in approximately 10% of cells from the villous stroma. A photo of the whole villous showing the presence of the XX cells in the villous stroma is provided in Supplementary Figure S1.

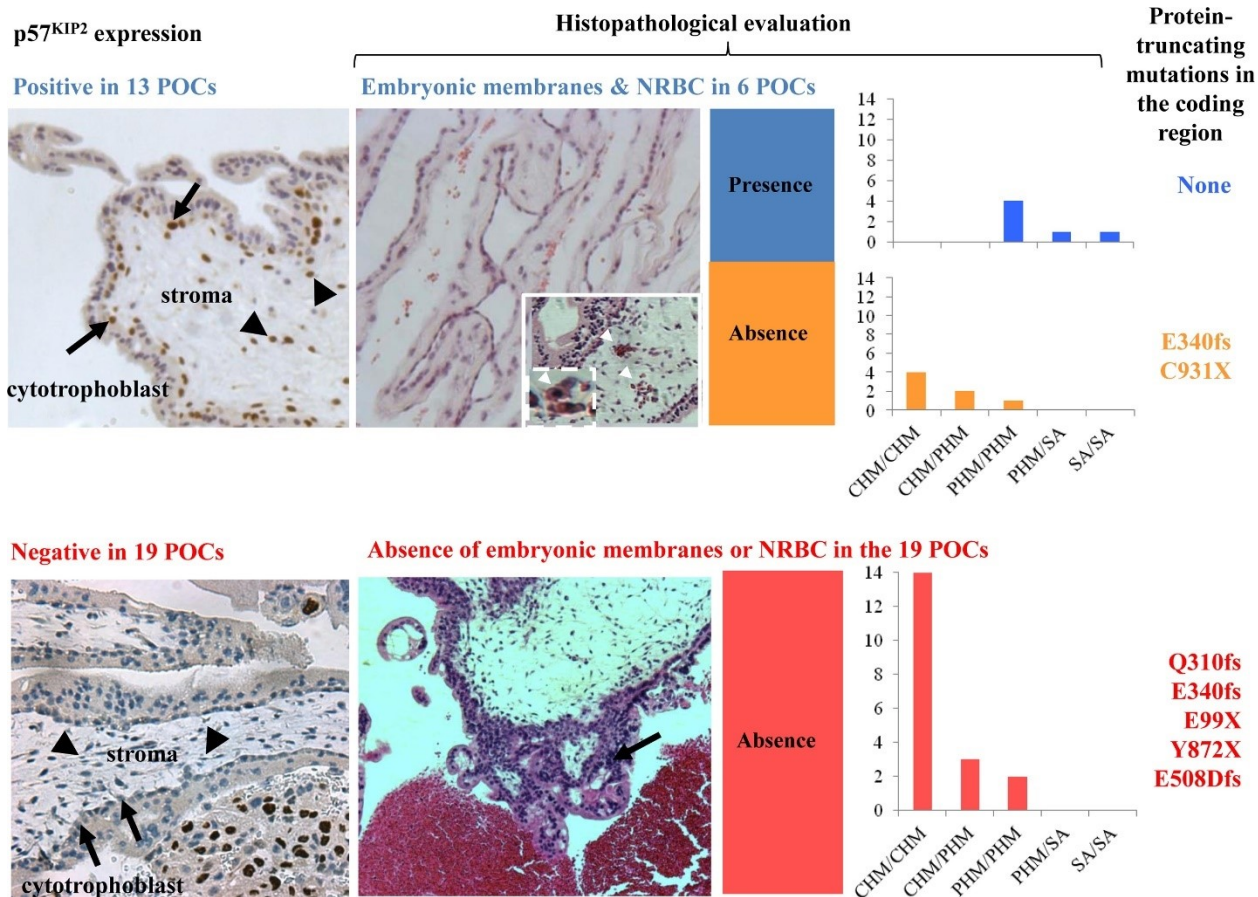


Figure 2.4. Recapitulation of p57^{KIP2} expression, histopathological features of the hydatidiform moles and *NLRP7* mutations in the patients. In the upper panel, from left to right, a representative view from one product of conception (POC) demonstrating positive p57^{KIP2} staining (brown colour) in both cytotrophoblast (arrow) and villous stroma (arrowhead) (200×); H&E staining of the same POC showing the presence of embryonic membranes (100×) and of another POC showing nucleated red blood cells inside a chorionic villous (200×); and final diagnoses made independently by two pathologists. Among the 13 POCs with some positive p57^{KIP2} staining, six (blue) had embryonic tissues of inner cell mass origin (embryonic membranes and/or nucleated red blood cells) and seven did not have (orange). In the lower panel, from left to right, a representative view from one POC demonstrating negative p57^{KIP2} staining in both cytotrophoblast (arrow) and villous stroma (arrowhead) (200×); H&E staining of the same POC showing circumferential trophoblastic proliferation (arrows) (100×); final diagnoses of the 19 POCs by two pathologists (red); and protein-truncating mutations in the coding region found in the patients who had these 19 p57^{KIP2}-negative POCs. Diagnoses by the two pathologists are separated by ‘/’. POC, product of conception; CHM, complete hydatidiform mole; PHM, partial hydatidiform mole; SA, spontaneous abortion; NRBC, nucleated red blood cells.

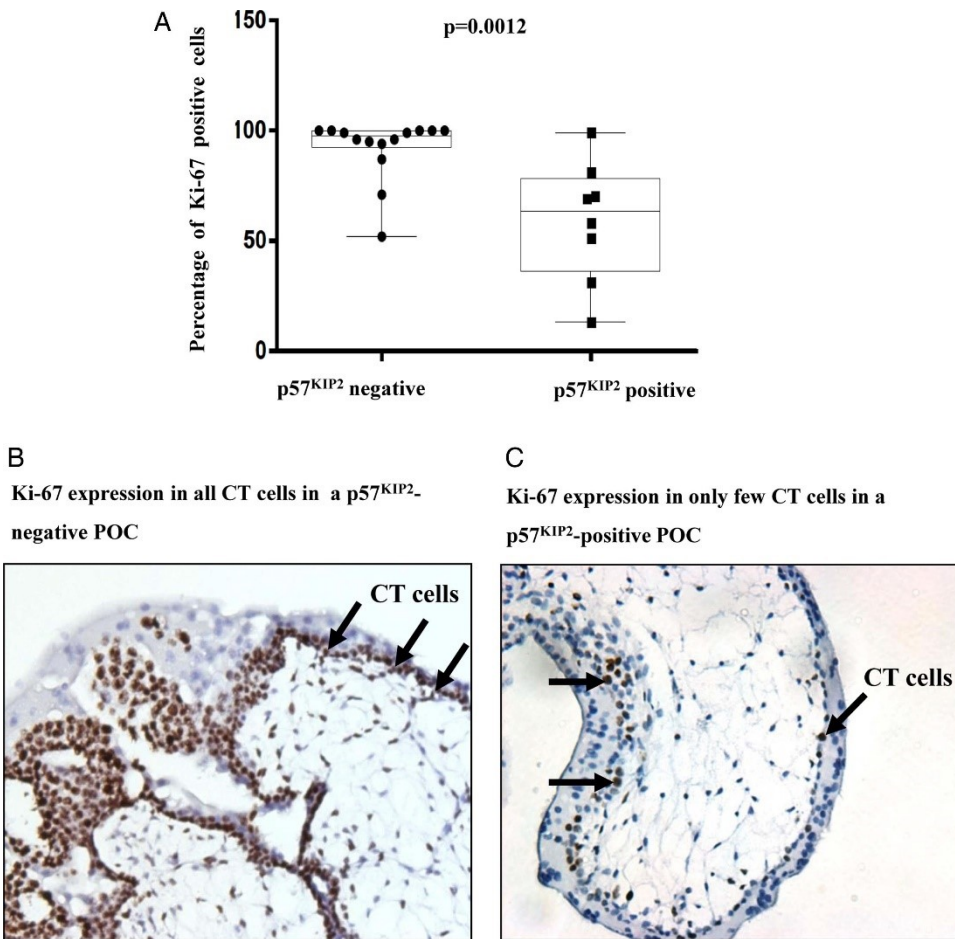


Figure 2.5. Ki-67 expression in 22 products of conceptions (POCs) from patients with two *NLRP7*-defective alleles. (A) Box plot comparing the expression of Ki-67 in moles that did not express p57^{KIP2} and moles that expressed p57^{KIP2}. Fourteen moles that were negative for p57^{KIP2} expression had significantly higher levels of Ki-67 expression in the nuclei of cytotrophoblast cells than eight moles with positive p57^{KIP2} expression (p=0.0012). (B) Examples of different levels of Ki-67 staining. (Left panel) POC 8508 (from patient 725) demonstrating positive Ki-67 staining (brown) in all nuclei of cytotrophoblast (CT) (arrow). This POC did not express p57^{KIP2} and is from a patient with one protein-truncating mutation in the coding region. (Right panel) POC 1554 (from patient 655) demonstrating positive Ki-67 staining in few CT cells (arrow). This POC expressed p57^{KIP2}, had embryonic membranes, mild trophoblastic proliferation and is from a patient with a missense mutation..

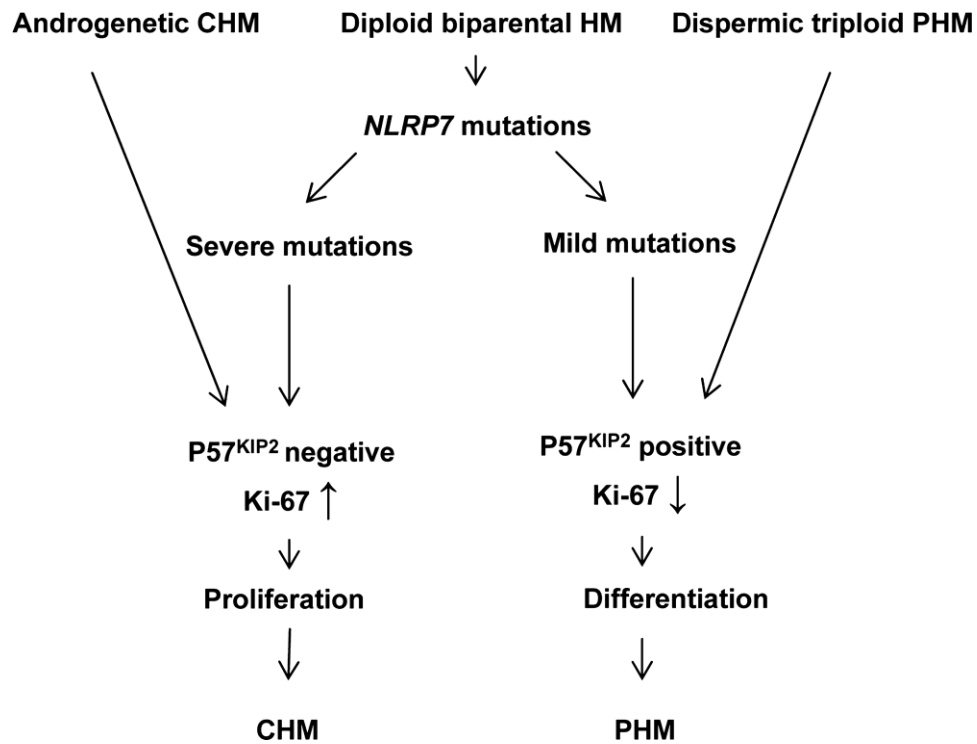


Figure 2.6. A suggested model of NLRP7 action upstream of p57^{KIP2} and Ki-67. Despite their different genotypes, both sporadic triploid dipsermic moles and some diploid biparental moles caused by mild NLRP7 mutations acquire p57^{KIP2} expression (positive) have low levels of Ki-67 expression and are therefore diagnosed as partial hydatidiform moles. However, sporadic androgenetic moles and most diploid biparental moles caused by NLRP7 protein-truncating mutations do not acquire p57^{KIP2} expression (negative), have higher levels of Ki-67 expression and are therefore diagnosed as complete hydatidiform moles. CHM, complete hydatidiform mole; PHM, partial hydatidiform mole.

Table 2.1. Recapitulation of p57^{KIP2} and Ki-67 expression by immunohistochemistry, presence of embryonic tissues of inner cell mass origin,

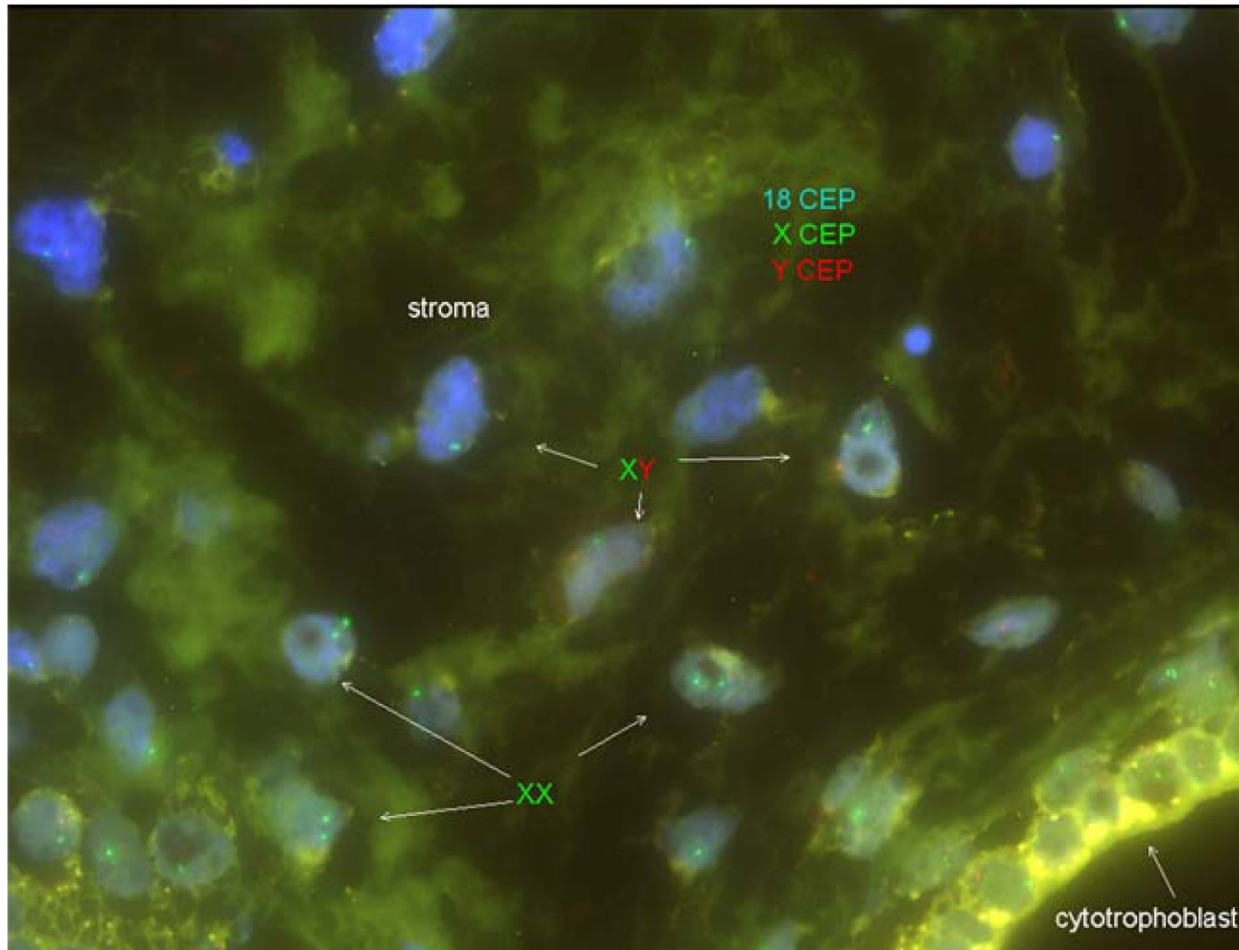
Case ID-Patient ID	Block ID (N)	GA in weeks	p57 ^{KIP2} expression		Inner cell mass derivatives	Ki-67 expression % of positive CT cells	Pathologists		NLRP7 mutations or NSVs in the patients
			CT	VM			1	2	
MoLb1-4	2151 (1)	8	+++	+++	No	n.a	CHM	CHM	p.[G118fs; V319I];[G118fs; V319I]
MoLb1-6	4199 (1)	11	+++	+++	No	70%	CHM	CHM	p.[G118fs; V319I];[G118fs; V319I]
MoUs99-655	6526 (6)	n.a.	+++	+++	Membranes	51%	PHM	PHM	p.[L750V];[L750]
MoUs99-657	238 (6)	17	+++	+++	Membranes	13%	PHM	PHM	p.[L750V];[L750]
Mous167-712	3932 (1)	n.a.	+++	+++	No	n.a	CHM	CHM	p.[V319I];[P716A];[Cys931X]
MoCa179-744	27404 (4)	8	+++	+++	No	69%	CHM	eCHM	p.[E340QfsX10];[R693W]
MoLb1-6	1524 (1)	n.a	+++	---	No	n.a	CHM	PHM	p.[G118fs; V319I];[G118fs; V319I]
MoLb1-6	6190 (1)	n.a	+++	---	No	n.a	CHM	PHM	p.[G118fs; V319I];[G118fs; V319I]
MoUs99-655	1554 (11)	9	+++	---	NRBC, membranes	31%	SA	SA	p.[L750V];[L750]
MoFr101-662	M251 (1)	9	+++ (45%), --- (55%)	---	Complete fetus with a mole	n.a	PHM	SA	p.[L964P];[L964]
Moln103-671	G1814 (1)	8	+++ (58%), --- (42%)	---	No	99%	PHM	PHM	p.[R693P];[R693]
MoUs99-655	7246 (3)	9	--- (95%), ++ (5%)	---	NRBC	81%	PHM	PHM	p.[L750V];[L750]
MoUs99-655	2777 (10)	9	--- (95%), ++ (5%)	---	NRBC	58%	PHM	PHM	p.[L750V];[L750]
MoLb1-4	5411 (2)	14	---	---	No	n.a	CHM	CHM	p.[G118fs; V319I];[G118fs; V319I]
Moln69-480	G1071 (2)	10	---	---	No	52%	HM	CHM	p.[N913S];[R693]
MoCh76-519	523 (1)	7	---	---	No	100%	CHM	CHM	p.[E99X;V319I];[D657V]
MoUs99-657	7814 (3)	n.a	---	---	No	99%	CHM	CHM	p.[L750V];[L750]
MoUs99-657	1858 (1)	n.a	---	---	No	96%	PHM	CHM	p.[L750V];[L750]
Moln104-674	G574 (2)	10	---	---	No	n.a	PHM	PHM	p.[R693P];[R693]
MoNz 170-725	7759 (1)	n.a	---	---	No	n.a	CHM	CHM	p.[Q310Hfs;A481T];[R693W]
MoNz 170-725	8508 (1)	n.a	---	---	No	100%	CHM	CHM	p.[Q310Hfs;A481T];[R693W]
MoUs171-733	15636 (5)	n.a	---	---	No	71%	CHM	CHM	p.[L750V];[L750]
MoUs171-733	3005 (2)	n.a	---	---	No	100%	CHM	CHM	p.[L750V];[L750]
MoCa179-744	21689 (1)	9	---	---	No	100%	CHM	PHM	p.[E340Qfs];[R693]
MoMx341-1074	9449 (6)	8	---	---	No	96%	CHM	CHM	p.[Tyr872X];c.[2810+2T>G]
MoCa179-744	100090 (3)	n.a	---	---	No	n.a	CHM	eCHM	p.[E340QfsX10];[R693W]
MoCa179-744	10282 (3)	n.a	---	---	No	99%	CHM	eCHM	p.[E340QfsX10];[R693W]
MoUs420-1200	8454 (3)	11.5	---	---	No	94%	CHM	CHM	p.[R693Q];c.2130-2A>G=A/G]
MoUs420-1200	5644 (15)	8	---	---	No	87%	PHM	PHM	p.[R693Q];c.2130-2A>G=A/G]
MoCa408-2000	10509 (2)	10.5	---	---	No	95%	CHM	CHM	p.[G487E;Glu508Aspfs*27];[G487E;Glu508Aspfs*27]
MoCa408-2000	17467 (1)	n.a	---	---	No	n.a	CHM	CHM	p.[G487E;Glu508Aspfs*27];[G487E;Glu508Aspfs*27]
MoCa408-2000	3661 (1)	8	---	---	No	100%	CHM	CHM	p.[G487E;Glu508Aspfs*27];[G487E;Glu508Aspfs*27]

The presence or absence of p57^{KIP2} expression in villous cytotrophoblast (CT) and mesenchyme (VM) are indicated by "+" or "-"; +++, indicates 100% of cells are positive; ++, 20-50% of cells are positive; ---, all cells are negative. Different populations of chorionic villi with discordant p57^{KIP2} expression are separated by a comma. The percentage of chorionic villi in each population compared to the total number of chorionic villi on the analyzed slide is indicated between parentheses. Family ID is provided in the first column followed by the patient ID. Histopathological diagnosis of products of conception was made independently by two pathologists. N, indicates number of available blocks for each POC; HM, hydatidiform mole (HM is used when the pathologist did not distinguish between partial and complete HM); CHM, complete HM; PHM, partial HM, SA, spontaneous abortion; NRBC, nucleated red blood cells. Mutations are in bold, rare or low-frequency non-synonymous variants (NSV) are underlined; common NSVs are in black.

Table 2.2. Correlations between the severity of the mutations, p57^{KIP2} expression, and the HM features

	Embryonic development		p57^{KIP2} expression	
	Present	Absent	Positive	Negative
Mutation severity				
Missense	6	14	11	9
Truncating	0	12	2	10
	p =0.04277		p=0.03191	
P57^{KIP2} expression				
Positive	6	7		
Negative	0	19		
	p=0.00189			

Supplementary figure and table



Supplementary figure S2.1. Whole villous showing the presence of the XX cells in the villous stroma. Two cellular populations, diploid XY and diploid XX in the villous stroma.

Supplementary Table 2.1. Recapitulation of the reproductive outcomes, mutation analysis, and characterization of 36 POCs from patients with 2 <i>NLRP7</i> defective alleles													
Case ID	Patient DNA ID	Reproductive outcomes as per the referral (pathology report or clinician)	<i>NLRP7</i> sequencing results	Block ID	GA in weeks	Pathologist		Flow	Karyotype	FISH	p57 ^{NP2}	Genotype & Conclusion	Reference
						1	2						
MoLb1	4	LB ^{RUQ} , SB, END, PHM, 2 HM-PTD, CHM*, SA, PHM	p.[G118fs;V319I][G118fs;V319I]	5411	14	CHM	CHM	2n	46,XX(91)/46,X X(6)t(9:17)		-	Biparental XX	Helwani et al., 1999 & this study
MoLb1	4	LB ^{RUQ} , SB, END, PHM, 2 HM-PTD, CHM, SA*, PHM	p.[G118fs;V319I][G118fs;V319I]	2151	8	CHM	CHM	2n		Di XX (18,X,Y)	+	Biparental XX	this study
MoLb1	6	5 SA, SB, 2 HM*, 3 SA, 2 HM, CHM, PHM	p.[G118fs;V319I][G118fs;V319I]	1584	na	CHM	PHM	inconc.			inconc.	Biparental XY	this study
MoLb1	6	5 SA, SB, 2 HM*, 3 SA, 2 HM, CHM, PHM	p.[G118fs;V319I][G118fs;V319I]	4406	na	HM	HM	2n			inconc.	Biparental XX	this study
MoLb1	6	5 SA, SB, 2 HM, 3 SA, 2 HM*, CHM, PHM	p.[G118fs;V319I][G118fs;V319I]	1524	na	CHM	PHM	2n		Di XY (X,Y,18)	+/-	Biparental XY	this study
MoLb1	6	5 SA, SB, 2 HM, 3 SA, 2 HM*, CHM, PHM	p.[G118fs;V319I][G118fs;V319I]	6190	na	CHM	PHM	2n		Di XY+XX (X,Y,18)	+/-	Biparental XY	this study
MoLb1	6	5 SA, SB, 2 HM, 3 SA, 2 HM, CHM*, PHM	p.[G118fs;V319I][G118fs;V319I]	1631	7.5	CHM	CHM	2n	46,XX+22		inconc.	Biparental XX	Helwani et al., 1999 & this study
MoLb1	6	5 SA, SB, 2 HM, 3 SA, 2 HM, CHM, PHM*	p.[G118fs;V319I][G118fs;V319I]	4199	11	CHM	CHM	na.	46,XY		+	Biparental XY	Helwani et al., 1999 & this study
MoIn69	480	HM-GTN, PHM, PHM-GTN-IM	p.[N913S][R693P]	G1071	10	HM	CHM	2n		Di XX (18,X,Y)	-	Biparental XX	this study
MoCh76	519	CHM-GTN, 2 CHM, PHM	p.[E99X;V319I][D657V]	523	7	CHM	CHM	2n			-	Biparental XY	Qian et al., 2007; this study
MoUs99	655	PHM*, CHM, SA, PHM	p.[L750V][L750V]	6526	na	PHM	PHM	2n		Di XX (18,X,Y)	+	Biparental XX	Deveault et al., 2009; this study
MoUs99	655	PHM, CHM*, SA, PHM	p.[L750V][L750V]	7246	9	PHM	PHM	2n		Di XX (X,Y, 18, 11)	+/-	Biparental XX	Deveault et al., 2009; this study
MoUs99	655	PHM, CHM, SA*, PHM	p.[L750V][L750V]	1554	9	SA,PHM	SA	2n		Di XX (18,X,Y)	+/-	Biparental XX	Deveault et al., 2009; this study
MoUs99	655	PHM, CHM, SA, PHM*	p.[L750V][L750V]	2777	9	PHM	PHM	2n		Di XX (18,X,Y)	+/-	Biparental XX	Deveault et al., 2009; this study
MoUs99	657	PHM*, PHM, CHM	p.[L750V][L750V]	238	17	PHM	PHM	2n		Di XX (18,X,Y,3,12)	+	Biparental XX	This study
MoUs99	657	PHM, PHM*, CHM	p.[L750V][L750V]	1858	na	PHM	PHM	2n			-	Biparental XY	This study
MoUs99	657	PHM, PHM, CHM*	p.[L750V][L750V]	7814	na	CHM	CHM	2n			-	Biparental XY	This study
MoFr101	662	PHM (+fetus)-GTN, 2 SA, PHM* (+ fetus)-GTN	p.[L964P][L964P]	M251	9	PHM	SA	na.		Di XY (X,Y,18)	-	Biparental XY	Candelier et al., 2012; this study
MoIn103	671	BO, HM	p.[R693P][R693P]	G1814	8	PHM	PHM	inconc.		Di XX (18,X,Y)	+/-	Biparental XX	This study
MoIn104	674	2 BO, PHM*-GTN	p.[R693P][R693P]	G574	10	PHM	PHM	inconc.		Di XX (18,X,Y)	-	Biparental XX	This study
MoUs167	712	SA, PHM*, PHM	p.[V319I][P716A(C);Cys931X]	3932	na	CHM	CHM	2n			+	Biparental XX	This study
MoNz 170	725	CHM*-GTN, SA, CHM, HM	p.[Q310Hfs;A481T][R693W]	7759	na	CHM	CHM	2n		Di XY (X,Y,13,18,21)	-	Biparental XY**	This study
MoNz 170	725	CHM-GTN, SA, CHM*, HM	p.[Q310Hfs;A481T][R693W]	8508	na	CHM	CHM	2n		Di XY (X,Y,18)	-	Biparental XY	This study
MoUs171	733	2 HM, SA, 2 HM, IVF-PGD-HM, HM, HM	p.[L750V][L750V]	15636	na	CHM	CHM	2n		Di XX (18,X,Y,3,12)	-	Biparental XX	This study
MoUs171	733	2 HM, SA, 2 HM, IVF-PGD-HM, HM, HM	p.[L750V][L750V]	3005	na	CHM	CHM	2n		Di XX (18,X,Y,3, 11,12)	-	Biparental XX	This study
MoCA179	744	PHM*, BO, 2 SA, HM, SA, CHM	p.[E340Q6 X10][R693W]	100090	na	CHM	eCHM	2n			-	Biparental XY	This study
MoCA179	744	PHM, BO*, 2 SA, CHM, SA, CHM	p.[E340Q6 X10][R693W]	10282	na	CHM	eCHM	2n			-	Biparental XY	This study
MoCA179	744	PHM, BO, 2 SA, CHM*, SA, CHM	p.[E340Q6 X10][R693W]	27404	8	CHM	eCHM	2n			+	Biparental XY	This study
MoCA179	744	PHM, BO, 2 SA, HM, SA, CHM*	p.[E340Q6 X10][R693W]	21689	9	CHM	CHM	2n		Di XY (18,X,Y,11,3)	-	Biparental XY	This study
MoMs341	1074	SA, PHM-CC, 5 SA, HM, CHM*	p.[Tyr872X]c.[2810+2T>G]	9449	8	CHM	CHM	na			-	Biparental XY	This study
MoIn381	1142	SA, CHM, PHM*	p.[R693P][R693P]	G 4721	na	CHM	PHM	2n		Di XY (18,X,Y)	inconc.	Biparental XY	This study
MoUs420	1200	CHM*, CHM	p.[R693Q]c.[2130-	8454	11.5	CHM	CHM	2n			-	Biparental XY	This study
MoUs420	1200	CHM, CHM*	p.[R693Q]c.[2130-	5644	8	PHM	PHM	2n			-	Biparental XY	This study
MoCa408	2000	CHM*, SA, CHM-GTN, CHM-GTN	p.[G487E;Glu508 Aspfs*27];[G487E;Glu508 Aspfs*27]	10509	10.5	CHM	CHM	2n			-	Biparental XY	This study
MoCa408	2000	CHM, SA, CHM-GTN*, CHM-GTN	p.[G487E;Glu508 Aspfs*27];[G487E;Glu508 Aspfs*27]	17467	na	CHM	CHM	2n			-	Biparental XX	This study
MoCa408	2000	CHM, SA, CHM-GTN, CHM-GTN*	p.[G487E;Glu508 Aspfs*27];[G487E;Glu508 Aspfs*27]	3661	8	CHM	CHM	2n			-	Biparental XY	This study

Reproductive outcomes are listed in chronological order from left to right. Mutations are in bold; rare or low-frequency non-synonymous variants (NSVs) are underlined; common NSVs are in black; NP, indicates normal pregnancy; SB, still birth; END, early neonatal death; CC, choriocarcinoma; BO, blighted ovum; SA, spontaneous abortion; HM, hydatidiform mole; PHM, partial HM; CHM, complete HM; GTN, gestational trophoblastic neoplasia; PTD, persistent trophoblastic disease; IVF, in-vitro fertilization; IM, invasive mole; FISH, fluorescent in-situ hybridization; Di XX, diploid biparental XX; Di XY, diploid biparental XY; na., not available; inconc., inconclusive. Chromosome tested by FISH are given between parenthesis. *, indicates the corresponding POC that was analyzed in that specific row. **, amelogenin marker failed to amplify to determine the gender of this POC.

PREFACE TO CHAPTER 3

The comprehensive characterization of the HMs from patients with RHM helped us to understand the differences between HMs from patients with and without mutations in the known genes at that time and helped us identify the 3 new genes. This study, described in Chapter 3, required tremendous efforts from different lab members, mainly to recruit a high number of patients and retrieve their archived HM tissues from several laboratories. The results of this study and the categorization of the patients into appropriate subgroups facilitated our work on the identification of new genes for this condition and allowed us to demonstrate the mechanism of their HM.

CHAPTER 3

The genetics of recurrent hydatidiform moles: new insights and lessons from a comprehensive analysis of 113 patients

Ngoc Minh Phuong Nguyen¹, Yassemine Khawajkie³, Nawel Mechtouf¹, Maryam Rezaei¹, Magali Breguet⁴, Elvira Kurvinen⁵, Sujatha Jagadeesh⁶, Asli Ece Solmaz⁷, Monica Aguinaga⁸, Reda Hemida⁹, Mehmet Ibrahim Harma¹⁰, Cécile Rittore¹¹, Kurosh Rahimi¹², Jocelyne Arseneau¹³, Karine Hovanes¹⁴, Ronald Clisham¹⁵, Tiffanee Lenzi¹⁶, Bonnie Scurry¹⁷, Marie-Claude Addor¹⁸, Rashmi Bagga¹⁹, Genevieve Girardet Nendaz²⁰, Vildana Finci²¹, Gemma Poke²², Leslie Grimes²³, Nerine Gregersen²⁴, Kayla York²⁵, Pierre-Adrien Bolze²⁶, Chirag Patel²⁷, Hossein Mozdarani²⁸, Jacques Puechberty²⁹, Jessica Scotchie³⁰, Majid Fardaei³¹, Muge Harma¹⁰, R.J. McKinlay Gardner²²², Trilochan Sahoo¹⁴, Tracy Dudding-Byth³², Radhika Srinivasan³³, Philippe Sauthier⁴, Rima Slim^{1,2,3*}

¹Departments of Human Genetics and ²Obstetrics and Gynecology, ³Division of Experimental Medicine,

¹³Department of Pathology, McGill University Health Centre, Montreal, Quebec, Canada

⁴Department of Obstetrics and Gynecology, Centre Hospitalier de l'Université de Montréal (CHUM), Centre Intégré de Cancérologie du CHUM, Registre des Maladies Trophoblastiques du Québec, Montréal, Québec, Canada

⁵Medical geneticist, Tartu University Hospital United Laboratories, Department of Clinical Genetics, 6 Hariduse Street, Tallinn 10119, Estonia

⁶Mediscan Systems, 197, Dr. Natesan Road, Mylapore, Chennai-4, India

⁷Ege University Faculty of Medicine, Department of Medical Genetics, Turkey

⁸Genetics and Genomics Department, Instituto Nacional de Perinatologia, Mexico City

⁹Obstetrics and Gynecology, Mansoura University, Egypt

¹⁰Departments of Obstetrics and Gynecology and Gynecologic Oncology, Bulent Ecevit University, Medical Faculty, 67100 Kozlu, Zonguldak, Turkey

¹¹Unité médicale des maladies Auto-inflammatoires, Hôpital Arnaud de Villeneuve, 371 avenue du Doyen Gaston Giraud, 34295 Montpellier Cedex 5, France

¹²Department of Pathology, Hôpital Notre-Dame, Université de Montréal, Montréal, Québec, Canada

¹⁴CombiMatrix Diagnostics, Irvine, California, USA

¹⁵Departments of Obstetrics & Gynecology, Tulane University School of Medicine. Los Angeles, USA

- ¹⁶ Maternal Fetal Medicine and Genetics, Tennessee Maternal Fetal Medicine PLC, 300 20th Avenue North, Suite 702, Nashville TN, USA 37203
- ¹⁷ Pathology Queensland, Royal Brisbane and Women's Hospital and Lady Cilento Children's Hospital, Queensland, Australia
- ¹⁸ Service de Médecine Génétique, CHUV - 1011 Lausanne, Switzerland
- ¹⁹ Department of Obstetrics & Gynecology, Post Graduate Institute of Medical, Education and Research, PGIMER, Chandigarh, India
- ²⁰ FMH Gynécologie-Obstétrique, Genève, Suisse
- ²¹ Département de médecine génétique et de laboratoire, Service de pathologie clinique, Centre Médical Universitaire (CMU), CH-1211 Genève 4, Genève, Suisse
- ²² Genetic Health Service, Central Hub, Wellington Hospital, Private Bag 7902, Wellington 6242, New Zealand
- ²³ University of Colorado Hospital, Colorado, USA
- ²⁴ Genetic Health Service New Zealand – Northern Hub, Auckland City Hospital, P/Bag 92024, Auckland, 1142, New Zealand
- ²⁵ Essentia Health, Duluth Clinic, Duluth MN 55805-1983, USA
- ²⁶ Department of Gynecological Surgery and Oncology, Obstetrics, and †French Center for Trophoblastic Diseases, University Hospitals of Lyon, Lyon, France
- ²⁷ Genetic Health Queensland, Royal Brisbane & Women's Hospital, Brisbane, Australia
- ²⁸ Department of Medical Genetics, Faculty of Medical Sciences, Tarbiat Modares University, Tehran, Iran
- ²⁹ Département de Génétique Médicale, Hôpital Arnaud de Villeneuve, 371 avenue du Doyen Gaston Giraud, 34295 Montpellier cedex 5, France
- ³⁰ Tennessee Reproductive Medicine, 6031 Shallowford Rd, Suite 101, Chattanooga, TN, 37421 USA
- ³¹ Department of Medical Genetics, Shiraz University of Medical Sciences, Shiraz, Iran
- ³² Hunter Genetics and University of Newcastle, GrowUpWell Priority Research Centre, Newcastle, NSW, Australia
- ³³ Cytology & Gynecological Pathology, Post Graduate Institute of Medical Education And Research, PGIMER, Chandigarh, India

Manuscript published in **Modern Pathology**, February 2018

(PMID: 29463882)

Abstract

Hydatidiform mole is aberrant human pregnancy characterized by early embryonic arrest and excessive trophoblastic proliferation. Recurrent hydatidiform moles are defined by the occurrence of at least two hydatidiform moles in the same patient. Fifty to eighty percent of patients with recurrent hydatidiform mole have bi-allelic pathogenic variants in *NLRP7* or *KHDC3L*. However, in the remaining patients, the genotypic types of the moles are unknown. We characterized 80 new hydatidiform mole tissues, 57 of which were from patients with no mutations in the known genes, and we reviewed the genotypes of a total of 123 molar tissues. We also reviewed mutation analysis in 113 patients with recurrent hydatidiform moles. While all hydatidiform moles from patients with bi-allelic *NLRP7* or *KHDC3L* mutations are diploid biparental, we demonstrate that those from patients without mutations are highly heterogeneous and only a small minority of them are diploid biparental (8%). The other mechanisms that were found to recur in patients without mutations are diploid androgenetic monospermic (24%), and triploid dispermic (32%); the remaining hydatidiform moles were misdiagnosed as moles due to errors in the analyses and/or their unusual mechanisms. We compared three parameters of genetic susceptibility in patients with and without mutations and show that patients without mutations are mostly from non-familial cases, have fewer reproductive losses, and more live births. Our data demonstrate that patients with recurrent hydatidiform moles and no mutations in the known genes are, in general, different from those with mutations; they have a milder genetic susceptibility and/or a multifactorial etiology underlying their recurrent hydatidiform moles. Categorizing these patients according to the genotypic types of their recurrent hydatidiform moles may facilitate the identification of novel genes for this entity.

Introduction

Hydatidiform mole is an aberrant human pregnancy characterized by abnormal embryonic development and excessive proliferation of the trophoblast. It occurs once in every 600-1000 pregnancies in Western countries but at higher frequencies in Latin America, Africa, the Middle East, and the Far East [3; 4](#). Among women with one hydatidiform mole (sporadic hydatidiform mole), about 1%-9% develops a second mole (recurrent hydatidiform moles), depending on populations and studies [8-13](#).

At the histopathological level, hydatidiform mole is classified as complete hydatidiform mole or partial hydatidiform mole. Complete hydatidiform moles have marked circumferential trophoblastic proliferation and, in general, lack embryonic tissues with the exception of extremely rare cases where inner cell derivatives were observed [156; 157](#). Partial hydatidiform moles have moderate focal trophoblastic proliferation and may contain embryonic tissues [138](#). At the genotypic level, complete hydatidiform moles are mostly diploid androgenetic (both chromosome complements are of paternal origin), while partial hydatidiform moles are mostly triploid dispermic (one maternal chromosome and two paternal chromosome complements). Non-molar miscarriages lack significant trophoblastic proliferation and are mostly diploid biparental (one maternal and one paternal chromosome complements) with or without aneuploidies. As microscopic evaluation of products of conception is mainly descriptive and not always sufficient to classify subgroups of hydatidiform moles and distinguish them from non-molar miscarriages, various methods have been developed to determine the parental contribution to such tissues and establish a more reliable diagnosis based on histopathological examination and parental contribution to the product of conception. Among these methods, short tandem repeat genotyping is used to identify the ploidy of the product of conception and the parental contribution to their

genomes; immunohistochemistry of p57^{KIP2} (a paternally imprinted, maternally expressed gene) is used to distinguish diploid androgenetic hydatidiform mole from most other genotypic types due to the lack of p57^{KIP2} expression in the cytotrophoblast and villous stroma of androgenetic hydatidiform mole; and flow cytometry is used to determine the ploidy of the tissues. Fluorescent in situ hybridization (FISH) is also used for determining the ploidy of the tissues, as well as for investigating the presence of mosaicisms. Previous studies have shown an important improvement in the diagnosis of hydatidiform mole by using different methods and integrating their results [139](#); [142](#).

By studying familial cases of recurrent hydatidiform moles, *NLRP7* and *KHDC3L* were found to be responsible for recurrent hydatidiform moles [57](#); [80](#). To date (including this study), ~70 and 6 pathogenic variants, observed in a recessive state, have been described in *NLRP7* (<http://fmf.igh.cnrs.fr/ISSAID/infevers/>) and *KHDC3L*, respectively. Recently, we demonstrated a high frequency of Alu-mediated deletions and rearrangements in *NLRP7* [158](#). All recurrent hydatidiform moles from patients with mutations in these two genes are diploid biparental with the exception of three cases, one reported to be triploid dispermic [134](#) and two reported to be triploid digynic [130](#).

In this study, we report ten novel pathogenic variants in *NLRP7*, two of which mediated by Alu repeats, and review our mutation analysis in *NLRP7* and *KHDC3L* on 113 unrelated patients with at least two hydatidiform moles. We used different approaches to comprehensively characterize the parental contribution to 23 and 57 products of conception from patients with and without recessive mutations in the known genes, respectively. We show that all products of conception from patients with *NLRP7* or *KHDC3L* recessive mutations are diploid biparental, while those from patients without mutations are highly heterogeneous and only a minority of them

are diploid biparental. We compared various parameters of genetic susceptibility between patients with and without mutations and found that a family history of moles is very rare among patients without mutations in the known genes. In addition, these patients have less reproductive losses and more live births. Our data suggest that patients with recurrent hydatidiform moles and no mutations in the known genes have a milder genetic susceptibility to reproductive losses and some of them may have polygenic and/or multifactorial aetiologies underlying their recurrent hydatidiform moles.

Materials and methods

Patients

The study was approved by the McGill Institutional Review Board (IRB# A01-M07-98 03A). Patients with at least 2 hydatidiform moles (all forms combined) were referred to our laboratory between 2002 and 2017 from various collaborators or recruited at the Quebec Trophoblastic Disease Registry (<http://www.rmtq.ca/en/>). All patients provided written consents to participate in our study, gave blood samples for mutation analysis, and agreed for us to retrieve their products of conception, from various histopathology laboratories, for research purposes.

Mutation analysis

NLRP7 and *KHDC3L* mutation analyses were performed on genomic DNA by PCR amplification of all their exons and Sanger sequencing in the two directions as previously described [81](#); [120](#). PCR conditions and the sequences of the primers used to amplify the junction fragments are provided in Supplementary Table 3.1. Variants nomenclature of *NLRP7* is given according to the following

references, NM_001127255.1 (cDNA), NG_008056.1 (genomic), and Q8WX94 (protein). Exon numbering is as in NG_008056.1.

Histopathological review

Morphological evaluation of the products of conception was performed on tissue sections stained with hematoxylin and eosin independently by at least two experts in the histology of molar pregnancies (JA, RK, and RS) according to standard criteria [138](#).

Parental contribution to the molar tissues

p57^{KIP2} immunohistochemistry. P57^{KIP2} immunohistochemistry was performed on 4- μ m sections of formalin-fixed paraffin-embedded tissues as previously described [122](#). For each product of conception, the p57^{KIP2} immunostaining result was interpreted as negative when maternal decidua and/or extravillous trophoblastic cells, which serve as internal positive control, exhibited nuclear p57^{KIP2} staining but villous stromal and cytotrophoblast cells did not exhibit staining. The result was interpreted as positive when villous stromal and cytotrophoblast cells showed nuclear staining of p57^{KIP2}.

Flow cytometry. Flow cytometry was performed on formalin fixed paraffin embedded tissues that were prepared according to standard methods. Cellular preparation for flow cytometry was performed according to a Hedley's protocol [159](#) as previously described [160](#). Briefly, two sections of 60 μ m were cut from each formalin fixed paraffin embedded block, deparaffinized with xylene, and gradually rehydrated. The proteins were digested in 1 ml of 5 mg/ml pepsin (Sigma-Aldrich, St Louis, USA) in 0.9% NaCl (adjusted to pH 1.5 with HCl). The cellular suspension was then

suspended in propidium iodide solution (0.1 mg/μl, Sigma-Aldrich) and 50 μl RNase (1 mg/ml) and incubated at 37°C for 30 min. Finally, they were filtered through a 48 μm mesh nylon filter and analyzed using a BD FACS Canto II at the Immunophenotyping Core Facility of the McGill University Health Centre Research Institute. Data files were analyzed using FCSalyzer (Wien, Austria).

Microsatellite DNA genotyping. On the basis of the quantity of chorionic villi in the formalin fixed paraffin embedded blocks, 5-12 serial 10 μm sections were prepared from the blocks with the largest amount of chorionic villi that are separated from maternal tissues. The sections were mounted on slides and stained with hematoxylin and eosin (H&E). Under a stereomicroscope, chorionic villi were collected from the slides using Kimwipes and forceps and used for DNA extraction using the QIAamp DNA formalin fixed paraffin embedded Tissue Kit (Qiagen, Hilden, Germany). Extracted DNA was quantified using a Nanodrop and loaded on an agarose gel to evaluate its quality and the required amount for multiplex fluorescent microsatellite genotyping with the PowerPlex 16 HS System (Promega, Corporation, Fitchburg, Wisconsin, USA). The reaction consists of short tandem repeat multiplex PCR assay that amplifies DNA at 15 different short tandem repeat loci and a fragment from the Amelogenin gene. DNA from the products of conception and their available parents was amplified, and the PCR products were resolved by capillary electrophoresis using an Applied Biosystems 3730xl DNA Analyzer (Applied Biosystems, Foster City, CA, USA) at the Centre for Applied Genomics (<http://www.tcag.ca>). The data were analyzed with PeakScanner, version 1.0 (Applied Biosystems, Foster City, CA, USA) and the product of conception alleles were compared to the parental alleles to determine their origin.

Fluorescent in situ hybridization. Fluorescent in situ hybridisation (FISH) was performed on 4 µm sections, which were hybridised systematically with centromeric probes from chromosomes, X, Y and 18, as previously described [31](#). On some tissues, other probes were also used. At least 100 cells for each product of conception, from different microscopic fields, were scored with each probe.

Microarray analysis. Microarray analysis was performed on blood DNA from patients with no identified mutations in either *NLRP7* or *KHDC3L* to search for large deletions or rearrangements using Cytoscan HD (Affymetrix, Santa Carla, CA, USA). We note that the Cytoscan HD microarray contains 32 markers in the genomic sequence of *NLRP7*, of which 6 are single nucleotide polymorphisms (SNP); most of these markers are located in the region spanning from intron 4 to exon 11. Consequently, this microarray is not sensitive to detect *NLRP7* deletion upstream of intron 4. For *KHDC3L*, because of its small genomic size (1495-bp, from the first nucleotide of exon 1 to the last nucleotide of exon 3), there are only two markers from its genomic sequence on the Cytoscan HD microarray and only one of them is a SNP marker. Consequently, the Cytoscan HD does not allow reaching a conclusion on the presence of deletions or rearrangements in *KHDC3L*. Another SNP microarray platform was performed at Combimatrix to search for aneuploidies in formalin fixed paraffin embedded tissues from one product of conception as previously described [161](#).

Search for deletions by quantitative real time PCR (qPCR) and multiplex ligation-dependent probe amplification. qPCR on genomic DNA from patient 1566 was performed using Quantifast SYBR-

green PCR kit (Qiagen, Toronto, ON, Canada). Each sample was checked in duplicates using the Bio-Rad MiniOpticon Real Time PCR system (Bio-Rad Laboratories, Mississauga, ON, Canada) and analyzed by the Opticon Monitor software (Bio-Rad Laboratories). The comparative CT method ($\Delta\Delta$ CT method) was used for relative quantification, and data was normalized against an endogenous control primer that amplifies exon 11 of *NLRP7*, for which the two alleles are amplified based on the presence of a heterozygous SNP. For the other samples, patient 1 and her family members and patient 6, multiplex ligation-dependent probe amplification was performed, as previously described [162](#).

Results

Ten novel pathogenic variants in *NLRP7*

To date, our laboratory has performed *NLRP7* mutation analysis on a total of 113 unrelated patients with at least 2 hydatidiform moles. This analysis revealed *NLRP7* pathogenic variants observed in a recessive state in 62 out of 113 unrelated patients (55%). Many of these variants were previously reported by our group [57-59](#); [115](#); [137](#); [158](#); [163](#) and others [60](#); [132](#); [164](#) and ten are novel. The novel variants are a missense, three stop codon gain, four small deletions, an insertion of Alu Yb element, and an Alu-mediated large deletion removing 9287-bp from the promoter region. All these variants are listed in Table 3.1 and their chromatograms are shown in Figure 3.1 and Supplementary Figures S3.1A and S3.1B. The missense variant affects a conserved amino acid and is predicted to be pathogenic (polyphen score=0.998); eight variants lead to protein truncations and one removes part of the promoter region and is predicted to affect *NLRP7* transcription. Consequently, these ten mutations are most likely pathogenic.

Mutation analysis of patient 1590 was initially performed by Whole Exome Sequencing by the referring laboratory and revealed only a previously reported missense pathogenic variant, c.2077C>T, p.(Arg693Trp), in a heterozygous state. Exome sequencing analysis had shown a significant low coverage in exon 4 with high number of recurrent soft-clipped reads (sequences that did not align with the reference sequence) that displayed significant similarities with Alu sequences when compared to databases. Because the patient had three recurrent hydatidiform moles and such phenotype is considered to be severe in our judgment and is associated with recessive mutations, we then repeated the search for *NLRP7* mutations by PCR amplification of genomic DNA followed by Sanger sequencing. Analysis of the amplified fragments by gel electrophoresis revealed an abnormal amplicon with primers located in exon 4 that is approximately 350-bp larger than the normal fragment in the patient and in her father (Figure 3.1). Gel extraction and sequencing of the abnormal fragment showed that it contains an Alu Yb8 element inserted in exon 4 at position c.1548 and identified a duplication of 18-bp at the site of the Alu Yb8 insertion, c. [1548_1566dup;1566_1567insAF15169.2: g.106_419] (Figure 3.1).

In patient 1566, only a stop gain variant c.2227G>T, p.(Glu743*), was found in a heterozygous state in exon 6. Because the patient had five recurrent hydatidiform moles and again such phenotype is in our judgment severe, we suspected the presence of a deletion on the other allele. Cytoscan HD microarray did not reveal any deletion (Supplementary Figure S3.2) but since this microarray does not cover the region upstream of intron 4 of *NLRP7*, we performed quantitative PCR (qPCR) with three amplicons located in the region of the suspected deletion. The result of this analysis with two amplicons suggested the presence of hemizygoty (Supplementary Figure S3.3). We next sequenced *NLRP7* amplicons containing common SNP, intronic, and promoter regions not covered by our standard *NLRP7* mutation analysis in this patient and in her

mother and grandmother. We also used long range PCR to amplify various large fragments covering the suspected deleted region. The results of these analyses led to the identification of a large deletion of 9287-bp that starts 6950-bp upstream of exon 1 and ends 2300-bp downstream of exon 1, that we define at the nucleotide level to c.-7026_-40+2300del (Figure 3.1 and Supplementary table 3.1). This deletion removes the entire *NLRP7* promoter that is predicted by the Eukaryote Promoter Database (<http://epd.vital-it.ch/>), which spans from 499-bp upstream of exon 1 to 63-bp downstream of exon 1. This variant is therefore most likely pathogenic and is the first regulatory mutation to be described in *NLRP7*.

From the aforementioned analysis, 51 patients were found negative for recessive *NLRP7* pathogenic variants and were then screened for *KHDC3L* mutations. This analysis revealed recessive *KHDC3L* pathogenic variants in six out of the 51 patients (12%), all of which were previously reported [82](#); [158](#). In conclusion, among the 113 unrelated patients with at least 2 hydatidiform moles, recessive *KHDC3L* pathogenic variants accounted for 5% of patients with at least 2 hydatidiform moles, which is in agreement with previous findings [80](#); [130](#)

Comprehensive analysis of the parental contribution to the molar tissues

Strategy of the analysis

To better understand the pathology of recurrent hydatidiform moles in patients with no mutations in the known genes, we made extensive efforts to retrieve archived formalin fixed paraffin embedded tissues from their products of conception from various hospitals. From most products of conception, formalin fixed paraffin embedded blocks were retrieved, which gave us the possibility to use various methods to determine the parental contribution to their genomes. From others, only sections on microscopic slides were available, which limited our investigation. All

products of conception referred to us as molar pregnancies were systematically assessed by morphology by two experts in the histopathology of hydatidiform mole, and by flow cytometry, p57^{KIP2} immunohistochemistry, and microsatellite DNA genotyping. The results of the various methods were compared and in cases of discrepancies, the experiments were repeated and/or FISH was used to clarify discrepancies. On several triploid dispermic partial hydatidiform moles, FISH was also used to investigate the presence of mosaicisms. On most tissues, probes that detect chromosomes X, Y, and 18 were used. Additional probes from other chromosomes were also used on some products of conception to clarify discrepancies between our results and those sent to us from the referring laboratories or to clarify distortions between the heights of alleles observed with the microsatellite genotyping.

Hydatidiform moles from patients with recessive pathogenic variants in *NLRP7* or *KHDC3L* are all diploid biparental

We previously reported the parental contribution to the genotypes of 41 molar tissues, 36 from patients with recessive pathogenic variants in *NLRP7* [163](#) and 5 from patients with recessive pathogenic variants in *KHDC3L* [81](#) and found them all diploid biparental. Other groups obtained similar results on most of their patients with only three exceptions reported to date [130](#): [134](#). In an effort to better understand the mechanisms leading to mole formation in patients with mutations in either gene and better understand the functions of these genes, we extended our genotypic analysis to 23 additional hydatidiform mole tissues, 22 from patients with recessive pathogenic variants in *NLRP7* and one from a patient with a recessive pathogenic variant in *KHDC3L*. Our analysis demonstrated that all the 23 products of conception are diploid biparental.

In conclusion, all 64 products of conception from patients with recessive mutations in the two known genes analyzed by our laboratory to date were found diploid biparental.

Hydatidiform moles from patients with no recessive mutations in *NLRP7* or *KHDC3L* are highly heterogeneous and a minority of them are diploid biparental

From the aforementioned analysis, a total of 45 unrelated patients did not have any variant in a recessive state in *NLRP7* or *KHDC3L* that are believed to be pathogenic. To better understand the aetiologies of their recurrent hydatidiform moles, extensive efforts were done and allowed retrieving 57 “hydatidiform mole” tissues from 25 patients that we comprehensively genotyped using various approaches. A summary of the results is recapitulated in Figure 3.2 and the detailed results with the various approaches are provided in Supplementary table 3.2. To our surprise, only a minority of patients (8%) were found to have diploid biparental hydatidiform moles. Six other patients (24%) had recurrent diploid androgenetic monospermic complete hydatidiform moles, 8 patients (32%) had recurrent triploid dispermic partial hydatidiform moles, and 3 patients had, each, only one hydatidiform mole available for analysis. The remaining 6 patients did not have recurrent hydatidiform moles because one or two of their “hydatidiform mole” were revised to non-molar miscarriages. Below a summary of our analyses and results.

Patients with recurrent hydatidiform moles

Two unrelated patients with diploid biparental complete hydatidiform moles. Patient 1 has a half-sister, who also had recurrent hydatidiform moles. Six products of conceptions from these two sisters were re-examined by us and five fulfilled the morphological criteria of complete hydatidiform mole; all were evaluated for p57^{KIP2} expression, two were found positive, two

negative, and two with negative and positive cells; three complete hydatidiform moles, from patient 1's sister, were genotyped and found diploid biparental. The full description and the characterization of these tissues are described by Scurry *et al.* (in preparation). From patient 2, three products of conception were analyzed, all fulfilled the criteria of complete hydatidiform mole; two were evaluated for p57^{KIP2} expression, one was found positive and one was found negative; and two were genotyped and found diploid biparental. These are the only patients out of 25 (without mutations in the two known genes) and with recurrent diploid biparental hydatidiform moles (8%).

Because 1) these patients were found to have diploid biparental complete hydatidiform moles, 2) most patients with diploid biparental complete hydatidiform moles are found to have *NLRP7* recessive mutations, and 3) *NLRP7* has a high frequency of Alu-mediated deletions [158](#), we performed microarray analysis using Cytoscan HD (Supplementary Figure 3.2) and multiplex ligation-dependent probe amplification for *NLRP7* (Supplementary Figure S3.3) on blood DNA from patient 1, her half-sister and father, and on patient 2. However, we did not detect any deletion or rearrangement in *NLRP7* or *KHDC3L*. These three patients are the only ones in our cohort of 113 patients with recurrent hydatidiform moles, for which we found evidence for diploid biparental complete hydatidiform moles but without mutations in the known genes. Another atypical finding in these two patients is that both of them had complete hydatidiform moles that expressed p57^{KIP2} in cytotrophoblast and villous stroma cells, which we have never seen in any other sample.

Six patients with diploid androgenetic complete hydatidiform moles. Six patients, 3-8, each had 2-4 available hydatidiform mole tissues and their analysis revealed their diploid androgenetic

monospermic origin. The morphological evaluation of all these tissues fulfilled the criteria of complete hydatidiform mole and all analyzed tissues were negative for p57^{KIP2} expression.

Eight patients with triploid dispermic partial hydatidiform moles. Eight patients, 9 -16, each had two triploid dispermic conceptions. Morphological evaluation confirmed the diagnosis of partial hydatidiform mole with the exception of one product of conception (from patient 15) that did not fulfill the morphological criteria of partial hydatidiform mole and was diagnosed as non-molar miscarriage. Indeed, the triploidy of this case was discovered incidentally by flow cytometry while analyzing the partial hydatidiform mole from this patient. Patient 10 had, in addition to her two partial hydatidiform moles, one complete hydatidiform mole that was confirmed by microscopic morphological evaluation and found to be diploid androgenetic monospermic by microsatellite DNA genotyping.

Three patients with various genotypes and only one available tissue. Patients 17-19 each had 2 hydatidiform moles but we were able to have access or reach a conclusive result on only one of the two hydatidiform moles. This group consisted of patient 17 with 1 triploid dispermic partial hydatidiform mole and 1 complete hydatidiform mole that is diploid by karyotype analysis but no tissues were available for p57^{KIP2} and genotyping from the complete hydatidiform mole; patient 18 had 1 diploid dispermic complete hydatidiform mole, and patient 19 with 1 androgenetic monospermic complete hydatidiform mole.

Patients with “hydatidiform mole” revised to non-molar miscarriages

Four patients with diploid biparental non-molar miscarriages. Patients 20-23 were each referred with a history of two hydatidiform mole conceptions; however, after morphological

evaluation, the hydatidiform moles from these patients were revised to non-molar miscarriage (Figure 3.2). These products of conception did have some, but not all the morphological features of hydatidiform mole and mainly lacked significant trophoblastic proliferation. p57^{KIP2} immunohistochemistry on these products of conception revealed that three of them are positive for p57^{KIP2} expression, which is in agreement with their diagnosis as miscarriage; two products of conception were not available for p57^{KIP2} expression analysis; one product of conception was inconclusive, and 2 products of conception from patient 23 were negative for p57^{KIP2} expression.

The absence of p57^{KIP2} expression in two products of conception from patient 23 was in contradiction with their histopathological diagnosis as non-molar miscarriage mainly due to the lack of trophoblastic proliferation (Figure 3.3a-d). Microsatellite genotyping on the first product of conception showed the presence of a non-maternal, 173-bp, and the lack of the maternal allele, 176-bp, at marker TH01 located on 11p15. However, this product of conception had the maternal allele, 232-bp, on a proximal marker, D11S1983, located on 11q12-13 suggesting a partial deletion of chromosome 11 (Figure 3.3c). Microarray analysis at Combimatrix on DNA from formalin fixed paraffin embedded tissues from this product of conception revealed a terminal microduplication of 3.9-Mb on 4p16.3 and a microdeletion of 3.6-Mb on 11p15.5-p15.4 (NCBI build GRCh37/hg, Feb. 2009) (Figure 3.3f) that removes *CDKN1C*, the gene coding for p57^{KIP2}. The microarray data in combination with those of microsatellite genotyping demonstrate that the 3.6-Mb deletion is on the maternal chromosome 11 and explains the lack of p57^{KIP2} expression in this product of conception. The second product of conception from this patient, which was also diploid biparental by microsatellite genotyping, was uninformative for marker TH01, which showed a single allele of 176-bp that could be in a hemi- or homozygous state. Since the partner DNA was not available, no conclusion could be reached on marker TH01 in the second product of

conception and there were not enough tissues from this product of conception for microarray analysis. Consequently, we could not further investigate why this product of conception is negative for p57^{KIP2} expression.

Two patients with tetraploid non-molar miscarriages. Two patients, 24 and 25, were referred to us because they each had 2 hydatidiform moles, but after comprehensive analysis, only one product of conception from each patient was found triploid dispermic and fulfilled morphological criteria of partial hydatidiform mole. The two other products of conception did not fulfill morphological criteria of hydatidiform mole and were therefore diagnosed as non-molar miscarriage. In patient 24, the tetraploid genome was not detected by microsatellite genotyping since the tissues had two identical maternal and two identical paternal genomes (XXYY) and displayed a normal diploid biparental genotype. Because the microsatellite genotyping result was in contradiction with a medical report indicating a trisomy for chromosome 17, obtained by FISH on tissue sections by the referring laboratory, we performed FISH on tissue sections with probes from chromosomes X, Y, 10, 11, and 17. Our results showed a tetraploid genotype with XXYY in more than 100 analyzed cells. In patient 25, microsatellite genotyping did not lead to a conclusive result on her first product of conception because of the presence of several non-maternal alleles and the absence of DNA from the first partner of the patient with whom she had the tetraploid conception. FISH on this tissue failed to reach a conclusion because of a technical reason (the provided slides by the referring laboratory were not positively charged). However, karyotype analysis from the referring laboratory documented a tetraploid karyotype, 92, XXXY, which most likely does not originate from contamination with maternal cells and therefore we concluded that this tissue is tetraploid.

Comparison of the genetic susceptibility for recurrent hydatidiform moles between patients with and without recessive mutations in *NLRP7* or *KHDC3L*

Less familial cases of recurrent hydatidiform moles among patients without recessive mutations in the known genes. Our laboratory has been analyzing patients for mutations in *NLRP7* and *KHDC3L* genes since their identification in 2006 [57](#) and 2011 [80](#), respectively. Our consistent observation over these years has always been that most patients from familial cases of recurrent hydatidiform moles are found to have to have recessive mutations mostly in *NLRP7* and the remaining in *KHDC3L*. Among the 113 unrelated patients with recurrent hydatidiform moles that we analyzed, 68 had recessive mutations in either gene and of these, 19 patients were from familial cases and had other relatives with recurrent hydatidiform moles. However, among a total of 45 unrelated patients with no recessive mutations in either gene, only one patient has a half-sister with recurrent hydatidiform moles. The difference in the number of familial cases between patients with and without mutations is statistically significant $p=0.00027$ (Fisher exact test, 95% confidence) (Figure 3.4a).

Less reproductive losses and more live births among patients without recessive mutations in the known genes. Another consistent observation is that most patients with high number of recurrent hydatidiform moles, even those who are not from familial cases, turn out to have recessive mutations mainly in *NLRP7* or in *KHDC3L*. To investigate the relevance of this observation, we compared the number of pregnancy losses in patients with (mutations positive) and without recessive pathogenic variants (mutations negative) (Figure 3.4b). In this analysis, we included the patients and their affected relatives (a total of 137 patients) and counted all their reproductive losses. We also combined all reproductive losses (hydatidiform moles and miscarriages) to avoid variations due to histopathological misdiagnosis of hydatidiform mole since not all the

reproductive losses were available to us for re-evaluation. The numbers of pregnancy losses were divided into three groups, at least 7 (≥ 7) pregnancy losses, 4 to 6 (4-6) pregnancy losses, and less or equal to 3 (≤ 3) pregnancy losses and their analysis showed that the highest numbers of pregnancy losses, ≥ 7 and 4-6, are more frequent in patients with recessive pathogenic variants in either *NLRP7* or *KHDC3L* while the lowest number of pregnancy losses (≤ 3) was more frequent among patients with no mutations in either gene and this difference was statistically significant ($p=0.01088$). In addition, patients with identified recessive pathogenic variants had less live births than patients with no recessive pathogenic variants (8 live births out of a total of 429 pregnancies in patients with mutations versus 28 live births out of 196 in patients with no mutations, respectively) (p -value=0).

Discussion

In this study, we report the identification of seven novel variants in *NLRP7*, two of which are mediated by Alu elements, an insertion in exon 4 and a deletion in the promoter regulatory region. Both Alu-mediated variants, the insertion in the coding region and the deletion that affects only the regulatory non-coding region, are described here for the first time in *NLRP7*. Our data confirm our previous observation on the high frequency of Alu-mediated deletions and rearrangements in *NLRP7* [158](#). Among the 113 unrelated patients referred with at least two hydatidiform moles analyzed to date by our laboratory, 68 had pathogenic variants in a recessive state, 62 (55%) in *NLRP7* and 6 in *KHDC3L* (5%); the remaining 45 patients did not have any detectable pathogenic variants in a recessive state by the used methods (Figure 3.5).

We previously reported a comprehensive analysis of the parental contribution to 41 products of conceptions from patients with two defective alleles in *NLRP7* [163](#) or *KHDC3L* [81](#) and demonstrated that they are all diploid biparental. In this study, we extended our comprehensive

analysis to 23 additional products of conception and found all of them again diploid biparental. Other groups have also reported that molar tissues from such patients are mostly diploid biparental [133](#). Deviation from this genotype has thus been reported only in three hydatidiform mole tissues [130](#); [134](#). However, these three tissues were not comprehensively analyzed with various methods. Based on our data and our extensive experience in genotyping formalin fixed paraffin embedded archived tissues, we believe that no single genotyping method is perfect and all methods have their own limitations, especially when working with formalin fixed paraffin embedded tissues. It was the integration and reconciliation of the results from various methods that revealed several mistakes and inaccuracies of results obtained by some methods. We therefore recommend that any deviation from the diploid biparental genotype, in patients with recessive pathogenic variants in *NLRP7* or *KHDC3L*, be investigated and documented by various methods. This will improve our understanding of the consequences of mutations in the two genes on oogenesis and normal fertilization.

Because recurrent hydatidiform moles may have different genotypes, in an effort to homogenize the category of patients with no mutations and facilitate the identification of novel genes responsible for this entity, we retrieved 57 hydatidiform mole conceptions (as per referral) from 25 patients without recessive pathogenic variants in the known genes. Genotypic analysis of these 57 hydatidiform moles using various approaches demonstrated that recurrent hydatidiform moles from these patients are highly heterogeneous. The three mechanisms that were found to recur in our cohort of 25 patients are diploid biparental in 8%, diploid androgenetic monospermic in 24%, and triploid dispermic in 32%. In 6 patients, one or two of their tissues were misdiagnosed as hydatidiform mole because of two main reasons, (i) errors in the analyses (at the level of histopathology and/or genotyping) and (ii) the presence of very rare mechanisms such as the 3.6-

Mb deletion on 11p15 and the tetraploid non-molar miscarriages. In such unusual cases, the use of additional characterization methods helped reaching a correct diagnosis. Interestingly, the breakpoint on 11p15 in our patient is very close to a previously reported deletion in two patients with a molar like-phenotype and deletions of 3.2-Mb and 3.6-Mb from the short arm telomere of chromosome 11 [165](#), which suggests the presence of repetitive elements in this region that could be mediating these different deletions that remain to be investigated in the future. The presence of a small deletion on 11p15 and duplication on 4p16.3 suggests that the patient may be a carrier for a cryptic balanced reciprocal translocation involving 11p15 and 4p16.3 that may be responsible for her four miscarriages.

In our cohort, the number of triploid dispermic partial hydatidiform moles did not exceed two in any of the eight patients, which is in agreement with a previous observation [166](#) and suggests a mild genetic susceptibility underlying the genotypic entity of triploid dispermic partial hydatidiform mole. However, androgenetic monospermic complete hydatidiform mole recurred 3-4 times in three out of six patients. In general, recurrent hydatidiform moles in the same patients tended to have the same genotypes with only three exceptions. One patient had 2 triploid dispermic partial hydatidiform moles and 1 complete hydatidiform mole by histopathology and two others had each one tetraploid and one triploid dispermic product of conception.

We compared various parameters and indicators of genetic susceptibility between patients with and without recessive mutations in the two known genes. Our analysis demonstrated that a family history of recurrent hydatidiform moles is very rare among patients without pathogenic variants in the two genes and is significantly associated with the presence of pathogenic variants in *NLRP7* or *KHDC3L* ($p=0.00027$). In addition, low numbers of pregnancy losses (hydatidiform

moles or miscarriages) and high numbers of live births were significantly associated with patients without recessive pathogenic variants in the known genes ($p=0.01088$ and $p=0.0000$, respectively).

Altogether, our data demonstrate that recurrent hydatidiform moles from patients without mutations in the known genes are highly heterogeneous and a minority of them (8%) have diploid biparental genomes. Moreover, our data suggest that patients without recessive pathogenic variants in the known genes have a milder genetic susceptibility for recurrent hydatidiform moles. Consequently, a genetic defect segregating in their families may not always manifest as molar pregnancies. One explanation for this observation is that recurrent hydatidiform moles in some of these patients may have polygenic and/or multifactorial aetiologies that may decrease their manifestation in other siblings since only those who inherited variants in several genes may manifest the defect.

In conclusion, patients with no recessive mutations in the known genes are different from those with mutations and have other mechanisms and molecular bases at the origin of their recurrent hydatidiform moles that remain to be elucidated in future studies.

Acknowledgement

We thank the patients and their families for their cooperation. We thank Sam Dougaparsad from Affymetrix for his kind technical assistance in the analysis of Cytoscan HD; Urvashi Surti and Lori Hoffner for performing FISH on tissue sections; and Judith St-Onge for her help in the primer design for long-range PCR. We acknowledge the use of the McGill University and Génome Québec Innovation Centre for Sanger sequencing. We also thank the Departments of Pathology of the following hospitals and medical centers, Greater Nashville Perinatology (TN, USA), Nashville

Fertility Center (TN, USA), INTEGRIS Baptist Medical Center (OK, USA), Wellington Hospital-Genetics Health Service (New Zealand), Essentia Health Duluth (MN, USA), Falls Memorial Hospital (MN, USA), Maisonneuve Rosemont Hospital (QC, Canada), Notre Dame Hospital (QC, Canada), Pathology Queensland Laboratory (Australia), Toowoomba Hospital (Australia), Auckland City Hospital (New Zealand), Touro Laboratory (NO, USA), Saint Justine Hospital (QC, Canada), Vaudois University Hospital (Switzerland), Evergreen Hospital Medical Center (Kirkland, USA), Providence Regional Laboratories (Portland, USA), St Mary's Hospital Center (QC, Canada), Johnston Memorial Hospital (NC, USA), Erlanger Medical Center (TN, USA), Pole Hospitalo-Universitaire Naissance Et Pathologie De La Femme (Montpellier, France), East Tallinn Central Hospital (Estonia), IWK Health Centre (Halifax, Canada), Victoria General Hospital (Nova Scotia, Canada), for providing archived molar tissues.

Funding

NMPN was supported by fellowships from Réseau Québécois en Reproduction, McGill Faculty of Medicine, RI-MUHC Desjardins Studentship in Child Health Research, and CRRD. Yasmine Khawajkie was supported by a CRRD trainee fellowship. RS is supported by the Canadian Institute of Health Research (MOP-86546, POP-122897, and MOP-130364).

Figures

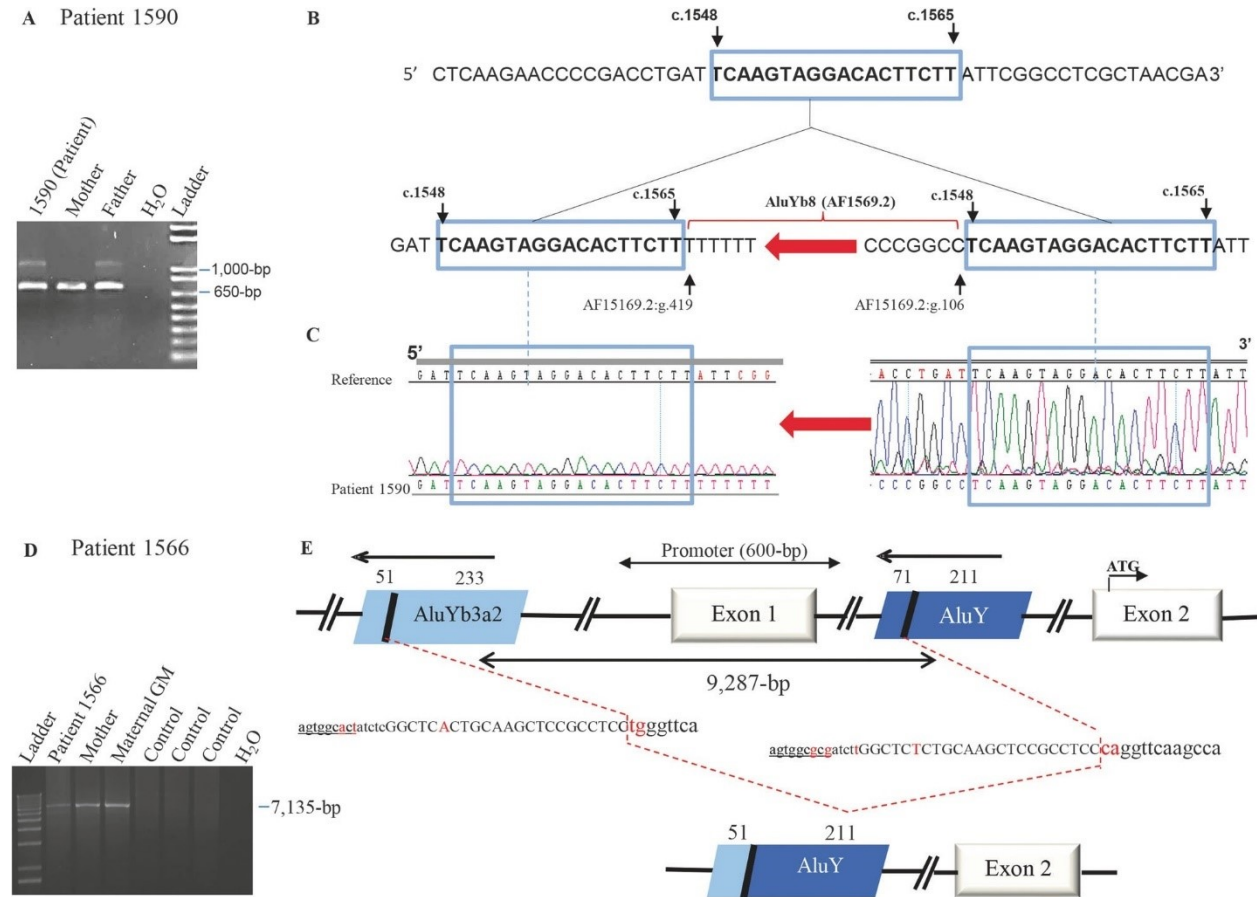
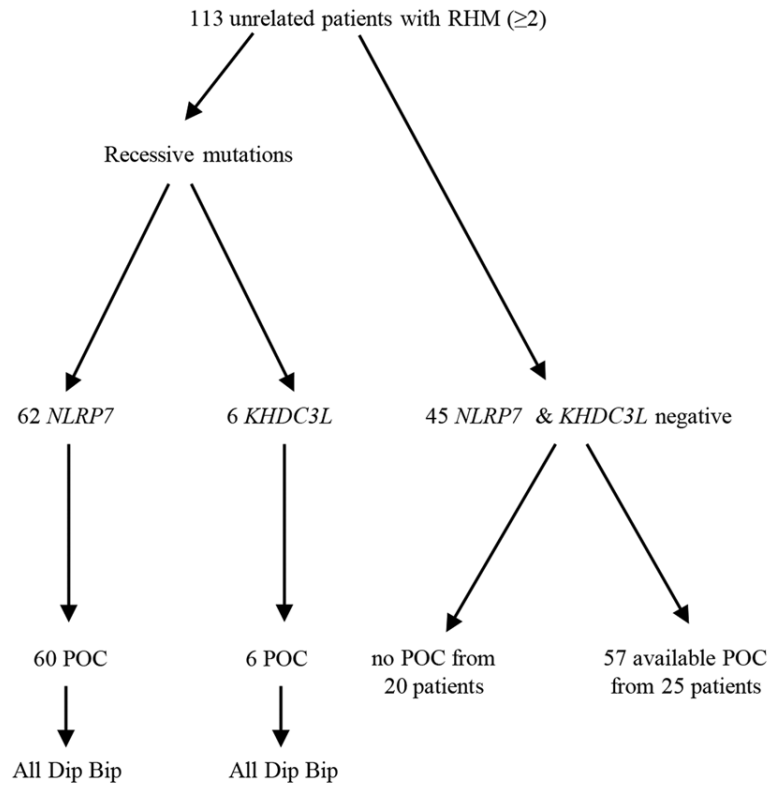


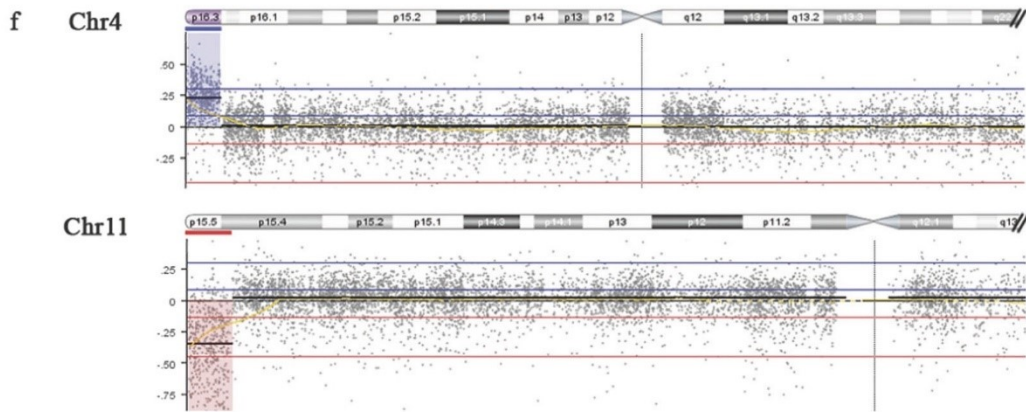
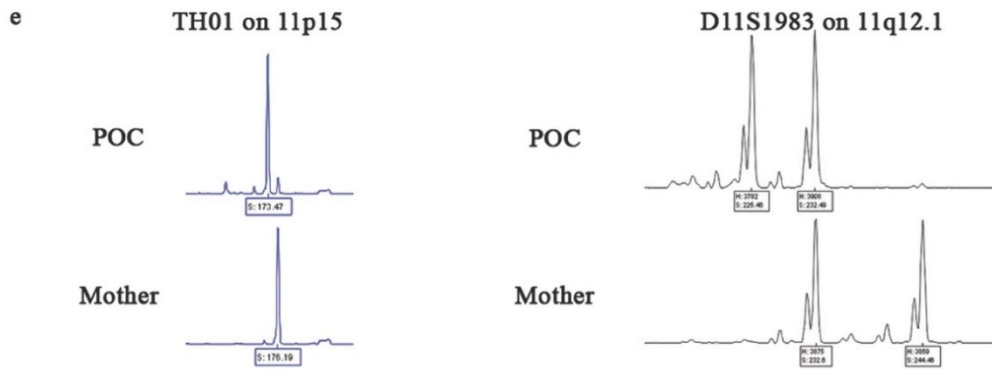
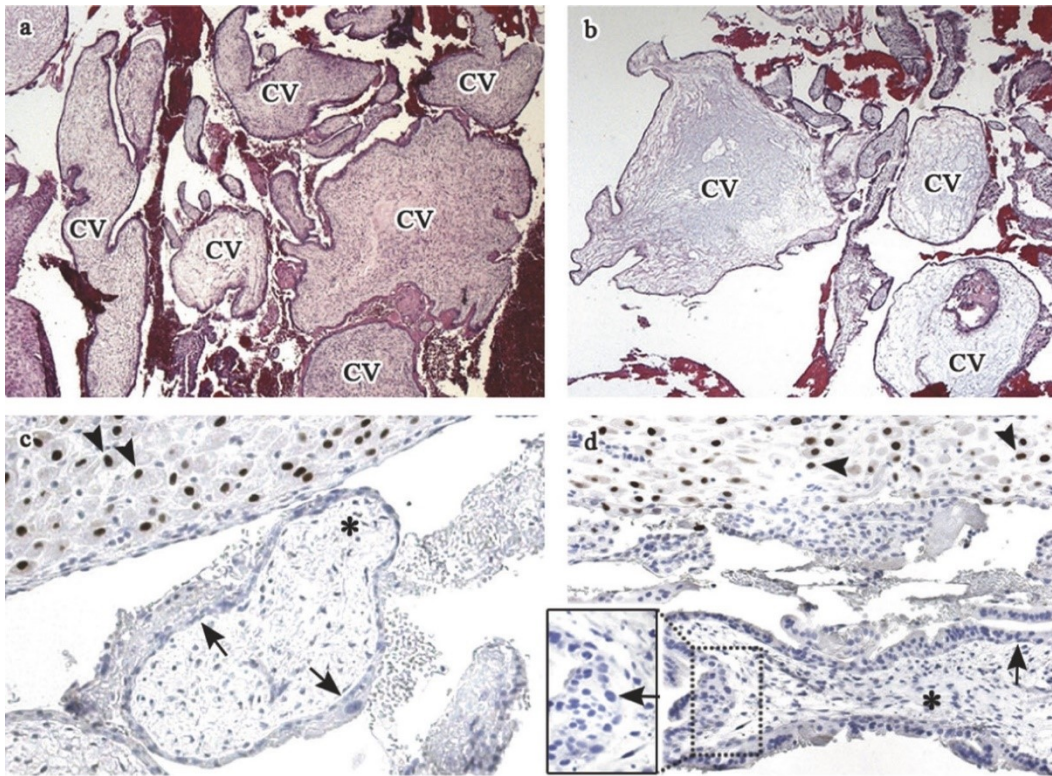
Figure 3.1. Location of the Alu insertion in exon 4 of *NLPR7*. (a) PCR amplification of genomic DNA from exon 4 followed by gel electrophoresis analysis revealed a second larger fragment by approximately 350-bp in patient 1590 and her father but not in her mother who carries a missense variant p.(Arg693Trp) in a heterozygous state. (b) A schematic of the region of exon 4 where the Alu Yb8 element is inserted between nucleotides c.1548 and c.1565 and results in a 18-bp duplication (blue box) at the site of the insertion. The red arrow indicates the 5' to 3' orientation of the inserted Alu Yb8 element that begins at genomic position g.106 and ends at g.419 in the poly (A) tract (poly(T) in the reverse complementary strand) of reference sequence AF15169.2. (c) Chromatograms showing the 5' and 3' junctions of the 18-bp duplication flanking the inserted Alu Yb8 element. (d) Long- range PCR amplification showing the amplification of an abnormal genomic DNA fragment of 7135-bp overlapping the deletion in patient 1566, her mother, and maternal grandmother, but not in three control subjects. The promoter region predicted by the

“Eukaryotic Promoter Database” (<http://epd.vital-it.ch/>) is indicated above exon 1 and starts 499-bp upstream of exon 1 and ends 63-bp downstream of exon 1. “GM” stands for Grandmother. e. Schematic of the deletion that is mediated by recombination between two Alu Y elements and a microhomology of 23-bp shown in capital letters



	Histopathology	Flow or FISH or Karyotype	p57 ^{KIP2}	Microsatellites	Conclusion
Patients with RHM					
½ sisters	1. CHM	2n	-	Inconcl.	Diploid biparental CHM
	5 CHM	2n; n.a.; 2n, 2 n.a., 2n	+; -/+; -/+; +; -	3 Dip Bip	
	2. 3 CHM	2 n.a.; 2n	-; n.a.; +	n.a.; 2 Dip Bip	Diploid androgenetic monospermic CHM
	3. 2 CHM	n.a.; 2n	-; n.a.	2 An Mo	
	4. 2 CHM	2 n.a.	2 n.a.	2 An Mo	
	5. 2 CHM	2 2n	-; -	2 An Mo	
	6. 3 CHM	3 n.a.	-; -; -	3 An Mo	
	7. 3 CHM	3 2n	-; -; -	3 An Mo	
	8. 4 CHM	3 2n; n.a.	-; -; -	4 An Mo	
	9. 2 PHM	2 3n	+; +	2 Tri Dis	
	10. 2 PHM; CHM	2 3n; 2n	+; +; -	2 Tri Dis; n.a.	
	11. 2 PHM	2 3n	+; +	2 Tri Dis	
	12. 2 PHM	2 3n	+; +	2 Tri Dis	
	13. 2 PHM	2 n.a.	+; +	2 Tri Dis	
	14. 2 PHM	2 3n	+; +	2 Tri Dis	
	15. PHM; NM	2 3n	+; +	2 Tri Dis	
	16. 2 PHM	2 69,XXY ^{kar}	2 n.a.	2 n.a.	Various genotypes
	17. PHM; CHM	3n; 46,XX ^{kar}	+; n.a.	Tri Dis; n.a.	
	18. CHM	n.a.	n.a.	Dip Dis	
19. CHM	n.a.	n.a.	An Mo		
Patients with "RHM" revised to nonmolar miscarriages					
20.	2 NM	n.a.; 2n	n.a.; +	2 Dip Bip	Diploid biparental NM MC
21.	2 NM	2n; Dip XY ^{FISH}	+; +	2 Dip Bip	
22.	2 NM	2 n.a.	2 n.a.	2 Dip Bip	
23.	2 NM	2 2n	-; -	2 Dip Bip	
24.	PHM; NM	3n; XXXY ^{FISH}	+; +	Tri Dis; Dip Bip	Tetraploid NM MC & Triploid dispermic PHM
25.	NM; PHM	92, XXXY ^{kar} ; 3n	+; n.a.	n.a.; Tri Dis	

Figure 3.2. Summary of the comprehensive characterization of 57 hydatidiform mole tissues from 25 patients with no recessive pathogenic variants in *NLRP7* or *KHDC3L*. Recapitulation of the characterization of the referred hydatidiform mole tissues with the various results obtained by morphological analysis, flow cytometry, karyotype analysis, and fluorescent in situ hybridization, p57^{KIP2} immunohistochemistry, microsatellite genotyping, and the conclusion of the analyses. Unrelated patients are numbered from 1 to 25, and only one of them has a half-sister with recurrent hydatidiform moles. The number of analyzed tissues for each patient is provided under the “Histopathology” column. More than one tissue of the same type are indicated by their numbers; lack of a number indicates one such tissue or item. In the other columns, results on the different tissues are listed by their chronological order. POC stands for product of conception; NM, for non-molar; MC, miscarriage; CHM, complete hydatidiform mole; PHM, partial hydatidiform mole; n.a., indicates result not available and is used to indicate an inconclusive result or not available samples; Dip, diploid; Bip, biparental; Dis, dispermic; Tri, triploid.



◀ **Figure 3.3. Histopathology and genotyping data of the two non-molar miscarriages from patient 4.** Microphotographs of hematoxylin and eosin-stained sections of the 1st (a) and 2nd (b) product of conception (POC) showing that chorionic villi (some of which are indicated by “CV”) lack trophoblastic proliferation. c and d Microphotographs of p57^{KIP2} immunostaining on the 1st (c) and 2nd (d) product of conception showing negative staining of the cytotrophoblast (arrows) and villous mesenchyme (asterisks) nuclei, in contrast to the positive staining of the endometrial nuclei (arrowheads), which serve as an internal positive control. (e) Deletion of the distal end of chromosome 11 is shown by the loss of the maternal allele (176-bp) in the 1st product of conception at TH01 marker located on 11p15. Marker D11S1983, located on 11q12.1, shows the presence of one maternal (232-bp) and one non-maternal (225-bp) alleles, demonstrating the diploid biparental origin of alleles at this locus in the 1st product of conception. (f) Combimatrix microarray results on the 1st product of conception demonstrating a duplication of 3.9-Mb on chromosome 4p16.3 and a deletion of 3.6-Mb on 11p15.5-p15.4

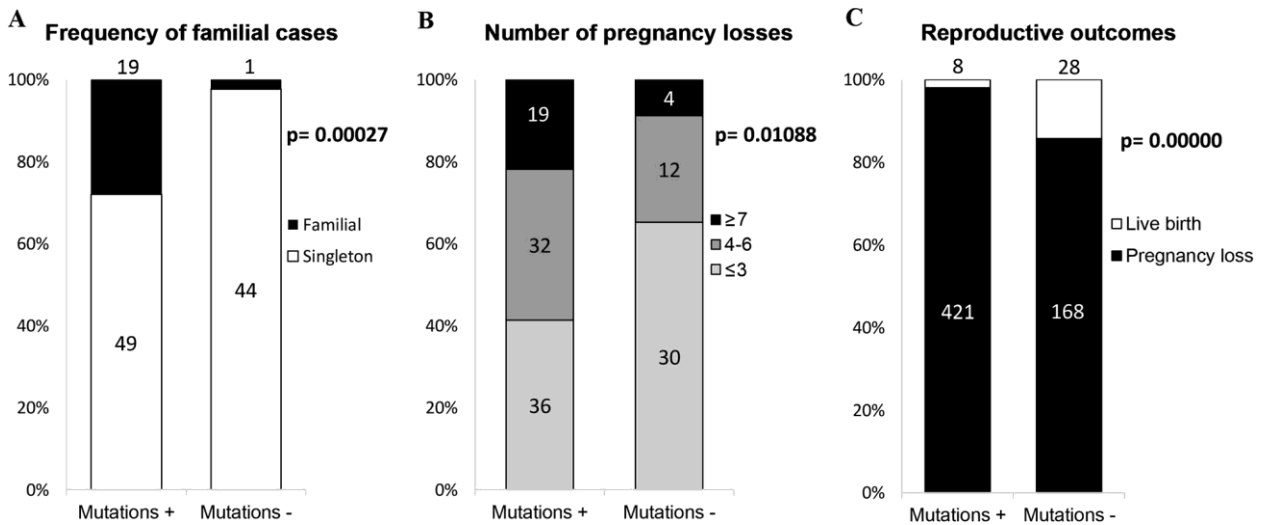


Figure 3.4. Comparison of the genetic susceptibility for recurrent hydatidiform moles between patients with and without recessive mutations in *NLRP7* or *KHDC3L*. (a) A significantly lower number of familial cases was found in patients without *NLRP7* or *KHDC3L* mutations ($p = 0.00029$). (b) A history of <3 pregnancy losses was more frequent in patients without mutations in either gene while a history of 4–6 pregnancy losses or at least 7 pregnancy losses was more frequent in patients with *NLRP7* or *KHDC3L* mutations. (c) Patients without mutations in either gene had a significantly higher number of live births than patients with mutations ($p = 0$).

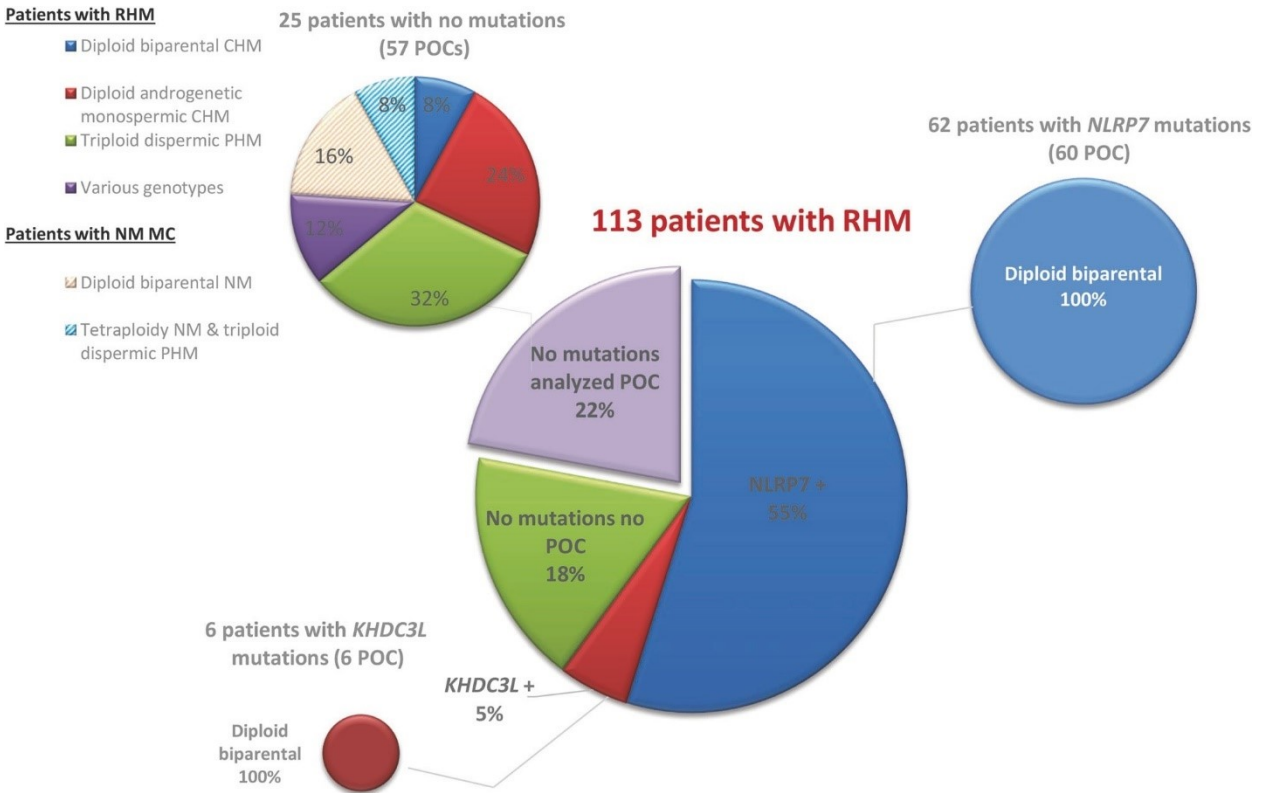


Figure 3.5. A recapitulation of the mutation screening in 113 patients and comprehensive characterization of their hydatidiform mole tissues. Among 113 patients, 55% (62 patients) have *NLRP7* and 5% have *KHDC3L* pathogenic variants in recessive state; the remaining 40% do not have mutations in either gene. In patients with *NLRP7* and *KHDC3L* recessive mutations, all analyzed products of conception (60 and 6, respectively) were found diploid biparental. In patients without mutations in these two genes, the genotypes were highly heterogeneous and diploid biparental moles were found in only a minority of cases (8%). The sizes of the pies are proportional to the number of patients. HM stands for hydatidiform mole; CHM, complete HM; PHM, partial HM; RHM, recurrent hydatidiform mole; NM MC, non- molar miscarriages; POC, product of conception.

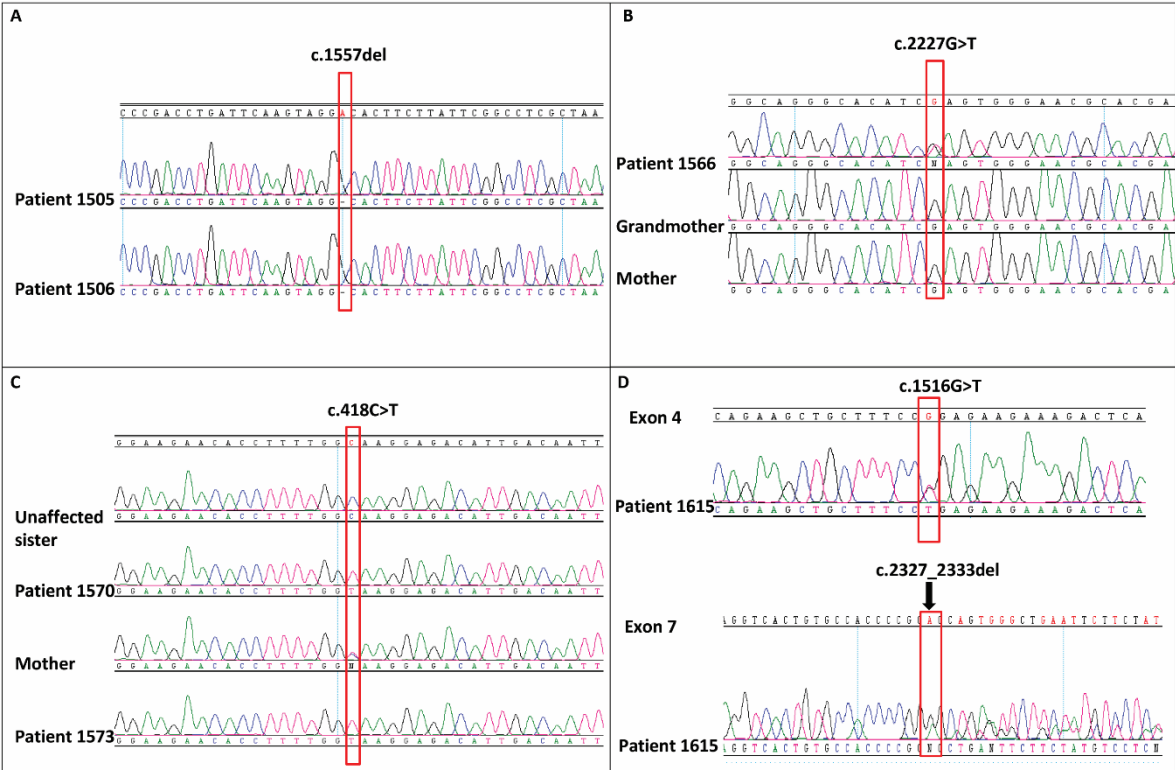
Table 3.1 Recapitulation of the ten novel protein-truncating variants in *NLRP7* with the ethnicities and reproductive histories of the patients

ID		Origin/ Ethnicity	Exon	Variants		Reproductive history and relevant medical information
Family	Patient			cDNA	Predicted protein	
MoTu594	1505	Turkey/Kurdish	4	c.[1557del];[1557del]	p.(His520Thrfs*46);(His520Thrfs*46)	11 HM
	sister, 1506			c.[1557del];[1557del]	p.(His520Thrfs*46);(His520Thrfs*46)	13 HMs
MoIn649	1566	Indian	Before exon 1 & exon 6	c.[-7026_-40+230del];[2227G>T]	p.(?);(Glu743*)	SA, 5 HM
MoTu650	1570	Turkey	4	c.[418C>T];[418C>T]	p.(Gln140*);(Gln140*)	7 HM, HM-GTN (1:5)
	sister, 1573			c.[418C>T];[418C>T]	p.(Gln140*);(Gln140*)	6 HM
MoTu682	1615	Turkey	4 & 7	c.[1516G>T];[2327_2333del]	p.(Gly506*);(Glu776Glyfs*14)	HM, MC, MC/HM, MC/HM, 2 PHM
	sister (not tested)				not tested	RHM
MoEs675	1590	Estonia	4 & 5	c.[1548_1566dup;1566_1567insAF15169.2:g.106_419];[2077C>T]	p.(?);(Arg693Trp)	3 HM, hysterectomy
MoMx628	1546	Mexican	4	c.[1168del];[1168del]	p.(Arg390Alafs*26);(Arg390Alafs*26)	CHM, PHM
	Other family members (not tested)					RHM
MoEg720	1693	Egyptian	4	c.[394_395del];[394_395del]	p.(Leu132Glyfs*12);(Leu132Glyfs*12)	3 CHM, SA
MoIn688	1630	Indian	5	c.[2002T>C];[2002T>C]	p.(Cys668Arg);(Cys668Arg)	7 HM

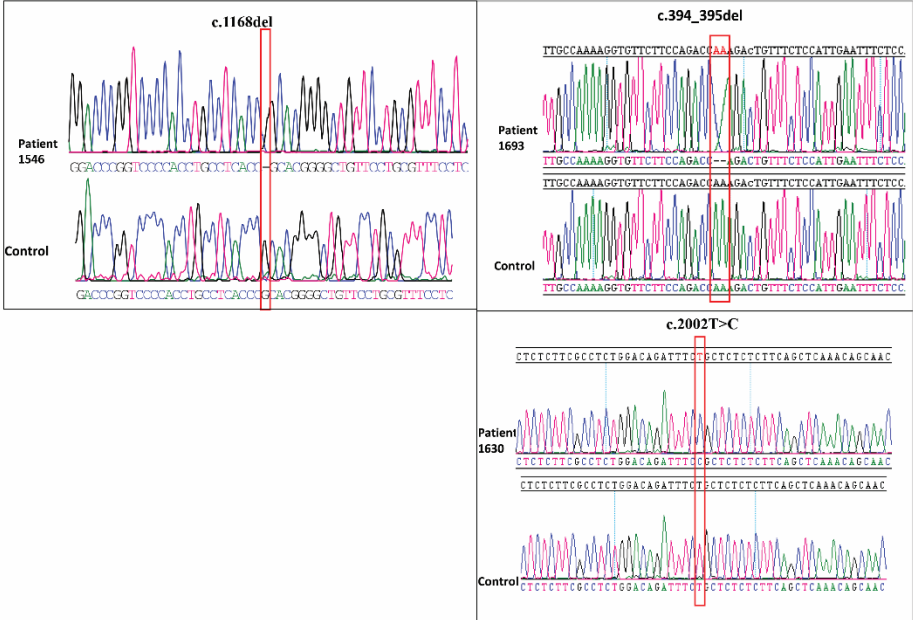
Novel variants are in bold font. HM, stands for hydatidiform mole and is used when no tissues were available to re-evaluate the diagnosis and available pathology report or provided information did not distinguish between partial and complete HM; PHM, for partial HM; RHM, for recurrent hydatidiform moles; MC, for miscarriage. The positions of different mutations in exons or introns are separated by "&"; Variants nomenclature is given according to the following references, NM_001127255.1 (cDNA), NG_008056.1 (genomic), and Q8WX94 (protein). Exon numbering is according to NG_008056.1

Supplementary Figures and Tables

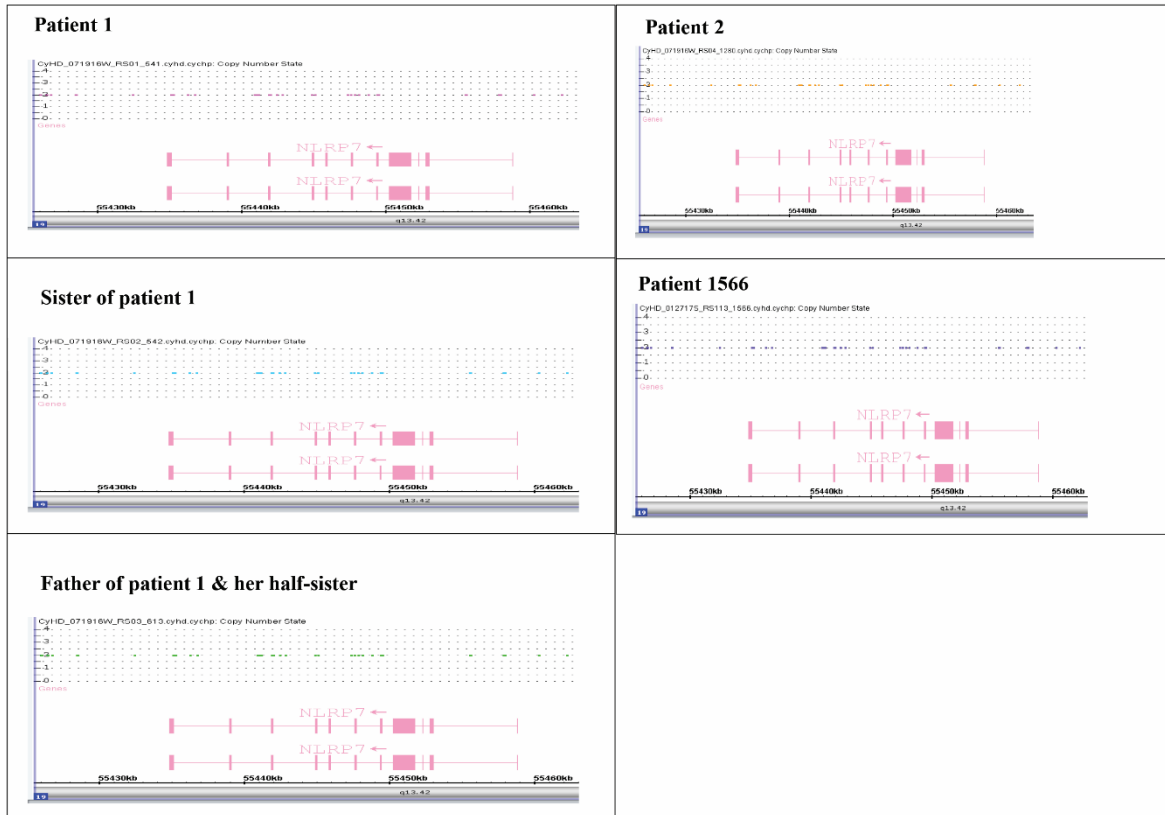
Supplementary Figure 3.1A



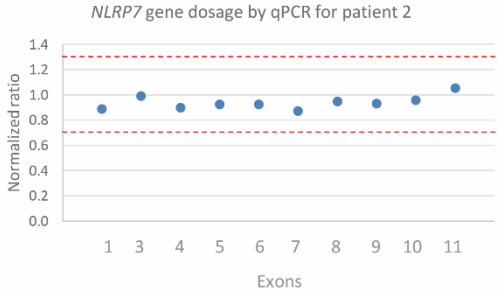
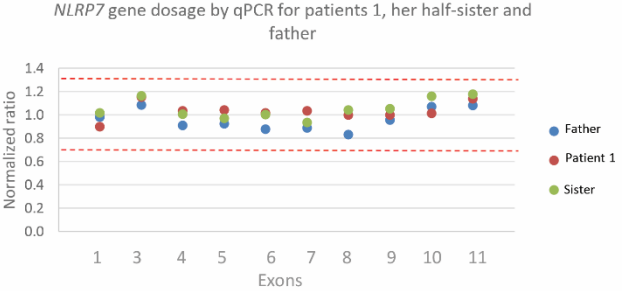
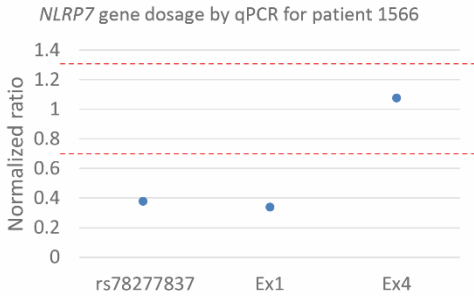
Supplementary Figure 3.1B



Supplementary Figure 3.2



Supplementary Figure S3.3



Supplementary Table 3.1: Table showing the sequences of the primers used to amplify the junction fragments and the sizes of the PCR-amplified fragments with

Patient ID	Primer name	Primer sequence (5'-3')	Expected size for WT allele	Size of PCR-amplified fragment	Causation	Condition
1590	Ex43F	TGCTGAAGAGGAAGATGTTACCC	720bp	1100bp	Alu Yb8 insertion	6ul (10ng/ul) of genomic DNA with Taq polymerase and Q solution (Qiangen) (denatured at 95°C for 5min, followed by 35 cycles under the following condition: 94°C for 45 sec, 58°C for 45 sec and 72°C for 1 min, and final extension of 72°C for 10min
	Ex43R	CGAGGCCGAATAAGAAGTGCCTAC				
1566	LRPCR-1566F1	CTTCTCCCTACTTCTCCTAAGTGCAATG	16422bp	7135bp	Alu-mediated deletion	5ul (500ng/ul) of genomic DNA with TaKaRa LA PCR kit (TaKaRa BIO INC) (denatured at 94°C for 15 sec, followed by 2 rounds of 15 cycles under the following condition: 94°C for 10 sec, 68°C for 14 min and 94°C for 10 sec, 68°C for 16 min
	LRPCR-1566R3	CAAAGACTGAATTAAGAGACTGAAAATCTGG				

Supplementary table 3.2. Comprehensive genotypic analyses of the POC of the 25 patients with various methods as well as their full reproductive histories

Patient	Reproductive history as referred	BlockID (t)	POC analyzed	Revised histopathology	Flow	FISH	Karyotype	n57 ^{KR2}	Microsatellites	Our Conclusion
Patients with RHM										
Two unrelated patients with diploid biparental CHM										
1	CHM-GTN, CHM, MC; 6 MC, CHM, MC, CHM	99-73	3rd CHM half-sister of 1							
		05-55	3 CHM; 2 2nd CHM	CHM	2n				n.a	CHM
		05-62	3rd CHM	CHM	2n				n.a	CHM
		09-17	4th CHM	CHM	2n				n.a	CHM
		12-74	4th MC	CHM	n.a.				Diploid biparental XY	Diploid biparental CHM
		14-66	6th CHM	CHM	2n				Diploid biparental	Diploid biparental CHM
		14-66	6th CHM	CHM	2n				n.a	
		14-66	6th CHM	CHM	2n				Diploid biparental XX	Diploid biparental CHM
2	PHM, LB, 5 HM	92-13	2nd HM 94-86	CHM	3rd HM				n.a	
		04-16	6th HM	CHM	n.a.				Diploid biparental XX	Diploid biparental CHM
		04-16	6th HM	CHM	n.a.				Diploid biparental XX	Diploid biparental CHM
		04-16	6th HM	CHM	2n				Diploid biparental XX	Diploid biparental CHM
Six patients with diploid androgenetic monospermic CHM										
3	2 CHM, 2 LB	41-08	1st CHM	CHM	n.a.				Androgenetic monospermic XX	Androgenetic monospermic CHM
		41-09	2nd CHM	CHM	2n				Androgenetic monospermic XX	Androgenetic monospermic CHM
4	2 ET, CHM, CHM, LB		1st CHM	CHM	n.a.				Androgenetic monospermic XX	Androgenetic monospermic CHM
			2nd CHM	CHM	n.a.				Androgenetic monospermic XX	Androgenetic monospermic CHM
5	LB, ET, HM, 2 MC, CHM	05-14	1st CHM	CHM	2n				Androgenetic monospermic XX	Androgenetic monospermic CHM
		10-09	2nd CHM	CHM	2n				Androgenetic monospermic XX	Androgenetic monospermic CHM
6	2 MC, LB, MC, CHM, HM, MC, HM, BO, LB	07-90	CHM	CHM	n.a.				Androgenetic monospermic XX	Androgenetic monospermic CHM
		09-57	1st HM	CHM	n.a.				Androgenetic monospermic XX	Androgenetic monospermic CHM
		09-94	2nd MC	MC	2n		Diploid XX (X, Y, 18)	+	Androgenetic monospermic XX	Diploid biparental MC (with high maternal contamination)
		12-49	2nd HM	CHM	n.a.				Androgenetic monospermic XX	Androgenetic monospermic CHM
7	LB, PHM, 2 CHM, 2 LB	836	PHM	CHM	2n		Diploid XX (X, Y, 18)	-	Androgenetic monospermic XX	Androgenetic monospermic CHM
		522	1st CHM	CHM	2n				Androgenetic monospermic XX	Androgenetic monospermic CHM
		868	2nd CHM	CHM	2n				Androgenetic monospermic XX	Androgenetic monospermic CHM
8	4 MC, 2 CHM, PHM, CHM	12-94	1st CHM	CHM	2n				Androgenetic monospermic XX	Androgenetic monospermic CHM
		14-21	2nd CHM	CHM	2n				Androgenetic monospermic XX	Androgenetic monospermic CHM
		07-69	PHM	CHM	2n				Androgenetic monospermic XX	Androgenetic monospermic CHM
		04-07	3rd CHM	CHM	n.a.				Androgenetic monospermic XX	Androgenetic monospermic CHM
Eight patients with triploid dispermic PHM										
9	EFL, LB, CHM, EFL, PHM, EFL, LB	06-79	CHM	PHM	3n		Trploid XYY + 5% XX (X, Y, 18, 8, 11)	+ , few -	Trploid dispermic XYY	Trploid dispermic PHM with mosaicism
		07-46	PHM	PHM	3n		Trploid XXX (X, Y, 18)	+	Trploid dispermic XYY	Trploid dispermic PHM
10	3 HM, LB	104	1st HM	PHM	3n		Trploid XXY (X, Y, 18, 8, 11)	+	Trploid dispermic XYY	Trploid dispermic PHM
		605	2nd HM	CHM	2n		Diploid XX (X, Y, 18, 13, 21, 8)	-	Androgenetic monospermic XX	Androgenetic monospermic CHM
		07-95	3rd HM	PHM	3n		Trploid XXX (X, Y, 18, 8)	+	Trploid dispermic XXX	Trploid dispermic PHM
11	LB, 2 PHM, LB	08-30	1st PHM	PHM	3n			+	Trploid dispermic XYY	Trploid dispermic PHM
		09-55	2nd PHM	PHM	3n		Trploid XXY (X, Y, 18)	+	Trploid dispermic XYY	Trploid dispermic PHM
12	LB, MC, EP, CP, 2 PHM	10-69	1st PHM	PHM	3n		Trploid XXY (X, Y, 18, 16)*	70, XXY +16	Trploid dispermic XYY	Trploid dispermic PHM
		11-99	2nd PHM	PHM	3n		Trploid XXY (X, Y, 18)	69, XXY	Trploid dispermic XYY	Trploid dispermic PHM
13	ET, 2 PHM	11-17	PHM	PHM	n.a.				Trploid dispermic XYY	Trploid dispermic PHM
14	PHM, MC, LB, MC, PHM, LB	07-14	1st PHM	PHM	3n		Trploid XXX (X, Y, 18)	+	Trploid dispermic XXX	Trploid dispermic PHM
		10-64	2nd PHM	PHM	3n		Trploid XXX (X, Y, 18)	+	Trploid dispermic XXX	Trploid dispermic PHM
15	2 MC, PHM, LB	13-41	2nd MC	MC	3n			+	Trploid dispermic XYY	Trploid dispermic PHM
		13-35	PHM	PHM	3n			+	Trploid dispermic XYY	Trploid dispermic PHM
16	2 PHM		1st PHM						69,XXY	Trploid PHM
			2nd PHM						69,XXY	Trploid PHM
Three patients with various genotypes on a single HM										
17	PHM, CHM, died from Adenocarcinome	73	PHM	PHM	3n		Trploid XXX (X, Y, 18, 8)	+	Trploid dispermic XXX	Trploid dispermic PHM
		25	CHM	CHM	n.a.				n.a	Androgenetic CHM
18	LB, HM, CHM	91-57	2nd CHM	CHM					Androgenetic monospermic XX	Androgenetic monospermic CHM
19	2 HM	91-31	2nd HM	CHM	n.a.				Androgenetic dispermic XY	Androgenetic dispermic CHM
Patients with "HM" revised to nonmolar miscarriages										
Four patients with diploid biparental nonmolar miscarriages										
20	3 HM	01-68	1st HM	MC	n.a.				n.a	
		05-22	2nd HM	MC	2n				Diploid biparental	Diploid biparental MC
21	PHM, 2 MC, PHM	79	1st PHM	MC	2n		Diploid XX (X, Y)	+	Diploid biparental XX	Diploid biparental MC
		M264-2	2nd PHM	MC	2n		Diploid XY (X, Y)	+	Diploid biparental XY	Diploid biparental MC
22	CHM, CHM-GTN, IVF_PGS failed ET	09-02	1st CHM	MC	n.a.				Diploid biparental XY	Diploid biparental MC
		09-14	2nd CHM	MC	n.a.				Diploid biparental XX	Diploid biparental MC
23	CHM, 2 MC, CHM	13-89	CHM	MC	2n				Diploid biparental XY, loss of maternal TH01 allele	Diploid biparental MC
		15-75	CHM	MC	2n				Diploid biparental XX	Diploid biparental MC
Two patients with 1 tetraploid MC and 1 triploid PHM										
24	MC, PHM, 3 MC, PHM	08-93	1st PHM	PHM	3n		Trploid XXX (X, Y, 18)	+	Trploid dispermic XXX	Trploid dispermic PHM
		13-72	2nd PHM	MC	2n		Tetraploid XYYY (17, 10, 11)	+	Diploid biparental XY	Tetraploid MC
25	PHM, MC, PHM	10-59	1st PHM	MC	n.a.		n.a	92, XXXY	n.a	Tetraploid MC
		13-21	2nd PHM	PHM	3n		Trploid XXX (X, Y, 18)	+/-	Trploid dispermic XYY	Trploid dispermic PHM

*. FISH on tissue sections revealed 20-25% of cells with four copies of Chromosome 16

PREFACE TO CHAPTER 4

When I started my PhD project, a previous lab colleague had sent and analyzed exome sequencing data of 20 patients who were negative for mutations in both genes; however, we were not able to identify recessive mutations in the same genes in at least two patients. The main factors that hinder the work of gene identification can be 1- the great variability in the patients' reproductive outcomes, which can range from complete HM and partial HM to miscarriages and live births (as demonstrated from Chapter 3), 2- the high genetic heterogeneity in the causation of RHM, and the fact that some of them were misdiagnosed with RHM. Genetic heterogeneity in breast cancer can serve as a model for complex disorders. Breast cancer can result from mutations in any one of different genes, all implicated in the same or related pathways ¹⁶⁷. RHM can be similar to breast cancer in this aspect. In Chapter 4, we describe the work on gene identification in patients with recurrent androgenetic HM and reveal 3 causative genes with known roles in the same pathway.

CHAPTER 4

Causative mutations and mechanism of androgenetic hydatidiform moles

Ngoc Minh Phuong Nguyen,^{1,15} Zhao-Jia Ge,^{1,15} Ramesh Reddy,¹ Somayyeh Fahiminiya,^{1,2} Philippe Sauthier,³ Rashmi Bagga,⁴ Feride Iffet Sahin,⁵ Sangeetha Mahadevan,⁶ Matthew Osmond,^{1,2} Magali Breguet,³ Kurosh Rahimi,⁷ Louise Lapensee,^{8,9} Karine Hovanes,¹⁰ Radhika Srinivasan,¹¹ Ignatia B. Van den Veyver,⁶ Trilochan Sahoo,¹⁰ Asangla Ao,^{1,12} Jacek Majewski,^{1,2} Teruko Taketo,^{12,13,14} Rima Slim^{1,12,*}

¹ Department of Human Genetics, McGill University Health Centre, Montréal, Québec, H4A 3J1, Canada

² Genome Québec Innovation Center, Montréal, Québec, H3A 0G1, Canada

³ Department of Obstetrics and Gynecology, Gynecologic Oncology Division, Centre Hospitalier de l'Université de Montréal, Réseau des Maladies Trophoblastiques du Québec, Montréal, H2X 0C1

⁴ Department of Obstetrics & Gynecology, Post Graduate Institute of Medical, Education and Research, PGIMER, Chandigarh, 160012, India

⁵ Department of Medical Genetics, Faculty of Medicine, Baskent University, 06810 Ankara, Turkey

⁶ Department of Obstetrics and Gynecology, Baylor College of Medicine, Houston, Texas, 77030, USA.

⁷ Department of Pathology, Centre Hospitalier de l'Université de Montréal, Montréal, Québec, H2X 0C1, Canada

⁸ Ovo Clinic, Montréal, Québec, H4P 2S4, Canada

⁹ Department of Obstetrics and Gynecology, Centre Hospitalier de l'Université de Montréal, Montréal, H2X 0C1

¹⁰ Invitae, Irvine, CA 92618, USA

¹¹ Cytology & Gynecological Pathology, Post Graduate Institute of Medical Education and Research PGIMER, Chandigarh, 160012, India

¹² Department of Obstetrics and Gynecology, McGill University Health Centre, Montréal, QC, H4A 3J1, Canada

¹³ Department of Surgery, McGill University Health Centre, Montréal, Québec, H4A 3J1, Canada

¹⁴Department of Biology, McGill University, Montréal, Québec, H3A 0G4, Canada

¹⁵ These authors contributed equally to this work

Manuscript published in the **American Journal of Human Genetics**, November 2018

(PMID: 30388401)

Abstract

Androgenetic complete hydatidiform moles are human pregnancies with no embryos and affect 1 in every 1400 pregnancies. They have mostly androgenetic monospermic genomes with all the chromosomes originating from a haploid sperm and no maternal chromosomes. Androgenetic complete hydatidiform moles were described in 1977, but how they occur has remained an open question. We identified bi-allelic deleterious mutations in *MEI1*, *TOP6BL/C11orf80*, and *REC114*, with roles in meiotic double-strand breaks formation in women with recurrent androgenetic complete hydatidiform moles. We investigated the occurrence of androgenesis in *Mei1*-deficient female mice and discovered that 8% of their oocytes lose all their chromosomes by extruding them with the spindles into the first polar body. We demonstrate that *Mei1*^{-/-} oocytes are capable of fertilization and 5% produce androgenetic zygotes. Thus, we uncover a meiotic abnormality in mammals and a mechanism for the genesis of androgenetic zygotes that is the extrusion of all maternal chromosomes and their spindles into the first polar body.

Introduction

Hydatidiform mole (HM) (MIM: 231090) is a human pregnancy with abnormal embryonic development and excessive trophoblastic proliferation. The common form of HM is sporadic, non-recurrent, and affects 1 in every 600 pregnancies.³ Based on microscopic morphological evaluation, half of common HMs belong to the histological type of partial HMs (PHMs) and have a triploid dispermic genome with two sets of paternal chromosomes and one set of maternal chromosomes. The second half belongs to the histological type of complete HMs (CHMs) and has a diploid androgenetic genome with all the chromosomes originating from one (monospermic) or two sperms (dispermic) and no maternal chromosomes. CHM affects approximately 1 in every 1400 pregnancies.³ Among androgenetic CHMs (AnCHMs), monospermic ones account for 85% of the cases and dispermic ones for 15% of the cases.²⁵ Androgenetic monospermic CHMs were first described in 1977²⁶, but the proposed mechanisms of their occurrence remained hypothetical. It is believed that after fertilization between a haploid sperm and an oocyte that has lost its nuclear DNA (for simplicity referred hereafter as empty oocyte), the paternal genome endoduplicates to reconstitute diploidy. Then, because the paternal and maternal genomes have different roles in cellular proliferation and embryonic differentiation, the androgenetic genome that results from such a zygote leads to the molar phenotype. However, in decades of *in vitro* fertilization, no one has seen or reported individuals who produced systematically empty oocytes. A new mechanism for the origin of AnCHMs was suggested: that dispermic fertilization of a haploid oocyte followed by postzygotic diploidization is more likely to be at the origin of the different genotypic types of sporadic HMs as well as of their association with mosaicisms and twin pregnancies consisting of one fetus with a normal placenta and a HM.²⁸

Recurrent HMs (RHM)s affect 1.5-9% of women with a prior HM.⁸⁻¹³ There are two genes, *NLRP7* (MIM: 609661)⁵⁷ and *KHDC3L* (MIM: 611687)⁸⁰, responsible for RHMs. Bi-allelic mutations in these two genes explain the etiology of RHMs in 60% of affected women.¹⁶⁸ Recurrent molar tissues from women with bi-allelic mutations in the two known genes are all diploid biparental while those from women without mutations are heterogeneous. Among women with no recessive mutations in the known genes, a minority of women have diploid biparental RHMs, half of the remaining women have triploid dispermic PHMs, and the second half have androgenetic monospermic CHMs.¹⁶⁸ Available data on women with diploid androgenetic monospermic RHMs indicate that 17-37% of them fail to have live births suggesting that these women may have a strong genetic defect underlying their RHMs.^{168; 169}

To identify mutations responsible for RHMs, we performed whole exome sequencing (WES) on a total of 65 women with RHM (including all histopathological and genotypic types), miscarriages, and infertility, who were negative for mutations in *NLRP7* and *KHDC3L*. We identified bi-allelic deleterious mutations in meiotic double-stranded break formation protein 1 (*MEI1*) (MIM: 608797), type 2 DNA topoisomerase 6 subunit B-like (*TOP6BL/C11orf80*) (MIM: 616109), and REC114 meiotic recombination (*REC114*) genes in five unrelated women, of which two had other family members with recurrent miscarriages and infertility. We demonstrated that their HMs have the histopathological features of CHMs and have androgenetic monospermic genomes. All three genes are conserved during evolution and known to play roles during early homologous chromosome pairing and recombination in the mouse oocyte.¹⁷⁰⁻¹⁷² *In vitro* maturation of oocytes from *Mei1*-deficient female mice has previously been reported, but the number of obtained mature oocytes was very small and consequently, mature oocytes were not further examined.¹⁷⁰ In the current study, we focused on the segregation of chromosomes at the

first meiotic division and the possibility of androgenetic embryonic development. We confirm that most *Mei1*^{-/-} oocytes have abnormal spindle morphology, misaligned chromosomes on the spindles, and 63% of them fail to extrude the first polar body (PB). However, 20% of oocytes extruded morphologically abnormal first PB and some extruded all their chromosomes together with the spindle microtubules into the PB and were empty with no chromosomes. We demonstrate that *Mei1*^{-/-} oocytes are capable of fertilization and that 5% lead to androgenetic zygotes. We finally show that the zygotes derived from *Mei1*-deficient oocytes are capable of initiating embryonic development but mostly arrest at the 2- to 4-cell stage.

Material and Methods

Subjects

Written informed consents were obtained from all participants and the study was performed accordance to the McGill University Research Ethics guidelines (Institutional Review Board # A01-M07-98 03A). Blood or saliva from affected women and their family members were collected. Genomic DNA was isolated from whole blood cells using Flexigene DNA Kit (Qiagen, Toronto, ON, Canada). The products of conception from different Pathology laboratories were retrieved for genotype analysis.

Mutation analyses

Mutation analyses of *NLRP7* and *KHDC3L* were performed to exclude the presence of mutations in these two genes before sending for whole-exome sequencing. PCR conditions and the sequences of primers were previously described and samples were sent for Sanger sequencing in both directions.⁵⁷

Whole-exome sequencing

Whole exome library preparation, capturing, sequencing and bioinformatics analyses were carried out at the McGill University and Genome Quebec Innovation Center, Montreal, Canada as previously described.¹⁷³ Whole exome was captured using either SureSelect Human All Exon Kit version 5 (Agilent Technologies, Inc., Santa Clara, CA) or the Roche Nimblegen SeqCap EZ Human Exome capture kit on 3ug or 500ng gnomonic DNA, respectively, and sequenced on an Illumina HiSeq 2000 sequencer with paired-end 100-base pair reads. The paired-end sequences were trimmed and aligned to the human reference genome hg19 using BWA (v.0.5.9)¹⁷⁴. The Genome Analysis Toolkit (GATK)¹⁷⁵ was used to perform local realignment around small insertions and deletions (indels) and assess capture efficiency and coverage for all samples. The latter was calculated after marking duplicate reads by Picard. Variants were called individually for each individual using Samtools (v.0.1.17)¹⁷⁶ and annotated by Annovar¹⁷⁷. Subsequently, several filtering criteria were applied to prioritize the potential causal variants from non-pathogenic polymorphisms and sequence errors. The variants were excluded when they were seen at a minor allele frequency (MAF) greater than 0.01 in public databases (ExAC, 1000 Genome, NHLBI exome databases) or in-house exomes database (>1000 exomes). Finally, only the most likely damaging variants (nonsense, canonical splice-site, conserved missense, and coding indels) were considered and manually examined in IGV¹⁷⁸ if they were predicted to be deleterious by at least 2 bioinformatics algorithms (PolyPhen, SIFT, MutationTaster, CADD-Combined Annotation Dependent Depletion).

Sanger sequencing validation of identified mutations

Sanger sequencing was used to validate the mutations identified by exome sequencing and to check the segregation of the mutations in other family members. Primers were designed using

Primer Blast. PCR conditions and sequences of the primers are provided in Table S4.1. Variant nomenclature is provided according to GeneBank references for *MEI1* (GenBank: NM_152513.3, NP_689726.3), *TOP6BL/C11orf80* (GenBank: NM_024650.3, NP_078926.3), *REC114* (GenBank: NM_001042367.1, NP_001035826.1).

Targeted sequencing

The candidate genes were screened in additional affected women with milder phenotypes (Table S4.3). *MEI1* and *REC114* were screened in 99 affected women (of which 53 had at least 1 HM and the remaining had ≥ 3 miscarriages). *TOP6BL/C11orf80* was screened in 246 affected women (46 women with at least 1 HM and the remaining had ≥ 3 miscarriages).

RT-PCR on lymphoblastoid cell line and human oocytes

RNA was extracted from EBV-transformed lymphoblastoid cell line (LCL) from affected women and controls using Trizol (Invitrogen, Carlsbad, CA, USA). Human oocytes at different stages (total 4-8 oocytes each stage) were obtained from women undergoing IVF/ICSI and were collected by removing the zona pellucida with acidified Tyrode's solution and washed in 1X PBS before putting them in lysis buffer as previously described.¹⁷⁹ cDNA synthesis was performed using a reverse transcription kit (Life Technologies, Thermo Scientific, Carlsbad, CA, USA). PCR conditions and primers for RT-PCR are provided in table S4.1.

H&E staining, p57^{KIP2} immunohistochemistry, flow cytometry, microsatellite genotyping, and SNP microarray analysis.

Sections of formalin-fixed, paraffin-embedded (FFPE) tissues were prepared for H&E staining, p57 immunohistochemistry, flow cytometry, microsatellite genotyping as previously described.¹⁶⁸ Microarray analysis search for aneuploidies in products of conception of affected women was performed at Invitae as previously described.¹⁶¹

Mice

Mei1 heterozygous mice (B6.129S1-*Mei1*^{m1Jcs/Mmnc})¹⁸⁰ were purchased from the MMRRC (Mutant Mouse Resource & Research Centers Supported by NIH, USA) (MMRRC#31721), maintained on the C57BL/6J background (Jackson Laboratory, Main), and crossed to produce homozygous null *Mei1*. Genotyping was done according to the MMRRC protocol. The mice were fed in a temperature- and light-controlled room at the Animal Resource Division of the McGill University Health Centre Research Institute. All the procedures and Ethics were approved by the McGill University Animal Care Committee in accordance with the Canadian Council on Animal Care. Food and water were provided *ad libitum*.

RT-PCR on mouse tissues

Ovaries, germinal vesicle-stage (GV) oocytes, and metaphase II (MII) oocytes (Total of 70-100 oocytes) were collected from 12.5dpc (days postcoitum), 17.5dpc, new born, 5 dpp (days postpartum), and adult wild-type females. Total RNA was extracted using the RNeasy plus Micro and Mini Kit (Qiagen) according to the manufacturer's instructions. cDNA was synthesized (Invitrogen, Canada) and used as template for RT-PCR. β -actin was used as a control. The primers and conditions used for RT-PCR are provided in Table S4.2. The transcript levels of genes were checked using 2% agarose gel.

Mouse oocyte maturation *in vitro* and *in vivo*

For *in vitro* oocyte maturation, female mice at 25-27dpp were intraperitoneally injected with 10 IU eCG (equine Chorionic Gonadotropin) per mouse. The mice were killed by cervical dislocation 46-48h later and the ovaries collected to retrieve cumulus cell-oocyte complexes (COCs). COCs were cultured in α -MEM medium containing 5IU/ml FSH (follicle-stimulating hormone, Sigma),

5% HI-FBS (Heat Inactivated Fetal Bovine Serum), 7.5µl/ml 100X penicillin/streptomycin, and 0.25mM sodium pyruvate (GIBCO, Thermo-Fisher Sci, MA) for 17 to 19h for all experiments¹⁸¹ except for the experiment to assess meiotic progression and delay. For this experiment, maturation was extended to 24 hours of *in vitro* of culture. For *in vivo* oocyte maturation, females at 25-27dpp were intraperitoneally injected with 10IU eCG, and 46-48h later, with 7.5IU hCG (Human Chorionic Gonadotropin (Sigma) per mouse. 15h later, oocytes were collected from oviduct ampullae.

Mouse embryo culture *in vitro*

Hormonal treatment with dCG followed by hCG was done as described above at 25-27dpp and the females were left with DBA/2 males (Charles River Laboratories, Canada) overnight. 20h after hCG injection, zygotes were collected from oviduct ampullae and cumulus cells were removed using 1% hyaluronidase. Washed zygotes were used for immunofluorescence staining or cultured in KSOM (Millipore) for 5 days under 5% CO₂ with humidity at 37 °C. Embryo development was recorded daily.

Immunofluorescence

Immunofluorescence staining was carried out as previously described¹⁸². Briefly, oocytes were fixed in 4% paraformaldehyde (PFA) in PBS for 30 min and then transferred to membrane permeabilization solution (0.5% Triton X-100) in water for 20 min. Thereafter, oocytes were blocked in 1% BSA (bovine serum albumin) in PBS for 1h. The oocytes were then incubated with primary antibodies diluted with 1% BSA overnight at 4°C. After incubation with secondary antibodies at room temperature for 1h, oocytes were placed in mounting medium with DAPI (Vector, Canada). Fluorescence was visualized using Zeiss LSM780 Scanning Confocal

Microscope at the Molecular Imaging Facility of the Research Institute of the McGill University Health Centre.

Antibodies

The following antibodies were used; mouse-anti-H3K9me2 (1:50, Abcam), mouse-anti- α -tubulin (1:100, Santa Cruz), and donkey-anti-mouse IgG-Alexa fluor 488 (1:500, Invitrogen).

Live imaging

COCs were cultured for maturation in α -MEM as previous described for 12h, and then cumulus cells were removed using 1% hyaluronidase. The denuded oocytes were incubated with 5 ng/ml Hoechst 33342 in α -MEM supplemented as above without FSH for 30 min. Thereafter, the oocytes were transferred to Zeiss LSM780 Scanning Confocal Microscope to monitor the first polar body extrusion, by scanning every 20 min, for 7h.

Results

Identification of bi-allelic mutations in *MEI1*, *TOP6BL/C11orf80*, and *REC114*

We performed WES on 65 women with RHM (including all histopathological and genotypic types) and without mutations in *NLRP7* or *KHDC3L* and 18 of their relatives. After aligning the WES reads to the reference genome, variants-calling and filtering for rare variants with minor-allele frequency <0.01 , we analyzed the data under the recessive mode of inheritance because of its compatibility with the inheritance of the disease in all reported cases of RHM (with or without mutations in the two known genes). We identified rare bi-allelic deleterious mutations (nonsense, canonical splice-site, evolutionary conserved missense, and coding indel) in seven important candidate genes. We next performed targeted sequencing of the seven candidate genes on 99 to

246 women with milder defects (2 HM or ≥ 3 miscarriages with or without one HM) (from all genotypic types) (Table S4.3). The two approaches led to the identification of bi-allelic potentially deleterious mutations in three genes in five unrelated affected women, including two from familial cases.

In *MEII*, exome sequencing revealed a novel homozygous protein-truncating mutation in exon 28, c.3452G>A, p.Trp1151*, in proband 1333 (Figure 4.1A, Table S4.4) with a history of four miscarriages followed by four HM, all from spontaneous conceptions. In addition, she had one failed cycle of *in vitro* fertilization by intra-cytoplasmic sperm injection (Table S4.5). Analyzing additional samples from other family members identified the same mutation in a homozygous state in two sisters who had one and three miscarriages, respectively, and both underwent total abdominal hysterectomy because of several uterine fibroids. The mother of the three sisters was found to be a heterozygous carrier of their mutation (Figure 4.1A). Using RT-PCR on total RNA from a lymphoblastoid cell line (LCL) from the proband 1333, we found that the mutation leads to, in addition to the normal splicing isoform, two abnormal splicing isoforms: a larger cDNA fragment caused by the insertion of intron 27 between exons 27 and 28, and a smaller cDNA fragment due to the skipping of exon 28 (Figure 4.1B). This aberrant splicing was seen only in the affected woman and not in control subjects and is most likely mediated by the nonsense-mediated decay.^{[183](#)}^{[184](#)}

The second family consists of a woman (proband 880) with six miscarriages and one CHM and her brother, who is infertile, with non-obstructive azoospermia and no Y-chromosome deletions. Both were found compound heterozygous for an invariant splice site mutation, c.1196+1G>A, affecting the splice donor of exon 10, and a 1-bp deletion, c.2206del, p.Val736Serfs*31, in exon 19 (Figure 4.1C, Table S4.4). The two mutations segregated in the

family, one from each parent. Using RT-PCR on total RNA from a LCL from the proband 880, we found that the invariant splice site mutation, c.1196+1G>A, leads to a smaller cDNA fragment that corresponds to the skipping of exon 11 (Figure 4.1D) located in one of the two predicted Armadillo-type fold domains (Figure 4.1E). These two mutations were identified in proband 880 by targeted sequencing and then in her other family members by Sanger sequencing.

In *TOP6BL/C11orf80*, we found in one woman (ID 1031), with one miscarriage and two HMs, a 1-bp insertion, c.783dup (p. Glu262*) in a homozygous state (Figure 4.2A, Table S4.4). The mutation segregated from both parents who were found to be heterozygous carriers. In a second woman with RHM (ID HM74, previously reported as the affected woman 2¹⁸⁵), we found a homozygous missense variant c.1501T>C, p.Ser501Pro that affects a highly conserved amino acid (Polyphen=0.9, CADD=22.5) (Figure 4.2B, Table S4.4). The c.783dup mutation leads to the truncation of the protein before the transducer domain. The second mutation, c.1501T>C (p.Ser501Pro), affects a conserved amino acid residue also involved in the interaction of TOP6BL transducer domain with SPO11, a component of topoisomerase 6 complex required for the formation of double-strand breaks in mice.¹⁷¹ These two mutations in *TOP6BL* were identified by exome sequencing.

In *REC114*, using exome sequencing, we found in one woman (ID 978) with a miscarriage and three CHMs, a novel splice acceptor mutation, c.334-1G>A, in a homozygous state (Figure 4.2C, Table S4.4). Of note that the last CHM of this woman was conceived with the help of intrauterine insemination because of her infertility. We did not detect *REC114* transcripts in LCL and consequently could not check the effect of this mutation on gene splicing. The mutation segregated in the family and the two parents were found to be heterozygous carriers (Figure 4.2C).

MEI1, *TOP6BL/C11orf80*, and *REC114* are conserved from yeast to human and their

functions have been examined in several organisms including yeast^{186: 187}, plants¹⁸⁸, worms¹⁸⁹, and mice¹⁷⁰⁻¹⁷². It was striking to see that all three genes play a key role in the formation of double-strand breaks, which is essential for homologous chromosome synapsis and recombination during meiosis I. Mutations in these three genes have never been reported in any human disease with the exception of a recent case of two infertile brothers with a homozygous bi-allelic *MEII* mutation.¹⁹⁰ Therefore, the presence of bi-allelic mutations in five unrelated women and three affected siblings establishes their causal role in recurrent HMs and miscarriages, and in male and female infertility in humans.

Affected women with bi-allelic *MEII* mutations have AnCHMs

We next retrieved all HM tissues from affected women 1333 and 880 with *MEII* mutations and comprehensively analyzed them. By morphological evaluation, all tissues fulfilled the histopathological criteria of CHMs did not express p57^{KIP2} in the nuclei of the cytotrophoblast and villous mesenchyme cells, were diploid by flow cytometry, androgenetic monospermic by microsatellite DNA markers genotyping, and did not have aneuploidies by SNP microarrays (Figure S4.1-S4.4). Two CHM tissues from affected woman 978, with bi-allelic *REC114* mutations, were genotyped by the referring laboratory and found androgenetic monospermic. The tissues from affected woman HM74, with bi-allelic mutations in *TOP6BL/C11orf80*, were reported to be most likely androgenetic CHM.¹⁸⁵ Therefore, HMs from affected women with mutations in the three genes are androgenetic and have a different mechanism at their origin than HM from women with bi-allelic mutations in *NLRP7* or *KHDC3L*.

A complete hCG follow up after HM evacuation was available for affected women 880 and 1031 and both had low risk persistent trophoblastic diseases after the last conception. The non-

molar miscarriages of all affected women with mutations in the three genes did not require dilatation and curettage and therefore are not available for evaluation.

Taken together, these data indicate that the bi-allelic mutations in three genes we identified may not be responsible only for recurrent androgenetic CHM, but also for recurrent miscarriages and female and male infertility.

Expression of *Mei1*, *Top6bl/C11orf80*, and *Rec114*

In humans, the three genes are transcribed in ovaries and some other somatic tissues (Figure 4.1B, Figure S4.5A), but were not detected in oocytes (4-8 oocytes per sample). In mice, the three genes were detected in ovaries from embryonic day 12 to 5 days postpartum (dpp) (Figure S4.5B), and these data are in agreement with a previous report.¹⁸⁰ While *Top6bl* and *Rec114* were found expressed in germinal vesicles (GV) and metaphase II (MII) oocytes from 25dpp mice, *Mei1* expression was not detectable in GV or MII mouse oocytes (70-100 oocytes per sample).

Evidence of empty oocytes from null *Mei1* females

In humans, it is unknown how an androgenetic monospermic CHM forms and such an entity has never been reported in animals. To elucidate the mechanism(s) leading to androgenetic monospermic CHM and possibly model some of its features in mice, we used a mouse knockout for *Mei1* that was available when we identified the mutations in the affected women.¹⁷⁰ The mutation in the *Mei1* knockout (c.984-2A>T) is very close to one of the mutations, p.Val736Serfs*31, found in proband 880 (Figure 4.1E), and results in 2 abnormal splice isoforms which are predicted to lead to premature stop codons. *Mei1*^{-/-} males and females are infertile, but

otherwise healthy.¹⁷⁰ While the males have no spermatozoa in their testes, the females have oocytes in all follicular stages at young ages, albeit in reduced numbers. The development of oocytes during *in vitro* maturation has been reported for *Mei1*^{-/-} and it was found that 94% of the oocytes arrest at metaphase I and have abnormal spindles with misaligned chromosomes scattered on the spindles; only 6% of *Mei1*^{-/-} oocytes progress to metaphase II and extrude the first PB (. To better understand the mechanism of AnCHM formation, we compared the development of oocytes from *Mei1*^{-/-} with those of wild-type after *in vitro* maturation. Under our experimental conditions of *in vitro* maturation for 17-24 h, we found that oocytes from *Mei1*^{-/-} have delayed meiotic progression (Figure 4.3A). We found that 96% of oocytes from the wild-type and only 8% of oocytes from *Mei1*^{-/-} extruded the first PB of normal size and shape. However, 63% of oocytes from *Mei1*^{-/-} failed to extrude the first PB, 20% extruded abnormal PB, either one PB of normal size and with a rough surface, one large PB, or two PBs (despite not being fertilized); the remaining 6% of oocytes appeared to be 2-4-cell-like or degenerating (Figure 4.3B-D). These PB abnormalities were also observed in *in vivo* matured *Mei1*^{-/-} oocytes (Figure 4.3D) with the exception that more oocytes were seen without PB in both mutant and wild-type, probably because the first PB had degenerated, a well-documented phenomenon of *in vivo* maturation.¹⁹¹

We next examined the spindle morphology and chromosome congregation in the *in vitro* matured oocytes using immunofluorescence localization of α -tubulin and DAPI staining of the chromosomes. We found that all oocytes without PB had chromosomes, but the chromosomes were misaligned on the spindles of abnormal shapes (Figure 4.4B). Of the oocytes that extruded PB, approximately 70% appeared at telophase, i.e., the spindles were seen between the two sets of chromosomes without clear separation between the oocytes and the PB. Some oocytes with two PB had tripolar spindles with chromosomes at each pole and two of them forming two first PB

(Figure 4.4, C and D). Other oocytes had bipolar spindles with chromosomes at both ends, but both the spindles and the chromosomes at their poles were altogether extruded into the first PB leaving the oocytes with few chromosomes (Figure S4.6) or empty with no chromosomes (Figure 4.4, D-F). Empty oocytes were also observed in *in vivo* matured oocytes (Figure S4.7). Such empty oocytes were observed only among those that extruded abnormal PB and accounted for approximately 8% of oocytes with ≥ 1 PB matured *in vitro* or *in vivo*. Empty oocytes were not observed in wild-type or *Mei1*^{+/-} mice after either *in vitro* or *in vivo* maturation. In addition, we did not see spindles or chromosomes congregation abnormalities in oocytes from *Mei1*^{+/-}, which behaved like those from wild-type mice. Using live imaging, we monitored *in vitro* maturation of oocytes from *Mei1*^{-/-} and confirmed the extrusion of all the chromosomes into the PB in some oocytes (Video S4.1).

Evidence of androgenetic zygotes from null *Mei1* oocytes

We next asked whether oocytes from null *Mei1*^{-/-} are capable of fertilization. Because the rate of fertilization and embryonic development *in vitro* is lower than *in vivo*, we used superovulation and natural mating in all subsequent experiments of embryonic development. To distinguish maternal from paternal chromosomes in the zygotes, we used immunofluorescence with an antibody against dimethylated histone 3 at lysine 9 (H3K9me2). H3K9me2 is an epigenetic marker that is acquired during oogenesis, but not during spermatogenesis; consequently, it distinguishes maternal from paternal chromosomes up to pronuclear fusion in late zygotes.¹⁹² We first confirmed similar immunofluorescence staining of H3K9me2 between wild-type and *Mei1*^{-/-} oocytes at GV to MII stages (Figure 4.5A). We next examined the oocytes after fertilization and confirmed that H3K9me2 stains only the maternal but not paternal chromosomes in control zygote (Figure S4.8).

Among the 113 oocytes from *Mei1*^{-/-} females analyzed, 68 (60%) had evidence of fertilization and contained paternal DNA. Some zygotes were penetrated by cumulus cells (Figure S4.9 & S4.10) and such zygotes were fertilized by two or three spermatozooids. Among all the zygotes, approximately 5% were androgenetic and did not contain maternal chromosomes. Figure 5B shows a zygote that had lost all maternal DNA into the PB (positive for anti-H3K9me2) and started the first mitotic division of the male pronucleus. All z axis stack sections of this zygote are shown in Video S2. We also observed zygotes that had retained very few maternal chromosomes and others that had undergone asymmetrical cleavage into 2-cell-like, with one cell containing paternal pronucleus or sperm head and the other containing maternal pronucleus (Figure S4.11).

Zygotes from null *Mei1* oocytes can initiate embryonic development

We next investigated whether the zygotes derived from *Mei1*^{-/-} oocytes can initiate embryonic development. We crossed *Mei1*^{-/-} females with wild-type males overnight, collected oocytes, and monitored their daily development in culture for up to 5 days using phase contrast microscopy (Figure 4.6). Our analysis demonstrated that 72% of embryos (n=200) derived from *Mei1*^{-/-} females underwent cleavage, but most were arrested at the 2-cell or 4-cell stage, only 2% reached the blastocyst stage after 120h post-fertilization, and none hatched (Figure 4.6). For comparison, 78% of oocytes from wild-type mice reached the blastocyst stage 96h post-fertilization and all hatched. In conclusion, oocytes from *Mei1*^{-/-} females can be fertilized and undergo embryonic development, but their chance to reach the stage for implantation is limited. Their development in uterus or on the genetic background other than C57/B6 remains an open question.

Discussion

Here we provide evidence implicating bi-allelic mutations in three genes, *MEI1*, *TOP6BL*, and *REC114*, in the causation of recurrent androgenetic monospermic hydatidiform moles, miscarriages, and infertility in humans. This evidence is based on the identification of bi-allelic mutations in *MEI1* in two familial cases, in *TOP6BL* in two unrelated women, and in *REC114* in one woman. The implication of *REC114* is also based on the known interaction of its protein with MEI4, an interactor of MEI1 in yeast and mice [172](#); [187](#). These three genes have been studied in various organisms and model systems and all are required for double-strand breaks formation in the early phase of meiosis in oocytes. Analyzing five HM from two unrelated women with *MEI1* mutations demonstrated that the five tissues fulfill the histopathological criteria of CHM, lack p57^{KIP2} expression, and have diploid androgenetic monospermic genomes. Tissues from proband 978 with mutations in *REC114* were referred to us as androgenetic monospermic CHM and those from woman HM74, with mutations in *TOP6BL*, are believed to be androgenetic CHM. Taken together, these data establish the role of *MEI1*, and possibly the two other genes, in the genesis of androgenetic CHM.

Among the three identified genes, *Mei1* is the most studied and its functional role has been investigated in several species [170](#); [186](#); [188](#); [189](#), of which mouse is the closest, evolutionarily, to human. Null mouse mutants fail to complete the first meiotic division due to defective double-strand breaks formation. *MEI1* was the first of the three genes, in which we found mutations in two unrelated families, and we were able to access the HM tissues and demonstrate their androgenetic monospermic genomes, we therefore set out to investigate whether androgenetic pregnancies or conceptions occur in *Mei1*-null mice. Because *Mei1*-null female mice were documented to be infertile, we hypothesized that perhaps androgenesis occurs in them but such

conceptions do not implant and lead to detectable pregnancies. We asked three main questions: (i) Do *Meil*-deficient females produce empty oocytes with no maternal chromosomes? (ii) When do *Meil*-deficient oocytes lose their chromosomes, before or after fertilization? (iii) By which mechanism do *Meil*-deficient oocytes lose their chromosomes? To answer these questions, we followed the development of oocytes from null *Meil* in *in vitro* maturation. We found that 8% of *Meil*^{-/-} extruded all their chromosomes together with the spindles into the first PB. Our results are in agreement with some observations made on null *meil* in *C. elegans*, which either fail to produce PB, produce PB with variable numbers of maternal chromosomes, or produce large PB appearing to contain all maternal chromosomes.[189: 193](#) Furthermore, we showed that the oocytes from *Meil*-null females can be fertilized and 5% of the zygotes had lost all their maternal chromosomes into the PB, and were therefore androgenetic. In addition, some of the zygotes retained very few maternal chromosomes, which may be unable to fuse with the paternal pronucleus and result also in androgenetic embryos. From our analysis, another potential mechanism that would lead to androgenesis may occur during postzygotic cleavage of a fertilized nucleated oocyte, resulting in the separation of paternal DNA into one cell and maternal DNA into another (Figure S4.11). Such aberrant cells with different genomes may have different growth rates, be subject to some selection, and lead to mosaic conceptions including AnCHMs. However, based on our observations, such events are unlikely to be at the origin of RHM in women with *MEII* mutations because they were not recurrent in *Meil*-deficient females. Some of the androgenetic zygotes we observed had cumulus cells under the zona pellucida, which indicates its abnormal permeability; indeed, some of these eggs were fertilized by two or three spermatozoa. This suggests that androgenetic dispermic CHMs, known to account for approximately 15% of sporadic androgenetic CHM²⁵, may involve the same mechanism and occur also in conceptions from women with bi-allelic *MEII*

mutations.

The earliest defect that has been demonstrated in the oocytes from *Meil*^{-/-} and *Top6bl*^{-/-} is the impaired double-strand breaks formation, which is essential for homologous chromosome synapsis and recombination. The absence of synapsis renders the meiotic silencing of unsynapsed chromatin regions, named MSUC, and affects subsequent meiotic processes depending on the silenced gene repertoire.¹⁹⁴⁻¹⁹⁷ Consequently, *Meil*^{-/-} oocytes may have accumulated several defects including deficiency in cytoplasmic components in addition to chromosomes segregation errors. In humans, the MSUC can also be triggered by abnormal homologous chromosome synapsis in carriers of reciprocal translocations, which are well-documented to be associated with infertility and recurrent miscarriages in male and female carriers.¹⁹⁸⁻²⁰⁰ With respect to HMs, two of the original reports about androgenetic monospermic CHM found that 4-6% of affected women had balanced chromosomal translocations, which is higher than the frequency of reciprocal translocation in the general population (0.6%).^{26; 201} Miscarriages are a well-known risk factor for sporadic HM²⁰² and sporadic HM are more frequent in women with recurrent miscarriages than in women from the general population^{20; 203}. However, only weak associations have been reported between infertility problems, difficulties in conception, and irregular menstrual cycles and CHMs^{204; 205}, which may need to be revisited in the light of our findings. In *Meil null* oocytes, the spectrum of abnormalities ranged from oocytes with normal appearing chromosome complement (that would lead to euploid conceptions or aneuploid conceptions involving few chromosomes) to oocytes with few chromosomes (that would lead to severely aneuploid conceptions that may not survive implantation and lead to infertility) and empty oocytes (that would lead to androgenetic HM), which support the commonalties between HM, miscarriages, and infertility observed in our affected women. In addition to the role of normal *Meil* in double-strand breaks formation, in *C.*

elegans, *meil* has been shown to have a role in microtubule-severing activity similar to katanin²⁰⁶; consequently, its bi-allelic mutations may have prevented the disassembly of microtubules and the separation of the two sets of chromosomes at the spindle poles and favored their extrusion altogether into the PB. Investigating the possible occurrence of empty oocytes in null mice for *Top6bl* and *Rec114*, with no known roles in microtubule-disassembly, will help clarifying which *Meil* function is most likely at the origin of the extrusion of the oocyte chromosomes and spindles into the PB.

In conclusion, we unravel a mechanism, i.g. the extrusion of all the oocytes chromosomes with their spindles into the first PB, for the genesis of androgenetic zygotes in mammals and therefore a plausible mechanism for the genesis of AnCHM in humans.

Accession Numbers

The patient accession numbers for *MEI1* variants are LOVD: 00181110, 00181111, for *C11orf80* variants are LOVD: 00181112, 00181113, for *REC114* variants is LOVD: 00181114

Supplemental Data

Supplemental Data include eleven figures, five tables, and two videos.

Acknowledgements

We thank Maria Galvez for her help in communicating with some individuals and coordinating the collection of samples from family members; Nawel Mechtouf and Yasmine Khawajkie for recruiting individuals, retrieving and analyzing some HM tissues; Xiao Yun Zhang for her help in the collection of human oocytes; Conceptions Reproductive Associates of Colorado for providing medical information; and Jyun-Yuan Huang, Pao-Lin Kuo, Farah Khan, Surksha Agrawal for providing samples from individuals with recurrent miscarriages. We acknowledge the use of the McGill University and Génome Québec Innovation Centre for whole exome, Sanger, and targeted sequencing. We also acknowledge the use of Molecular Imaging Platform of the Research Institute of the McGill University Health Centre and thank Min Fu and Shibo Feng for their invaluable help. N.M.P.N. was supported by the RQR, McGill Faculty of Medicine, RI-MUHC, Desjardins Studentship in Child Health Research, and the CRRD. This work was supported by the Canadian Institute of Health Research (MOP-130364) to R.S.

Declaration of interest

The authors declare no competing interests.

Web resources

OMIM, <http://www.omim.org>

Combined Annotation Dependent Depletion (CADD), <http://cadd.gs.washington.edu/>

MutationTaster, <http://www.mutationtaster.org/>

PolyPhen-2, <http://genetics.bwh.harvard.edu/pph2/>

SIFT, <http://sift.bii.a-star.edu.sg/>

ExAC, <http://exac.broadinstitute.org/>

1000 Genomes, <http://www.internationalgenome.org/home>

NHLBI exome database, <http://evs.gs.washington.edu/EVS/>

MMRRC, <http://www.csbio.unc.edu/MMRRC/index.py>

Picard, <http://picard.sourceforge.net/>

NCBI homogene, protein multiple alignment,
<https://www.ncbi.nlm.nih.gov/homogene/69381>

Leiden Open Variation Database (LOVD), <http://www.lovd.nl/3.0/home>

Movie titles and legends

Video S4.1. Empty oocyte observed during *in vitro* maturation by live imaging. Video showing the extrusion of maternal chromosomes into the first polar body.

https://drive.google.com/file/d/117gI3cYAzDcQOgDBNVuxJI5_qG9i2_o1/view?usp=sharing

Video S4.2. Androgenetic zygote observed after *in vivo* fertilization. All Z-Axis stack positions of the androgenetic zygote that had lost all maternal chromosomes into the polar body using confocal immunofluorescence.

<https://drive.google.com/file/d/1N1HcormjwSfc7DQIEfDTFrOCaO8vHKTW/view?usp=sharin>

g

Figures

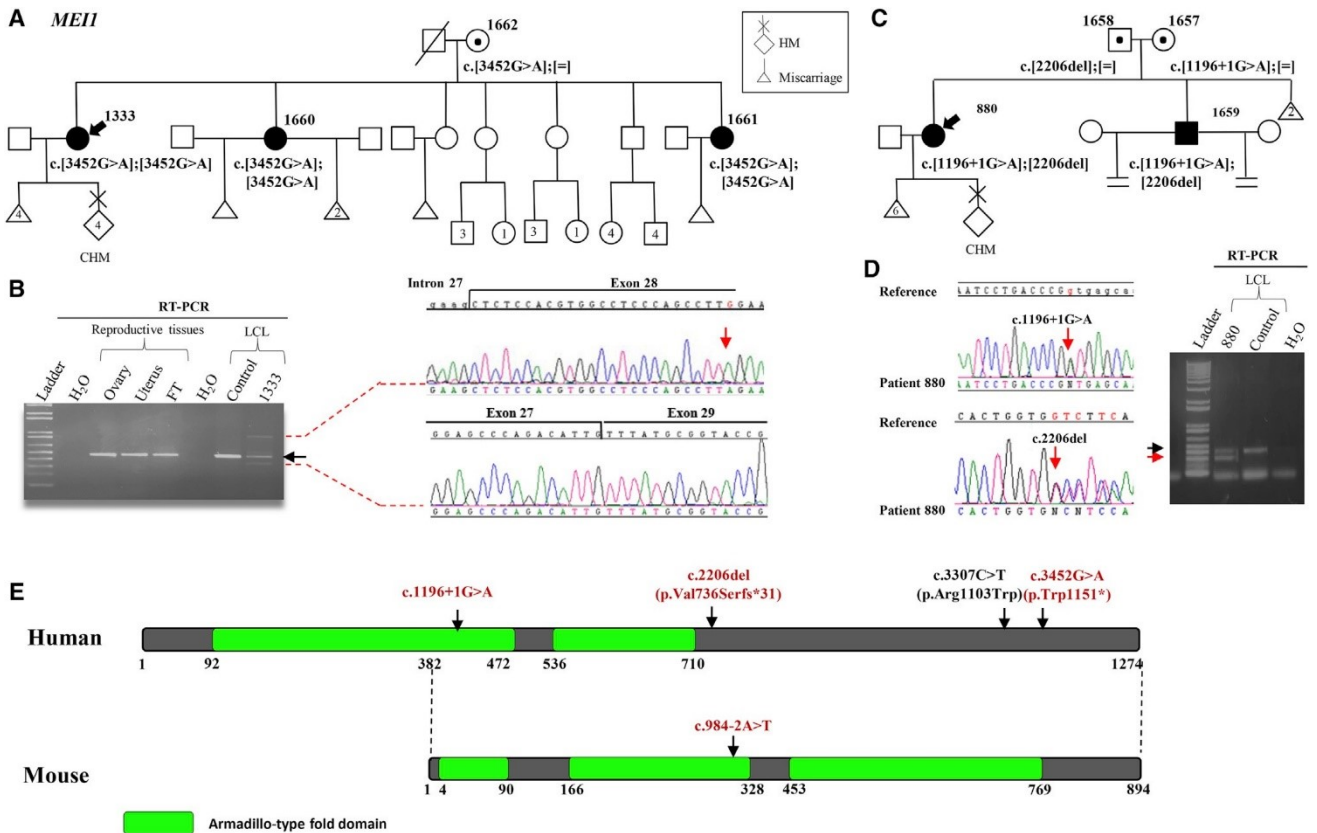


Figure 4.1. Pedigree structure, reproductive outcomes, and mutation analysis of two families with bi-allelic *MEII* mutations

(A) Sanger sequencing and segregation of the mutation identified in *MEII* in the family of proband 1333 (indicated by an arrow).

(B) RT-PCR demonstrating abnormal splicing caused by the nonsense mutation (c.3452G>A) and the generation of three cDNA fragments, the normal fragment indicated by a black arrow and two abnormal fragments indicated by dashed red lines (a larger fragment that includes intron 27 and a smaller fragment that skips exon 28).

(C) Sanger sequencing and segregation of the mutations identified in *MEII* in the family of proband 880 (indicated by an arrow).

(D) Abnormal splicing in affected individual 880 showing the amplification of a smaller cDNA fragment that corresponds to the skipping of exon 11 (red arrow) and another cDNA fragment corresponding to the normal splicing isoform (black arrow). RNA was from lymphoblastoid cell lines (LCL) of the affected women.

(E) Schematic presentation of the domains of human and mouse *MEII*. The positions of the mutations are

indicated by arrows. The mutations identified in this study are shown in red. In black is a recently reported mutation in two infertile brothers with non-obstructive azoospermia. The mutation in the *Meil* knockout is shown on the mouse protein.

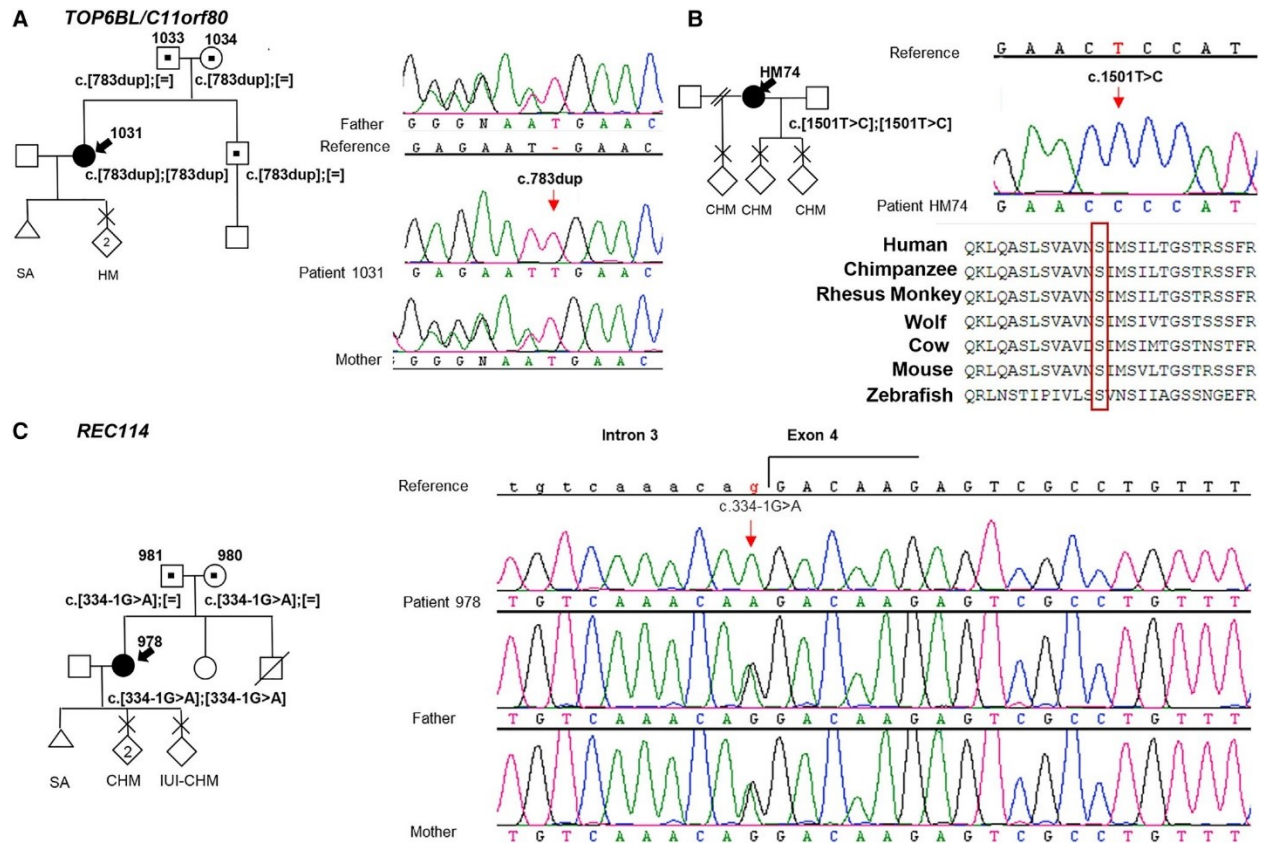


Figure 42. Pedigree structure, reproductive outcomes, and mutation analyses OF *TOP6BL/C11orf80* and *REC114* in three affected women with bi-allelic mutations

(A) Pedigree of proband 1031 showing the segregation of *TOP6BL/C11orf80* mutations and the chromatograms.

(B) Pedigree of proband HM74 showing the chromatogram of her mutation in *TOP6BL/C11orf80* and the conservation of the changed amino acid in different species by multiple alignment from NCBI.

(C) Pedigree of proband 978 with *REC114* mutation and the chromatograms.

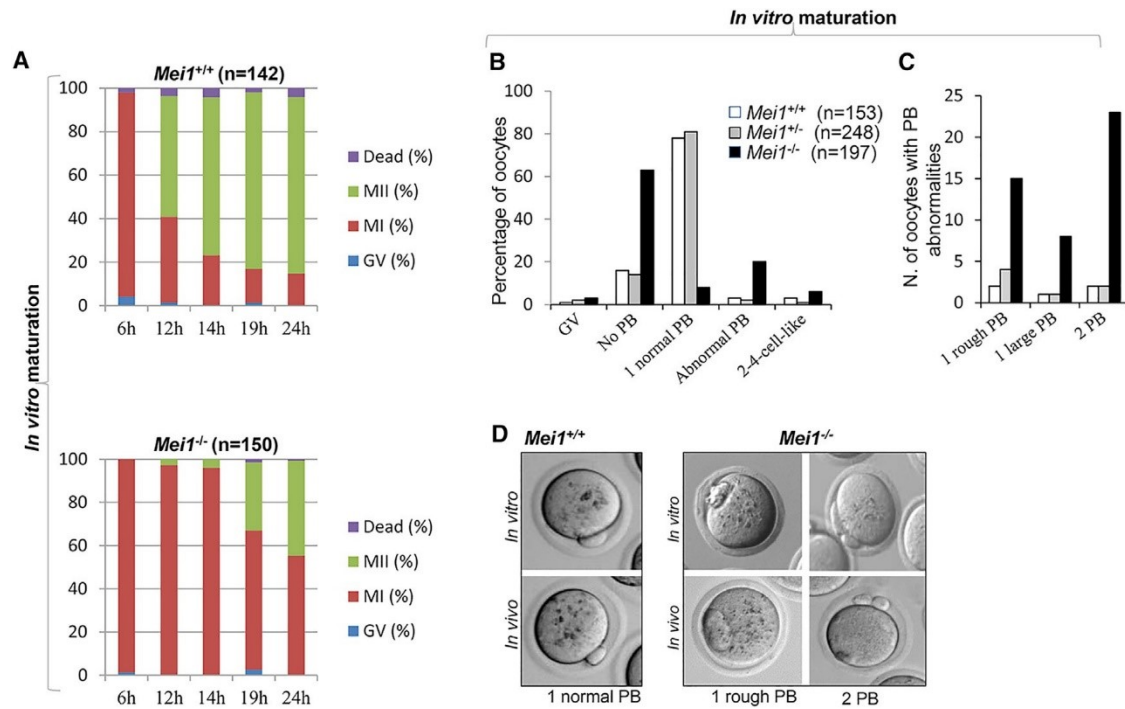


Figure 4.3 Meiosis I abnormalities in oocytes from wild-type, heterozygous, and homozygous mice

(A) Fully grown oocytes from *Mei1^{b/p}* and *Mei1^{-/-}* mice were cultured *in vitro* and the frequency of various stages at different time point were recorded by phase contrast microscopy. The absence of polar body (PB) 17–19 hr after germinal vesicle (GV) breakdown was our criterion for arrest before metaphase I stage (MI) and the presence of at least one PB was our criterion for progression to metaphase II arrest (MII).

(B) Percentages of oocytes with or without abnormalities observed after *in vitro* maturation.

(C) Numbers (N) of oocytes with various PB abnormalities observed after *in vitro* maturation.

(D) Examples of oocytes with abnormal polar bodies after *in vitro* or *in vivo* maturation.

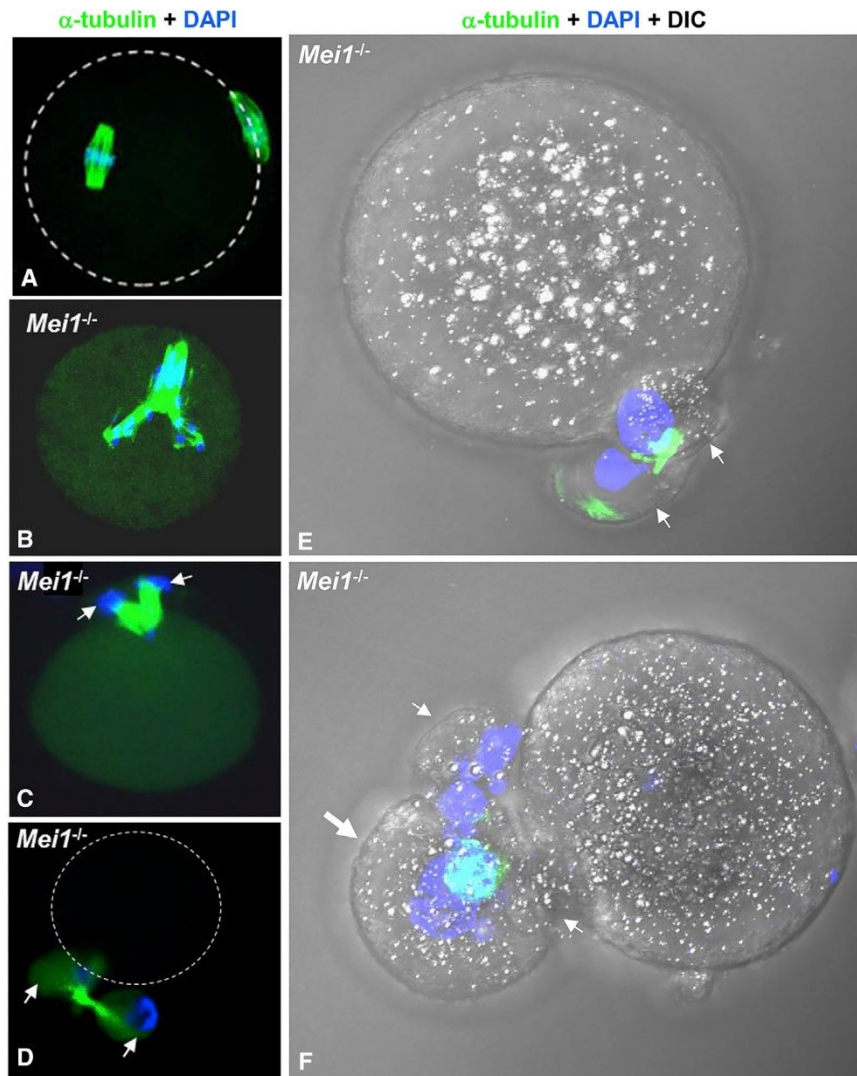


Figure 4.4. Various spindle and chromosome congression abnormalities after in vitro maturation

- (A) Oocyte from wild-type at MII displaying two normal spindles, one in the oocyte with aligned chromosomes and another in the polar body (PB).
- (B) An oocyte from *Meil*^{-/-} with tripolar spindles within the oocyte and misaligned chromosomes.
- (C) An oocyte from *Meil*^{-/-} with tripolar spindles that had extruded DNA at two poles into the PB (arrows).
- (D) An empty oocyte from *Meil*^{-/-} that had extruded the spindles and the chromosomes at their two poles into two PB (arrows).
- (E) Another empty oocyte from *Meil*^{-/-} that had extruded all its DNA with the spindles into the PB (arrows).
- (F) An oocyte that extruded one large (large arrow) and two normal-size PB (small arrows).

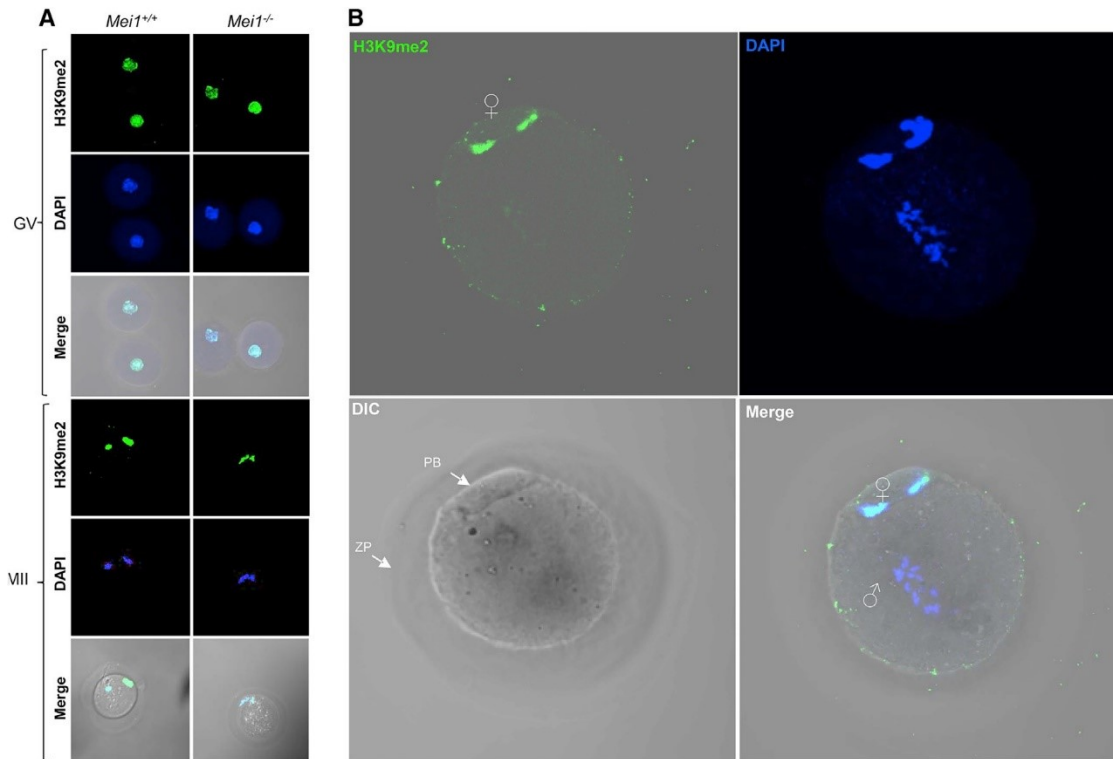


Figure 4.5 H3K9me2 staining of maternal chromosomes in oocytes and zygotes from wild-type and *Mei1*^{-/-}

(A) H3K9me2 immunofluorescence of GV and MII oocytes from wild-type and *Mei1*^{-/-} females, demonstrating that H3 methylase is not impaired in *Mei1*-deficient oocytes.

(B) H3K9me2 immunofluorescence on zygotes showing the staining of maternal but not paternal chromosomes in a zygote from *Mei1*^{-/-} females. GV stands for germinal vesicle; MII, metaphase II; PB, polar body; ZP, zona pellucida; ♀, maternal chromosomes; ♂, paternal chromosomes; and DIC, differential interference contrast.

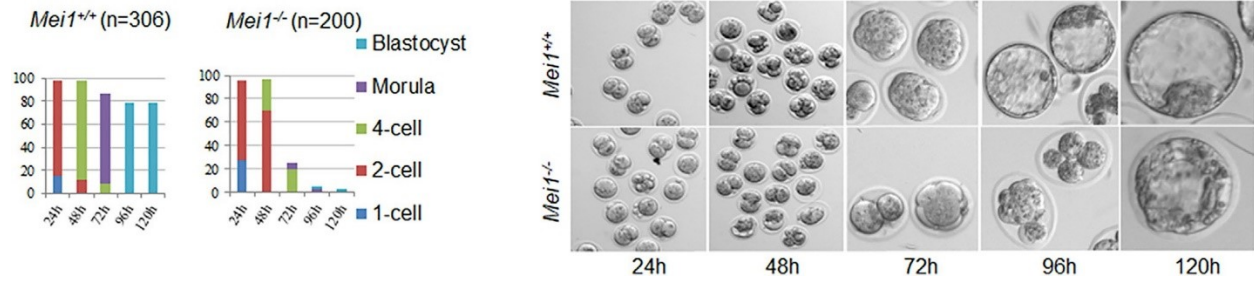


Figure 4.6 Preimplantation Development of *Meil*^{-/-} Oocytes in Culture

Zygotes were collected from wild-type or *Meil*^{-/-} females 20 hr after hCG injection and mating with wild-type males and cultured *in vitro*. Embryonic development was analyzed daily using phase contrast microscopy. The embryos that failed to develop by the next day were removed for further analysis. Embryos derived from *Meil*^{-/-} oocytes were arrested mainly at the 2- to 4-cell stage. A few reached the morula or blastocyst stages but appeared disorganized and none hatched.

Supplementary figures and tables

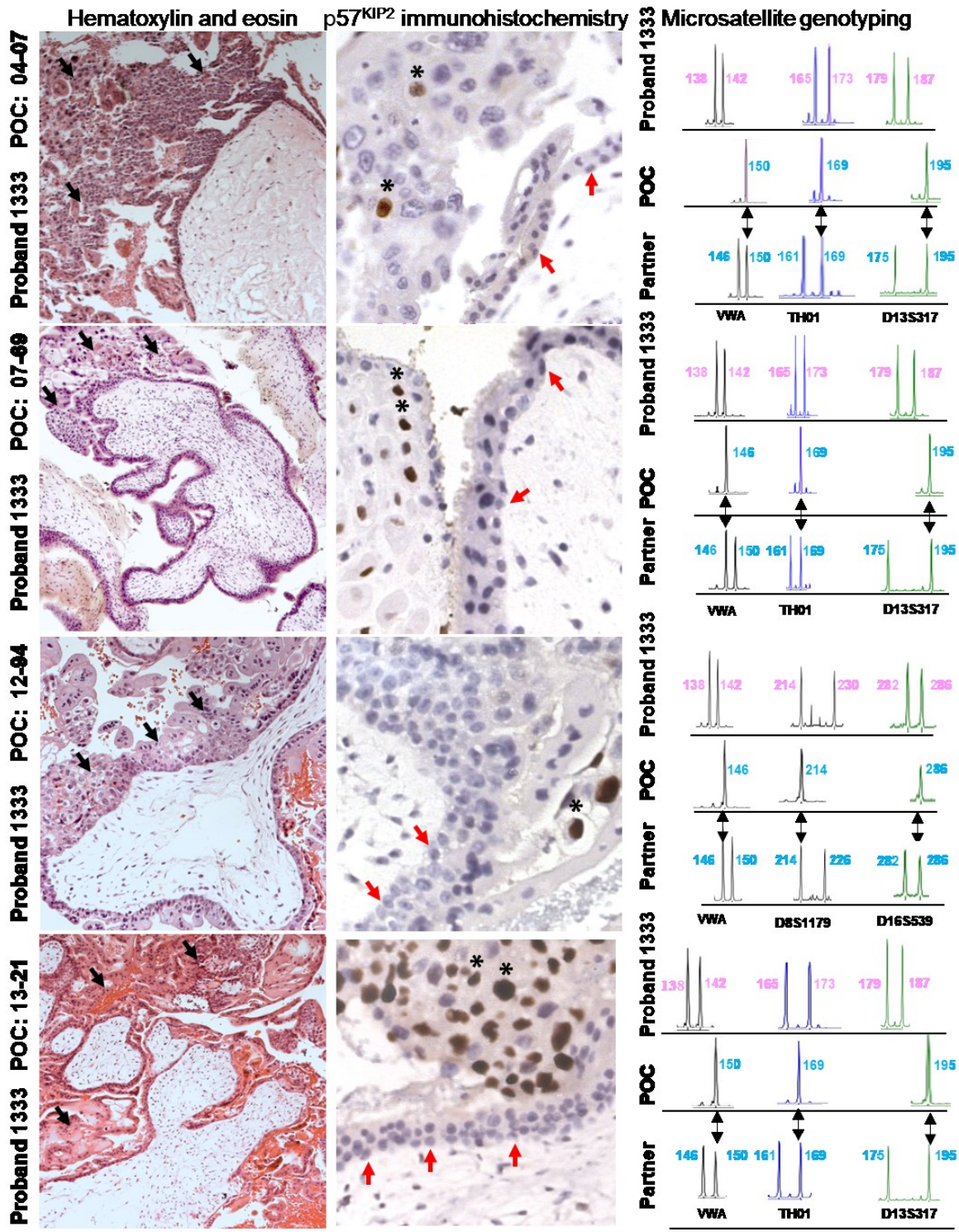


Figure S4.1. Characterization of four HM tissues from proband 1333 with bi-allelic *MEII* mutations. Left panel shows haematoxylin and eosin staining demonstrating excessive trophoblastic proliferation in the different conceptions (black arrows). Middle panel shows p57^{KIP2} immunohistochemistry showing negative staining in the cytotrophoblast (red arrows) while the internal control, the nuclei of the extravillous trophoblast cells are positive (asterisks). Right panel shows examples of HM tissue genotypes at 3 microsatellite markers demonstrating the androgenetic monospermic contribution to the molar genome with one paternal allele at each marker. POC stands for product of conception.

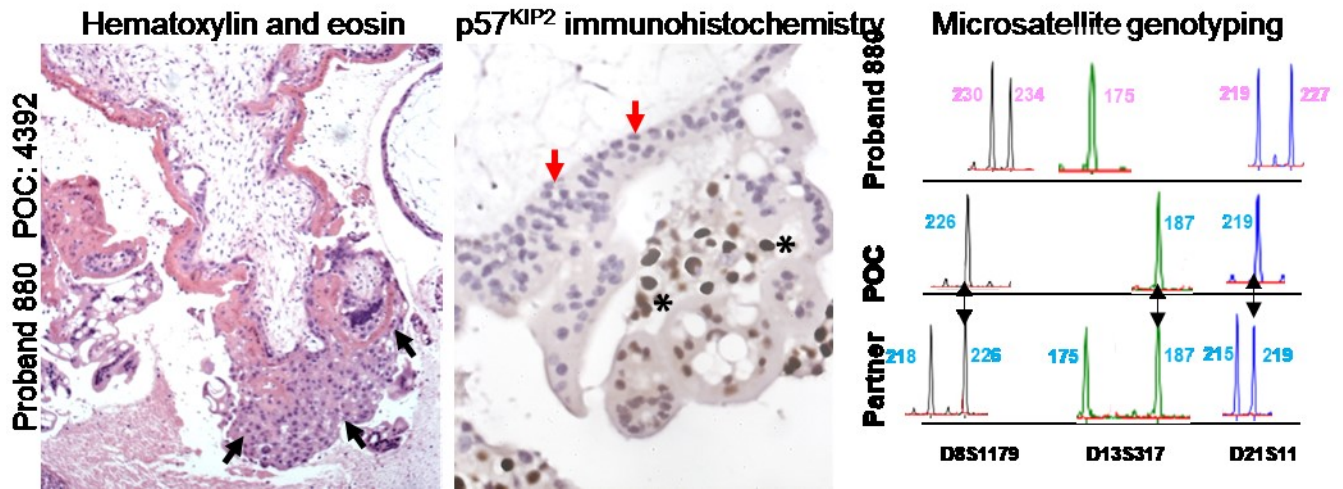


Figure S4.2. Characterization of one HM tissue from proband 880 with bi-allelic *MEII* mutations. Left panel shows haematoxylin and eosin staining demonstrating excessive trophoblastic proliferation in the different conceptions (black arrows). Middle panel shows p57^{KIP2} immunohistochemistry showing negative staining in the cytotrophoblast (red arrows) while the internal control, the nuclei of the extravillous trophoblast cells are positive (asterisks). Right panel shows examples of HM tissue genotypes at 3 microsatellite markers demonstrating the androgenetic monospermic contribution to the molar genome with one paternal allele at each marker. POC stands for products of conception.

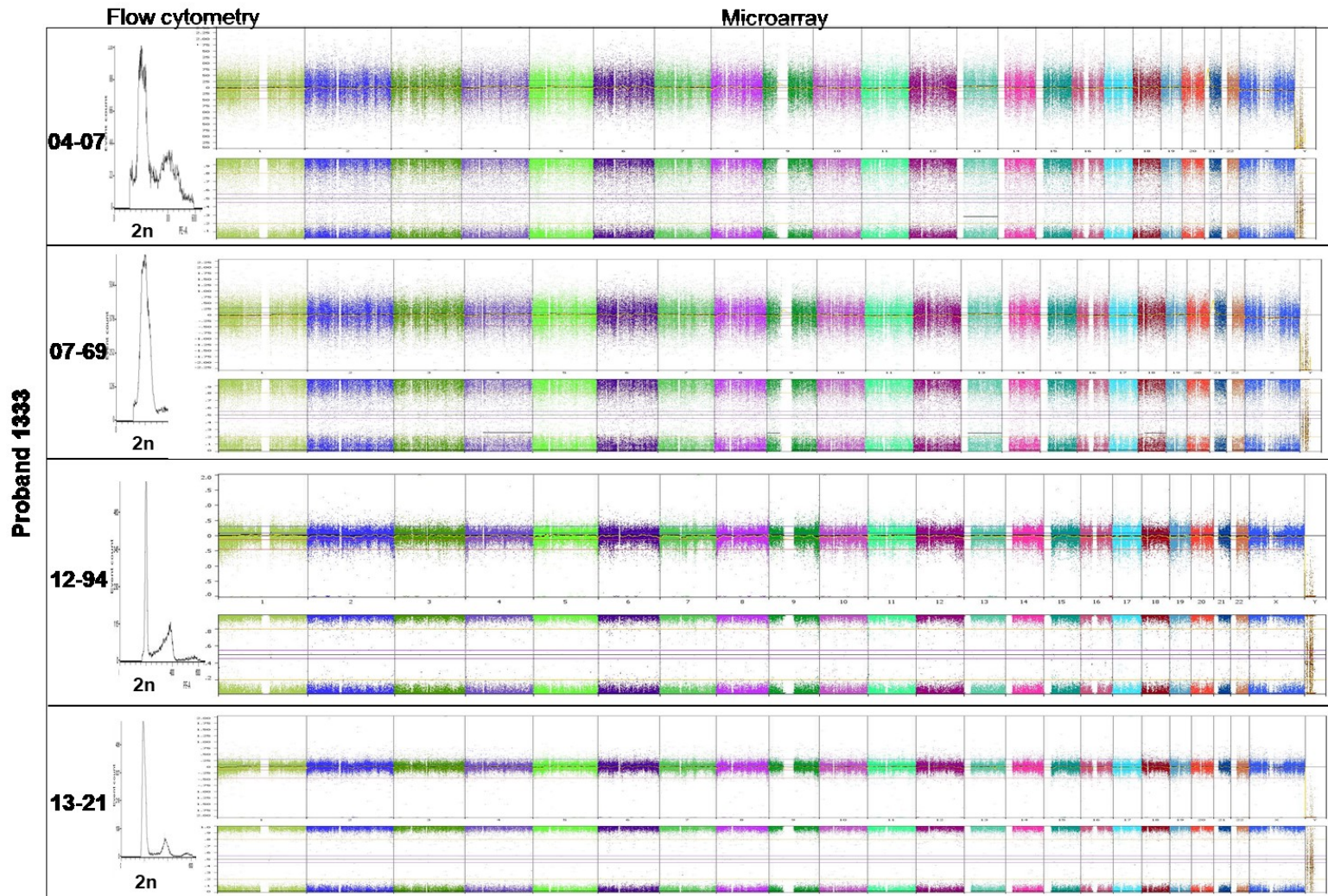


Figure S4.3. Microarray and flow cytometry analyses on 4 HM from proband 1333 with bi-allelic mutations in *MEI1* showing their diploid genomes (indicated by 2n) and the absence of aneuploidies. The peak on the right of the diploid peak corresponds to 4n and represent cells in G2.

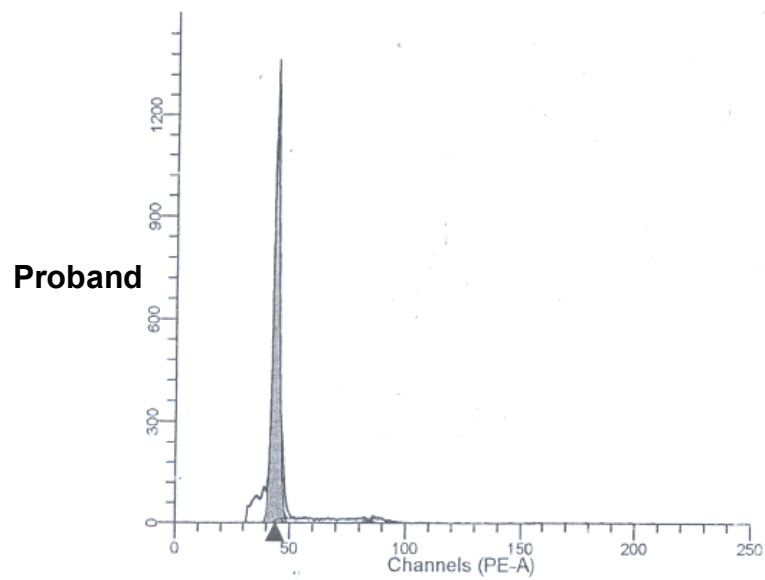


Figure S4.4. Flow cytometry analysis of the HM from proband 880 with bi-allelic mutations in MEI1 showing its diploid genome.

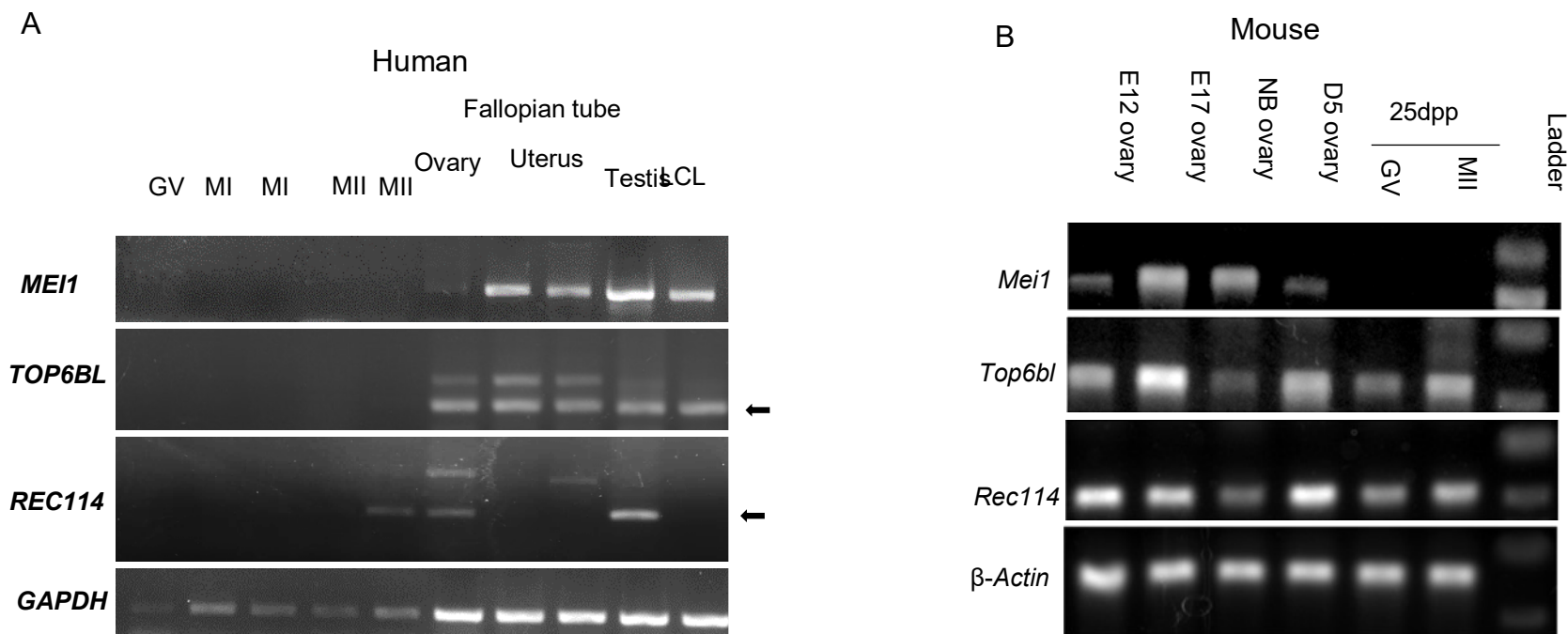


Figure S4.5. Transcription of *MEI1*, *TOP6BL*, and *REC114* in different stages of oocytes and reproductive tissues. (A) Transcription of *MEI1*, *TOP6BL*, and *REC114* in different stages of human oocytes and reproductive tissues. The arrows indicate the isoforms observed in most tissues, which have the expected sizes (340 bp for *TOP6BL* and 259 bp for *REC114*). (B) Transcription of *Mei1*, *Top6bl*, and *Rec114* in wild-type mouse ovaries from embryonic day 12 (E12), embryonic day 17 (E17), newborn (NB), day 5 postpartum (D5) and oocytes at two stages from mice at day 25 postpartum (25 dpp). *GAPDH* and β -actin serve as internal controls. LCL, stands for lymphoblastoid cell line; GV, for germinal vesicle; MII, for metaphase II; dpp, for day postpartum; NB, for newborn.

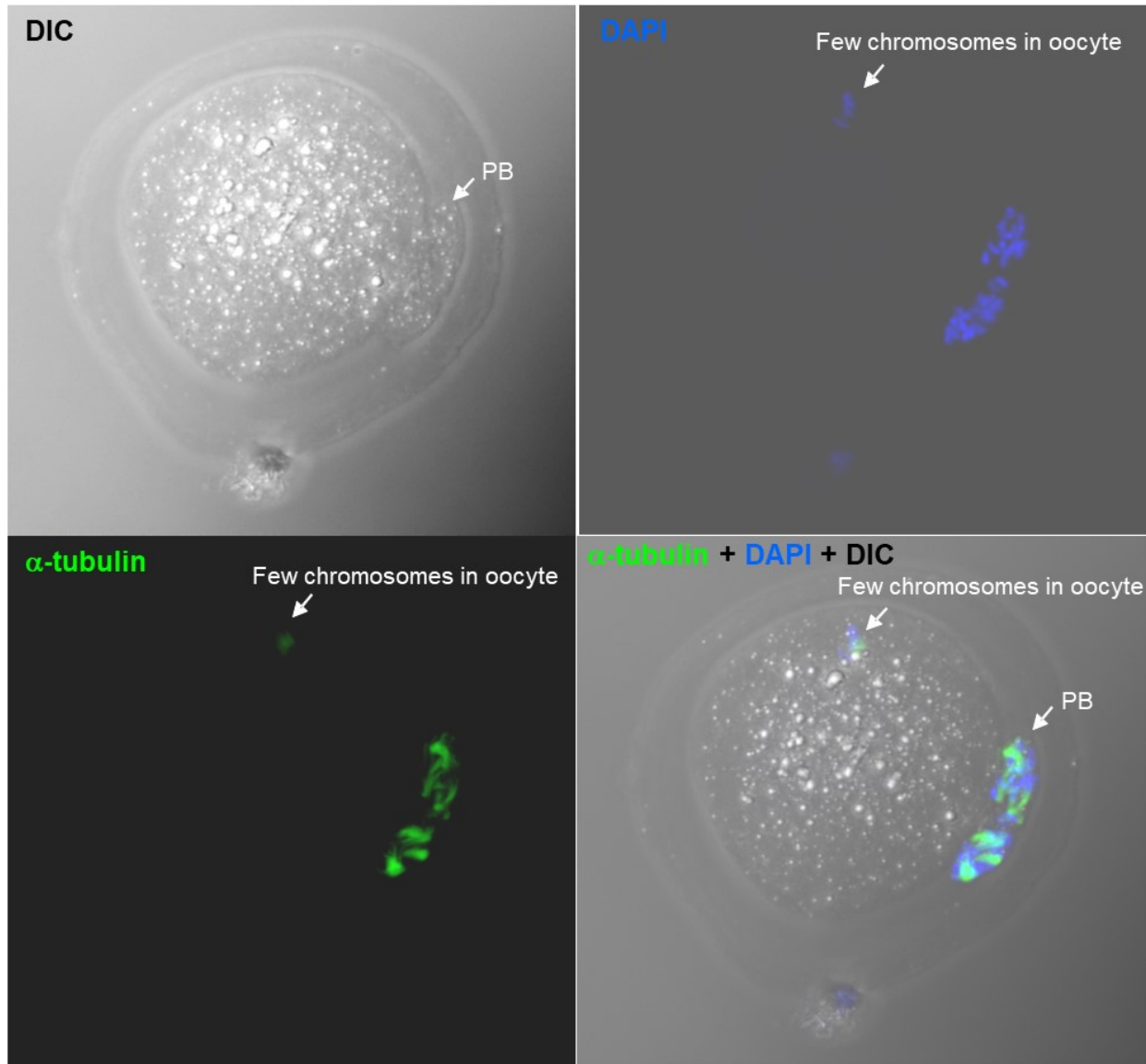


Figure S4.6. Oocyte matured *in vitro* stained with anti α -tubulin (green) and DAPI (blue). Note that the oocyte had lost most of maternal chromosomes and extruded them into the polar body (PB).

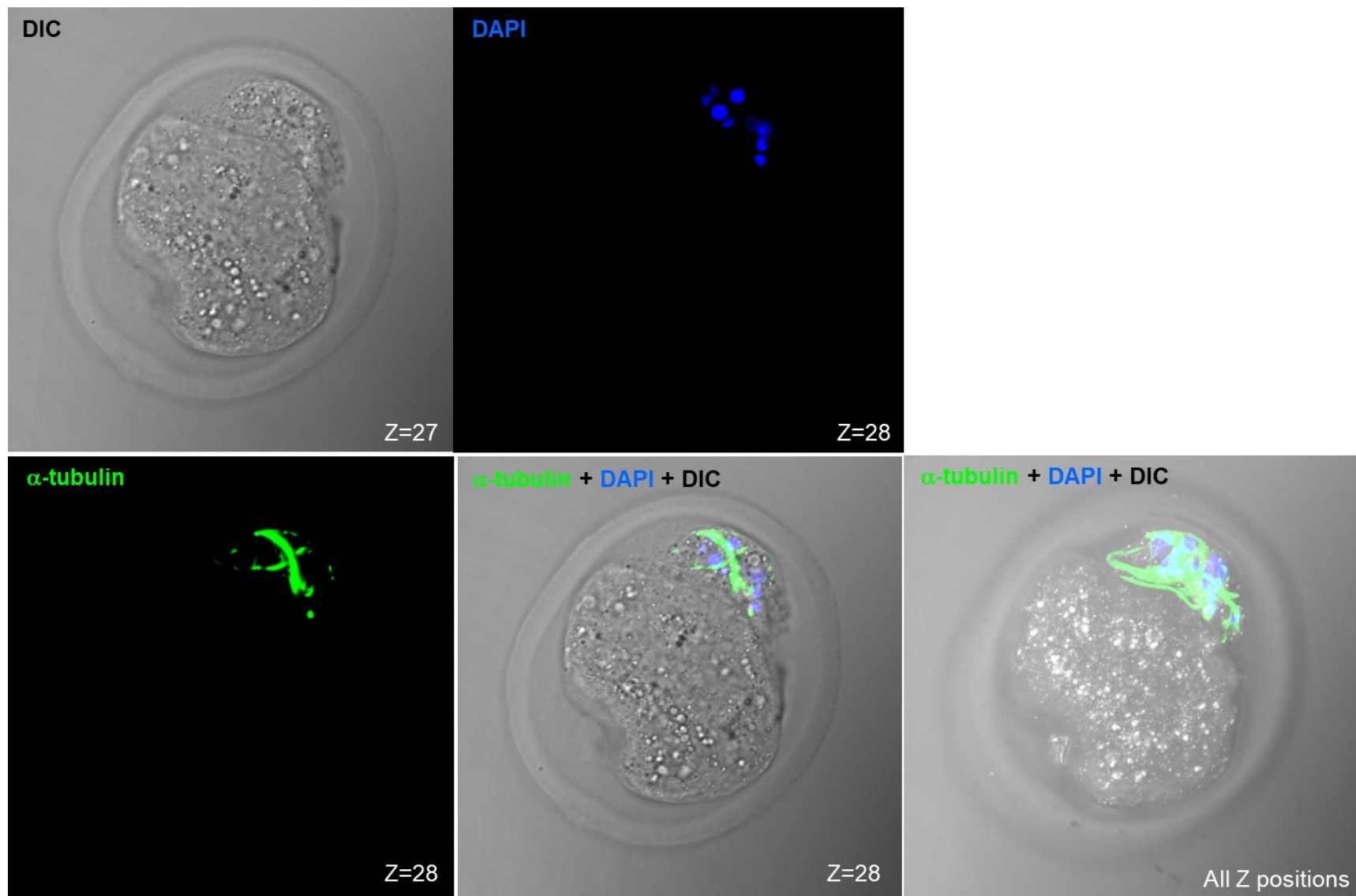


Figure S4.7. An empty oocyte matured *in vivo* and displaying all maternal DNA that had been extruded into the polar body. Z indicates the confocal Z-Axis position.

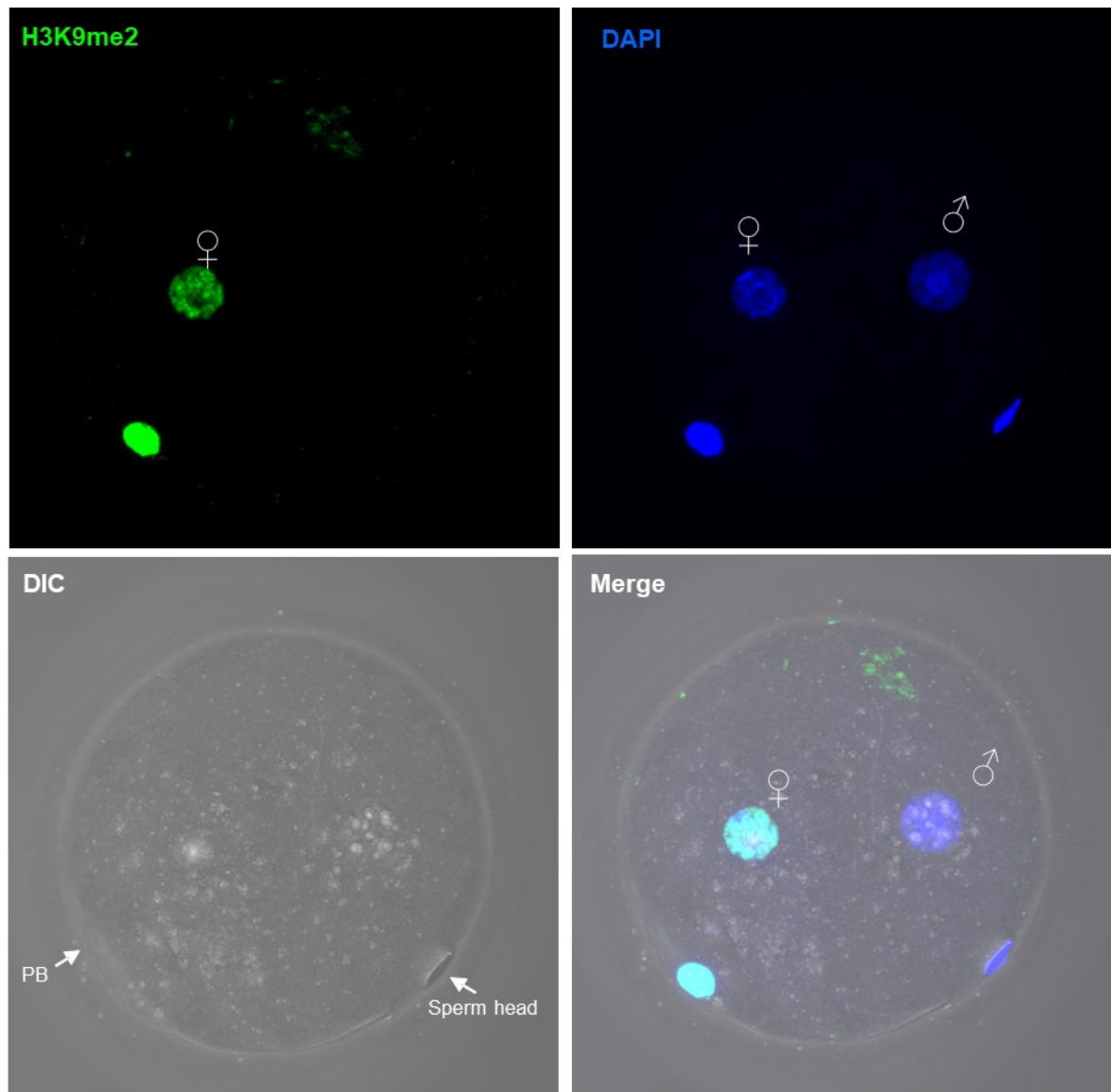


Figure S4.8. H3K9me2 immunofluorescence showing the staining of maternal but not paternal chromosomes in a *Meil*^{+/-} zygote. PB, polar body; ZP, zona pellucida; ♀, maternal chromosomes; ♂, paternal chromosomes; and DIC, differential interference contrast.

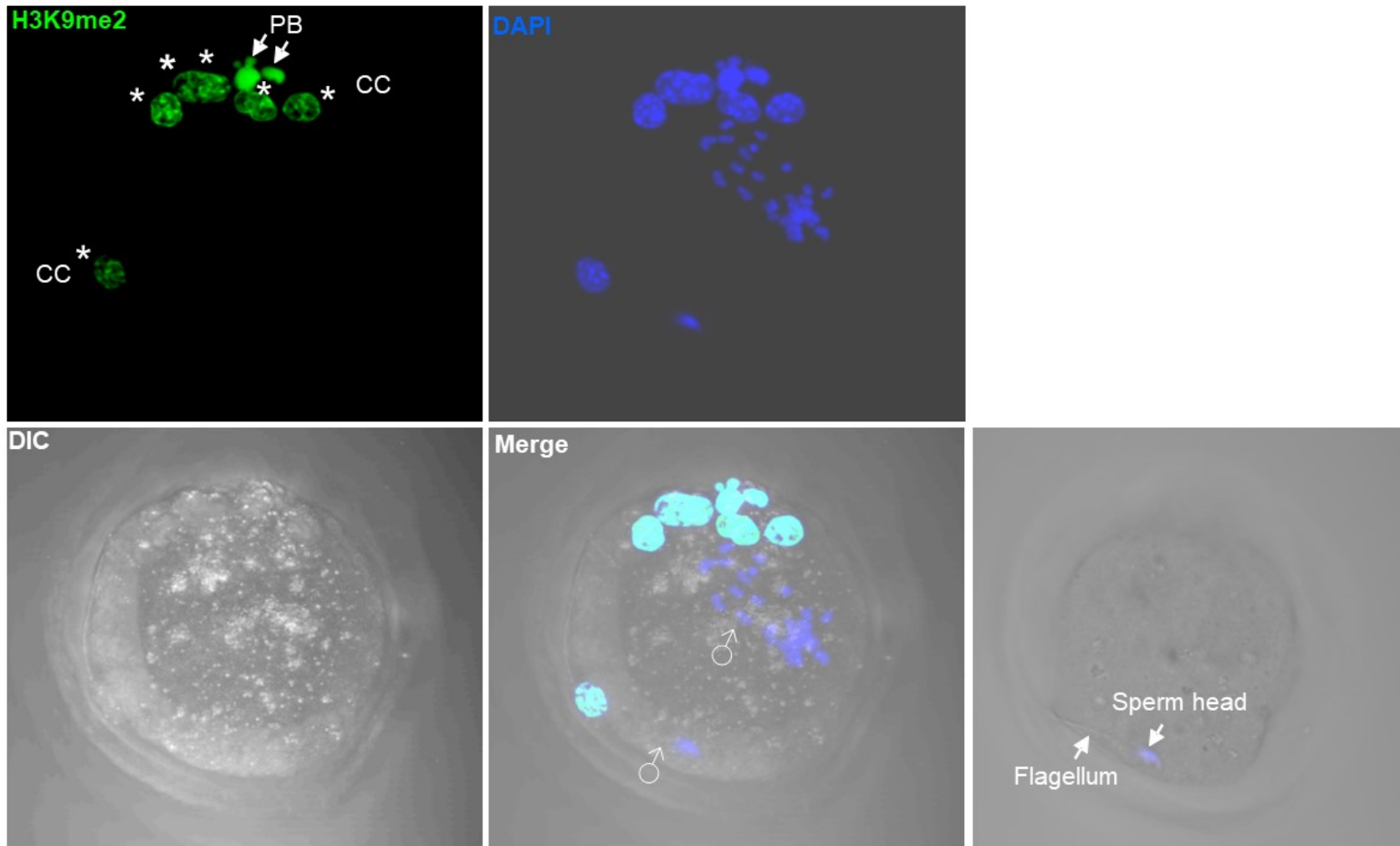


Figure S4.9. An in vivo fertilized oocyte stained with anti-H3K9me2 and DAPI. No maternal chromosomes were observed in the oocyte. Maternal chromosomes were extruded into the polar body (PB). The asterisks indicate cumulus cells (CC) that had penetrated under the zona pellucida. The oocyte displays paternal chromosomes that had started the first mitotic division and another spermatozoid (arrows) that is still condensed.

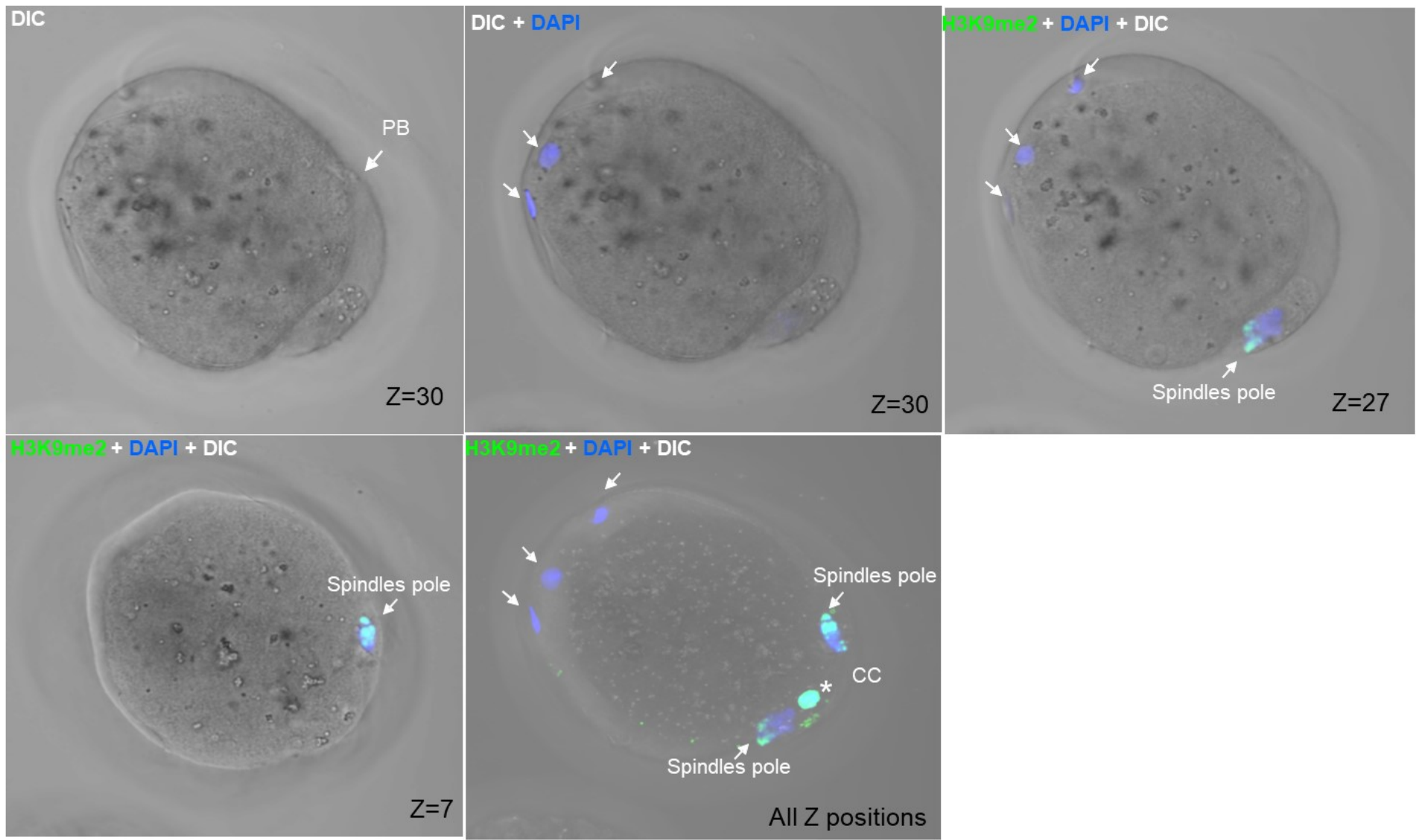


Figure S4.10. An empty in vivo fertilized oocyte from *Meil*-deficient female stained with anti-H3K9me2 (green) and DAPI (blue). The oocyte had extruded all maternal DNA with their spindles into the polar body (PB) and is fertilized by three sperm, all of which are still condensed. The asterisk indicates a cumulus cell (CC) that had penetrated under the zona pellucida. Z indicates the confocal Z-Axis position.

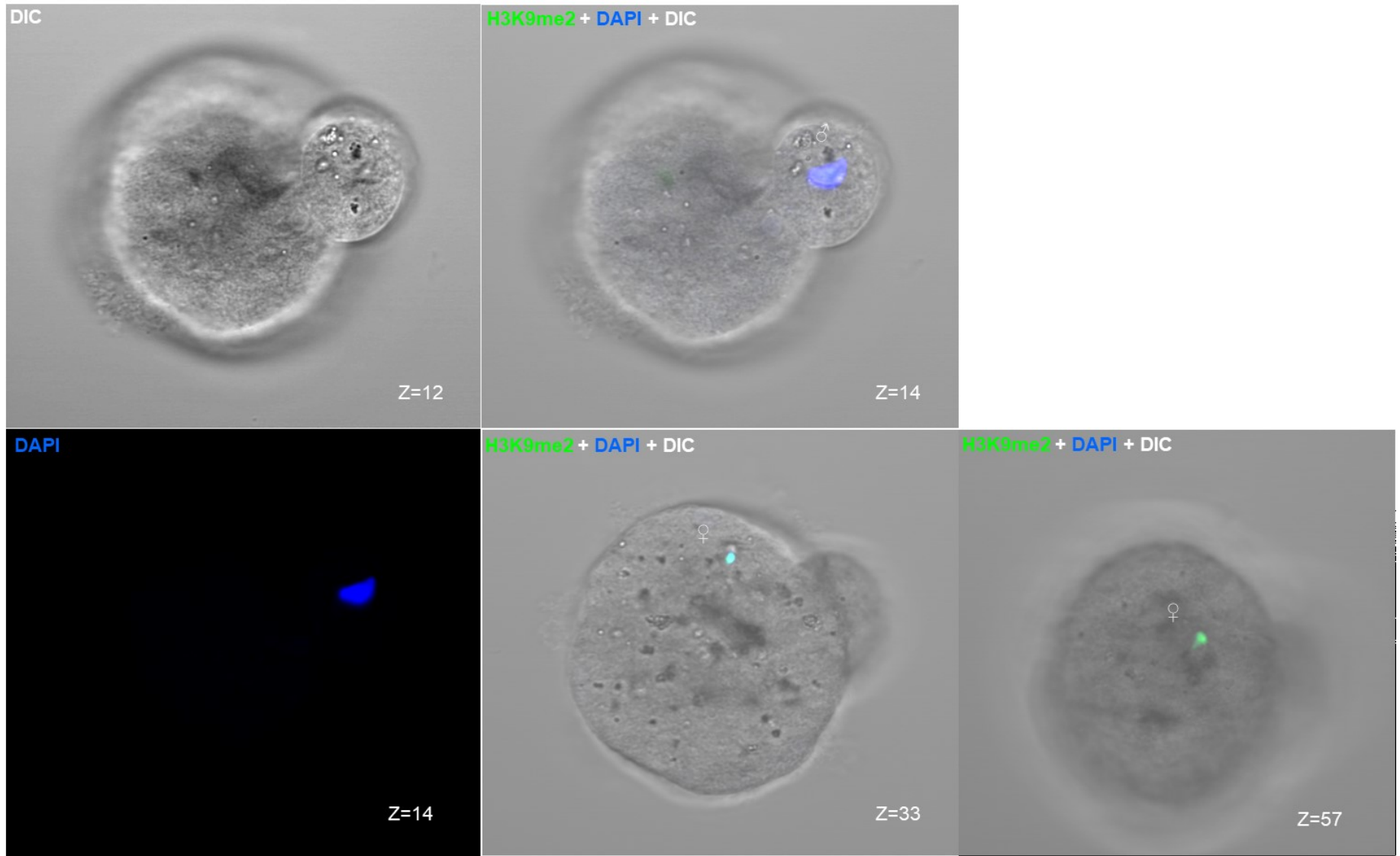


Figure S4.11. An in vivo fertilized oocyte from *Meil*-deficient female stained with anti-H3K9me2 (green) and DAPI. Maternal chromosomes appear in green/blue in the oocyte and a spermhead in a protruding smaller cell. Z indicates the confocal Z-Axis position.

Table S4.1: Primers used to amplify human genomic and complementary DNA

Gene	Proband	Mutation in cDNA and Protein	Primer name	Primer (5' to 3')	Application
PCR for Sanger Sequencing					
<i>MEI1</i>	1333	c.3452G>A, p.Trp1151*	<i>MEI1_ex28_W1151X_f</i>	CTTACTGCCTGCCTTCCACA	PCR for Sanger Sequencing
			<i>MEI1_ex28_W1151X_r</i>	GTCCCTGGAGTGAGGAGAT	
<i>MEI1</i>	880	c.1196+1G>A	<i>MEI1_ex11_A438S_f</i>	GAGCCTGTCACCTCTTCTGG	PCR for Sanger Sequencing
			<i>MEI1_ex11_A438S_f</i>	CACAATTATGAAGGGCCAAC	
<i>MEI1</i>	880	c.2206del, p. Val736Serfs*31	<i>MEI1_V736Sfs_Ex19F</i>	CCTTGCACAAGGCACAGAAC	PCR for Sanger Sequencing
			<i>MEI1_V736Sfs_Ex19R</i>	CCTCCCAGGAAGGCTGAGAT	
<i>C11orf80/TOP6BL</i>	1031	c.783dup, p. Glu262*	<i>C11orf80_ex11F</i>	TTTGCAGGTCAGATTTCATTCA	PCR for Sanger Sequencing
			<i>C11orf80_ex11R</i>	AAGCTGACACCTGGCACTTACAAA	
<i>C11orf80/TOP6BL</i>	HM74	c.1501T>C, p. Ser501Pro	<i>C11orf80_Ex13F2</i>	CCCTCTGGGATTCTCTAAACC	PCR for Sanger Sequencing
			<i>C11orf80_Ex13F2</i>	TCCCAATCCCAATCTCTACTA	
<i>REC114</i>	978	c.334-1G>A	<i>REC114_ex4_splice_F</i>	ATACCTTCTCCTCCGCAAG	PCR for Sanger Sequencing
			<i>REC114_ex4_splice_R</i>	CAAACCTCCACTGTCATTTGG	
RT-PCR					
<i>MEI1</i>			RT <i>MEI1_ex26F</i>	CATCTTATGCTTCCTGCGGAC	splicing effect of c.3452G>A (patient 1333)
			RT <i>MEI1_ex29R</i>	TGGTGTTTCGAGAGGGTAGACA	
<i>MEI1</i>			RT <i>MEI1_Splicing_Ex10F</i>	CAGTGAAGTGCTCGTCTGGT	Splicing effect of c.1196+1G>A (patient 880)
			RT <i>MEI1_Splicing_Ex13R</i>	CGCACATCGGTTTAGCATGG	
<i>MEI1</i>			RT <i>MEI1_Ex18F</i>	CTGAAAGCCTTGCCTTCTCTGT	Expression of <i>MEI1</i> in different tissues
			RT <i>MEI1_Ex20R</i>	AACCAAAGTTCAGGACACGG	
<i>C11orf80/TOP6BL</i>			<i>C11orf80_N262ter_F</i>	GGACTTCAGAGGAAGGCAGC	Expression of <i>C11orf80/TOP6BL</i> in different tissues
			<i>C11orf80_N262ter_R</i>	GGATGTCTAGCACAGGGTG	
<i>REC114</i>			RT <i>REC114_new_F</i>	GCAGGTGCCTGATGGAAACA	Expression of <i>Rec114</i> in different tissues
			RT <i>REC114_new_R</i>	TTCTGCACCCCATGCAGATT	

Table S4.2: Primers used in RT-PCR to amplify mouse genes

Gene	Primer (5' to 3')	Annealing temperature (°C)	Length (bp)
<i>Meil</i> -Forward	TTATCTCAAGCCTGTATT	50	285
<i>Meil</i> -Reverse	CTGGAGTGTATCGTTTGA		
<i>Rec114</i> -Forward	GTGTTCTACAGGAAAGGA	58	274
<i>Rec114</i> -Reverse	AAGGTGCTTGGAATAATAC		
<i>Gm960</i> -Forward	ATCAGTCTCAGAATATGAACGCACAG	50	101
<i>Gm960</i> -Reverse	TCCCCAGATTTTCGCTTGTTGTA		
Actin-Forward	TATTGGCAACGAGCGGTTCC	50	139
Actin-Reverse	GGCATAGAGGTCTTTACGGATGTC		

Table S4.3: Subjects screened by targeted sequencing for mutations in the three genes.

	<i>MEI1</i>	<i>C11orf80/TOP6BL</i>	<i>REC114</i>
2 HM	5	14	5
1 HM+ \geq 3RM	48	32	48
only \geq 3RM	46	200	46
Total number of subjects	99	246	99

HM stands for hydatidiform mole; RM stands for recurrent miscarriages.

Table S4.4: Summary of data about the mutations found in the 3 genes.

Gene	Proband	Ethnicity	Mutation	Predicted consequence	State	rs ID	MAF	Polyphen	CADD	SIFT	MutationTaster	Run of Homozygosity
<i>MEI1</i>	1333	Mexican	c.3452G>A, p.Trp1151*	Stopgain	Homozygous	rs749779829	0.000008					yes
	880	French Canadian	c.1196+1G>A	Aberrant splicing	Compound heterozygous	Novel	n.a					
	880		c.2206del, p.Val736Serfs*31	Frameshift	Compound heterozygous	rs759915989	0.00003					
<i>C11orf80</i>	1031	Indian	c.783dup, p.Glu262*	Frameshift	Homozygous	rs779402951	0.0001					yes
	HM74	Mexican	c.1501T>C, p. Ser501Pro	Conserved missense	Homozygous	Novel	n.a	Damaging	22.5*	Damaging	Amino acid change. Splice site might be changed	yes
<i>REC114</i>	978	Turkish	c.334-1G>A	Aberrant splicing	Homozygous	rs780169159	0.000025					yes

* CADD score ≥ 20 indicates deleterious variants. Variants nomenclature for *MEI1* is given according to the following references, NM_152513.3, NP_689726.3. For *C11orf80*, the references are NM_024650.3, NP_078926.3. For *REC114*, the references are NM_001042367.1, NP_001035826.1. MAF stands for minor allele frequency.

Table S4.5: Summary of oocyte stages at time of collection from proband 1333 (at 36 years) and comments on embryo development after ICSI

Right ovary: There were 5 follicles measuring >16 mm. An oocyte was obtained from each of these follicles. There were also 3 follicles between 11 mm and 16 mm.

Left ovary: There were 2 follicles measuring >16 mm. An oocyte was obtained from each of these follicles. There were also 3 follicles between 11 mm and 16 mm

The quality of the oocytes was reported to be poor as most were dark, grainy, and had sticky cytoplasm. **Several oocytes had multiple PB.** Fertilization rate was noted to be below average.

No.	Oocyte stage & comments	Fertilization	Day 3	Day 5
1	MII	Normal	normal with minimal fragmentation	High quality blastocyst. Sent for PGD and found to be digynic triploid.
2	MII	Normal	normal with minimal fragmentation	In progress. Rechecked on day 6 and did not develop to high quality blastocyst.
3	MII	Normal	asymmetrical cells with minimal fragmentation	Arrested
4	MII	Normal	asymmetrical cells with minimal fragmentation	Arrested
5	MII	Normal	asymmetrical cells with minimal fragmentation	Arrested
6	MII	Atretic	n.a	n.a
7	MII	Atretic	n.a	n.a
8	MII	Abnormal with uneven pronuclei	n.a	n.a
9	MII	Abnormal with uneven pronuclei	n.a	n.a
10	MII	n.a.	n.a	n.a
11	MII	n.a.	n.a	n.a
12	Fractured zona	n.a	n.a	n.a
13	Fractured zona	n.a	n.a	n.a
14	Fractured zona	n.a	n.a	n.a
15	Fractured zona	n.a	n.a	n.a
16	atretic	n.a	n.a	n.a
17	atretic	n.a	n.a	n.a
18	atretic	n.a	n.a	n.a
19	2-cell	n.a	n.a	n.a

n.a., stands for data not available; PB for polar body; PGD, for preimplantation genetic diagnosis; MII, for metaphase II; ICSI, for intra-cytoplasmic sperm injection.

CHAPTER 6: GENERAL DISCUSSION

As an MSc student who fast-tracked to the PhD program, I had the opportunity to investigate the pathogenesis of diploid biparental RHM caused by recessive mutations in *NLRP7* or *KHDC3L* mutations and diploid androgenetic RHM caused by recessive mutations in *MEI1*, *TOP6BL*, and *REC114*. Despite their genotypic, and perhaps many other, differences between these conceptions, all lead to the same phenotype, hydropic chorionic villi, excessive trophoblastic proliferation and no, or abnormal, embryonic development. In this discussion, I will review our findings and compare the two mechanisms that my work has revealed from studies on *NLRP7* (which represents a model for diploid biparental HM formation) and *MEI1* (which represents a model for androgenetic HM formation). Understanding the differences, similarities, and the effects caused by these genes provides us with profound insights into the genetics of RHM specifically and HM in general.

1- NLRP7 and recurrent diploid biparental HM:

Our study in Chapter 2 was the first to report the positive expression of p57^{KIP2} in diploid biparental RHM caused by *NLRP7* mutations. However, it is possible that prior reported cases overlooked the positive expression of p57^{KIP2} since its expression is limited. Cells require sophisticated molecular machinery to determine the cells' fates toward proliferation, arrest, differentiation, quiescent, or apoptosis. p57^{KIP2} is a cell cycle regulator which was reported to induce the cell cycle exit and promote cell differentiation, while opposite effects occur in p57-deficient cells [108](#); [147](#); [148](#). In addition, the level of p57^{KIP2} expression was reported to peak at key stages of differentiation of several organs, highlighting its role in tissue differentiation [208](#). Therefore, silencing of p57^{KIP2} may indicate that the cytotrophoblast cells do not exit the cell cycle to differentiate normally, but rather continue cell division, leading to the high proliferation of trophoblast. The correlation between p57^{KIP2} expression, embryonic development, and mild trophoblastic proliferation (which result in a “less severe” phenotype) indicates some factors are regulated downstream of *NLRP7* to determine the cell fate between proliferation and differentiation in this pathway, allowing the tissues to develop into a severe form (CHM) or a milder form (PHM). Within the androgenic types of HM, the severe form with excessive trophoblastic proliferation and absence of embryonic development are consistently observed.

For patients with mutations in *NLRP7* or *KHDC3L*, it should be noted that their HMs are diploid biparental with a normal number of chromosomes, indicating appropriate chromosomal segregation. The fact that we were not able to detect mosaicism in these tissues may be due to the following: 1) DNA extracted from FFPE tissues is too degraded and requires more sensitive methods, or 2) HM tissues were collected at a later stage of the pregnancy, when the 2n diploid biparental derivatives outgrow other cell populations due to selective advantage, or 3) HM

tissues are diploid biparental after fertilization because there are no spindle defects in such conceptions, however, other defects in the oocytes before and after fertilization contributed to the HM morphology.

As *NLRP7* does not have a mouse orthologue and there are ethical restrictions on the use of human oocytes; consequently, the functional roles of *NLRP7* were characterized only using various cellular models such as human hematopoietic cells, embryonic stem cells, or in tissues of the HM and other conceptions of these patients (Introduction 1.2.1 *NLRP7*). Based on these data and on our work in chapter 2, we proposed a model that recapitulates the different aspects of the pathology of recurrent diploid biparental HM (Figure 6.1). In this model, the primary defect is in the oocytes, which includes the abnormal methylation of imprinted genes, the earliest defect demonstrated in diploid biparental HM tissues, and perhaps many other abnormalities that have not yet been studied. This defect does not affect fertilization but impairs early preimplantation development ⁷⁹ and the resulting molar tissues display a shift from normal tissue differentiation toward excessive trophoblastic proliferation (Chapter 2). The second defect comes from the inability of patients' cells to secrete sufficient amounts of cytokines and mount an appropriate inflammatory response to reject their arrested pregnancies.

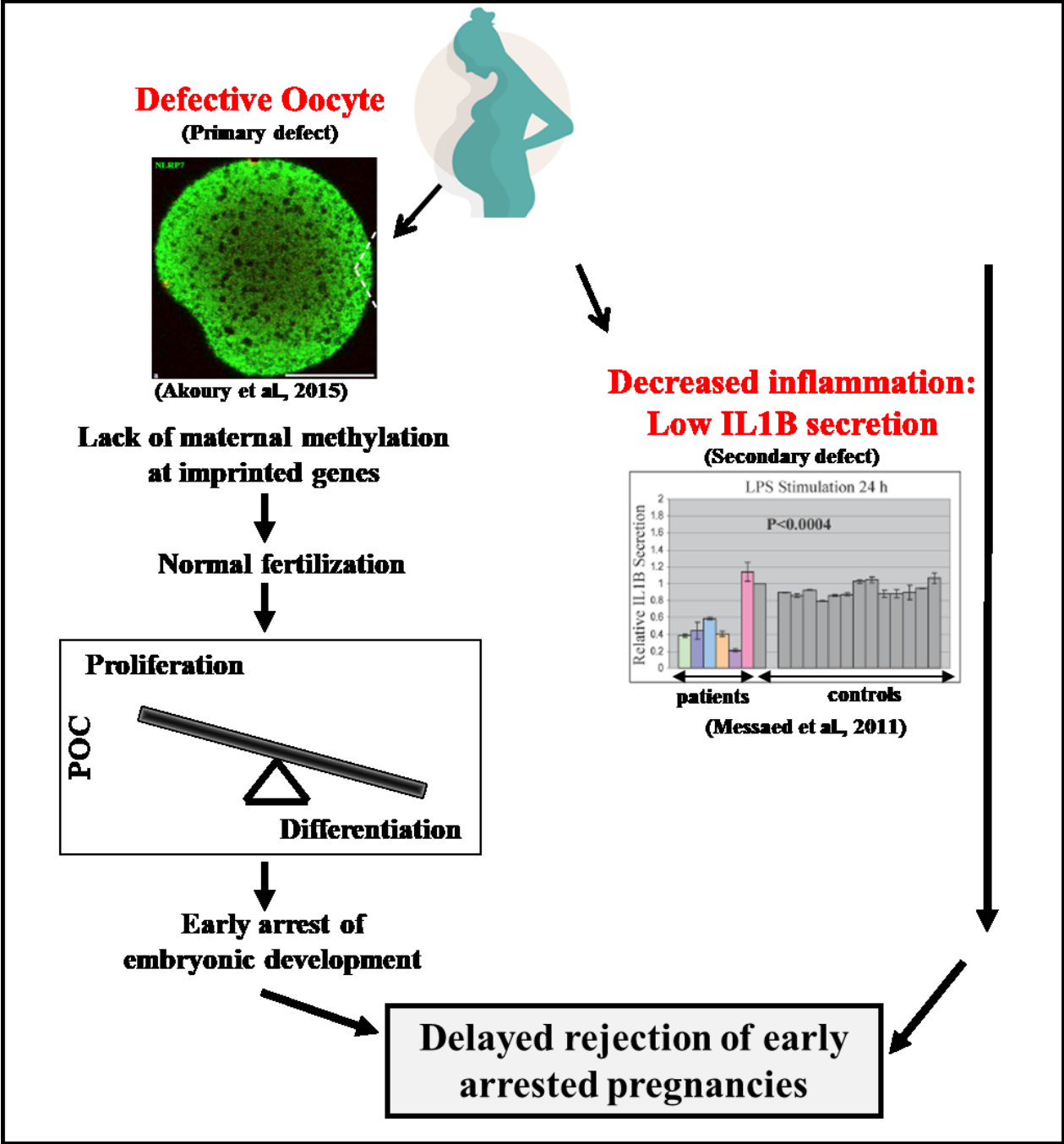


Figure 6.1. A suggested model that recapitulates the various roles of NLRP7 in the pathology of recurrent hydatidiform mole (RHM). (Figure 27.4 from Chapter 27 “Textbook of Autoinflammation”)

2- MEI and recurrent diploid androgenetic HM

The earliest defect that was observed in oocytes from mice KO for *Mei1*, *Top6 l*, *Rec114* is the defective double-strand break formation in prophase I [170](#); [171](#); [180](#); [209](#). During prophase I, homologous chromosomes pair with each other, undergo synapsis and initiate recombination. The process of matching, locking and moving chromosomes in meiosis is very crucial for gametes to obtain the right number of chromosomes. In meiosis, programmed DSB formation is essential to initiate meiotic recombination, which allows for the exchange of genetic information between homologous chromosomes and promotes accurate chromosomal segregation. In humans, approximately 30% of all miscarriages are aneuploid due to chromosome mis-segregation events [210](#).

It should be noted that *Mei1* has a restricted expression to prophase I (*Mei1* is highly expressed in embryonic day 17 ovaries and becomes undetectable in adult ovaries, indicating its specific role at this earliest stage of meiosis. Meanwhile, *NLRP7* and *KHDC3L* have ubiquitous expression in all stages of human oocytes (GV, MI, MII) and preimplantation embryos [72](#); [80](#); [85](#). However, it is worth mentioning that the transcription of these two genes, *NLRP7* and *KHDC3L*, was investigated in oocytes after birth (from patients with IVF/ICSI), and whether *NLRP7* and *KHDC3L* are also expressed in the early stage of prophase I (before birth) is still unknown.

As the defects in *Mei1*-null mice occur at the earliest stage of meiosis (prophase I), multiple downstream events are consequently affected and are expected to result in severe phenotype. Another critical aspect is the delayed progression of oocytes from *Mei1* null mice, with only about 8% reaching the MII stage. Oocytes from *Mei1* null mice could be fertilized in vivo but most arrested during in vitro culture at the 2-cell or 4-cell stage; only 2% reached the blastocyst stage. Indeed, all mouse knockout models for genes known to be involved in meiotic

DNA double-strand breaks formation were reported to be infertile and most of the resulting embryos arrest at the 2-4 cell stage [170-172](#); [209](#); [211-213](#). On the other hand, *Khdc3* null mice showed less catastrophic phenotype, with reduced fecundity due to the delay in embryonic development, rather than a complete arrest [84](#).

In line with these observations in mice, it is worth highlighting some differences in the developmental rate of oocytes after assisted reproductive technologies in two patients, one with bi-allelic mutations in *NLRP7* and another in *MEII*. For the patient with bi-allelic *NLRP7* mutations, in the study of Sills *et al.* 73% (11/15) of the oocytes reached MII, 66% (10/15) were fertilized with a single sperm, and all had a biparental contribution with some ploidy errors. In the patient with *MEII* mutations (Table S5, chapter 4), 58% (11/19) of oocytes reached MII, only 26% (5/19) were fertilized (noted as below fertilization rate by the patient's physician), and one of them developed to the blastocyst stage and was triploid digynic. It could be speculated that *MEII* defects reduces the fertilization rate, while *NLRP7* defects are compatible with normal fertilization but lead to the impaired establishment of methylation marks on imprinted genes (in the female germ cells as well as after fertilization). However, more data is needed to support this suggestion since it is only based on a small number of oocytes from only 2 patients. Such results may also vary between different IVF laboratories, stimulation protocols, and patients.

Figure 6.2 and 6.3 illustrates proposed mechanisms for pathogenesis of diploid biparental and androgenetic HMs.

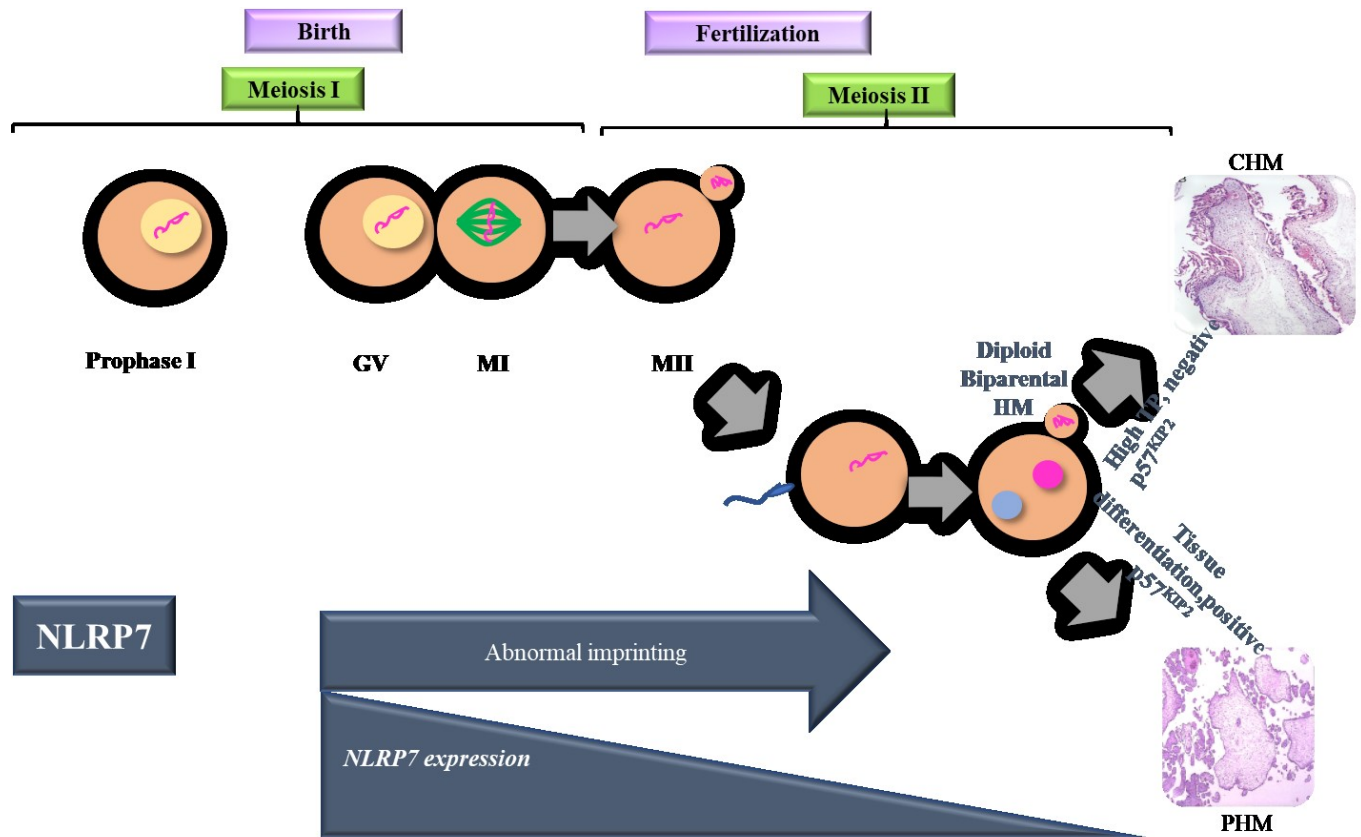


Figure 6.2. Schematic representation of proposed mechanisms of recurrent diploid biparental and androgenetic HMs.

Mutations in *NLRP7* (and *KHDC3L*) disrupted whole-genome maternal imprinting in the female germline, silencing the expression of maternally imprinted genes. However, chromosome segregation is not affected. Depending on the severity of the defects, the conceptions can develop into the severe form (CHM) or milder form (PHM).

The figure also illustrates the expression profile of *NLRP7*, with the peak is at GV stage. GV stands for germinal vesical oocytes; MI, Metaphase oocyte, MII, metaphase II; HM, hydatidiform mole; TP, trophoblastic proliferation.

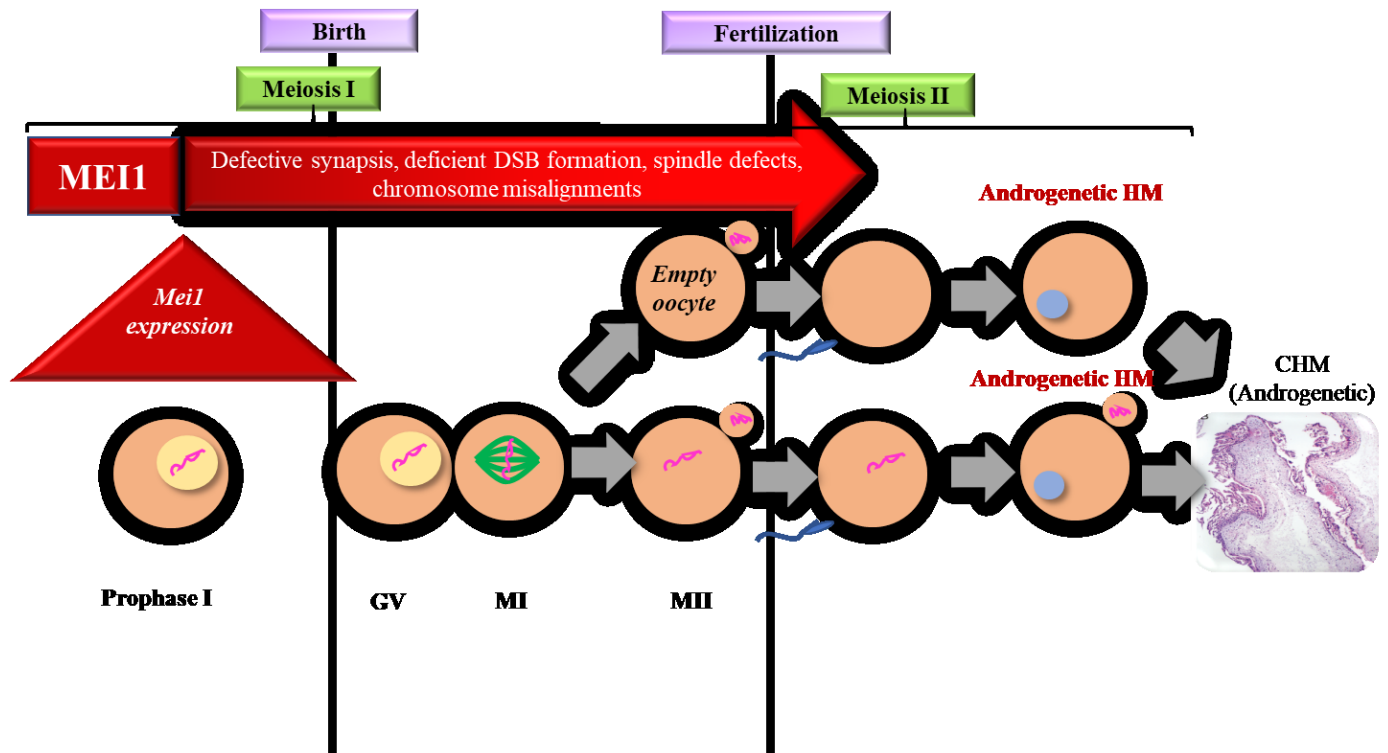


Figure 6.3. Schematic representation of proposed mechanisms of recurrent androgenetic HMs.

Mutations in *MEI1* (and *TOP6BL*, *REC114*) lead to defects in the earliest stage of meiosis (prophase I), resulting in multiple downstream abnormalities. Completion of meiosis I causes the extrusion of the first polar body (PB). At this stage, two scenarios may occur: i) all maternal chromosomes are extruded to the first PB, resulting in empty oocytes. Such empty oocytes can be fertilized and form androgenetic embryos; or ii) maternal chromosomes stay in the oocytes after meiosis I (nucleated oocytes), but fertilization triggers the extrusion of all maternal chromosomes into the PB, resulting in androgenetic embryos. Androgenetic embryos with the lack of maternal haploid genome (and therefore imprinting abnormalities) will result in the severe form of HM (CHM) with excessive trophoblastic proliferation and lack of embryonic tissues.

The figure also illustrates the expression profile of *MEI1*, with the peak expression of *MEI1* is at leptotene in prophase I. GV stands for germinal vesical oocytes; MI, Metaphase oocyte, MII, metaphase II; HM, hydatidiform mole; TP, trophoblastic proliferation.

3- Crossovers and the maternal age effect:

Meiotic recombination begins with DNA double-strand breaks introduced into the genome and is subsequently followed by DNA repair and the generation of crossovers. Crossovers are important to hold homologous chromosomes together and ensure accurate segregation of chromosomes. For example, three abnormal crossover configurations were reported to be associated with human trisomies: lack of crossovers (achiasmata bivalents), distal-only crossovers and proximal crossovers (reviews in Nagaoka 2012 [214](#)). It was reported that at least one chiasma (formed by crossover events) is required per chromosome pairs [215](#). The failure to form DNA double-strand breaks in *Mei1* null mice, and probably in patients with *MEI1* mutations, might lead to the failure of crossovers and therefore the misalignment of chromosomes, resulting in aneuploidies. It is also known that aneuploidy in human pregnancy increases with maternal age. This “maternal age effect” is often attributed to the age-related loss of cohesion [214](#). It was suggested that the loss of cohesion in older women can lead to loss of chiasmata from crossover-containing bivalents or reduced mechanical linkage between chiasmata and kinetochores, and therefore an increased chance of mis-segregation [216](#). In four out of five patients with mutations in the 3 new causative genes, a similar pattern of reproductive outcomes was observed: several miscarriages were followed by androgenetic HM(s). The fact that androgenetic HM(s) were observed at a later time in the reproductive life of the patients suggests that maternal age may have exacerbated the genetic defects influencing crossovers and consequently led to a spectrum of chromosomal abnormalities, ranging from miscarriages (aneuploids for few chromosomes) at younger ages to androgenetic HM (loss of all maternal chromosomes) at later ages. This observation is consistent with the fact that advanced maternal age is the strongest risk factor for sporadic CHM (which are androgenetic) (see Introduction

1.1.2. Epidemiology). In light of this, exploring the mechanism of RHM will help understand the causes and risk factors of sporadic CHM, which affect 1 in every 1200 pregnancies in western countries.

4- Clinical benefits to patients with RHM

For patients with *NLRP7* mutations, ovum donation was successful in 3 patients, indicating that the defects come solely from the quality of the patients' oocytes. For patients with *MEII* mutations, IVF might not be a good option since the oocytes of these patients are defective. While ovum donation can be recommended based on the oocyte defect, it is not yet known if it allows the patients to achieve successful pregnancies. Patient 1333's two sisters (who also carry biallelic *MEII* mutations and had only miscarriages) underwent, at young ages, total abdominal hysterectomies due to several uterine fibroids, which are benign tumors that arise from the smooth-muscle cells of the uterus. Consequently, it is not known whether the uterus of such patients are healthy and can accommodate normal embryo development and whether replacing solely the oocytes can rescue the defects caused by *MEII* mutations.

CHAPTER 6: CONCLUSION AND FUTURE DIRECTIONS

RHM is, overall, a complex genetic trait. The current state of knowledge indicates that RHM is clearly not a single entity, but rather represents a large variety of subgroups, some that follow Mendelian trait (Recurrent Diploid Biparental, Recurrent Androgenetic), while others with possible multifactorial etiologies (a spectrum of reproductive losses including RHM, miscarriages, and live births).

The work published in Modern Pathology (Chapter 3) revealed the genetic heterogeneity of patients without mutations in *NLRP7* and *KHDC3L*, and in fact, we were able to identify mutations in only 5 patients with the most severe phenotype (Chapter 4). Finding genes in the remaining patients can be challenging, with the underlying causes can be monogenetic trait with incomplete penetrance and variable expressivity, or complex polygenic trait influenced by genetic and environmental factors. Considering such a rare disease as well as its high heterogeneity, it is highly challenging to identify mutations in the same gene in multiple patients. Rather, gene identification work should focus on different genes involved in the same mechanism.

Since the first report of androgenetic HM was described in 1977, an “empty” oocyte mechanism was suggested. However, with the lack of evidence for empty oocyte, another hypothesis at the origin of androgenetic HM was postulated, which is the loss or degeneration of maternal chromosomes after fertilization due to abnormal cleavages (Introduction 1.1.5). In our study, we provided evidence of empty oocytes as well as androgenetic zygotes. Whether these zygotes are derived from the empty oocytes is still an unanswered question. The mechanism demonstrated in our study can be applied to sporadic androgenetic HM, when such abnormalities

due to the spindles and abnormal cleavage can be caused by other factors (e.g. maternal age, ethnicity) in only one pregnancy and lead to androgenetic HM

CHAPTER 7: REFERENCES

1. Nguyen, N.M.P., and Slim, R. (2014). Genetics and Epigenetics of Recurrent Hydatidiform Moles: Basic Science and Genetic Counselling. *Current Obstetrics and Gynecology Reports* 3, 55-64.
2. Richardson, M.V., and Hertig, A.T. (1959). New England's first recorded hydatidiform mole; a historical note. *N Engl J Med* 260, 544-545.
3. Savage, P., Williams, J., Wong, S.L., Short, D., Casalboni, S., Catalano, K., and Seckl, M. (2010). The demographics of molar pregnancies in England and Wales from 2000-2009. *J Reprod Med* 55, 341-345.
4. Grimes, D.A. (1984). Epidemiology of gestational trophoblastic disease. *Am J Obstet Gynecol* 150, 309-318.
5. Bracken, M.B., Brinton, L.A., and Hayashi, K. (1984). Epidemiology of hydatidiform mole and choriocarcinoma. *Epidemiol Rev* 6, 52-75.
6. Steigrad, S.J. (2003). Epidemiology of gestational trophoblastic diseases. *Best Pract Res Clin Obstet Gynaecol* 17, 837-847.
7. Bagshawe, K.D., Dent, J., and Webb, J. (1986). Hydatidiform mole in England and Wales 1973-83. *Lancet* 2, 673-677.
8. Berkowitz, R.S., Im, S.S., Bernstein, M.R., and Goldstein, D.P. (1998). Gestational trophoblastic disease. Subsequent pregnancy outcome, including repeat molar pregnancy. *J Reprod Med* 43, 81-86.
9. Boufettal, H., Coullin, P., Mahdaoui, S., Noun, M., Hermas, S., and Samouh, N. (2011). [Complete hydatiforme mole in Morocco: epidemiological and clinical study]. *J Gynecol Obstet Biol Reprod (Paris)* 40, 419-429.
10. Horn, L.C., Kowalzik, J., Bilek, K., Richter, C.E., and Einenkel, J. (2006). Clinicopathologic characteristics and subsequent pregnancy outcome in 139 complete hydatidiform moles. *Eur J Obstet Gynecol Reprod Biol* 128, 10-14.
11. Kim, J.H., Park, D.C., Bae, S.N., Namkoong, S.E., and Kim, S.J. (1998). Subsequent reproductive experience after treatment for gestational trophoblastic disease. *Gynecol Oncol* 71, 108-112.
12. Kronfol, N.M., Iliya, F.A., and Hajj, S.N. (1969). Recurrent hydatidiform mole: a report of five cases with review of the literature. *J Med Liban* 22, 507-520.
13. Sebire, N.J., Fisher, R.A., Foskett, M., Rees, H., Seckl, M.J., and Newlands, E.S. (2003). Risk of recurrent hydatidiform mole and subsequent pregnancy outcome following complete or partial hydatidiform molar pregnancy. *BJOG: An International Journal of Obstetrics and Gynaecology* 110, 22-26.
14. Messerli, M.L., Lilienfeld, A.M., Parmley, T., Woodruff, J.D., and Rosenshein, N.B. (1985). Risk factors for gestational trophoblastic neoplasia. *Am J Obstet Gynecol* 153, 294-300.
15. Yen, S., and MacMahon, B. (1968). Epidemiologic features of trophoblastic disease. *Am J Obstet Gynecol* 101, 126-132.
16. Palmer, J.R., Driscoll, S.G., Rosenberg, L., Berkowitz, R.S., Lurain, J.R., Soper, J., Twigg, L.B., Gershenson, D.M., Kohorn, E.I., Berman, M., et al. (1999). Oral contraceptive use and risk of gestational trophoblastic tumors. *J Natl Cancer Inst* 91, 635-640.
17. Bracken, M.B. (1987). Incidence and aetiology of hydatidiform mole: an epidemiological review. *Br J Obstet Gynaecol* 94, 1123-1135.
18. Graham, I.H., Fajardo, A.M., and Richards, R.L. (1990). Epidemiological study of complete and partial hydatidiform mole in Abu Dhabi: influence age and ethnic group. *J Clin Pathol* 43, 661-664.
19. Vecchia, C.L., Franceschi, S., Parazzini, F., Fasoli, M., Decarli, A., Gallus, G., and Tognoni, G. (1985). RISK FACTORS FOR GESTATIONAL TROPHOBLASTIC DISEASE IN ITALY. *Am J Epidemiol* 121, 457-464.
20. Acaia, B., Parazzini, F., La Vecchia, C., Ricciardiello, O., Fedele, L., and Battista Candiani, G. (1988). Increased frequency of complete hydatidiform mole in women with repeated abortion. *Gynecol Oncol* 31, 310-314.
21. Parazzini, F., Mangili, G., La Vecchia, C., Negri, E., Bocciolone, L., and Fasoli, M. (1991). Risk factors for gestational trophoblastic disease: a separate analysis of complete and partial hydatidiform moles. *Obstet Gynecol* 78, 1039-1045.

22. Fisher, R.A., Povey, S., Jeffreys, A.J., Martin, C.A., Patel, I., and Lawler, S.D. (1989). Frequency of heterozygous complete hydatidiform moles, estimated by locus-specific minisatellite and Y chromosome-specific probes. *Hum Genet* 82, 259-263.
23. Kovacs, B.W., Shahbahrani, B., Tast, D.E., and Curtin, J.P. (1991). Molecular genetic analysis of complete hydatidiform moles. *Cancer Genet Cytogenet* 54, 143-152.
24. Lawler, S.D., Fisher, R.A., and Dent, J. (1991). A prospective genetic study of complete and partial hydatidiform moles. *Am J Obstet Gynecol* 164, 1270-1277.
25. Banet, N., DeScipio, C., Murphy, K.M., Beierl, K., Adams, E., Vang, R., and Ronnett, B.M. (2014). Characteristics of hydatidiform moles: analysis of a prospective series with p57 immunohistochemistry and molecular genotyping. *Mod Pathol* 27, 238-254.
26. Kajii, T., and Ohama, K. (1977). Androgenetic origin of hydatidiform mole. *Nature* 268, 633-634.
27. Wake, N., Takagi, N., and Sasaki, M. (1978). Androgenesis as a cause of hydatidiform mole. *J Natl Cancer Inst* 60, 51-57.
28. Golubovsky, M.D. (2003). Postzygotic diploidization of triploids as a source of unusual cases of mosaicism, chimerism and twinning. *Hum Reprod* 18, 236-242.
29. Sunde, L., Niemann, I., Hansen, E.S., Hindkjaer, J., Degn, B., Jensen, U.B., and Bolund, L. (2011). Mosaics and moles. *Eur J Hum Genet* 19, 1026-1031.
30. Hoffner, L., Dunn, J., Esposito, N., Macpherson, T., and Surti, U. (2008). P57KIP2 immunostaining and molecular cytogenetics: combined approach aids in diagnosis of morphologically challenging cases with molar phenotype and in detecting androgenetic cell lines in mosaic/chimeric conceptions. *Hum Pathol* 39, 63-72.
31. Surti, U., Hoffner, L., Kolthoff, M., Dunn, J., Hunt, J., Sniezek, L., and Macpherson, T. (2006). Persistent gestational trophoblastic disease after an androgenetic/biparental fetal chimera: a case report and review. *Int J Gynecol Pathol* 25, 366-372.
32. Borgulova, I., Soldatova, I., Putzova, M., Malikova, M., Neupauerova, J., Markova, S.P., Trkova, M., and Seeman, P. (2018). Genome-wide uniparental diploidy of all paternal chromosomes in an 11-year-old girl with deafness and without malignancy. *J Hum Genet* 63, 803-810.
33. McKone, M.J., and Halpern, S.L. (2003). The evolution of androgenesis. *Am Nat* 161, 641-656.
34. Pigneur, L.M., Hedtke, S.M., Etoundi, E., and Van Doninck, K. (2012). Androgenesis: a review through the study of the selfish shellfish *Corbicula* spp. *Heredity (Edinb)* 108, 581-591.
35. Komaru, A., Kawagishi, T., and Konishi, K. (1998). Cytological evidence of spontaneous androgenesis in the freshwater clam *Corbicula leana* Prime. *Dev Genes Evol* 208, 46-50.
36. Komaru, A., Ookubo, K., and Kiyomoto, M. (2000). All meiotic chromosomes and both centrosomes at spindle pole in the zygotes discarded as two polar bodies in clam *Corbicula leana*: unusual polar body formation observed by antitubulin immunofluorescence. *Dev Genes Evol* 210, 263-269.
37. Gard, D.L. (1992). Microtubule organization during maturation of *Xenopus* oocytes: assembly and rotation of the meiotic spindles. *Dev Biol* 151, 516-530.
38. Sawada, T., and Schatten, G. (1988). Microtubules in ascidian eggs during meiosis, fertilization, and mitosis. *Cell Motil Cytoskeleton* 9, 219-230.
39. Selman, G.G. (1966). Cell cleavage in polar body formation. *Nature* 210, 750-751.
40. Pichot, C., Borrut, A., and El Maâtaoui, M. (1998). Unexpected DNA content in the endosperm of *Cupressus dupreziana* A. Camus seeds and its implications in the reproductive process. *Sexual Plant Reproduction* 11, 148-152.
41. Pichot, C., Fady, B., and Hochu, I. (2000). Lack of mother tree alleles in zymograms of *Cupressus dupreziana* A. Camus embryos. *Annals of Forest Science* 57, 17-22.
42. Pichot, C., El Maataoui, M., Raddi, S., and Raddi, P. (2001). Surrogate mother for endangered *Cupressus*. *Nature* 412, 39.
43. Fournier, D., Estoup, A., Orivel, J., Foucaud, J., Jourdan, H., Le Breton, J., and Keller, L. (2005). Clonal reproduction by males and females in the little fire ant. *Nature* 435, 1230-1234.
44. Hedtke, S.M., and Hillis, D.M. (2011). The potential role of androgenesis in cytoplasmic-nuclear phylogenetic discordance. *Syst Biol* 60, 87-96.
45. Waldman, A.S. (2008). Ensuring the fidelity of recombination in mammalian chromosomes. *Bioessays* 30, 1163-1171.
46. Schwander, T., and Oldroyd, B.P. (2016). Androgenesis: where males hijack eggs to clone themselves. *Philos Trans R Soc Lond B Biol Sci* 371.

47. Koehler, K.E., Schrupp, S.E., Cherry, J.P., Hassold, T.J., and Hunt, P.A. (2006). Near-human aneuploidy levels in female mice with homeologous chromosomes. *Curr Biol* 16, R579-580.
48. McGrath, J., and Solter, D. (1984). Completion of mouse embryogenesis requires both the maternal and paternal genomes. *Cell* 37, 179-183.
49. Barton, S.C., Surani, M.A., and Norris, M.L. (1984). Role of paternal and maternal genomes in mouse development. *Nature* 311, 374-376.
50. Hoppe, P.C., and Illmensee, K. (1977). Microsurgically produced homozygous-diploid uniparental mice. *Proc Natl Acad Sci U S A* 74, 5657-5661.
51. Modlinski, J.A. (1980). Preimplantation development of microsurgically obtained haploid and homozygous diploid mouse embryos and effects of pretreatment with Cytochalasin B on enucleated eggs. *J Embryol Exp Morphol* 60, 153-161.
52. Markert, C.L. (1982). Parthenogenesis, homozygosity, and cloning in mammals. *J Hered* 73, 390-397.
53. Surani, M.A., and Barton, S.C. (1983). Development of gynogenetic eggs in the mouse: implications for parthenogenetic embryos. *Science* 222, 1034-1036.
54. Okamoto, I., Tan, S., and Takagi, N. (2000). X-chromosome inactivation in XX androgenetic mouse embryos surviving implantation. *Development* 127, 4137-4145.
55. van der Smagt, J.J., Scheenjes, E., Kremer, J.A., Hennekam, F.A., and Fisher, R.A. (2006). Heterogeneity in the origin of recurrent complete hydatidiform moles: not all women with multiple molar pregnancies have biparental moles. *Bjog* 113, 725-728.
56. Buyukkurt, S., Fisher, R.A., Vardar, M.A., and Evruke, C. (2010). Heterogeneity in recurrent complete hydatidiform mole: presentation of two new Turkish families with different genetic characteristics. *Placenta* 31, 1023-1025.
57. Murdoch, S., Djuric, U., Mazhar, B., Seoud, M., Khan, R., Kuick, R., Bagga, R., Kircheisen, R., Ao, A., Ratti, B., et al. (2006). Mutations in NALP7 cause recurrent hydatidiform moles and reproductive wastage in humans. *Nat Genet* 38, 300-302.
58. Qian, J., Cheng, Q., Murdoch, S., Xu, C., Jin, F., Chebaro, W., Zhang, X., Gao, H., Zhu, Y., Slim, R., et al. (2011). The Genetics of Recurrent Hydatidiform Moles in China: Correlations between NLRP7 Mutations, Molar Genotypes, and Reproductive Outcomes. *Mol Hum Reprod* 17, 612-619.
59. Slim, R., Bagga, R., Chebaro, W., Srinivasan, R., and Agarwal, N. (2009). A strong founder effect for two NLRP7 mutations in the Indian population: an intriguing observation. *Clin Genet* 76, 292-295.
60. Hayward, B.E., De Vos, M., Talati, N., Abdollahi, M.R., Taylor, G.R., Meyer, E., Williams, D., Maher, E.R., Setna, F., Nazir, K., et al. (2009). Genetic and Epigenetic Analysis of Recurrent Hydatidiform Mole. *Hum Mutat* 30, E629-639.
61. Estrada, H., Buentello, B., Zenteno, J.C., Fiszman, R., and Aguinaga, M. (2013). The p.L750V mutation in the NLRP7 gene is frequent in Mexican patients with recurrent molar pregnancies and is not associated with recurrent pregnancy loss. *Prenat Diagn*, 1-4.
62. Kinoshita, T., Wang, Y., Hasegawa, M., Imamura, R., and Suda, T. (2005). PYPAF3, a PYRIN-containing APAF-1-like Protein, Is a Feedback Regulator of Caspase-1-dependent Interleukin-1 β Secretion. *J Biol Chem* 280, 21720-21725.
63. Messaed, C., Akoury, E., Djuric, U., Zeng, J., Saleh, M., Gilbert, L., Seoud, M., Qureshi, S., and Slim, R. (2011). NLRP7, a nucleotide oligomerization domain-like receptor protein, is required for normal cytokine secretion and co-localizes with Golgi and the microtubule-organizing center. *J Biol Chem* 286, 43313-43323.
64. Khare, S., Dorfleutner, A., Bryan, N.B., Yun, C., Radian, A.D., de Almeida, L., Rojanasakul, Y., and Stehlik, C. (2012). An NLRP7-containing inflammasome mediates recognition of microbial lipopeptides in human macrophages. *Immunity* 36, 464-476.
65. Mahadevan, S., Wen, S., Wan, Y.W., Peng, H.H., Otta, S., Liu, Z., Iacovino, M., Mahen, E.M., Kyba, M., Sadikovic, B., et al. (2014). NLRP7 affects trophoblast lineage differentiation, binds to overexpressed YY1 and alters CpG methylation. *Hum Mol Genet* 23, 706-716.
66. Gerard, N., Caillaud, M., Martoriati, A., Goudet, G., and Lalmanach, A.C. (2004). The interleukin-1 system and female reproduction. *J Endocrinol* 180, 203-212.
67. Caillaud, M., Duchamp, G., and Gerard, N. (2005). In vivo effect of interleukin-1 β and interleukin-1RA on oocyte cytoplasmic maturation, ovulation, and early embryonic development in the mare. *Reprod Biol Endocrinol* 3, 26.

68. Zheng, H., Fletcher, D., Kozak, W., Jiang, M., Hofmann, K.J., Conn, C.A., Soszynski, D., Grabiec, C., Trumbauer, M.E., Shaw, A., et al. (1995). Resistance to fever induction and impaired acute-phase response in interleukin-1 beta-deficient mice. *Immunity* 3, 9-19.
69. Abbondanzo, S.J., Cullinan, E.B., McIntyre, K., Labow, M.A., and Stewart, C.L. (1996). Reproduction in mice lacking a functional type 1 IL-1 receptor. *Endocrinology* 137, 3598-3601.
70. Okada, K., Hirota, E., Mizutani, Y., Fujioka, T., Shuin, T., Miki, T., Nakamura, Y., and Katagiri, T. (2004). Oncogenic role of NALP7 in testicular seminomas. *Cancer Sci* 95, 949-954.
71. Ohno, S., Kinoshita, T., Ohno, Y., Minamoto, T., Suzuki, N., Inoue, M., and Suda, T. (2008). Expression of NLRP7 (PYPAF3, NALP7) protein in endometrial cancer tissues. *Anticancer Res* 28, 2493-2497.
72. Zhang, P., Dixon, M., Zucchelli, M., Hambiliki, F., Levkov, L., Hovatta, O., and Kere, J. (2008). Expression analysis of the NLRP gene family suggests a role in human preimplantation development. *PLoS ONE* 3, e2755.
73. Akoury, E., Zhang, L., Ao, A., and Slim, R. (2015). NLRP7 and KHDC3L, the two maternal-effect proteins responsible for recurrent hydatidiform moles, co-localize to the oocyte cytoskeleton. *Hum Reprod* 30, 159-169.
74. Li, L., Baibakov, B., and Dean, J. (2008). A subcortical maternal complex essential for preimplantation mouse embryogenesis. *Dev Cell* 15, 416-425.
75. Edwards, R., Crow, J., Dale, S., Macnamee, M., Hartshorne, G., and Brinsden, P. (1990). Preimplantation diagnosis and recurrent hydatidiform mole. *Lancet* 335, 1030-1031.
76. Edwards, R.G., Crow, J., Dale, S., Macnamee, M.C., Hartshorne, G.M., and Brinsden, P. (1992). Pronuclear, cleavage and blastocyst histories in the attempted preimplantation diagnosis of the human hydatidiform mole. *Hum Reprod* 7, 994-998.
77. Pal, L., Toth, T.L., Leykin, L., and Isaacson, K.B. (1996). High incidence of triploidy in in-vitro fertilized oocytes from a patient with a previous history of recurrent gestational trophoblastic disease. *Hum Reprod* 11, 1529-1532.
78. Reubinoff, B.E., Lewin, A., Verner, M., Safran, A., Schenker, J.G., and Abeliovich, D. (1997). Intracytoplasmic sperm injection combined with preimplantation genetic diagnosis for the prevention of recurrent gestational trophoblastic disease. *Hum Reprod* 12, 805-808.
79. Sills, E.S., Obregon-Tito, A.J., Gao, H., McWilliams, T.K., Gordon, A.T., Adams, C.A., and Slim, R. (2017). Pathogenic variant in NLRP7 (19q13.42) associated with recurrent gestational trophoblastic disease: Data from early embryo development observed during in vitro fertilization. *Clin Exp Reprod Med* 44, 40-46.
80. Parry, D.A., Logan, C.V., Hayward, B.E., Shires, M., Landolsi, H., Diggle, C., Carr, I., Rittore, C., Toutou, I., Philibert, L., et al. (2011). Mutations causing familial biparental hydatidiform mole implicate c6orf221 as a possible regulator of genomic imprinting in the human oocyte. *Am J Hum Genet* 89, 451-458.
81. Reddy, R., Akoury, E., Phuong Nguyen, N.M., Abdul-Rahman, O.A., Dery, C., Gupta, N., Daley, W.P., Ao, A., Landolsi, H., Ann Fisher, R., et al. (2013). Report of four new patients with protein-truncating mutations in C6orf221/KHDC3L and colocalization with NLRP7. *Eur J Hum Genet* 21, 957-964.
82. Rezaei, M., Nguyen, N.M., Foroughinia, L., Dash, P., Ahmadpour, F., Verma, I.C., Slim, R., and Fardaei, M. (2016). Two novel mutations in the KHDC3L gene in Asian patients with recurrent hydatidiform mole. *Hum Genome Var* 3, 16027.
83. Pierre, A., Gautier, M., Callebaut, I., Bontoux, M., Jeanpierre, E., Pontarotti, P., and Monget, P. (2007). Atypical structure and phylogenomic evolution of the new eutherian oocyte- and embryo-expressed KHDC1/DPPA5/ECAT1/OOEP gene family. *Genomics* 90, 583-594.
84. Zheng, P., and Dean, J. (2009). Role of Filia, a maternal effect gene, in maintaining euploidy during cleavage-stage mouse embryogenesis. *Proceedings of the National Academy of Sciences* 106, 7473-7478.
85. Liu, C., Li, M., Li, T., Zhao, H., Huang, J., Wang, Y., Gao, Q., Yu, Y., and Shi, Q. (2016). ECAT1 is essential for human oocyte maturation and pre-implantation development of the resulting embryos. *Sci Rep* 6, 38192.

86. Tong, Z.B., Gold, L., Pfeifer, K.E., Dorward, H., Lee, E., Bondy, C.A., Dean, J., and Nelson, L.M. (2000). Mater, a maternal effect gene required for early embryonic development in mice. *Nat Genet* 26, 267-268.
87. Yu, X.J., Yi, Z., Gao, Z., Qin, D., Zhai, Y., Chen, X., Ou-Yang, Y., Wang, Z.B., Zheng, P., Zhu, M.S., et al. (2014). The subcortical maternal complex controls symmetric division of mouse zygotes by regulating F-actin dynamics. *Nat Commun* 5, 4887.
88. Yurttas, P., Vitale, A.M., Fitzhenry, R.J., Cohen-Gould, L., Wu, W., Gossen, J.A., and Coonrod, S.A. (2008). Role for PADI6 and the cytoplasmic lattices in ribosomal storage in oocytes and translational control in the early mouse embryo. *Development* 135, 2627-2636.
89. Mahadevan, S., Sathappan, V., Utama, B., Lorenzo, I., Kaskar, K., and Van den Veyver, I.B. (2017). Maternally expressed NLRP2 links the subcortical maternal complex (SCMC) to fertility, embryogenesis and epigenetic reprogramming. *Sci Rep* 7, 44667.
90. Gao, Z., Zhang, X., Yu, X., Qin, D., Xiao, Y., Yu, Y., Xiang, Y., Nie, X., Lu, X., Liu, W., et al. (2018). Zbed3 participates in the subcortical maternal complex and regulates the distribution of organelles. *J Mol Cell Biol* 10, 74-88.
91. Alazami, A.M., Awad, S.M., Coskun, S., Al-Hassan, S., Hijazi, H., Abdulwahab, F.M., Poizat, C., and Alkuraya, F.S. (2015). TLE6 mutation causes the earliest known human embryonic lethality. *Genome Biol* 16, 240.
92. Xu, Y., Shi, Y., Fu, J., Yu, M., Feng, R., Sang, Q., Liang, B., Chen, B., Qu, R., Li, B., et al. (2016). Mutations in PADI6 Cause Female Infertility Characterized by Early Embryonic Arrest. *Am J Hum Genet* 99, 744-752.
93. Maddirevula, S., Coskun, S., Awartani, K., Alsaif, H., Abdulwahab, F.M., and Alkuraya, F.S. (2017). The human knockout phenotype of PADI6 is female sterility caused by cleavage failure of their fertilized eggs. *Clin Genet* 91, 344-345.
94. Qian, J., Nguyen, N.M.P., Rezaei, M., Huang, B., Tao, Y., Zhang, X., Cheng, Q., Yang, H., Asangla, A., Majewski, J., et al. (2018). Biallelic PADI6 variants linking infertility, miscarriages, and hydatidiform moles. *Eur J Hum Genet* 26, 1007-1013.
95. Ghazi, H., Magewu, A.N., Gonzales, F., and Jones, P.A. (1990). Changes in the allelic methylation patterns of c-H-ras-1, insulin and retinoblastoma genes in human development. *Dev Suppl*, 115-123.
96. Clarke, A. (1990). Genetic imprinting in clinical genetics. *Dev Suppl*, 131-139.
97. Miyamoto, S., Sasaki, M., Nishida, M., and Wake, N. (1991). [Identification of a chromosome carrying a putative tumor suppressor gene in human choriocarcinoma by microcell-mediated chromosome transfer]. *Hum Cell* 4, 38-43.
98. Kircheisen, R., and Schroeder-Kurth, T. (1991). [Familial hydatidiform mole syndrome and genetic aspects of this disturbed trophoblast development]. *Geburtshilfe Frauenheilkd* 51, 569-571.
99. Sunde, L., Vejerslev, L.O., Jensen, M.P., Pedersen, S., Hertz, J.M., and Bolund, L. (1993). Genetic analysis of repeated, biparental, diploid, hydatidiform moles. *Cancer Genet Cytogenet* 66, 16-22.
100. Judson, H., Hayward, B.E., Sheridan, E., and Bonthron, D.T. (2002). A global disorder of imprinting in the human female germ line. *Nature* 416, 539-542.
101. El-Maarri, O., Seoud, M., Coullin, P., Herbiniaux, U., Oldenburg, J., Rouleau, G., and Slim, R. (2003). Maternal alleles acquiring paternal methylation patterns in biparental complete hydatidiform moles. *Hum Mol Genet* 12, 1405-1413.
102. Djuric, U., El-Maarri, O., Lamb, B., Kuick, R., Seoud, M., Coullin, P., Oldenburg, J., Hanash, S., and Slim, R. (2006). Familial molar tissues due to mutations in the inflammatory gene, NALP7, have normal postzygotic DNA methylation. *Hum Genet* 120, 390-395.
103. Kou, Y.C., Shao, L., Peng, H.H., Rosetta, R., del Gaudio, D., Wagner, A.F., Al-Hussaini, T.K., and Van den Veyver, I.B. (2008). A recurrent intragenic genomic duplication, other novel mutations in NLRP7 and imprinting defects in recurrent biparental hydatidiform moles. *Mol Hum Reprod* 14, 33-40.
104. Sanchez-Delgado, M., Martin-Trujillo, A., Tayama, C., Vidal, E., Esteller, M., Iglesias-Platas, I., Deo, N., Barney, O., Maclean, K., Hata, K., et al. (2015). Absence of Maternal Methylation in Biparental Hydatidiform Moles from Women with NLRP7 Maternal-Effect Mutations Reveals Widespread Placenta-Specific Imprinting. *PLoS Genet* 11, e1005644.

105. Rugg-Gunn, P.J., Ferguson-Smith, A.C., and Pedersen, R.A. (2007). Status of genomic imprinting in human embryonic stem cells as revealed by a large cohort of independently derived and maintained lines. *Hum Mol Genet* 16 Spec No. 2, R243-251.
106. Beygo, J., Ammerpohl, O., Gritzan, D., Heitmann, M., Rademacher, K., Richter, J., Caliebe, A., Siebert, R., Horsthemke, B., and Buiting, K. (2013). Deep bisulfite sequencing of aberrantly methylated loci in a patient with multiple methylation defects. *PLoS One* 8, e76953.
107. Fisher, R.A., Hodges, M.D., Rees, H.C., Sebire, N.J., Seckl, M.J., Newlands, E.S., Genest, D.R., and Castrillon, D.H. (2002). The maternally transcribed gene p57(KIP2) (CDKN1C) is abnormally expressed in both androgenetic and biparental complete hydatidiform moles. *Hum Mol Genet* 11, 3267-3272.
108. Zhang, P., Liegeois, N.J., Wong, C., Finegold, M., Hou, H., Thompson, J.C., Silverman, A., Harper, J.W., DePinho, R.A., and Elledge, S.J. (1997). Altered cell differentiation and proliferation in mice lacking p57KIP2 indicates a role in Beckwith-Wiedemann syndrome. *Nature* 387, 151-158.
109. Fitzpatrick, G.V., Soloway, P.D., and Higgins, M.J. (2002). Regional loss of imprinting and growth deficiency in mice with a targeted deletion of KvDMR1. *Nat Genet* 32, 426-431.
110. Bhogal, B., Arnaudo, A., Dymkowski, A., Best, A., and Davis, T.L. (2004). Methylation at mouse *Cdkn1c* is acquired during postimplantation development and functions to maintain imprinted expression. *Genomics* 84, 961-970.
111. Diaz-Meyer, N., Day, C.D., Khatod, K., Maher, E.R., Cooper, W., Reik, W., Junien, C., Graham, G., Algar, E., Der Kaloustian, V.M., et al. (2003). Silencing of CDKN1C (p57KIP2) is associated with hypomethylation at KvDMR1 in Beckwith-Wiedemann syndrome. *J Med Genet* 40, 797-801.
112. Moglabey, Y.B., Kircheisen, R., Seoud, M., El Mogharbel, N., Van den Veyver, I., and Slim, R. (1999). Genetic mapping of a maternal locus responsible for familial hydatidiform moles. *Hum Mol Genet* 8, 667-671.
113. Akoury, E., Gupta, N., Bagga, R., Brown, S., Dery, C., Kabra, M., Srinivasan, R., and Slim, R. (2015). Live births in women with recurrent hydatidiform mole and two NLRP7 mutations. *Reprod Biomed Online* 31, 120-124.
114. Fisher, R.A., Lavery, S.A., Carby, A., Abu-Hayyeh, S., Swingler, R., Sebire, N.J., and Seckl, M.J. (2011). What a difference an egg makes. *Lancet* 378, 1974.
115. Deveault, C., Qian, J.H., Chebaro, W., Ao, A., Gilbert, L., Mehio, A., Khan, R., Tan, S.L., Wischmeijer, A., Coullin, P., et al. (2009). NLRP7 mutations in women with diploid androgenetic and triploid moles: a proposed mechanism for mole formation. *Hum Mol Genet* 18, 888-897.
116. Helwani, M.N., Seoud, M., Zahed, L., Zaatari, G., Khalil, A., and Slim, R. (1999). A familial case of recurrent hydatidiform molar pregnancies with biparental genomic contribution. *Hum Genet* 105, 112-115.
117. Sensi, A., Gualandi, F., Pittalis, M.C., Calabrese, O., Falciano, F., Maestri, I., Bovicelli, L., and Calzolari, E. (2000). Mole maker phenotype: possible narrowing of the candidate region. *Eur J Hum Genet* 8, 641-644.
118. Panichkul, P.C., Al-Hussaini, T.K., Sierra, R., Kashork, C.D., Popek, E.J., Stockton, D.W., and Van den Veyver, I.B. (2005). Recurrent biparental hydatidiform mole: additional evidence for a 1.1-Mb locus in 19q13.4 and candidate gene analysis. *J Soc Gynecol Investig* 12, 376-383.
119. Zhao, J., Moss, J., Sebire, N.J., Cui, Q.C., Seckl, M.J., Xiang, Y., and Fisher, R.A. (2006). Analysis of the chromosomal region 19q13.4 in two Chinese families with recurrent hydatidiform mole. *Hum Reprod* 21, 536-541.
120. Qian, J., Deveault, C., Bagga, R., Xie, X., and Slim, R. (2007). Women heterozygous for NLRP7/NLRP7 mutations are at risk for reproductive wastage: report of two novel mutations. *Hum Mutat* 28, 741.
121. Chilosi, M., Piazzola, E., Lestani, M., Benedetti, A., Guasparri, I., Granchelli, G., Aldovini, D., Leonardi, E., Pizzolo, G., Doglioni, C., et al. (1998). Differential expression of p57kip2, a maternally imprinted cdk inhibitor, in normal human placenta and gestational trophoblastic disease. *Laboratory investigation; a journal of technical methods and pathology* 78, 269-276.
122. Castrillon, D.H., Sun, D., Weremowicz, S., Fisher, R.A., Crum, C.P., and Genest, D.R. (2001). Discrimination of complete hydatidiform mole from its mimics by immunohistochemistry of the paternally imprinted gene product p57KIP2. *Am J Surg Pathol* 25, 1225-1230.

123. Wells, M. (2007). The pathology of gestational trophoblastic disease: recent advances. *Pathology* 39, 88-96.
124. Folkins, A., Cruz, L., Goldstein, D.P., Berkowitz, R.S., Crum, C., and Kindelberger, D. (2010). Utility of chromosomal chromogenic in situ hybridization as an alternative to flow cytometry and cytogenetics in the diagnosis of early partial hydatidiform moles: a validation study. *J Reprod Med* 55, 275-278.
125. Scholzen, T., and Gerdes, J. (2000). The Ki-67 protein: from the known and the unknown. *Journal of cellular physiology* 182, 311-322.
126. Xue, W.C., Khoo, U.S., Ngan, H.Y., Chan, K.Y., Chiu, P.M., Tsao, S.W., and Cheung, A.N. (2003). Minichromosome maintenance protein 7 expression in gestational trophoblastic disease: correlation with Ki67, PCNA and clinicopathological parameters. *Histopathology* 43, 485-490.
127. Olvera, M., Harris, S., Amezcua, C.A., McCourty, A., Rezk, S., Koo, C., Felix, J.C., and Brynes, R.K. (2001). Immunohistochemical expression of cell cycle proteins E2F-1, Cdk-2, Cyclin E, p27(kip1), and Ki-67 in normal placenta and gestational trophoblastic disease. *Mod Pathol* 14, 1036-1042.
128. Yapar, E.G., Ayhan, A., and Ergeneli, M.H. (1994). Pregnancy outcome after hydatidiform mole, initial and recurrent. *J Reprod Med* 39, 297-299.
129. Sand, P.K., Lurain, J.R., and Brewer, J.I. (1984). Repeat gestational trophoblastic disease. *Obstet Gynecol* 63, 140-144.
130. Fallahian, M., Sebire, N.J., Savage, P.M., Seckl, M.J., and Fisher, R.A. (2013). Mutations in NLRP7 and KHDC3L confer a complete hydatidiform mole phenotype on digynic triploid conceptions. *Hum Mutat* 34, 301-308.
131. Mahadevan, S., Wen, S., Wan, Y.W., Peng, H.H., Otta, S., Liu, Z., Iacovino, M., Mahen, E.M., Kyba, M., Sadikovic, B., et al. (2013). NLRP7 affects trophoblast lineage differentiation, binds to overexpressed YY1 and alters CpG methylation. *Hum Mol Genet*.
132. Dixon, P.H., Trongwongsa, P., Abu-Hayyah, S., Ng, S.H., Akbar, S.A., Khawaja, N.P., Seckl, M.J., Savage, P.M., and Fisher, R.A. (2012). Mutations in NLRP7 are associated with diploid biparental hydatidiform moles, but not androgenetic complete moles. *J Med Genet* 49, 206-211.
133. Sebire, N.J., Savage, P.M., Seckl, M.J., and Fisher, R.A. (2013). Histopathological features of biparental complete hydatidiform moles in women with NLRP7 mutations. *Placenta* 34, 50-56.
134. Ulker, V., Gurkan, H., Tozki, H., Karaman, V., Ozgur, H., Numanoglu, C., Gedikbasi, A., Akbayir, O., and Uyguner, Z.O. (2013). Novel NLRP7 mutations in familial recurrent hydatidiform mole: are NLRP7 mutations a risk for recurrent reproductive wastage? *Eur J Obstet Gynecol Reprod Biol* 170, 188-192.
135. Brown, L., Mount, S., Reddy, R., Slim, R., Wong, C., Jobanputra, V., Clifford, P., Merrill, L., and Brown, S. (2013). Recurrent pregnancy loss in a woman with NLRP7 mutation: not all molar pregnancies can be easily classified as either "partial" or "complete" hydatidiform moles. *Int J Gynecol Pathol* 32, 399-405.
136. Caliebe, A., Richter, J., Ammerpohl, O., Kanber, D., Beygo, J., Bens, S., Haake, A., Juttner, E., Korn, B., Mackay, D.J., et al. (2014). A familial disorder of altered DNA-methylation. *J Med Genet* 51, 407-412.
137. Messaed, C., Chebaro, W., Di Roberto, R.B., Rittore, C., Cheung, A., Arseneau, J., Schneider, A., Chen, M.F., Bernishke, K., Surti, U., et al. (2011). NLRP7 in the spectrum of reproductive wastage: rare non-synonymous variants confer genetic susceptibility to recurrent reproductive wastage. *J Med Genet* 48, 540-548.
138. Szulman, A.E., and Surti, U. (1978). The syndromes of hydatidiform mole. II. Morphologic evolution of the complete and partial mole. *Am J Obstet Gynecol* 132, 20-27.
139. Murphy, K.M., McConnell, T.G., Hafez, M.J., Vang, R., and Ronnett, B.M. (2009). Molecular genotyping of hydatidiform moles: analytic validation of a multiplex short tandem repeat assay. *J Mol Diagn* 11, 598-605.
140. Dressler, L.G., and Bartow, S.A. (1989). DNA flow cytometry in solid tumors: practical aspects and clinical applications. *Seminars in diagnostic pathology* 6, 55-82.
141. Fukunaga, M., Katabuchi, H., Nagasaka, T., Mikami, Y., Minamiguchi, S., and Lage, J.M. (2005). Interobserver and intraobserver variability in the diagnosis of hydatidiform mole. *Am J Surg Pathol* 29, 942-947.

142. Gupta, M., Vang, R., Yemelyanova, A.V., Kurman, R.J., Li, F.R., Maambo, E.C., Murphy, K.M., DeScipio, C., Thompson, C.B., and Ronnett, B.M. (2012). Diagnostic reproducibility of hydatidiform moles: ancillary techniques (p57 immunohistochemistry and molecular genotyping) improve morphologic diagnosis for both recently trained and experienced gynecologic pathologists. *Am J Surg Pathol* 36, 1747-1760.
143. Wachtel, M.S. (2005). Interobserver and intraobserver variability in the diagnosis of hydatidiform mole. *Am J Surg Pathol* 29, 1410.
144. Paradinas, F.J., Sebire, N.J., Fisher, R.A., Rees, H.C., Foskett, M., Seckl, M.J., and Newlands, E.S. (2001). Pseudo-partial moles: placental stem vessel hydrops and the association with Beckwith-Wiedemann syndrome and complete moles. *Histopathology* 39, 447-454.
145. Matsui, H., Iitsuka, Y., Yamazawa, K., Tanaka, N., Mitsuhashi, A., Seki, K., and Sekiya, S. (2003). Placental mesenchymal dysplasia initially diagnosed as partial mole. *Pathology international* 53, 810-813.
146. Meyer, E., Lim, D., Pasha, S., Tee, L.J., Rahman, F., Yates, J.R., Woods, C.G., Reik, W., and Maher, E.R. (2009). Germline mutation in NLRP2 (NALP2) in a familial imprinting disorder (Beckwith-Wiedemann Syndrome). *PLoS Genet* 5, e1000423.
147. Yan, Y., Frisen, J., Lee, M.H., Massague, J., and Barbacid, M. (1997). Ablation of the CDK inhibitor p57Kip2 results in increased apoptosis and delayed differentiation during mouse development. *Genes & development* 11, 973-983.
148. Tury, A., Mairet-Coello, G., and DiCicco-Bloom, E. (2011). The cyclin-dependent kinase inhibitor p57Kip2 regulates cell cycle exit, differentiation, and migration of embryonic cerebral cortical precursors. *Cereb Cortex* 21, 1840-1856.
149. Matsuoka, S., Edwards, M.C., Bai, C., Parker, S., Zhang, P., Baldini, A., Harper, J.W., and Elledge, S.J. (1995). p57KIP2, a structurally distinct member of the p21CIP1 Cdk inhibitor family, is a candidate tumor suppressor gene. *Genes Dev* 9, 650-662.
150. Zhang, P., Wong, C., Liu, D., Finegold, M., Harper, J.W., and Elledge, S.J. (1999). p21(CIP1) and p57(KIP2) control muscle differentiation at the myogenin step. *Genes & development* 13, 213-224.
151. Ito, Y., Takeda, T., Sakon, M., Tsujimoto, M., Monden, M., and Matsuura, N. (2001). Expression of p57/Kip2 protein in hepatocellular carcinoma. *Oncology* 61, 221-225.
152. Sato, N., Matsubayashi, H., Abe, T., Fukushima, N., and Goggins, M. (2005). Epigenetic down-regulation of CDKN1C/p57KIP2 in pancreatic ductal neoplasms identified by gene expression profiling. *Clinical cancer research : an official journal of the American Association for Cancer Research* 11, 4681-4688.
153. Itoh, Y., Masuyama, N., Nakayama, K., Nakayama, K.I., and Gotoh, Y. (2007). The cyclin-dependent kinase inhibitors p57 and p27 regulate neuronal migration in the developing mouse neocortex. *J Biol Chem* 282, 390-396.
154. Driver, A.M., Huang, W., Kropp, J., Penagaricano, F., and Khatib, H. (2013). Knockdown of CDKN1C (p57(kip2)) and PHLDA2 results in developmental changes in bovine pre-implantation embryos. *PLoS One* 8, e69490.
155. Ullah, Z., Kohn, M.J., Yagi, R., Vassilev, L.T., and DePamphilis, M.L. (2008). Differentiation of trophoblast stem cells into giant cells is triggered by p57/Kip2 inhibition of CDK1 activity. *Genes & development* 22, 3024-3036.
156. Baergen, R.N., Kelly, T., McGinniss, M.J., Jones, O.W., and Benirschke, K. (1996). Complete hydatidiform mole with a coexistent embryo. *Hum Pathol* 27, 731-734.
157. Zaragoza, M.V., Keep, D., Genest, D.R., Hassold, T., and Redline, R.W. (1997). Early complete hydatidiform moles contain inner cell mass derivatives. *Am J Med Genet* 70, 273-277.
158. Reddy, R., Nguyen, N.M., Sarrabay, G., Rezaei, M., Rivas, M.C., Kavasoglu, A., Berkil, H., Elshafey, A., Abdalla, E., Nunez, K.P., et al. (2016). The genomic architecture of NLRP7 is Alu rich and predisposes to disease-associated large deletions. *Eur J Hum Genet* 24, 1516.
159. Hedley, D.W. (1989). Flow cytometry using paraffin-embedded tissue: five years on. *Cytometry* 10, 229-241.
160. Khawajkie, Y., Buckett, W., Nguyen, N.M.P., Mechtouf, N., Ao, A., Arseneau, J., and Slim, R. (2017). Recurrent triploid digynic conceptions and mature ovarian teratomas: Are they different manifestations of the same genetic defect? *Genes Chromosomes Cancer* 56, 832-840.

161. Sahoo, T., Dzidic, N., Strecker, M.N., Commander, S., Travis, M.K., Doherty, C., Tyson, R.W., Mendoza, A.E., Stephenson, M., Dise, C.A., et al. (2017). Comprehensive genetic analysis of pregnancy loss by chromosomal microarrays: outcomes, benefits, and challenges. *Genet Med* 19, 83-89.
162. Pallares-Ruiz, N., Philibert, L., Dumont, B., Fabre, A., Cuisset, L., Cointin, E., Rittore, C., Soler, S., and Toutou, I. (2010). Combined mutation and rearrangement screening by quantitative PCR high-resolution melting: is it relevant for hereditary recurrent Fever genes? *PLoS One* 5, e14096.
163. Nguyen, N.M., Zhang, L., Reddy, R., Dery, C., Arseneau, J., Cheung, A., Surti, U., Hoffner, L., Seoud, M., Zaatari, G., et al. (2014). Comprehensive genotype-phenotype correlations between NLRP7 mutations and the balance between embryonic tissue differentiation and trophoblastic proliferation. *J Med Genet* 51, 623-634.
164. Wang, M., Dixon, P.H., Decordova, S., Hodges, M., Sebire, N.J., Ozalp, S., Fallahian, M., Sensi, A., Ashrafi, F., Repiska, V., et al. (2009). Identification of 13 novel NLRP7 mutations in 20 families with recurrent hydatidiform mole; missense mutations cluster in the leucine rich region. *J Med Genet* 46, 569-555.
165. Sunde, L., Lund, H., N, J.S., Grove, A., Fisher, R.A., Niemann, I., Kjeldsen, E., Andreasen, L., Hansen, E.S., Bojesen, A., et al. (2015). Paternal Hemizygoty in 11p15 in Mole-like Conceptuses: Two Case Reports. *Medicine (Baltimore)* 94, e1776.
166. Eagles, N., Sebire, N.J., Short, D., Savage, P.M., Seckl, M.J., and Fisher, R.A. (2015). Risk of recurrent molar pregnancies following complete and partial hydatidiform moles. *Hum Reprod* 30, 2055-2063.
167. Walsh, T., and King, M.C. (2007). Ten genes for inherited breast cancer. *Cancer Cell* 11, 103-105.
168. Nguyen, N.M.P., Khawajkie, Y., Mechtouf, N., Rezaei, M., Breguet, M., Kurvinen, E., Jagadeesh, S., Solmaz, A.E., Aguinaga, M., Hemida, R., et al. (2018). The genetics of recurrent hydatidiform moles: new insights and lessons from a comprehensive analysis of 113 patients. *Mod Pathol*.
169. Eagles, N., Sebire, N.J., Short, D., Savage, P.M., Seckl, M.J., and Fisher, R.A. (2016). Risk of recurrent molar pregnancies following complete and partial hydatidiform moles. *Hum Reprod* 31, 1379.
170. Libby, B.J., De La Fuente, R., O'Brien, M.J., Wigglesworth, K., Cobb, J., Inselman, A., Eaker, S., Handel, M.A., Eppig, J.J., and Schimenti, J.C. (2002). The mouse meiotic mutation *mei1* disrupts chromosome synapsis with sexually dimorphic consequences for meiotic progression. *Dev Biol* 242, 174-187.
171. Robert, T., Nore, A., Brun, C., Maffre, C., Crimi, B., Bourbon, H.M., and de Massy, B. (2016). The TopoVIB-Like protein family is required for meiotic DNA double-strand break formation. *Science* 351, 943-949.
172. Kumar, R., Bourbon, H.M., and de Massy, B. (2010). Functional conservation of *Mei4* for meiotic DNA double-strand break formation from yeasts to mice. *Genes Dev* 24, 1266-1280.
173. Reddy, R., Fahiminiya, S., El Zir, E., Mansour, A., Megarbane, A., Majewski, J., and Slim, R. (2014). Molecular genetics of the Usher syndrome in Lebanon: identification of 11 novel protein truncating mutations by whole exome sequencing. *PLoS One* 9, e107326.
174. Li, H., and Durbin, R. (2009). Fast and accurate short read alignment with Burrows-Wheeler transform. *Bioinformatics* 25, 1754-1760.
175. McKenna, A., Hanna, M., Banks, E., Sivachenko, A., Cibulskis, K., Kernytsky, A., Garimella, K., Altshuler, D., Gabriel, S., Daly, M., et al. (2010). The Genome Analysis Toolkit: a MapReduce framework for analyzing next-generation DNA sequencing data. *Genome Res* 20, 1297-1303.
176. Li, H., Handsaker, B., Wysoker, A., Fennell, T., Ruan, J., Homer, N., Marth, G., Abecasis, G., Durbin, R., and Genome Project Data Processing, S. (2009). The Sequence Alignment/Map format and SAMtools. *Bioinformatics* 25, 2078-2079.
177. Wang, K., Li, M., and Hakonarson, H. (2010). ANNOVAR: functional annotation of genetic variants from high-throughput sequencing data. *Nucleic Acids Res* 38, e164.
178. Thorvaldsdottir, H., Robinson, J.T., and Mesirov, J.P. (2013). Integrative Genomics Viewer (IGV): high-performance genomics data visualization and exploration. *Brief Bioinform* 14, 178-192.
179. Taylor, D.M., Handyside, A.H., Ray, P.F., Dibb, N.J., Winston, R.M., and Ao, A. (2001). Quantitative measurement of transcript levels throughout human preimplantation development: analysis of hypoxanthine phosphoribosyl transferase. *Mol Hum Reprod* 7, 147-154.

180. Libby, B.J., Reinholdt, L.G., and Schimenti, J.C. (2003). Positional cloning and characterization of *Mei1*, a vertebrate-specific gene required for normal meiotic chromosome synapsis in mice. *Proc Natl Acad Sci U S A* 100, 15706-15711.
181. Xu, B., Noohi, S., Shin, J.S., Tan, S.L., and Taketo, T. (2014). Bi-directional communication with the cumulus cells is involved in the deficiency of XY oocytes in the components essential for proper second meiotic spindle assembly. *Dev Biol* 385, 242-252.
182. Hu, M.W., Wang, Z.B., Jiang, Z.Z., Qi, S.T., Huang, L., Liang, Q.X., Schatten, H., and Sun, Q.Y. (2014). Scaffold subunit Aalpha of PP2A is essential for female meiosis and fertility in mice. *Biol Reprod* 91, 19.
183. Cartegni, L., Chew, S.L., and Krainer, A.R. (2002). Listening to silence and understanding nonsense: exonic mutations that affect splicing. *Nat Rev Genet* 3, 285-298.
184. Holbrook, J.A., Neu-Yilik, G., Hentze, M.W., and Kulozik, A.E. (2004). Nonsense-mediated decay approaches the clinic. *Nat Genet* 36, 801-808.
185. Mahadevan, S., Wen, S., Balasa, A., Fruhman, G., Mateus, J., Wagner, A., Al-Hussaini, T., and Van den Veyver, I.B. (2013). No evidence for mutations in *NLRP7* and *KHDC3L* in women with androgenetic hydatidiform moles. *Prenat Diagn* 33, 1242-1247.
186. Hiraoka, Y., Ding, D.Q., Yamamoto, A., Tsutsumi, C., and Chikashige, Y. (2000). Characterization of fission yeast meiotic mutants based on live observation of meiotic prophase nuclear movement. *Chromosoma* 109, 103-109.
187. Maleki, S., Neale, M.J., Arora, C., Henderson, K.A., and Keeney, S. (2007). Interactions between *Mei4*, *Rec114*, and other proteins required for meiotic DNA double-strand break formation in *Saccharomyces cerevisiae*. *Chromosoma* 116, 471-486.
188. Grelon, M., Gendrot, G., Vezon, D., and Pelletier, G. (2003). The Arabidopsis *MEI1* gene encodes a protein with five BRCT domains that is involved in meiosis-specific DNA repair events independent of *SPO11*-induced DSBs. *Plant J* 35, 465-475.
189. Mains, P.E., Kempthues, K.J., Sprunger, S.A., Sulston, I.A., and Wood, W.B. (1990). Mutations affecting the meiotic and mitotic divisions of the early *Caenorhabditis elegans* embryo. *Genetics* 126, 593-605.
190. Ben Khelifa, M., Ghieh, F., Boudjenah, R., Hue, C., Fauvert, D., Dard, R., Garchon, H.J., and Vialard, F. (2018). A *MEI1* homozygous missense mutation associated with meiotic arrest in a consanguineous family. *Hum Reprod*.
191. Miao, Y., Ma, S., Liu, X., Miao, D., Chang, Z., Luo, M., and Tan, J. (2004). Fate of the first polar bodies in mouse oocytes. *Mol Reprod Dev* 69, 66-76.
192. Liu, H., Kim, J.M., and Aoki, F. (2004). Regulation of histone H3 lysine 9 methylation in oocytes and early pre-implantation embryos. *Development* 131, 2269-2280.
193. Clark-Maguire, S., and Mains, P.E. (1994). Localization of the *mei-1* gene product of *Caenorhabditis elegans*, a meiotic-specific spindle component. *J Cell Biol* 126, 199-209.
194. Baarends, W.M., Wassenaar, E., van der Laan, R., Hoogerbrugge, J., Sleddens-Linkels, E., Hoeijmakers, J.H., de Boer, P., and Grootegoed, J.A. (2005). Silencing of unpaired chromatin and histone H2A ubiquitination in mammalian meiosis. *Mol Cell Biol* 25, 1041-1053.
195. Turner, J.M., Mahadevaiah, S.K., Fernandez-Capetillo, O., Nussenzweig, A., Xu, X., Deng, C.X., and Burgoyne, P.S. (2005). Silencing of unsynapsed meiotic chromosomes in the mouse. *Nature genetics* 37, 41-47.
196. Carofigli, F., Inagaki, A., de Vries, S., Wassenaar, E., Schoenmakers, S., Vermeulen, C., van Cappellen, W.A., Sleddens-Linkels, E., Grootegoed, J.A., Te Riele, H.P., et al. (2013). *SPO11*-independent DNA repair foci and their role in meiotic silencing. *PLoS genetics* 9, e1003538.
197. Schimenti, J. (2005). Synapsis or silence. *Nature genetics* 37, 11-13.
198. Ferguson, K.A., Chow, V., and Ma, S. (2008). Silencing of unpaired meiotic chromosomes and altered recombination patterns in an azoospermic carrier of a t(8;13) reciprocal translocation. *Hum Reprod* 23, 988-995.
199. Pujol, A., Durban, M., Benet, J., Boiso, I., Calafell, J.M., Egozcue, J., and Navarro, J. (2003). Multiple aneuploidies in the oocytes of balanced translocation carriers: a preimplantation genetic diagnosis study using first polar body. *Reproduction* 126, 701-711.
200. Anton, E., Vidal, F., and Blanco, J. (2008). Reciprocal translocations: tracing their meiotic behavior. *Genet Med* 10, 730-738.

201. Lawler, S.D., Povey, S., Fisher, R.A., and Pickthall, V.J. (1982). Genetic studies on hydatidiform moles. II. The origin of complete moles. *Ann Hum Genet* 46, 209-222.
202. Altieri, A., Franceschi, S., Ferlay, J., Smith, J., and La Vecchia, C. (2003). Epidemiology and aetiology of gestational trophoblastic diseases. *Lancet Oncol* 4, 670-678.
203. Coulam, C.B. (1991). Epidemiology of recurrent spontaneous abortion. *Am J Reprod Immunol* 26, 23-27.
204. La Vecchia, C., Franceschi, S., Parazzini, F., Fasoli, M., Decarli, A., Gallus, G., and Tognoni, G. (1985). Risk factors for gestational trophoblastic disease in Italy. *Am J Epidemiol* 121, 457-464.
205. Berkowitz, R.S., Bernstein, M.R., Harlow, B.L., Rice, L.W., Lage, J.M., Goldstein, D.P., and Cramer, D.W. (1995). Case-control study of risk factors for partial molar pregnancy. *American Journal of Obstetrics and Gynecology* 173, 788.
206. Srayko, M., Buster, D.W., Bazirgan, O.A., McNally, F.J., and Mains, P.E. (2000). MEI-1/MEI-2 katanin-like microtubule severing activity is required for *Caenorhabditis elegans* meiosis. *Genes Dev* 14, 1072-1084.
207. McNally, K., Audhya, A., Oegema, K., and McNally, F.J. (2006). Katanin controls mitotic and meiotic spindle length. *J Cell Biol* 175, 881-891.
208. Westbury, J., Watkins, M., Ferguson-Smith, A.C., and Smith, J. (2001). Dynamic temporal and spatial regulation of the cdk inhibitor p57(kip2) during embryo morphogenesis. *Mech Dev* 109, 83-89.
209. Kumar, R., Oliver, C., Brun, C., Juarez-Martinez, A.B., Tarabay, Y., and Massy, J.K.a.B.d. (July 18, 2018). Mouse REC114 is essential for meiotic DNA double-strand break formation and forms a complex with MEI4. *bioRxiv*.
210. Hassold, T., and Hunt, P. (2001). To err (meiotically) is human: the genesis of human aneuploidy. *Nat Rev Genet* 2, 280-291.
211. Baudat, F., Manova, K., Yuen, J.P., Jasin, M., and Keeney, S. (2000). Chromosome synapsis defects and sexually dimorphic meiotic progression in mice lacking Spo11. *Mol Cell* 6, 989-998.
212. Daniel, K., Lange, J., Hached, K., Fu, J., Anastassiadis, K., Roig, I., Cooke, H.J., Stewart, A.F., Wassmann, K., Jasin, M., et al. (2011). Meiotic homologue alignment and its quality surveillance are controlled by mouse HORMAD1. *Nat Cell Biol* 13, 599-610.
213. Stanzione, M., Baumann, M., Papanikos, F., Dereli, I., Lange, J., Ramlal, A., Trankner, D., Shibuya, H., de Massy, B., Watanabe, Y., et al. (2016). Meiotic DNA break formation requires the unsynapsed chromosome axis-binding protein IHO1 (CCDC36) in mice. *Nat Cell Biol* 18, 1208-1220.
214. Nagaoka, S.I., Hassold, T.J., and Hunt, P.A. (2012). Human aneuploidy: mechanisms and new insights into an age-old problem. *Nat Rev Genet* 13, 493-504.
215. Fledel-Alon, A., Wilson, D.J., Broman, K., Wen, X., Ober, C., Coop, G., and Przeworski, M. (2009). Broad-scale recombination patterns underlying proper disjunction in humans. *PLoS Genet* 5, e1000658.
216. Wang, S., Kleckner, N., and Zhang, L. (2017). Crossover maturation inefficiency and aneuploidy in human female meiosis. *Cell Cycle* 16, 1017-1019.

APPENDIX (ETHICS AND COPYRIGHT PERMISSION)



McGill

Faculty of Medicine
3655 Promenade Sir William Osler
Montreal, QC H3G 1Y6

Faculté de médecine
3655, Promenade Sir William Osler
Montréal, QC, H3G 1Y6

Fax/Télécopieur: (514) 398-3595

**CERTIFICATION OF ETHICAL ACCEPTABILITY FOR RESEARCH
INVOLVING HUMAN SUBJECTS**

The Faculty of Medicine Institutional Review Board consisting of:

ARTHUR CANDIB, MED

PATRICIA DOBKIN, PHD

CATHERINE GARDNER, BSC

LAWRENCE HUTCHISON, MD

WILSON MILLER, PHD, MD

ROBERT L. MUNRO, BCL

ROBERTA PALMOUR, PHD

LUCILLE PANET-RAYMOND, BA

has examined the research project **A01-M07-03A** entitled **"Identification of a Gene Responsible for Repeated Hydraditiform Moles"**

as proposed by: Rima Slim to _____
Applicant Granting Agency, if any

and consider the experimental procedures to be acceptable on ethical grounds for research involving human subjects.

January 24, 2003
Date

Neil Malhotra
Chair, IRB

De Montigny
Dean of Faculty

Institutional Review Board Assurance Number: M-1458



McGill

January 16, 2018

■ Dr. Rima Slim

Faculty of Medicine 3655 Promenade
Sir William Osler #633 Montreal, QC
H3G 1Y6

Faculté de médecine
3655, Promenade Sir William Osler #633
Montréal QC H3G 1Y6

Fax/Télécopieur: (514) 398-3870
Tél/Tel: (514) 398-3124

McGill University Health Center Research Institute
1001 Décarie Blvd, Room EM03210
Montréal, QC H4A 3J1

■ **RE: IRB study Number A01-M07-03A**

Identification of a Gene Responsible for Repeated Hydraditiform Moles, Spontaneous Abortions and Infertility of Unknown Clinical Etiology

■ **Dear Dr. Slim,**

Thank you for submitting an application for Continuing Review for the above-referenced study.

The study progress report was reviewed and an expedited re-approval was provided on January 15, 2018. The ethics certification renewal is valid from January 8, 2018 to January 7, 2019.

The Investigator is reminded of the requirement to report all IRB approved protocol and consent form modifications to the Research Ethics Offices (REOs) for the participating hospital sites. Please contact the individual hospital REOs for instructions on how to proceed. Research funds may be withheld and / or the studVs data may be revoked for failing to comply with this requirement.

Should any modification or unanticipated development occur prior to the next review, please notify the IRB promptly. Regulation does not permit the implementation of study modifications prior to IRB review and approval.

Regards,

■ **Carolyn Ells, PhD**

Co-Chair
Institutional Review Board

cc: Nawel Mechtouf
JGH/REB
SMH/REB
A01-M07-03A

McGill Faculty of Institutional Review Board



Medicine -

CONTINUING REVIEW FORM -

The completed form is to be submitted electronically to submit2irb.med@mcgill.ca. The continuing review form must be received at least one (1) month before the expiration of the last ethics approval. If you require additional information, please visit the IRB website at: <http://www.mcgill.ca/medresearch/ethics/> or by calling 514-398-3124.

Principal Investigator	Rima Slim
Faculty and Department	McGill University Health Center Research Institute - Human Genetics
Study Coordinator, if applicable	Nawel Mechtouf
Address:	1001 Decarie Blvd, Glen Site, Block E, EM03210 (office) E012379 (lab), Montreal QC, H4A
E-mail	3J1 QC Canada
	Identification of a Gene Responsible for Repeated Hydraditiform Moles, Spontaneous Abortions and Infertility of Unknown Clinical Etiology

rima.slim@muhc.mcgill.ca

Telephone: (514) 934-1934 ext 4455

study Title

Grant title, if different from study title. Identify new genes for recurrent Molar Pregnancies and characterize mechanisms of mole formation

IRB Study Number A01-M07-03A

Date of last approval 02/13/2017

Has there been a change or addition to the financial support for this study?
 YES @ NO

If yes, please specify the changes/additions.

700

0

Status of the Protocol

Recruitment complete

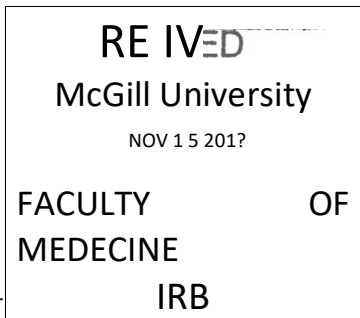
Recruitment on hold

Data analysis

Secondary Analysis only

Inactive/dormant••

Active enrolment When did this study begin? 04/01/2003



*If the study is inactive/ dormant (i.e., there are no participants enrolled in the study and no study activity is occurring), please specify the reason:

If the study is actively enrolling participants, or if enrolment is complete, please answer the following questions:

Study sample size. not defined

700

Total number of participants withdrawn

Total number enrolled in the study:

Number of participants that have completed this study:

Projected date of study completion:

04/01/2023

Projected date of completion of study enrolment:

Please provide a brief description of what has occurred since the IRB's last ethics approval.

- O YES
@ NO
O N/A

Has this new information been communicated to participants?

- O YES
O No
@ N/A

Have the adverse events been reported to the IRB? If no, submit alt adverse events with this form.

Has the study revealed any new findings or knowledge relevant to the potential benefits and/or study risks that may influence participants' willingness to continue in the study?

- Have there been any publications?
O YES What is the version 05/12/2015 date of the most recent IRB- approved protocol?
@ NO

If applicable, please describe the findings.

- O YES
@ NO
O N/A

Have consent form modifications been reported to the IRB?

- O YES
O NO
@ N/A

Has an amendment(s) to the protocol been submitted to the IRB in the past year?

Has the consent form(s) been revised in the past year?

Version date/s of the most recently approved consent form(s).

Have any adverse events occurred since the last approval?

April 14, 2003

YES

N/A

YES NO

@ YES

No

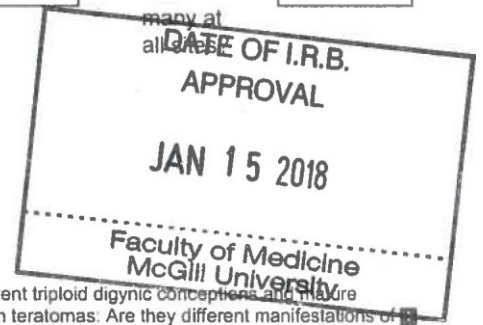
If yes, how many at
all sites?
McGill

How
many at
all sites

N/A

If yes, append list:

Recurrent triploid digynic conceptions and mature ovarian teratomas: Are they different manifestations of



SIGNATURES



Principal Investigator

11/14/2017

IRB Chair



Date

Jan 16, 2018



Title: Causative Mutations and Mechanism of Androgenetic Hydatidiform Moles

Author: Ngoc Minh Phuong
Nguyen,Zhao-Jia Ge,Ramesh Reddy,Somayyeh Fahiminiya,Philippe Sauthier,Rashmi Bagga,Feride Iffet Sahin,Sangeetha Mahadevan,Matthew Osmond,Magali Breguet,Kurosh Rahimi,Lo uise Lapensee, Karine Hovanes, Radhika Srinivasa n et al.

Publication: The American Journal of Human Genetics

Publisher: Elsevier

Date: 1 November 2018

© 2018 American Society of Human Genetics.

LOGINLOGIN
If you're a copyright.com user, you can login to RightsLink using your copyright.com credentials. Already a **RightsLink user** or want to [learn more?](#)

Please note that, as the author of this Elsevier article, you retain the right to include it in a thesis or dissertation, provided it is not published commercially. Permission is not required, but please ensure that you reference the journal as the original source. For more information on this and on your other retained rights, please visit: <https://www.elsevier.com/about/our-business/policies/copyright#Authorrights>

BACK

CLOSE WINDOW

Copyright © 2018 [Copyright Clearance Center, Inc.](#) All Rights Reserved. [Privacy statement.](#) [Terms and Conditions.](#)
Comments? We would like to hear from you. E-mail us at customercare@copyright.com

Re: Permission to include the article in the

thesis llacey@bmj.com on behalf of bmj.permissions

<bmj.permissions@bmj.com>

Thu 11/22/2018 4:49 AM

To: Ngoc Minh Phuong Nguyen <phuong.nguyen2@mail.mcgill.ca>;

Dear Phuong,

Thank you for your email. The author licence you agreed to when publishing in a BMJ Journal allows you to reuse your article in your thesis without acquiring permission from BMJ.

Further details about your rights as an author can be found here: <https://www.bmj.com/company/products-services/rights-and-licensing/author-self-archiving-and-permissions/>

Best wishes

Laura

On Tue, 20 Nov 2018 at 23:20, Ngoc Minh Phuong Nguyen <phuong.nguyen2@mail.mcgill.ca> wrote:

Dear BMJ/JMG,

My name is Ngoc Minh Phuong Nguyen, PhD candidate at McGill university. I would like to ask for your permission to include in my thesis the article published in **Journal of Medical Genetics**.

Please find below the information of the article:

Comprehensive genotype–phenotype correlations between NLRP7 mutations and the balance between embryonic tissue differentiation and trophoblast proliferation

Crossref DOI link: <https://doi.org/10.1136/JMEDGENET-2014-102546>

PMID: 25097207

Please let me know if further actions are needed,

Thank you and Regards,

Phuong

BMJ advances healthcare worldwide by sharing knowledge and expertise to improve experiences, outcomes and value. This email and any attachments are confidential. If you have received this email in error, please delete it and kindly notify us. If the email contains personal views then BMJ accepts no responsibility for these statements. The recipient should check this email and attachments for viruses because the BMJ accepts no liability for any damage caused by viruses. Emails sent or received by BMJ may be monitored for size, traffic, distribution and content. BMJ Publishing Group Limited trading as BMJ. A private limited company, registered in England and Wales under registration number 03102371. Registered office: BMA House, Tavistock Square, London WC1H 9JR, UK.

Title: The genetics of recurrent
hydatidiform moles: new insights and lessons
from a comprehensive analysis of 113 patients
Author: Ngoc Minh Phuong Nguyen et al
Publication: Modern Pathology
Publisher: Springer Nature
Date: Feb 20, 2018
Copyright © 2018, Springer Nature

LOGINLOGIN
If you're a **copyright.com user**, you can login to RightsLink using your copyright.com credentials. Already a **RightsLink user** or want to [learn more?](#)

Author Request

If you are the author of this content (or his/her designated agent) please read the following. If you are not the author of this content, please click the Back button and select no to the question "Are you the Author of this Springer Nature content?".

Ownership of copyright in original research articles remains with the Author, and provided that, when reproducing the contribution or extracts from it or from the Supplementary Information, the Author acknowledges first and reference publication in the Journal, the Author retains the following nonexclusive rights: To reproduce the contribution in whole or in part in any printed volume (book or thesis) of which they are the author(s).

The author and any academic institution, where they work, at the time may reproduce the contribution for the purpose of course teaching.

To reuse figures or tables created by the Author and contained in the Contribution in oral presentations and other works created by them.

To post a copy of the contribution as accepted for publication after peer review (in locked Word processing file, or a PDF version thereof) on the Author's own web site, or the Author's institutional repository, or the Author's funding body's archive, six months after publication of the printed or online edition of the Journal, provided that they also link to the contribution on the publisher's website. Authors wishing to use the published version of their article for promotional use or on a web site must request in the normal way.

If you require further assistance please read Springer Nature's online [author reuse guidelines](#).

For full paper portion: Authors of original research papers published by Springer Nature are encouraged to submit the author's version of the accepted, peer-reviewed manuscript to their relevant funding body's archive, for release six months after publication. In addition, authors are encouraged to archive their version of the manuscript in their institution's repositories (as well as their personal Web sites), also six months after original publication.

v1.0

BACK CLOSE WINDOW

Copyright © 2018 [Copyright Clearance Center, Inc.](#) All Rights Reserved. [Privacy statement](#). [Terms and Conditions](#).
Comments? We would like to hear from you. E-mail us at customercare@copyright.com

RE: Permission to reuse the article

Journalpermissions <journalpermissions@springernature.com>

Thu 11/22/2018 9:50 AM

To:Ngoc Minh Phuong Nguyen <phuong.nguyen2@mail.mcgill.ca>;

Dear Ngoc,

Thank you for your Springer Nature request. As an author, you are welcome to reuse this content in other works created by yourself, but we require a license for our records.

To obtain your permission, please access the following URL which will take you to the order entry page from which you can request your permission. Please apply for the 'thesis/disserta on' license, and make sure to select Yes in the author field.

Please note: we allow the use of the final accepted manuscript version of the article in the thesis, not the published version.

<https://s100.copyright.com/AppDispatchServlet?publisherName=SpringerNature&orderBeanReset=true&orderSource=OEP&openAccess=false&publication=2161-3303&title=Gene+cs+and+Epigene+cs+of+Recurrent+Hydroids+Moles:+Basic+Science+and+Gene+c+Counselling&author=Ngoc+Minh+Phuong+Nguyen;+Rima+Slim&contentID=10.1007/s13669-013-0076-1&publicationDate=01/21/2014&volumeNum=3&issueNum=1&startPage=55&endPage=64&imprint=Springer+US>

During the process, you will set up an account with RightsLink, who will invoice you if there are any fees incurred. You will be able to use your RightsLink account in the future to request (and pay for) permissions online both from Springer Nature and from other participating publishers. RightsLink will also email you confirmation that permission has been granted, in the form of a printable license.

Best wishes,
Oda

Oda Siqveland
Permissions Assistant

SpringerNature
The Campus, 4 Crinan Street, London N1 9XW,
United Kingdom
T +44 (0) 207 014 6851

<https://www.springer.com>

<http://www.palgrave.com>

From: Ngoc Minh Phuong Nguyen [mailto:phuong.nguyen2@mail.mcgill.ca]
Sent: 21 November 2018 22:03
To: Journalpermissions
Subject: Permission to reuse the article

Dear Springer team,

My name is Ngoc Minh Phuong Nguyen. I'm contacting you to ask for permission to reuse the review article below in my thesis (I am the first author in this review article). Please find below the info of the article:

Title: Genetics and Epigenetics of Recurrent Hydatidiform Moles: Basic Science and Genetic Counselling

Authors: Ngoc Minh Phuong Nguyen, Rima Slim

March 2014, Volume 3, [Issue 1](#), pp 55–64, Curr Obstet Gynecol Rep (2014).

Please let me know if further actions are required.

Regards,

Thank you for your order with RightsLink / Springer Nature

no-reply@copyright.com

Fri 11/23/2018 4:31 PM

To: Ngoc Minh Phuong Nguyen <phuong.nguyen2@mail.mcgill.ca>;



Thank you for your order!

Dear Ms. Ngoc Minh Phuong Nguyen,

Thank you for placing your order through Copyright Clearance Center's RightsLink® service.

Order Summary

Licensee: Ngoc Minh Phuong Nguyen
Order Date: Nov 23, 2018
Order Number: 4474960730678
Publication: Current Obstetrics and Gynecology Reports
Title: Genetics and Epigenetics of Recurrent Hydatidiform Moles: Basic Science and Genetic Counselling
Type of Use: Thesis/Dissertation Order
Total: 0.00 CAD

View or print complete [details](#) of your order and the publisher's terms and conditions.

Sincerely,

Copyright Clearance Center

Tel: +1-855-239-3415 / +1-978-646-2777

customer@copyright.com



<https://myaccount.copyright.com>

This message (including attachments) is confidential, unless marked otherwise. It is intended for the addressee(s) only. If you are not an intended recipient, please delete it without further distribution and reply to the sender that you have received the message in error.